Order Number 9130938

Investigation of stagnation flow heat transfer for a heated horizontal round plate

Wei, Ching-Hua, Ph.D.

New Jersey Institute of Technology, 1991

U·M·I
300 N. Zeeb Rd.
Ann Arbor, MI 48106

INVESTIGATION OF STAGNATION FLOW HEAT TRANSFER FOR A HEATED HORIZONTAL ROUND PLATE

BY

CHING-HUA WEI

A Dissertation

Submitted to the Faculty of the Graduate Division of the

New Jersey Institute of Technology

in Partial Fulfillment of the Requirements for the Degree of

Doctor of Philosophy

Department of Mechanical Engineering.

May 1991.

APPROVAL SHEET

Title of Dissertation: Investigation of stagnation flow heat transfer for a heated horizontal round plate.

Name of candidate: Ching-Hua Wei.

Doctor of Philosophy in Mechanical Engineering, 1991.

Dissertation and Abstract Approved by:

Dr. Peter Hrycak, Thesis Advisor
Professor of Mechanical Engineering, NJIT

Dr. Denis Blackmore, Committee Member
Professor of Mathematics and Associate Director of the Center for Applied Mathematics and Statistics, NJIT

Dr. Rajesh N. Dave, Commitee Member
Assistant Professor of Mechanical Engineering, NJIT

Dr. Avraham Harnoy, Committee Member
Associate Professor of Mechanical Engineering, NJIT

Prof. Lawrence J. Schmerzler, Commitee Member
Associate Professor of Mechanical Engineerion, NJIT

ABSTRACT

Investigation of Stagnation Flow Heat Transfer for a Heated Horizontal Round Plate

by
Ching-Hua, Wei

The heat transfer characteristics in stagnation flow are investigated through three cases in this study. The first is forced convection by an array of air jets; the second is free convection of a downward-facing heated round plate; the third is free convection of an upward-facing heated round plate.

The first case is investigated by systematic experiments which examine the heat transfer characteristics mainly by five air jets impinging normally to a flat plate, with varying nozzle diameters, and Reynolds numbers, at different distances between the nozzles and the plate. The empirical formulas of heat transfer around the stagnation point and over the entire plate are established. Compared to the single jet cooling, the Nusselt numbers do not increase significantly by increasing the numbers of jets.

The second case is a theoretical study. The analytical solutions for the velocity and the temperature profiles, using the Prandtl number in the moderate range, have been obtained through the similarity transformation of the governing equations applicable to laminar flow. The Nusselt number expression is found to be a function of the 1/4 power of the Rayleigh number, for the prescribed surface temperature condition; and a function of the 1/5 power of the modified Rayleigh number, for the prescribed surface flux condition.

The third case is formulated by a mathematical model similar to the second case; however, the analytical solutions for the velocity and the temperature profiles have not been obtained. Yet, the Nusselt number expression from the model shows the 1/4 power dependence on the Rayleigh number, which agrees with the results of the second approach and with experimental findings.

VITA

Name: Ching-Hua Wei.

Degree and date to be conferred: Doctor of Philosophy in Mechanical Engineering, 1991.

Secondary education: The High School of Taiwan Normal University, Taipei, Taiwan, 1977.

Collegiate Institutions attended.	Dates.	Degree.	Date of Degree.
Feng-Chia University, Taiwan.	1977-1981	B.S.M.E.	May, 1981.
N.J.I.T., Newark, N.J., U.S.A.	1985-1987	M.S.M.E.	May, 1987.
N.J.I.T., Newark, N.J., U.S.A.	1987-1991	Ph.D.	May, 1991.

Major: Mechanical Engineering.

Positions held : Engineer Assistant,
Chung-Shan Institute of Science & Technology,
Taiwan, 1984-1985.

Research Assistant,
N.J.I.T., Newark, New Jersey, 1985-1990

ACKNOWLEDGEMENTS

I wish to thank my advisor, Dr. Peter Hrycak, for his continued guidance, encouragement and instruction during my graduate studies in New Jersey Institute of Technology, and the members of the committee for their constructive suggestions.

Thanks are also due to the Department of Mechanical Engineering, for its financial support of a graduate assistantship, and to the staff of the Mechanical Engineering Department for their help in getting supplies for the experiments carried out in the Jet Research Laboratory that are described in part one of this dissertation.

I also wish to express my appreciation to Dr. M. J. Linden for his reading the dissertation in its early form and for making many valuable comments.

My friends, Vasil Hlinka, Orest Hrycak, and Samir Sethi, have helped me with collecting and processing data in the experiment on impinging jets. I express to them my thanks for their assistance.

I am indebted to my parents who have constantly supported me in pursuit of higher education and research.

TABLE OF CONTENTS

LIST OF SYMBOLS

a	free constant used for scaling, 1/sec
c	undetermined constant of equation
Cn	nozzle-to-nozzle spacing
C_p	specific heat at constant pressure, kJ/kg °C
D	diameter of nozzle, m
$f(\eta)$	similarity function
h	convective heat transfer coefficient, W/m^2 °C
k	undetermined constant in equation, Eq.(I.29); abbreviation of kilo, in Fig.I-4 and Fig.I-5 series
K	thermal conductivity, W/m °C
L	characteristic length, m
m	dimensionless constant to be determined by experiment
M	distance from the bottom position of the thermocouple hole to the top surface of calorimeter
N	distance between the top and the bottom thermocouple hole of calorimeter
p	pressure, N/m^2
q	heat flux, W/m^2
r	radial coordinate, m
R	radius of the heated round plate
t	thickness of nozzle plate shown in Fig.I-4 series
T	temperature, °C or °F
u	velocity component in radial coordinate, m/sec
U	radial velocity component outside of boundary layer, m/sec
U_{oc}	velocity at exit of nozzle, m/sec

V	velocity, m/sec
w	velocity component in vertical coordinate, m/sec
z	vertical coordinate, m
Zn	distance of nozzle to the heat transfer plate
α	thermal diffusivity, m^2/sec
β	volume coefficient of expansion, 1/ °K
η	similarity variable, dimensionless coordinate
$\theta(\eta)$	dimensionless temperature function
μ	viscosity, kg/m sec
ν	kinematic viscosity, m^2/sec
ρ	density, Kg/m^3
Φ	dissipation function
Ψ	stream function

Dimensionless Groups:

Ec	Eckert number, $V^2/C_p\ \Delta T$
Gr	Grashof number, $g\beta\Delta TL^3/\nu^2$
Gr^*	modified Grashof number, $GrNu=g\beta q_w L^4/K\nu^2$
Nu;(NU)	Nusselt number, hL/K, $q_w L/K\Delta T$; (used in Fig.I-4 series)
Pr	Prandtl number, ν/α, $\mu C_p/K$
Ra	Rayleigh number, $GrPr=g\beta\Delta TL^3/\nu\alpha$
Ra^*	modified Rayleigh number, $PrGr^*$
Re_D;(RED)	Reynolds number based on nozzle diameter and air properties at exit of nozzle, $U_{oc}D/\nu$; (used in Fig.I-4 series)
Sh	Sherwood number

Subscripts:

b	specified at bottom position

D;(d)	characteristic length based on diameter of nozzle; (used in Fig.I-4 series)
f	indicates fluid condition
i	index indicates interval between the points
L	characteristic length
o	indicates the condition at stagnation point region, otherwise indicated in special case
pl	based on heat transfer plate
r	at specified radial position of the heated plate
R	the characteristic length based on the radius of plate
s	indicates the solid condition; surface of plate
t	specified at top position
w	indicates the condition at wall or surface
wc	indicates the condition at the wall center of the round plate
∞	indicates far field

Superscripts:

"	represents the unit of inch (used in Fig.I-4 series)
_	overhead bar indicates the average value, or dimensionless function in Eq.(II.68) and (II.69)
*	indicates the modified dimensionless variable

LIST OF TABLES

LIST OF FIGURES

INTRODUCTION AND RESEARCH OBJECTIVES

The fluid which flows in a normal direction toward a plate is a type of stagnation flow. In this flow pattern, there is a spot where the velocity is zero and there is no unique direction for the streamlines. This point in the flow field is called the stagnation point. The fluid dynamic and heat transfer behavior around the vicinity of the stagnation point of the heated plate is important both theoretically and practically, because velocity distribution changes abruptly so as to affect heat transfer characteristics.

The analytical solution of fluid dynamic behavior around the stagnation point in impinging flow (Fig. 1.a) has been originally obtained by Homann and Froessling (as introduced by Schlichting, pp. 98-101, [22]). It is considered as an example of exact solution of the Navier-Stokes equation. Based on this solution, the heat transfer characteristics of the forced convection was then evaluated by Sibulkin [24]. This solution is of special interest, even if it is obtained from the governing equation of the boundary-layer type. The Sibulkin's theoretical expression is usually used as a guidance to the analyses of experimental results around the stagnation point for the single jet cooling [10]. Concerning an array of jets, it is interesting to see how is the cooling performance of a single jet impinging on a heated plate around the stagnation point can differ from the characteristics of a central jet performing as a part of an array of jets. This will be examined in Part I.

Since the analytical solution can be obtained in the case of the forced convection by impinging flow, it is worth trying to find the analytical solutions for the case of the free convection of a downward-facing heated plate (Fig. 1.b) because two flow patterns are similar to each other (i.e. fluid flows towards a flat plate). This will be analyzed in Part II. The discussion in Part III is an extension of the discussion from Part II. The purpose here is to see if the analytical solutions can be found when fluid flows in the reverse direction.

Therefore, in this thesis, it is intended to show the many common features existing between the stagnation flow generated by single jet and multiple jets issuing from nozzles; and thermal plumes generated by temperature differences. It is believed that some uncertainties still exist concerning the nature of such flow, and the resulting heat transfer. This will be clarified by uniform treatment of the subject based on the formulation of the fundamental equations and the analysis of the experimental results. The experimental results discussed are both the ones carried out by the author, and those available from the literature. All the efforts lead to develop empirical formulas or theoretical explanations for the prediction of the heat transfer under the stagnation flow by an array of air jets; and by natural convection to a heated horizontal round plate facing either upward or downward.

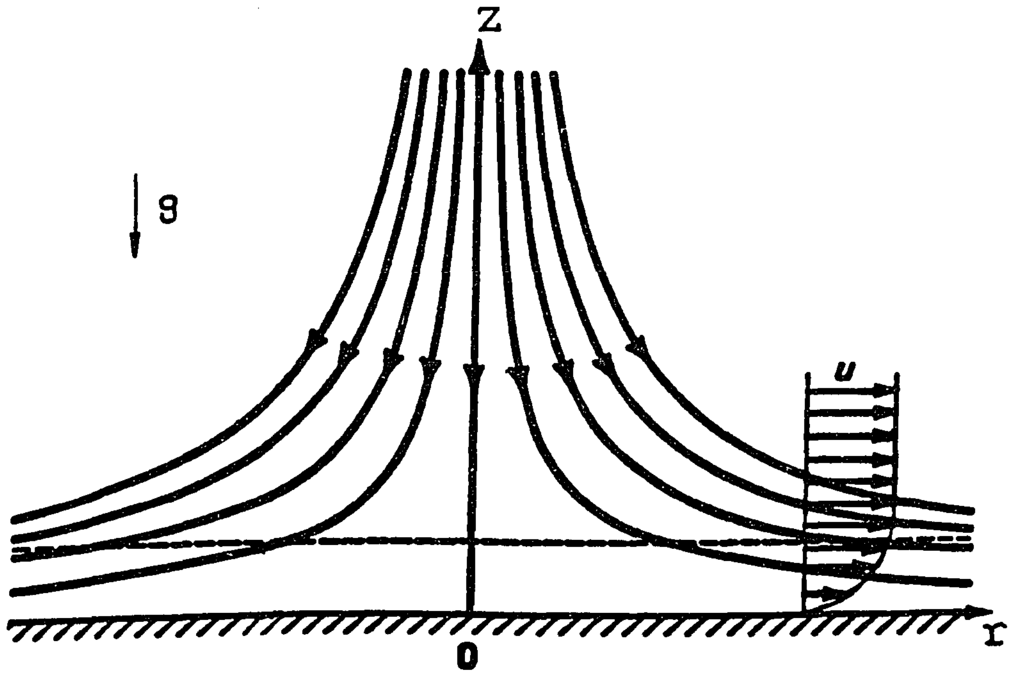

Fig.1.a The Impinging Stagnation Flow

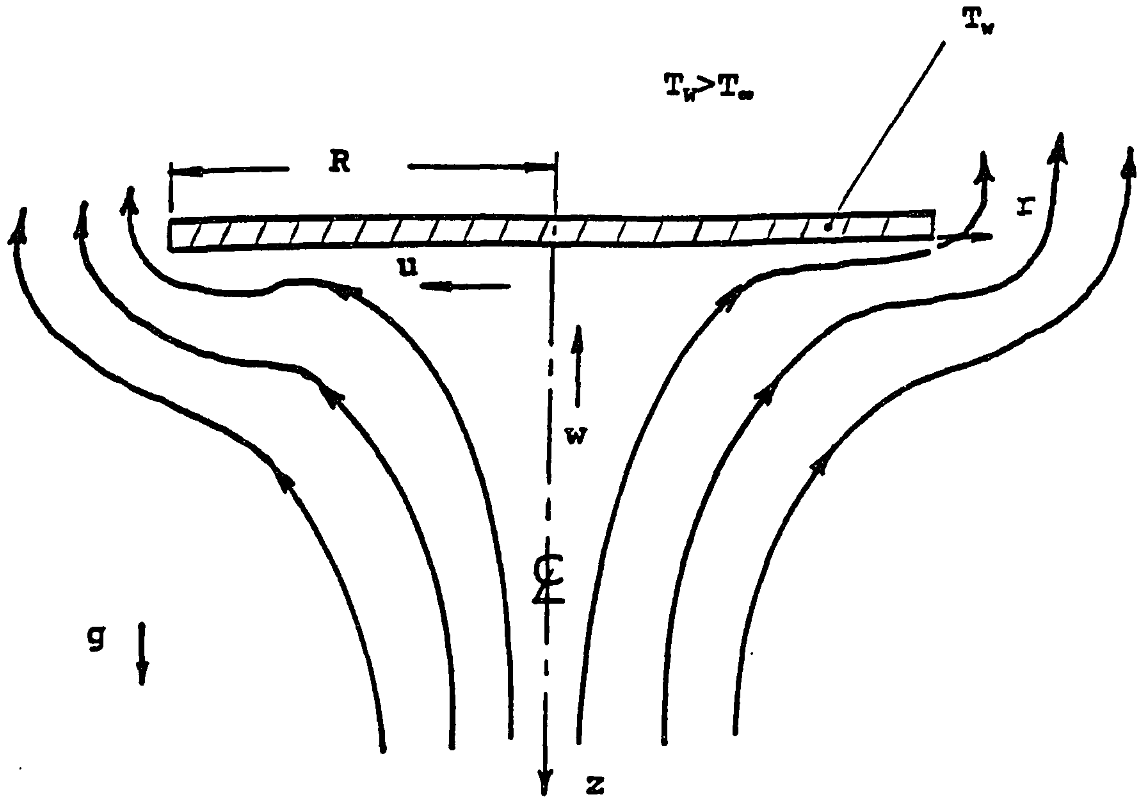

Fig.1.b Free Convection of a Downward-Facing Heated Plate

PART I FORCED CONVECTION BY AN ARRAY OF AIR JETS IMPINGING TO A HEATED ROUND PLATE

I-1 INTRODUCTION

1.1 General

Many industries use an array of air jets for the cooling of large hot surfaces. Such uses include the annealing of metal or plastic sheets, the tempering of glass, the cooling of turbine blades, the drying of textiles or paper, and the cooling of microelectronic parts in computers [17] and so on. This method supplies a cooling rate several times higher than those of conventional methods, such as fan or blower cooling. In addition, it provides more flexibility for meeting different surface heat transfer needs through simple alteration of air flow rates or through a variation in the distance between jets and the hot surface.

Although the study of the topics connected with the heat transfer from the impinging jet has been done for decades, there still exists a need for both analytical and experimental work, because the theoretical results obtained so far have differed somewhat with experimental results, and empirical equations have not met all requirements for cooling designs [11].

1.2 Subject of the Present Work

This study has experimentally examined the heat transfer of a horizontal heated plate by a square arrays of turbulent, round air jets (cf., Fig.I-3.2), impinging normally on it (cf., Fig.I-1.1), at steady state. Jets are issued from an array of five nozzles with diameters ranged at 3.18 mm (0.125 in.), 6.35 mm (0.25 in.) and 9.53 mm (0.375 in.). The nozzle exit Reynolds numbers are ranged at 14,000, 26,000, 35,000, and 54,000 (based on the diameter of nozzle, D; and the velocity at the exit of nozzle, U_{oc}). The ratio of the nozzle-to-heat-transfer-plate distance (Zn) to the diameter of nozzle (D), Zn/D, is varied at 3, 5, 7, 9, 12, and 15. The ratio of the nozzle-to-nozzle spacing (Cn) to the nozzle diameter, Cn/D, is varied at 2, 3, 4, and 5. Some tests have been made for jets issued from an array of nine nozzles with diameter at 3.18 mm.

This investigation has been carried out as a continuation of earlier work done by Kaya [14] and a single jet done by Datta [2]. Finally, these results are summarized into optimal empirical equations as a reference for further applications.

1-3 Previous Studies

Heat transfer near the stagnation point by axisymmetric flow impinging on a hot object has been studied since about 1950. As pointed out in Schlichting (cf., p.100, [22]), the basic fluid flow pattern for a laminar stagnation flow either two-dimensional or axisymmetric type was studied before then, so as to allow later calculation of heat transfer. Hrycak [9] did an extensive literature review about heat transfer from impinging jets up to 1980. Among those research works, some of the most important ones are worth mentioning:

Freidman and Mueller [4] presented experimental results of heat transfer for an array of air jets impinging on a heated plate.

Sibulkin [24] was among the first to study the stagnation point heat transfer of a body of revolution, however, the flow is an infinite stream.

Kezios [16] reported results from both analytical and experimental approaches for a jet impinging on an infinite plane. His results offered a very limited range for the distance from nozzle to surface.

Ott [21] investigated heat transfer experimentally by a triangular array of round jets.

Gardon and Cobonpue [6] reported experimental results by single jet and multiple jets; the maximum heat transfer rate was found at $6<Zn/D<7$ for a single jet. There were no correlation equations expressed for multiple jets at the stagnation point.

Hilgeroth [8] reported the heat transfer coefficients increased as the jet diameter increased while Cn/D, Zn/D, and exit velocity of nozzle remained constant.

Kercher and Tabakoff [15] tested the heat transfer relation by a square array of round air jets impinging on a flat heated plate and allowing spent air to flow out from one direction. The correlation formula of average Nusselt number was presented.

Datta [2] did a single jet cooling experiment with wide range of each of the corresponding parameters, such as diameter of nozzle, mass flow rate, and distance from jet to target. The stagnation region heat transfer rates were summarized into empirical equations. He found the maximum heat transfer occurred at Zn/D approximately at seven diameters downstream from the nozzle which was similar to Gardon and Cobonpue's finding.

Martin [19] edited heat transfer researches created by single and multiple jets, but the original experimental work was done by Krotzsch [18]. His report was adopted recently in a thermal design handbook [7]. However, his empirical equations can only be applied to evaluate average heat transfer.

Hrycak [10] reported single jet cooling results and a comprehensive survey of previous studies. He confirmed that at the stagnation point, the Nusselt number depends upon the half power of Reynolds number, and the maximum Nusselt number occurs when the heated plate is placed at about seven diameters downstream from the nozzle.

Behbahani and Goldstein [1] investigated heat transfer by an array of staggered air jets. An empirical equation of average Nusselt number was presented.

Experimental investigation of an array of five and nine air jets, has been carried out in Hrycak's laboratory since 1984. Sethi [23] reported systematic results about fluid dynamic behavior and patterns. Kaya [14] reported heat transfer results with limited tests, by an array of five jets with the diameter of nozzles at 6.25 mm.

From looking at previous works, single jet impinging heat transfer has been studied intensively. The experimental results as expressed in terms of the Nusselt number for the problem of heat transfer near the stagnation point are usually higher than the calculation based on the Sibulkin's solution [24]. Some common features for single jet cooling have been found by several investigators. These are the facts that the maximum heat transfer occurs at the tip of nominal potential core (cf., p.10, [9]), and the exponent of the Reynolds number shows very nearly the value of 0.5 in a heat transfer expression at the stagnation point [10]. The experimental method is commonly used for the study of multiple jets. Researchers have paid more attention to the study of average heat transfer under multiple jets than to the examination of heat transfer around the stagnation point. However, there is still an overall lack of agreement between the results of various researchers.

I-2 THEORETICAL BACKGROUND

2.1 Introduction

Generally, the fluid flow pattern along the exit of the jet can be partitioned into three zones [9, 23, 25]. They are the free jet zone, deflection zone, and wall jet zone respectively. The flow pattern is shown in Fig.I-1.1.

In the free jet zone, the fluid just leaving from the nozzle, is beyond the viscous boundary layer caused by the flat plate. It has been determined at the length of about 4/5 Zn (cf., Fig.I-1.1) measured from the exit of nozzle [12, 23]. If the impingement plate is placed far enough from jets, the free jet zone may be characterized into two parts. They are the potential core, where the centerline velocity remains the same as the exit of nozzle, and the fully developed region, where the velocity distribution is similar to that of the free jet diffusing into an infinite medium. In the deflection zone, where the fluid strikes the flat plate, a boundary layer is formed at the stagnation point. Actually, this is the region we are most interested in as far as the heat transfer at the stagnation point is concerned.

After jet air hits the flat plate, the air spreads radially toward the outside of the plate forming a flow pattern that is similar to the wall jet as discussed by Schlichting (cf., p.750, [22]). The average heat transfer characteristics of the plate are associated with the flow behavior in this "wall jet" zone. Although multiple jets are used in this experiment, the flow pattern behavior described above is still helpful, because the flow pattern of the multiple impinging jets can be considered as the combination of each jet. The interference between jets is not examined theoretically in this study, but it is investigated experimentally by dimensional analysis in section I-2.3.

2.2 Differential Formulation at Stagnation Point Region

The most general analytical approach for heat transfer and fluid dynamics at the stagnation point in deflection zone on a flat plate is to find the velocity expression from the continuity and momentum (i.e. Navier-Stokes) equations; and the temperature expression from the energy equation. Schlichting [22] discussed this problem. The Navier-Stokes and the continuity equations in cylindrical coordinate for rotational symmetry and steady state can be written as

$$u\frac{\partial u}{\partial r}+w\frac{\partial u}{\partial z}=-\frac{1}{\rho}\frac{\partial p}{\partial r}+\nu\left(\frac{\partial^2 u}{\partial r^2}+\frac{1}{r}\frac{\partial u}{\partial r}-\frac{u}{r^2}+\frac{\partial^2 u}{\partial z^2}\right) \qquad (I.1)$$

$$u\frac{\partial w}{\partial r}+w\frac{\partial w}{\partial z}=-\frac{1}{\rho}\frac{\partial p}{\partial z}+\nu\left(\frac{\partial^2 w}{\partial r^2}+\frac{1}{r}\frac{\partial w}{\partial r}+\frac{\partial^2 w}{\partial z^2}\right) \qquad (I.2)$$

$$\frac{\partial u}{\partial r}+\frac{u}{r}+\frac{\partial w}{\partial z}=0 \qquad (I.3)$$

If the velocity components outside of the boundary layer are assumed to be

$$U = ar \qquad (I.4)$$

$$W = -2az \qquad (I.5)$$

where " a " is a constant, then the expression of pressure in frictionless flow is

$$p_0-p=\frac{1}{2}\rho\left(U^2+W^2\right)=\frac{1}{2}\rho a^2\left(r^2+4z^2\right) \qquad (I.6)$$

where P_0 denotes the pressure around the stagnation point. The pressure differential term in the radial direction can be described by Euler equation as

$$-\frac{1}{\rho}\frac{\partial p}{\partial r}=U\frac{\partial U}{\partial r}=a^2 r \qquad (I.7)$$

However, Eq.(I.7) can also be used inside the boundary layer at the stagnation region and the expression of pressure can be assumed as (cf., p.101, [22])

$$p_0 - p = \frac{1}{2}\rho a^2 (r^2 + F(z)) \tag{I.8}$$

because the deflection zone is small and the boundary layer is very thin. The expressions of velocity distribution that are satisfied by Eq.(I.3) are as follows.

$$u = arf'(\eta) \tag{I.9}$$

$$w = -2\sqrt{a\nu}\, f(\eta) \tag{I.10}$$

In the above, a dimensionless coordinate is introduced as

$$\eta = \sqrt{\frac{a}{\nu}}\, z \tag{I.11}$$

By applying the similarity transformation, the partial differential equations Eq.(I.1), and (I.2) can then be transformed into total differential equations as follows.

$$f'''(\eta) + 2f(\eta)f''(\eta) - f'(\eta)^2 + 1 = 0 \tag{I.12}$$

$$f''(\eta) + 2f(\eta)f'(\eta) = \frac{1}{4}F'(z) \tag{I.13}$$

where the prime " ′ " denotes the differentiation with respect to η. Eq.(I.12) is independent of function F(z), therefore $f(\eta)$ can be determined by solving Eq.(I.12) along with proper boundary conditions. They are

$$(i) \quad \eta = 0\ (i.e.\ z=0) \quad ; \quad f(0) = f'(0) = 0$$

which indicates the velocity components to be zero on the plate surface, and

$$(ii)\quad \eta=\eta_\infty \;;\quad f'(\eta_\infty)=1$$

which indicates the radial coordinate velocity component u is approximately U outside of the boundary layer. Eq.(I.12) was first solved by Homann (cf., p.101, [22]). Froessling (cf., p.98, [22]) solved it numerically and determined when $f''(0)=1.312$, it will satisfy the boundary condition at $f'(\eta_\infty)=1$. The solution is verified by this study which is carried out by the Runge-Kutta method along with Newton's shooting method at step size equal to 0.001. The numerical calculation scheme is discussed in section II-3.1.

Substituting $f(\eta)$ and $f'(\eta)$ into Eq.(I.9), and Eq.(I.10), the velocity expression can be obtained. The temperature distribution governed by the energy equation can then be obtained from integrating the function $f(\eta)$. For steady state, incompressible flow with constant properties and negligible dissipation, the energy equation in cylindrical coordinate is

$$u\frac{\partial T}{\partial r}+w\frac{\partial T}{\partial z}=\alpha\left(\frac{\partial^2 T}{\partial r^2}+\frac{1}{r}\frac{\partial T}{\partial r}+\frac{\partial^2 T}{\partial z^2}\right) \qquad \text{(I.14)}$$

The dimensionless temperature function may be assumed as

$$\theta(\eta)=\frac{T-T_\infty}{T_w-T_\infty} \qquad \text{(I.15)}$$

where T_w is wall temperature, T_∞ is ambient temperature, and T is temperature function with dependent variable η only. For the prescribed constant wall temperature case, the boundary conditions are

$$(i)\quad \eta=0 \;;\quad \theta(0)=1$$

$$(ii)\quad \eta=\eta_\infty \ ; \quad \theta(\eta_\infty)=0$$

Combining Eq.(I.9), (I.10), and (I.15), the energy equation, Eq.(I.14), can be transformed into

$$\theta''(\eta)+2Prf(\eta)\theta'(\eta)=0 \tag{I.16}$$

Eq.(I.16) is a separable linear differential equation. Rearranging and integrating Eq.(I.16), it becomes

$$\int_0^\eta \frac{1}{\theta'(\eta)}d\theta'(\eta)=\int_0^\eta -2\,Prf(s)\,ds \tag{I.17}$$

then

$$\theta'(\eta)=C_1e^{\int_0^\eta -2Prf(s)\,ds} \tag{I.18}$$

$$\theta(\eta)=C_1\int_0^\eta e^{\int_0^t -2\,Prf(s)\,ds}\,dt+C_2 \tag{I.19}$$

With the above thermal boundary conditions, $\theta(\eta)$ can be expressed as

$$\theta(\eta)=1-\frac{\int_0^\eta e^{-2Pr\int_0^t f(s)\,ds}\,dt}{\int_0^\infty e^{-2Pr\int_0^\eta f(s)\,ds}\,d\eta} \tag{I.20}$$

then

$$\left.\frac{d\theta(\eta)}{d\eta}\right|_{\eta=0}=\theta'(0)=-\frac{1}{\int_0^\infty e^{-2Pr\int_0^\eta f(s)\,ds}\,d\eta} \tag{I.21}$$

where the Prandtl number varies within a moderate range (i.e. 10.7<Pr< 5). The results of Eq.(I.21) are expressed by Sibulkin [24] as follows.

$$\theta'(0) = -0.763 Pr^{0.4} \tag{I.22}$$

However, in the present study, the author has calculated Eq.(I.21) numerically by Simpson's rule; and found that the more accurate results may be expressed as

$$\theta'(0) = -0.762 Pr^{0.37} \tag{I.22.1}$$

The relative error is less than 1% between the two expressions for a Prandtl of 0.72; therefore, Eq.(I.22) is still applicable if air is used as heat transfer medium.

The heat flux on the wall is

$$\begin{aligned} q_w &= -K_f \frac{dT}{dZ}\bigg|_{z=0} = -K_f \theta'(0) \sqrt{\frac{a}{\nu}} (T_w - T_\infty) \\ &= h (T_w - T_\infty) \end{aligned} \tag{I.23}$$

therefore, h (convective heat transfer coefficient) is equal to

$$h = -K_f \theta'(0) \sqrt{\frac{a}{\nu}} \tag{I.24}$$

Substituting Eq.(I.4) and Eq.(I.22) into Eq.(I.24), the Nusselt number expression can be written as:

$$Nu_{0,r} = \frac{hr}{K_f} = 0.763 Pr^{0.4} \left(\frac{Ur}{\nu}\right)^{0.5} = 0.763 Pr^{0.4} Re_{r,U}^{0.5} \tag{I.25}$$

Eq.(I.25) is identical to the one derived by Sibulkin [24]. It is not convenient to make comparisons to experimental data, unless the Nusselt number based on D (diameter of nozzle) and the Reynolds number based on U_{0c} (exit velocity of jet) and D in Eq.(I.25) can be converted. Making Eq.(I.4) dimensionless and setting $a^* = aD/U_{0c}$, then

$$\frac{U}{U_{0c}} = \left(\frac{aD}{U_{0c}}\right) \frac{r}{D} = a^* \frac{r}{D} \tag{I.26}$$

This dimensionless formulation, Eq.(I.26), was introduced by Hrycak [10]. Substituting Eq.(I.26) into Eq.(I.25), the Nusselt number expression becomes

$$Nu_{0,D}=0.763Pr^{0.4}Re_{D,U_{0c}}^{0.5}\sqrt{a^{*}} \tag{I.27}$$

where a^{*} is a function of Zn/D and that can be determined by experiment. Sethi [23] reported experimental results of a^{*}, for five jets, nozzle diameter of 6.35 mm, Re_D=14,000, and Cn/D=2. The values of a^{*} are 1.14, 0.98, 0.62, 0.46, and 0.302 corresponding to the values of Zn/D at 5, 7, 9, 12, and 15 respectively. Substituting the a^{*} results into Eq.(I.27), the Nusselt number values are about 62% lower than the experimental results from this study. However, the 0.5 power of the Reynolds number in heat transfer expression matches the experimental results for the cases with the diameter of nozzles at 6.35 mm and 9.53 mm for the lower Zn/D values (i.e. 3≤Zn/D≤5) around the stagnation point.

Hrycak [10] explained that this may be due to turbulence effects around the stagnation point, and introduced an applicable technique, which is extended from laminar boundary-layer technique to turbulent flow. By his method, Eq.(I.27) can be modified as

$$Nu_{0,D}=1.312Pr^{0.4}Re_{D,U_{0c}}^{0.5}\sqrt{a^{*}} \tag{I.28}$$

Eq.(I.28) shows better agreement with experimental results than Eq.(I.27) does. The Nusselt number values calculated from Eq.(I.28) are about 28% lower for the value of Zn/D at five; and about 40% lower for the value of Zn/D from nine to fifteen than the present experimental results. It appears that the experimental results for the smaller value of Zn/D can fit better with the Eq.(I.28) than those for the larger value of Zn/D does.

2.3 Dimensional Analysis

The heat transfer analysis in the case of multiple turbulent impinging jets is usually difficult to perform accurately by analytical solutions from governing equations. The applicable analysis still relies greatly on experimental data. Therefore, the dimensional analysis is very useful in correlating experimental data [10, 2, 14]. The basic idea is to find the heat transfer formula expressed by the least number of parameters, which affect heat transfer phenomena. From the theoretical analysis (i.e. Eq.(I.27)) and the experience of experimental work, the general expression of the Nusselt number can be written as

$$Nu_D = kRe^{a}_{D,U_{0c}} Pr^{b} \left(\frac{Z_n}{D}\right)^{c} \left(\frac{D}{D_0}\right)^{d} \left(\frac{C_n}{D}\right)^{e} \left(\frac{D}{D_{pl}}\right)^{f} \qquad \text{(I.29)}$$

where k, a, b, c, d, etc., are all determined by experiment. The parameter of $(Zn/D)^c$ represents the effects of the various nozzle-to-heat-transfer-plate distance. The $(D/D_0)^d$ term is used to correlate with experimental results, obtained from different diameters of the nozzles, for the Nusselt number of the stagnation point. The D_0 represents the reference diameter of the nozzle. The effects of interference in a cluster of jets are expressed by $(Cn/D)^e$. The $(D/D_{pl})^f$ represents the aspect ratio of the diameter of the nozzle to the diameter of the heat transfer plate; this term is used to correlate with the results of the average Nusselt number.

For boundary-layer type stagnation flow, a=0.5 and b=0.4 associated with Sibulkin's analysis [24] are applied. For turbulent flow in the wall jet zone, a=0.7 and b=0.33 are commonly used [9].

I-3 EXPERIMENT SET-UP AND PROCEDURES

3.1 Air Supply System

The compressed air used for cooling the heated plate is supplied by a compressor equipped with a 15-horse-power A.C. motor. The air flows trough the piping system, which includes an oil trap, storage tank, regulator, orifice, plenum chamber, and finally from the nozzle plate to the test plate (cf., Fig.I-3.1 and Fig.I-3.2). The air pressure on the inlet side of the rotameter is kept at 25 psi. to ensure a proper setting for the rotameters, which are used to control the air flow rate. The real flow rates are measured by the pressure difference between both sides of an orifice plate, which is inserted on outlet side of the rotameter (cf., Fig.I-3.1). In the plenum chamber, two screens and a coarse wool-like material are stuffed in so as to eliminate internal turbulence and create a uniform air output from the nozzle plate.

3.2 Heating System and Test Plate Configuration

The test plate is heated by 100 °C (212 °F) steam from the bottom of the plate under atmospheric pressure. The steam is generated from boiling water, contained in a boiler, heated by a 1500 W electric heater element. Its output power is regulated by a transformer, commonly known as Variac. Inside the boiler, a metal screen is installed just above water level to prevent water from splashing and to help the steam uniformly heat the bottom of the test plate.

The test plate (cf., Fig.I-3.3) consists of the heat transfer plate, calorimeters, calorimeter insulators, thermocouples (copper-constantan T type, diameter is 0.005 in.), and the brass support plate. On the heat transfer plate, fourteen temperature measurement locations are prepared. One is located at the center, the others are distributed around five different concentric rings on the heat transfer plate shown in Fig.I-3.4. At each location is embedded one calorimeter (cf., Fig.I-3.5), at which two thermocouples are installed. In order to reduce measurement error of the temperature, silver-based high conductivity grease is used to fill in the gaps between thermocouples and calorimeters. To obtain a one-dimensional heat flux measurement, the calorimeters are surrounded by insulators. The heating system and test plate assembly are put together into a wooden box with glass fiber stuffed in between to prevent heat loss. On the top of the box, an acrylic plate is used to cover the space between the edge of the heat transfer plate and the edge of the box to ensure a continuous plane that will minimize the possibility of forming vortexes. The assembly graph is shown in Fig.I-3.3.

3.3 Temperature Measurement System

The temperature measurement system diagram is shown in Fig.I-3.6. All the thermocouple wires and one common reference junction thermocouple are connected with a set of selection switches for selecting each location where the temperature is to be measured.

The temperatures are measured by a potentiometer (Leed and Northrop made, 7555 type K-5) in conjunction with a galvanometer. These pieces of equipment are recalibrated every two years to meet the requirement of the National Bureau of Standard. The error of the whole measurement system is estimated within 0.2 °C to 0.3 °C. The test of accuracy of temperature measurement is made by measuring the temperatures of boiling water and of an ice bath. A well-charged 1.5 Volt D.C. battery and a standard cell (1.01938 Volt) are required for the proper function of the potentiometer.

3.4 Operation Procedure

The step-by-step procedures are described as follows :

(1) Load a nozzle plate on the plenum chamber.

(2) Adjust the center line of the central nozzle aligned with the center line of the central calorimeter.

(3) Adjust the cross, formed by the nozzles on the nozzle plate (cf., Fig.I-3.2), aligned with the cross, formed by calorimeters numbered as 10, 11, 12, 13 and 14 on the heat transfer plate (cf., Fig.I-3.4).

(4) Adjust the surface of the nozzle plate parallel to the surface of the heat transfer plate.

(5) Set up a specified nozzle-to-heat-transfer-plate distance.

(6) Fill the boiler up with water; set the heater in full power until the water is boiling, then turn down the heater at a proper setting to maintain water at the boiling state. The setting value depends on different tests of cooling rate carried out by the jets.

(7) Turn on the air compressor, and set the pressure at 25 psi. at the inlet side of the rotameter.

(8) Adjust the rotameter for the specified Reynolds number of the test.

(9) Take temperature readings of each thermocouple when the system reaches steady state. (It is determined by experiment that the steady state should be achieved two hours after procedure (8) is completed).

(10) Take readings of the pressure difference, including the pressure difference between each side of orifice (P_1-P_2), plenum chamber and barometric pressure (P_3-P_0), and downstream of orifice and barometric pressure (P_2-P_0).

I-4 DATA PROCESSING AND RESULTS

4.1 General Description

The data processing is done by a computer program listed in appendix A. It is written in procedures described as follows:

(1) Input data of the temperature readings (in units of milli volts).

(2) Convert the temperature readings into degrees Celsius and Fahrenheit, according to the copper-constantan T type thermocouple conversion table by Omega Engineering Co. [20].

(3) Calculate the average temperature of each ring.

(4) Calculate the heat transfer coefficient of each ring (i.e. local heat transfer coefficients).

(5) Calculate the local Nusselt number.

(6) Calculate the average Nusselt number by subroutine (SUB1).

(7) Calculate the actual Reynolds number in the pipe.

(8) Extrapolate or interpolate the Nusselt number to the corresponding nominal Reynolds number.

(9) Stop.

4.2 Local Heat Transfer Coefficients

Calculating the heat transfer coefficient of each ring on the surface of the heated plate is one of the most important steps of this calculation. At steady state, the heat flux conducted from the calorimeter is equal to the heat flux convected by air. The relation can be expressed as follows.

$$q_{conduc.}=-K_s\frac{dT}{dZ}=q_{convec.}=h(T_w-T_{jet}) \qquad (I.30)$$

were K_s is thermal conductivity of the material of the calorimeter, and T_{jet} is the temperature of air leaving the nozzle. The temperature gradient is obtained from the ratio of the temperature difference between the top (T_t) and the bottom (T_b) positions to the distance (N shown in Fig.I-3.5) between them.

By T_t, T_b, and T_{jet} measured from the thermocouples, the temperature on the surface of the heat transfer plate (T_w) can be found by extrapolating the temperature gradient between T_t and T_b.

$$T_w = T_b + (T_t - T_b)\frac{M}{N} \tag{I.31}$$

where M denotes the distance between the surface of the heated plate and the bottom position of the thermocouple (shown in Fig. I-3.5). From Eq.(I.30) and (I.31), the heat transfer coefficient can be expressed as

$$h = \frac{K_s}{N}\left(\frac{T_b - T_t}{T_w - T_{jet}}\right) \tag{I.32}$$

where K_s is the thermal conductivity of the calorimeter material -Invar (the alloy of iron and nickel, containing 36% nickel with minor amounts of manganese, silicon and carbon, amounting to less than 1% in all). Its formula (cf.,[3]), a function of temperature, used in this calculation is

$$K_s = 7.856 + 0.005478(T-32) + (3.4568\times10^{-6})T^2 \tag{I.33}$$

where T is average temperature of T_b and T_t in degrees Fahrenheit.

4.3 Stagnation Point Nusselt Number

After the local heat transfer coefficients have been obtained, the local Nusselt number can be calculated by the following equation.

$$Nu(r)=\frac{h(r)D}{K_{air}} \tag{I.34}$$

Where K_{air}, thermal conductivity of air, varies with temperature. The formula used in this calculation is

$$K_{air}=[1.33+0.41\times(\frac{T}{200})]\times 0.01 \tag{I.35}$$

where T, in degrees Fahrenheit, is an average value from the temperature of the jet and the ambient temperature. Compared with the table of air properties in Kay's [13], Eq.(I.35) has a maximum deviation of 1.3% between 50 °F and 100 °F under one atmosphere of pressure.

From Eq.(I.34), the stagnation point Nusselt number (Nu_0) can be obtained at r being equal to zero. The results of the five jets cooling with the nozzle diameter of 6.35 mm, and 9.53 mm, for various Reynolds numbers and Zn/D, are plotted from Fig.I-4.1 to Fig.I-4.8. Each curve, represented by a cubic polynomial, in the figures is obtained by using a least squares curve-fitting technique (cf., p.534, [5]). The experimental data points are more scattered corresponding to the larger Reynolds number in each figure. The maximum relative deviation of the data points to the regression curves are within ±10%.

The results can be summarized by the following formulas: For $3\leq Zn/D\leq 5$, the stagnation point Nusselt number formula is

$$Nu_{0,D}=1.61Re_{D,U_{0c}}^{0.5}Pr^{0.4}(\frac{Z_n}{D})^{0.14}(\frac{D}{D_0})^{0.4}F(\frac{C_n}{D}) \tag{I.36}$$

where D_0=6.35 mm,

for D=6.35 mm, $F(Cn/D)=0.943(Cn/D)^{0.08}$, the formula values fit the curves within ±5% , except for the maximum 11% at Cn/D=4; for D=9.53 mm, $F(Cn/D)=1.0643(Cn/D)^{-0.09}$, the formula values fit the curves within ±8%.

For Zn/D≥7, the formulas are

$$Nu_{0,D}=0.984Re_{D,U_{0c}}^{0.5755}Pr^{0.4}\left(\frac{D}{D_0}\right)^{0.25}\left(1.155-0.031\frac{Z_n}{D}\right)F\left(\frac{C_n}{D}\right) \qquad (I.37)$$

for D=6.35 mm, $F(Cn/D)=0.946(Cn/D)^{0.07}$, the formula values fit the curves within +10% and -2%; and

$$Nu_{0,D}=2.842Re_{D,U_{0c}}^{0.5755}Pr^{0.4}\left(\frac{Z_n}{D}\right)^{-0.545}\left(\frac{D}{D_0}\right)^{0.25}F\left(\frac{C_n}{D}\right) \qquad (I.38)$$

for D=9.53 mm, $F(Cn/D)=0.953(Cn/D)^{0.07}$, the formula values fit the curves within ±10%.

For the diameter of nozzles at 3.18 mm, the size of the nozzle plate is reduced to a diameter of 58 mm (named "reduced nozzle plate") to avoid the "tunneling problem" (flow constricted to a narrow space between the bottom of the plenum chamber and the heat transfer plate) [11]. The results obtained from the reduced nozzle plate of five jets and nine jets for various Zn/D and Cn/D are plotted from Fig.I-4.9 to Fig.I-4.14. The maximum relative deviation of the data points to the regression curves are within ±10%. The results are summarized by formulas as follows:

For Zn/D≤7,

$$Nu_{0,D}=1.47Re_{D,U_{0c}}^{0.5}Pr^{0.4} \qquad (I.39)$$

the formula values fit the curves of five jets within ±6% and of nine jets within -13% to 5%.

For Zn/D≥7,

$$Nu_{0,D}=4.38Re_{D,U_{0c}}^{0.5}Pr^{0.4}\left(\frac{Z_n}{D}\right)^{-0.568} \tag{I.40}$$

the formula values fit the curves of five jets within ±10% and of nine jets within ±11%, except for the maximum -25% for Cn/D=4.

The exponent of the Prandtl number, 0.4, in the heat transfer correlation shown in the above formulas is used in accordance with the theoretical results by Sibulkin [24].

4.4 Average Nusselt Number

The average Nusselt number is found from the following equation as.

$$\overline{Nu}=\frac{1}{\pi R^2}\int_0^R 2\pi Nu(r)\,rdr \tag{I.41}$$

where Nu(r) denotes a radially dependent function. However, it has only six ring average values evaluated from the temperature measurement of the fourteen calorimeters. In order to get accurate results for the average Nusselt number, a continuous function of Nu(r) is expected. The method developed in this calculation applies the cubic spline method to generate cubic polynomials connecting each ring average Nusselt number in each interval. To achieve a smooth and continuous curve, the slope and the curvature must be the same for the two polynomials which join at a common point. The cubic polynomial for the *ith* interval, which lies between the point (x_i, y_i) and (x_{i+1}, y_{i+1}) is represented as

$$y_i=a_i(x-x_i)^3+b_i(x-x_i)^2+c_i(x-x_i)+d_i \tag{I.42}$$

where a_i, b_i, c_i, d_i are the coefficients of the cubic polynomial. The method of finding those coefficients are explained in Gerald's book "Applied Numerical Analysis" [5].

In this calculation, three additional Nusselt number points are either interpolated or extrapolated from six measured ring average Nusselt number points. The first additional point, between the first ring (center) and the second ring, is obtained by taking two times the Nusselt number of the first ring and then adding the average Nusselt number of the second ring divided by three. The second additional point, between the fifth ring and the sixth ring, is evaluated by taking the average Nusselt number of the fifth ring and then adding two times the average Nusselt number of the sixth ring divided by three. The third additional point, at the edge of the plate, is extrapolated from the straight line formula joining the point of the average Nusselt number of the sixth ring and the "second additional point". Therefore, a total eight cubic polynomials, representing continuous function of Nu(r), are generated between eight intervals from nine points.

If r and dr are replaced by x and dx in Eq.(I.41), then it becomes

$$\overline{Nu}=\frac{2}{R^2}\sum_{i=1}^{8}\int_{x_i}^{x_{i+1}}[a_i(x-x_i)^3+b_i(x-x_i)^2+c_i(x-x_i)+d_i]\,x\,dx \tag{I.43}$$

The integral in Eq.(I.43) can be decomposed and rearranged as

$$\overline{Nu}=\frac{2}{R^2}\sum_{i=1}^{8}[a_i(\frac{1}{5}x_{i+1}^5-\frac{3}{4}x_{i+1}^4x_i+x_{i+1}^3x_i^2-\frac{1}{2}x_{i+1}^2x_i^3+\frac{1}{20}x_i^5)$$
$$+b_i(\frac{1}{4}x_{i+1}^4-\frac{2}{3}x_{i+1}^3x_i+\frac{1}{2}x_{i+1}^2x_i-\frac{1}{12}x_i^4)$$
$$+c_i(\frac{1}{3}x_{i+1}^3-\frac{1}{2}x_{i+1}^2x_i+\frac{1}{6}x_i^3)$$
$$+d_i(\frac{1}{2}x_{i+1}^2-\frac{1}{2}x_i^2)] \tag{I.44}$$

The method introduced above is converted into a computer subroutine (SUB1) attached to the main program listed in appendix A.

The results of five jets cooling by the nozzle diameter of 6.35 mm, and 9.53 mm, for the various Reynolds numbers and Zn/D are plotted from Fig.I-4.15 to Fig.I-4.22. Each curve, represented by a cubic polynomial, in the figures is obtained by using a nonlinear least squares curve-fitting technique. The maximum relative deviation of the data points to the regression curves are within ±10%. The results can be summarized by formulas as follows:

For Zn/D<7 , the average Nusselt number is

$$\overline{Nu_D}=5.084Re_{D,U_{0c}}^{0.7}Pr^{\frac{1}{3}}(\frac{D}{D_{pl}})^{1.226}F(\frac{C_n}{D}) \tag{I.45}$$

where D_{pl} is diameter of the heat transfer plate (154 mm); for D=6.35 mm, $F(Cn/D)=0.846(Cn/D)^{0.08}$, the formula values fit the curves within ±9%; and for D=9.53 mm, $F(Cn/D)=1.012(Cn/D)^{-0.03}$, the formula values fit the curves within ±5%.

For Zn/D≥7, the formulas are

$$\overline{Nu_D}=5.084Re_{D,U_{0c}}^{0.7}Pr^{\frac{1}{3}}(\frac{D}{D_{pl}})^{1.226}F(\frac{C_n}{D}) \tag{I.46}$$

for D=6.35 mm, $F(Cn/D)=1.18(Cn/D)^{-0.08}$, the formula values fit the curves within +3% and -5%; and

$$\overline{Nu_D}=5.084Re_{D,U_{0c}}^{0.7}Pr^{\frac{1}{3}}(\frac{D}{D_{pl}})^{1.226}(1.19-0.027\frac{Z_n}{D})F(\frac{C_n}{D}) \qquad (I.47)$$

for D=9.53 mm, $F(Cn/D)=1.082(Cn/D)^{-0.055}$, the formula values fit the curves within +10% and -5%.

The results of five jets or nine jets cooling from the reduced nozzle plate, with the diameter of nozzles at 3.18 mm, are plotted in Fig.I-4.23 to Fig.I-4.28. The results are summarized into the formulas which cover the whole range of Zn/D (i.e. $3 \le Zn/D \le 15$) as follows. For five jets,

$$\overline{Nu_D}=17.3Re_{D,U_{0c}}^{0.58}Pr^{\frac{1}{3}}(0.858+0.047\frac{Z_n}{D})(\frac{D}{D_{pl}})^{1.278} \qquad (I.48)$$

the formula values fit the curves of Cn/D=3 or 4 within ±20%, but it does not fit well for Cn/D=2.

For nine jets,

$$\overline{Nu_D}=28.16Re_{D,U_{0c}}^{0.58}Pr^{\frac{1}{3}}(0.865+0.044\frac{Z_n}{D})(\frac{D}{D_{pl}})^{1.278} \qquad (I.49)$$

the formula values fit the curves within ±18%. The exponent of the Prandtl number, 1/3, in the heat transfer correlation shown in the above formulas is used in accordance with the theoretical analysis for the heat transfer of turbulent boundary layer on a flat plate at zero incidence (cf., p.299, [22]).

I-5 DISCUSSIONS

5.1 Stagnation Point Nusselt Number

From observing the figures (Fig.I-4.1 to Fig.I-4.8) of stagnation point Nusselt number (Nu_0) vs. Zn/D, each curve has only one peak where the maximum Nusselt number occurs for the corresponding Zn/D. Datta [2] obtained a similar trend that the maximum Nusselt number occurred at Zn/D about seven, for the experiment of single jet cooling, with nozzle diameters greater than or equal to 6.35 mm. Sethi's investigation [23] of fluid dynamic behavior for five impinging air jets, with the diameters of the nozzles at 6.35 mm and 9.53 mm, has indicated that the theoretical dimensionless length of potential core is at Zn/D about six. Kaya [14] investigated five jets cooling, with nozzle diameter of 6.35 mm, and Cn/D ranged at two, three, four. His results reveal that the maximum stagnation point Nusselt number has a tendency to peak out at Zn/D within five to seven. This phenomenon is explained by Hrycak et al. [11] as the combination of turbulence and velocity in the tip of the potential core generated by the optimal mixing effect at the center jet.

In the present experiment, some features of five jets cooling, for the nozzle diameters of 6.35 mm and 9.53 mm, are observed as follows:

(1) The maximum stagnation point Nusselt numbers are found to occur at Zn/D within 4.5 to 6.5. This fact incorporated with Sethi's investigation proves that the maximum heat transfer occurs at the tip of nominal potential core.

(2) For the same nozzle plate, the location of the maximum Nusselt number corresponding to Zn/D will increase with

increasing the Reynolds number. This trend also meets with that of Sethi's investigation which indicates the length of potential core increasing with the Reynolds number (cf., pp.72-73; pp.80-81, [23]).

(3) The exponent of the Reynolds number in heat transfer correlation is 0.5 within the potential core (i.e. $3 \le Zn/D \le 7$), which is supported by Sibulkin's theoretical result [24]. Outside of the potential core (i.e. $7 \le Zn/D \le 15$), the exponent of the Reynolds number in heat transfer correlation is 0.5755. This fact indicates that the turbulent flow has started even at the stagnation point [11].

(4) A weak function of Cn/D in heat transfer correlation is found at the range of Zn/D from three to fifteen. This is shown in Fig.I-5.1 and Fig.I-5.2, which are plotted by scaling from the Reynolds number of 26,000, 35,000, 54,000 (abbreviated as 26k, 35k, 54k in the figures) down to the Reynolds number of 14,000. This fact can be interpreted as that the effects of fluid mixing do not rely strongly on changing the spacing of the nozzles.

(5) Compared with the results of the stagnation point Nusselt number from single jet cooling [2] (shown in Fig.I-5.3 and Fig.I-5.4), the results of five jets cooling (shown from Fig.I-4.1 to Fig.I-4.8) do not increase proportionally with increasing the mass flow rates. For the diameter of 6.35 mm nozzles, the results of single jet cooling are about 10% lower than the results of five jets at Zn/D from three to nine; and then the results are close to each other at Zn/D from nine to fifteen. A similar trend is found for the diameter of 9.53 mm nozzles except Cn/D of two. This fact indicates that the flow pattern

around the stagnation point of both the single jet cooling and the five jets cooling cases are similar to each other.

For the reduced nozzle plate, with five jets and nine jets, the diameter of nozzles at 3.18 mm, the repeatability of the experiment has not been well examined. However, from the results of the limited tests, some features are observed to be different from those with 6.35 mm or 9.53 mm nozzles. They are : (1) The maximum Nusselt number seems to occur at the smaller Zn/D. (2) The exponent of the Reynolds number in heat transfer correlation is 0.5 within the full range of Zn/D. These findings can be interpreted as that the length of potential core is shorter and the mixing effect is weaker for the case with 3.18 mm nozzles.

5.2 Average Nusselt Number

From observing the figures (Fig.I-4.15 to Fig.I-4.28) of average Nusselt number vs. Zn/D, each figure has at least two curves associated with two different Reynolds numbers. Therefore, the relation of the Reynolds number's exponent to the average Nusselt number can be calculated. This relation for multiple jets cooling has been suggested by Gardon and Cobonpue [6] as 0.623, by Martin [19] as 0.67, and by Behbahani and Goldstein [1] as 0.78. According to the theoretical result of heat transfer in turbulent boundary layer on a flat plate at zero incidence (cf., p.299, [22]), the exponent of Reynolds number in heat transfer correlation is 0.8.

The dependence of Zn/D and Cn/D is shown from Fig.I-5.5 to Fig.I-5.6. In order to summarize their effects, the figures are shown by scaling the results from different Reynolds numbers to the nominal Reynolds number of 14,000 (abbreviated as 14k in the figures).

In the present experiment, for five jets, with the nozzle diameters of 6.35 mm and 9.53 mm, some features are observed as follows:

(1) The exponent of the Reynolds number in heat transfer correlation is 0.7 within the full range of Zn/D. This is within the range between the experimental results by the previous mentioned investigators [1,6,19] and the theoretical results in turbulent boundary layer [22].

(2) The Zn/D dependence of average Nusselt number for 6.35 mm nozzles is not noticeable. However, for the nozzles of 9.53 mm, the average Nusselt number curves have a peak at about Zn/D at seven and then start to decrease with Zn/D greater than seven. This reason may be explained in (4) as follows.

(3) The average Nusselt number increases with the increasing of the nozzle diameter. This is due to the increasing of mass flow rate of air.

(4) The dependence of Cn/D in heat transfer correlation is weak. However, for the nozzle diameter of 6.35 mm and Zn/D from three to seven, the average Nusselt number seems to increase with the increasing of Cn/D. This phenomenon may be caused by the stronger mixing effect created by the peripheral nozzles at the larger spacing of nozzles. For the values of Zn/D from seven to fifteen, the average Nusselt number seems to decrease with the increasing of Cn/D. The reason may be the "limited size of the heat transfer plate" which is unable to take the benefit of heat transfer by the entrainment effect of the peripheral nozzles at the larger Cn distance. For the nozzle

diameter of 9.53 mm, the average Nusselt number decreases with the increasing of Cn/D values even at Zn/D from three to seven. This may be caused by the distance of Cn for the nozzle plate with diameter of 9.53 mm nozzles is larger than that for the nozzle plate with diameter of 6.35 mm nozzles at the same Cn/D values. The reason of "the limit size of heat transfer plate" seems to apply.

(5) Compared with the results of single jet cooling [2] (shown in Fig.I-5.7 and Fig.I-5.8), the results of five jets cooling (shown from Fig.I-4.15 to Fig.I-4.22) increase only about 20% to 50%. Therefore, the method of superposition from the results of single jet cooling is not directly applicable.

For the reduced nozzle plate, with five jets and nine jets respectively, and the nozzle diameter of 3.18 mm, the exponent of the Reynolds number in heat transfer correlation is 0.58 which is less than that of the five jets with the nozzle diameters of 6.35 mm or 9.53 mm. This indicates the turbulent effects are less strong for this small diameter nozzle than that for the other two large diameter nozzles.

I-6 *CONCLUSIONS*

6.1 Stagnation Point Nusselt Number

The theoretical heat transfer analysis at the stagnation point in the stagnation flow shown in Eq.(I.27) can only be fit closely to the experimental results of five air jets. However, the modified theoretical equation, Eq.(I.28), combined with Sethi's experimental results shows an improvement; but it is still below the results of this investigation by about 28% to 40%. The experimental results of single jet cooling do not increase proportionally (i.e. as the effects of superposition) with the results of five jets. The increments of five jets cooling are about 10%, comparing with single jet cooling, for the Zn/D from three to nine. Beyond the Zn/D of nine, the results are close to each other.

The exponent of the Reynolds number, 0.5, in heat transfer correlation derived by the theoretical analysis fits well with the experimental results within the potential core of the jets. Beyond the distance of the potential core, the exponent of the Reynolds number becomes 0.5755 for the nozzle diameters of 6.35 mm and 9.53 mm, but remains at 0.5 for the reduced nozzle plate with the nozzle diameter of 3.18 mm.

The experimental results show that the Zn/D dependence is very noticeable, but Cn/D dependence is not very noticeable. Higher values of Nusselt number are observed for Zn/D within the potential core than that for Zn/D beyond the potential core. The maximum Nusselt numbers occur at Zn/D within 4.5 to 6.5 for the nozzle diameters of 6.35 mm or 9.53 mm. The stagnation point Nusselt numbers are always larger than the average Nusselt number for the same experimental set-up. The empirical formulas in terms of Reynolds number, Prandtl number, Zn/D, Cn/D and dimensionless nozzle ratio D/D_0 are obtained.

6.2 Average Nusselt Number

For the average Nusselt number, this investigation shows that the exponent of the Reynolds number in heat transfer correlation is 0.7, with the nozzle diameters of 6.35 mm and 9.53 mm. This result is in good agreement with the analytical result, 0.8, for the heat transfer in a turbulent boundary layer on a flat plate. However, an exponent of the Reynolds number of 0.58, for the reduced nozzle plate with the nozzle diameter of 3.18 mm, is obtained from this investigation.

The experimental results show that the Cn/D dependence is weak in the empirical equations which are expressed in terms of Reynolds number, Prandtl number, Zn/D, Cn/D and D/D_{p1}. The results of five jets cooling are increased about 20% to 50% when they are compared with the results of the single jet cooling.

6.3 Recommendations

(1) Larger diameter of the nozzles, say diameter of 12.7 mm, may be worth testing to see if the trends of heat transfer are consistent with the fact found in this experiment.

(2) The exponent of the Prandtl number can be examined by changing to a different heat transfer fluid which has not been done in this experiment.

(3) Heat transfer tests under more jets are worth trying.

PART II FREE CONVECTION OF A FINITE SIZE DOWNWARD-FACING HEATED HORIZONTAL ROUND PLATE

II-1 INTRODUCTION

1.1 General Introduction and Research Objective

The free convection is caused by the density difference of the transport medium in the gravitational field. In this case, the density of the heated medium under the plate is smaller than that of the surrounding medium. Therefore, the heated fluid would flow from the central region toward the edge of the plate along the surface and induce unheated fluid flowing from the deep bottom to the central region, also known as the stagnation region. The flow pattern of this type is shown in Fig.II.1.1.

It seems that this problem has received less attention in the natural convection heat transfer field [44]. However, its applications still can be found in industries such as in nuclear power generation [52] and glass tempering processes [47]. In the theoretical point of view, it is always expected that an analytical solution for this physical phenomenon would be found. The difficult points appear to be the finite size of the plate making it difficult to determine the thickness of the boundary layer at the edge of the plate, and that the governing equations are strongly-coupled.

In this study, a mathematical model is suggested as valid for the laminar flow, of single plume type, at steady state, around the central region of the plate, and for the moderate range of the Prandtl numbers of fluids (i.e. $0.7 \le Pr \le 5$). The velocity and the temperature distributions are obtained by solving the Navier-Stokes and the energy equations with the thermal boundary conditions both prescribed at approximately constant surface temperature and constant surface flux beneath the center of the plate. Heat transfer formulas for the vicinity of the stagnation point and the approximate average heat transfer formulas are presented.

1.2 Previous Studies

The investigation of heat transfer for a downward-facing heated plate for laminar flow started experimentally by Saunders, Fishenden and Mansion [51] in 1935. They tested a rectangular plate heated in air. In the same year, Weise [58] did a similar test of a square plate heated on both sides. From their investigation, the heat transfer correlation was shown as

$$Nu = cRa^{\frac{1}{4}}$$

A theoretical approach by an integral method based on the boundary layer approximation was introduced by Levy [48], and Wagner [56]. In 1969, Singh et al. [54] published both theoretical and experimental results with the Prandtl number being equal to 0.7. In their theoretical works, two-dimensional flow and an integral method with boundary layer approximation were used to deal with infinite strip, circular plate, and square plate. The boundary layer thickness at the edge of the plate was assumed to be zero. The heat transfer correlation was suggested as

$$Nu=cRa^{\frac{1}{5}}$$

Their experimental results confirmed the 1/5 power correlation, but the experimental results were higher than analytical ones.

Clifton et al. [33] introduced a method, adopted from hydraulics of an open channel, to estimate a critical boundary layer thickness at the edge of the plate in an integral analysis using a two-dimensional flow. But their experimental results show a 1/4 power of the Rayleigh number different from his analytical formula in heat transfer expression.

Chen [31] introduced a differential formulation of two-dimensional flow in Cartesian coordinates. His theoretical analysis supported the 1/4 power of the Rayleigh number in heat transfer correlation.

Birkebak et al. [28] reported experimental results for a square plate in water. Their results had good agreement with Singh's [54] analytical results.

Aihara et al. [26] concluded from their experimental work, for rectangular plates in air, that the similarity solution could not be obtained at the edge of the plate, but may be obtained in the stagnation region. Their heat transfer correlation result was similar to Fujii and Imura's [37] experimental result for a square plate in air. The 1/5 power of the Rayleigh number in heat transfer correlation was shown to apply.

Fujii and Honda et al. [38] did a theoretical analysis based on an integral method for a wide range of the Prandtl numbers of the fluids (i.e. $0.001 \leq Pr < \infty$), for an infinite strip, square plate, and circular plate. The 1/5 power of the Rayleigh number in the heat transfer formula was suggested.

Restrepo and Glicksman [50] made a test of heat transfer rates with different extension at the edge of plate. Their reports showed the average Nusselt number was highest for the plate with vertical heated extension, higher for the plate with vertical cooled extension, and lowest for the plate with horizontal adiabatic extension. The 1/5 power of the Rayleigh number in heat transfer correlations were observed in all cases.

Faw and Dullforce [34, 35] used holographic interferometry measurement to investigate the heat transfer rate and temperature distribution for square plate and circular plate. They adopted Singh's [54] method to analyze their experimental data. The average Nusselt number expression for circular plate had very good agreement with Singh's result.

Hatfield et al. [43] summarized their experimental data into a new type of heat transfer correlation formula which included edge and aspect ratios for different test plates.

Goldstein et al. [39] formulated the problem in the differential form and solved it by a finite difference method. Two-dimensional flow under an infinite strip was studied.

Schulenberg [52, 53] studied this problem theoretically by a differential formulation based on simplified governing equations. Two thermal boundary conditions, constant surface temperature and surface flux, were analyzed for both very large Prandtl number and very small Prandtl number fluids. His analysis covered both infinite strips and circular disks. The average heat transfer correlations were suggested at 1/5 power of the Rayleigh number for the constant surface temperature case and at 1/6 power of the modified Rayleigh number for the constant flux case, even though his analysis was based on the stagnation region.

Gryzagoridis [40] suggested, from his experimental data, that the formula of heat transfer correlation should not be dependent only on the Rayleigh number, but also on the temperature difference between the surface and the ambient region.

Chang et al. [30] published a theoretical analysis for a rectangular plate in air. Their results supported the 1/4 power of the Rayleigh number in the heat transfer correlation.

Hrycak [44, 45] published an analytical results for circular plates for fluids at moderate Prandtl numbers. A new free constant was introduced in heat transfer correlation to match experimental analysis; the 1/4 power of the Rayleigh number in heat transfer formula was found to apply.

The results of the past studies are listed in Table II-1.1. The characteristic length of the Nusselt number and the Rayleigh number are the side length of a square plate, the width of a rectangular plate, the width of an infinite strip, or the radius of a circular plate respectively. Those formulas, based on the half side length, in the original documents, are converted into full side length here. An asterisk, * , is used to denote the converted formulas.

II-2 MATHEMATICAL MODEL OF DIFFERENTIAL FORMULATION

The appropriate governing equations for three-dimensional, axisymmetric, steady state, laminar flow are still the continuity, the Navier-Stokes, and the energy equations. However, in the case of natural convection, the density cannot be treated as constant, because density variation combined with gravitational force is the primary cause of fluid motion. If density is treated as a function of temperature in each direction of the momentum equation, the governing equations would be more complicated. Therefore, the Boussinesq approximation is used to treat density as constant in all terms except the buoyancy term in the governing equations [27, 41]. Following these simplifications, the governing equations for natural convection in cylindrical coordinates with the gravitational vector parallel to the z-axis are usually written as follows [41].

$$\frac{\partial u}{\partial r}+\frac{u}{r}+\frac{\partial w}{\partial z}=0 \qquad \text{(II.1)}$$

$$u\frac{\partial u}{\partial r}+w\frac{\partial u}{\partial z}=-\frac{1}{\rho}\frac{\partial p}{\partial r}+\nu\left(\frac{\partial^2 u}{\partial r^2}+\frac{1}{r}\frac{\partial u}{\partial r}+\frac{\partial^2 u}{\partial z^2}-\frac{u}{r^2}\right) \qquad \text{(II.2)}$$

$$u\frac{\partial w}{\partial r}+w\frac{\partial w}{\partial z}=-\frac{1}{\rho}\frac{\partial p}{\partial z}-g\beta(T-T_\infty)+\nu\left(\frac{\partial^2 w}{\partial r^2}+\frac{1}{r}\frac{\partial w}{\partial r}+\frac{\partial^2 w}{\partial z^2}\right) \qquad \text{(II.3)}$$

$$u\frac{\partial T}{\partial r}+w\frac{\partial T}{\partial z}=\alpha\left(\frac{\partial^2 T}{\partial r^2}+\frac{1}{r}\frac{\partial T}{\partial r}+\frac{\partial^2 T}{\partial z^2}\right)+\frac{\nu}{C_p}\Phi \qquad \text{(II.4)}$$

$$\Phi=2\left(\frac{\partial u}{\partial r}\right)^2+2\left(\frac{u}{r}\right)^2+2\left(\frac{\partial w}{\partial z}\right)^2+\left(\frac{\partial u}{\partial z}+\frac{\partial w}{\partial r}\right)^2 \qquad \text{(II.5)}$$

The momentum equation of the angular coordinate is neglected due to the axisymmetric flow. The contribution of heat transfer is mainly dependent on the fluid flowing parallel to the surface of the plate and the dominant term in the z-direction momentum equation is the pressure differential term which is related to buoyant and gravitational forces. Therefore, the z-direction momentum equation, Eq.(II.3), can be simplified as

$$0=-\frac{1}{\rho}\frac{\partial p}{\partial z}-g\beta\,(T-T_{\infty}) \qquad \text{(II.6)}$$

Integrate Eq.(II.6) and assume the pressure would not vary beyond Z_0 which is the vertical distance away from the plate. The pressure near the surface of the central region of the plate (P_s) can be approximately expressed as

$$P_s \approx P_{\infty}+\rho g\beta\,(T-T_{\infty})\,Z_0 \qquad \text{(II.7)}$$

where Z_0 also represents the place where the temperature is equal to the ambient temperature (T_{∞}). Z_0 may be assumed to be proportional to the radius of the plate as

$$Z_0 = m\ R \qquad \text{(II.8)}$$

where m denotes a proportional constant, to be determined by experiment. In order to transform the partial differential equations into O.D.E.s, the unknown temperature distribution may be assumed in certain forms which will be discussed in the following sections.

2.1 One Assumed Function in Temperature Distribution

2.1.1 Prescribed Surface Temperature Case

The temperature distribution should be a dependent variable of two independent coordinates, r and z. Therefore, an assumption of separation of variable can be applied. From observation of the streamlines and isothermal lines beneath the downward-facing heated plate [26, 28], the temperature distribution underneath the plate may be assumed to be of a parabolic shape, such as

$$\frac{T-T_{\infty}}{T_{wc}-T_{\infty}}=\theta(\eta)\,(1-\frac{r^2}{2R^2}) \qquad \text{(II.9)}$$

where T_{wc} denotes the wall temperature at the center of the plate. The η, the similarity variable or vertical dimensionless coordinate, can be assumed as

$$\eta=\sqrt{\frac{a}{\nu}}\,z \tag{II.10}$$

where " a " is a free constant, to be determined by scaling of the momentum equation. Let's choose the Stokes stream function, Ψ, in three-dimensional and axisymmetric flow to be

$$\Psi=\sqrt{a\nu}\,r^2 f(\eta) \tag{II.11}$$

Hence, the velocity components can be expressed as [58].

$$u=\frac{1}{r}\frac{\partial\Psi}{\partial z}=arf'(\eta) \tag{II.12}$$

$$w=-\frac{1}{r}\frac{\partial\Psi}{\partial r}=-2\sqrt{a\nu}\,f(\eta) \tag{II.13}$$

where u, w denote the velocity components in radial and vertical down directions respectively; the prime " ' " denotes the differentiation with respect to η. The partial derivative terms in the momentum equations can be derived from Eq.(II.12), and Eq.(II.13). They are

$$\begin{aligned}&\frac{\partial u}{\partial r}=af'(\eta)\,;\ \frac{\partial^2 u}{\partial r^2}=0\,;\ \frac{\partial u}{\partial z}=a\sqrt{\frac{a}{\nu}}\,rf''(\eta)\,;\ \frac{\partial^2 u}{\partial z^2}=\frac{a^2}{\nu}rf'''(\eta)\,;\\ &\frac{\partial w}{\partial r}=0\,;\ \frac{\partial^2 w}{\partial r^2}=0\,;\ \frac{\partial w}{\partial z}=-2af'(\eta)\,;\ \frac{\partial^2 w}{\partial z^2}=-2a\sqrt{\frac{a}{\nu}}\,f''(\eta)\end{aligned} \tag{II.14}$$

With relations in Eq.(II.12), (II.13), and (II.14), the continuity equation, Eq.(II.1), is satisfied. From Eq.(II.7), (II.9), the pressure derivative with respect to r is

$$-\frac{1}{\rho}\frac{\partial p}{\partial r}=g\beta\,(T_{wc}-T_\infty)\,\theta(\eta)\,\frac{r}{R^2}Z_0 \tag{II.15}$$

Substituting Eq.(II.8) and multiplying ($R^2\nu^2$) in both the numerator and the denominator of Eq.(II.15), it becomes

$$-\frac{1}{\rho}\frac{\partial p}{\partial r}=r\frac{mGr_R\nu^2}{R^4}\theta(\eta) \tag{II.16}$$

Set $a^2=(m\ Gr_R\ \nu^2)/R^4$, hence

$$\sqrt{\frac{a}{\nu}}=\frac{(mGr_R)^{\frac{1}{4}}}{R} \tag{II.17}$$

$$-\frac{1}{\rho}\frac{\partial p}{\partial r}=a^2 r\theta(\eta) \tag{II.18}$$

where Gr_R is the Grashof number based on the characteristic length, R, the radius of the plate. With the relations in Eq.(II.14), (II.18), the momentum equation in radial coordinate (i.e. Eq.(II.2)) can be transformed into

$$f'''(\eta)+2f(\eta)f''(\eta)-f'(\eta)^2+\theta(\eta)=0 \tag{II.19}$$

With the temperature distribution in Eq.(II.9), the partial derivative terms in energy equation, Eq.(II.4), are derived as

$$\begin{aligned}
\frac{\partial T}{\partial r}&=-(T_{wc}-T_\infty)\theta(\eta)\frac{r}{R^2}\\
\frac{\partial^2 T}{\partial r^2}&=-(T_{wc}-T_\infty)\theta(\eta)\frac{1}{R^2}\\
\frac{\partial T}{\partial z}&=(T_{wc}-T_\infty)(1-\frac{r^2}{2R^2})\theta'(\eta)\sqrt{\frac{a}{\nu}}\\
\frac{\partial^2 T}{\partial z^2}&=(T_{wc}-T_\infty)(1-\frac{r^2}{2R^2})\theta''(\eta)\frac{a}{\nu}
\end{aligned} \tag{II.20}$$

From Eq.(II.12), (II.13) and (II.20), the energy equation, Eq.(II.4), and dissipation function, Eq.(II.5), are then transformed into

$$\begin{aligned}
&-arf'(\eta)\theta(\eta)\frac{r}{R^2}-2\sqrt{a\nu}f(\eta)\theta'(\eta)\sqrt{\frac{a}{\nu}}(1-\frac{r^2}{2R^2})\\
&=\alpha[-\frac{2}{R^2}\theta(\eta)+(1-\frac{r^2}{2R^2})\theta''(\eta)\frac{a}{\nu}]+\frac{\nu}{C_p(T_{wc}-T_\infty)}\\
&\qquad[12a^2f'(\eta)^2+r^2\frac{a^3}{\nu}f''(\eta)^2]
\end{aligned} \tag{II.21}$$

The coefficients of the r^0 and r^2 terms in the right hand side of Eq.(II.21) should be equal to those in the left hand side. Therefore, two equations would be derived from the energy equation. However, around the stagnation point (i.e. r close to zero), the r^2 terms can be neglected. Hence, collecting r^0 terms leads to

$$-2af(\eta)\theta'(\eta)=\alpha[-\frac{2}{R^2}\theta(\eta)+\theta''(\eta)\frac{a}{\nu}]+\frac{\nu}{C_p(T_{wc}-T_\infty)}[12a^2f'(\eta)^2] \qquad (II.22)$$

Rearranging Eq.(II.22), it becomes

$$\theta''(\eta)+2\,Pr\,f(\eta)\theta'(\eta)-\frac{2}{\sqrt{mGr_R}}\theta(\eta)+12\,Pr\,Ec\,f'(\eta)^2=0 \qquad (II.23)$$

where Pr denotes the Prandtl number, a fluid property; Gr denotes the Grashof number, a parameter describing the ratio of buoyancy to viscous force; and Ec denotes the Eckert number. The magnitude of the product Pr Ec is a parameter of the importance in viscous dissipation; its value is small in most natural convection cases for fluids with the moderate Prandtl numbers (i.e. $0.7<Pr<5$) [27]. In this present geometry, for instance, the radius can be made to vary within the range from 15 mm to 80 mm and the temperature difference between the hot surface and the surrounding fluid is approximately 80 °C. The order of magnitude for the Grashof number is about 10^4 to 10^6. Hence, the last two terms of Eq.(II.23) can be neglected, becoming

$$\theta''(\eta)+2Prf(\eta)\theta'(\eta)=0 \qquad (II.24)$$

Looking at Eq.(II.19) and (II.24), one can realize they are strongly coupled equations, which means both function $f(\eta)$ and $\theta(\eta)$ are involved in the momentum and energy equations. Substituting Eq.(II.19) into Eq.(II.24), a fifth order, nonlinear, ordinary differential equation can be obtained as

$$f^{(5)}(\eta)+2(1+Pr)f(\eta)f^{(4)}(\eta)+2f'(\eta)f'''(\eta)+4Prf(\eta)^2f'''(\eta)=0 \qquad (II.25)$$

The boundary conditions are:

(i) at $\eta = 0$: $w = 0$, $u = 0$, T = surface temperature,

(ii) at $\eta = \eta_\infty$: w = finite constant, $u = 0$, $T = T_\infty$.

With relations in Eq.(II.12), (II.13), and (II.9), the boundary conditions for $f(\eta)$ and $\theta(\eta)$ are

(i) at $\eta = 0$: $f(0) = 0$, $f'(0) = 0$, $\theta(0) = 1$,

(ii) at $\eta = \eta_\infty$: $f(\eta_\infty) = \text{constant}$, $f'(\eta_\infty) = 0$, $\theta(\eta_\infty) = 0$.

The boundary conditions for $\theta(\eta)$ can be converted into $f(\eta)$ associated conditions by using Eq.(II.19). Hence, $\theta(0)=1$ is equivalent to $f'''(0)=-1$, and $\theta(\eta_\infty)=0$ is equivalent to $f'''(\eta_\infty)=0$.

In order to solve Eq.(II.25), it may be decomposed into five coupled first-order O.D.E.s. Let's set $U_1=f(\eta)$, $U_2=f'(\eta)$, $U_3=f''(\eta)$, $U_4=f'''(\eta)$, $U_5=f^{(4)}(\eta)$, then Eq.(II.25) becomes

$$\begin{aligned} U_1' &= U_2 \\ U_2' &= U_3 \\ U_3' &= U_4 \\ U_4' &= U_5 \\ U_5' &= -2(1+Pr)U_1U_5 - 2U_2U_4 - 4PrU_1^2U_4 \end{aligned} \tag{II.26}$$

The boundary conditions for Eq.(II.26) are

(i) $U_1(0) = 0$, $U_1(\eta_\infty) = \text{constant}$,

(ii) $U_2(0) = 0$, $U_2(\eta_\infty) = 0$,

(iii) $U_3(0) = \text{unknown}$, $U_3(\eta_\infty) = 0$,

(iv) $U_4(0) = -1$, $U_4(\eta_\infty) = 0$,

(v) $U_5(0) = \text{unknown}$, $U_5(\eta_\infty) = 0$.

2.1.2 Prescribed Constant Surface Flux Case

In this case, the thermal boundary condition, the heat flux of the plate, is prescribed to be constant. The temperature distribution is assumed as

$$T - T_\infty = \frac{q_w R}{K(mGr_R^*)^{\frac{1}{5}}}\theta(\eta)\left(1-\frac{r^2}{2R^2}\right) \tag{II.27}$$

where q_w denotes heat flux at the wall of the plate; $Gr^*_R=(g\beta q_w R^4)/(K\nu^2)$ denotes the modified Grashof number. The procedures of mathematical formulation are the same as the prescribed surface temperature case in section II-2.1.1. Use the same Stokes stream function as Eq.(II.11), and similarity variable as in

Eq.(II.10), but the free constant " a ", under a new scaling condition, is modified to

$$a=\frac{\nu}{R^2}(mGr_R^*)^{\frac{2}{5}}\ ,\ and$$
$$\sqrt{\frac{a}{\nu}}=\frac{(mGr_R^*)^{\frac{1}{5}}}{R} \qquad \text{(II.28)}$$

The governing equations can then be transformed into the same forms as Eq.(II.19), and (II.24). Therefore, Eq.(II.25) and (II.26), valid around the stagnation point, are the same for this case. However, the thermal boundary condition would be changed as shown in the following:

$$\begin{aligned}&q_{wc}\ (\textit{heat flux in the plate center})\\&=-K\frac{\partial T}{\partial z}\bigg|_{z=0}=-K\frac{\partial T}{\partial \eta}\bigg|_{\eta=0}\frac{\partial \eta}{\partial z}\\&=-K\frac{q_w R}{K(mGr_R^*)^{1/5}}\theta'(0)\sqrt{\frac{a}{\nu}}\\&=-\theta'(0)\,q_w\end{aligned} \qquad \text{(II.29)}$$

Hence, the boundary conditions are

(i) at $\eta = 0$: $f(0) = 0$, $f'(0) = 0$, $\theta'(0) = -1$,

(ii) at $\eta = \eta_\infty$: $f(\eta_\infty)$ = constant, $f'(\eta_\infty) = 0$, $\theta'(\eta_\infty) = 0$.

Taking the derivative of Eq.(II.19) with respect to η, and substituting $\theta'(0)=-1$ into it, then $f^{(4)}(0)=-\theta'(0)=1$. Changing the boundary conditions from f(0) and its consecutive derivatives to $U_1(0)$, $U_2(0)$, $U_3(0)$, $U_4(0)$, and $U_5(0)$, the conditions corresponding to the governing Eq.(II.26) become

(i) $U_1(0) = 0$, $U_1(\eta_\infty)$ = constant,

(ii) $U_2(0) = 0$, $U_2(\eta_\infty) = 0$,

(iii) $U_3(0)$ = unknown, $U_3(\eta_\infty) = 0$,

(iv) $U_4(0)$ = unknown, $U_4(\eta_\infty) = 0$,

(v) $U_5(0) = 1$, $U_5(\eta_\infty) = 0$.

2.2 Two Assumed Functions in Temperature Distribution

2.2.1 Prescribed Surface Temperature Case

In previous sections, the terms with r^2 in energy equation are neglected by assuming r close to zero, which is interpreted as being concerned with the heat transfer in the vicinity of the stagnation point only. In this section, the solutions attempt to include the previous dropped terms. This is done by using a temperature distribution expressed as follows.

$$\frac{T-T_\infty}{T_{wc}-T_\infty}=\theta_1(\eta)-\frac{r^2}{2R^2}\theta_2(\eta) \tag{II.30}$$

Using the same transformation method, introduced in section II.2.1.1, the momentum equations are transformed into

$$f'''(\eta)+2f(\eta)f''(\eta)-f'(\eta)^2+\theta_2(\eta)=0 \tag{II.31}$$

Two equations, one from the coefficients of r^0 terms, the other from the coefficients of the r^2 terms, are obtained from the transformation of the energy equation. They are

$$\theta_1''(\eta)+2Prf(\eta)\theta_1'(\eta)=0 \tag{II.32}$$

$$\theta_2''(\eta)-2Pr[\theta_2(\eta)f'(\eta)-\theta_2'(\eta)f(\eta)]=0 \tag{II.33}$$

Eq.(II.31) and (II.33) can be combined as follows.

$$\begin{aligned} &f^{(5)}(\eta)+2(1+Pr)f(\eta)f^{(4)}(\eta)+2(1-Pr)f'(\eta)f'''(\eta) \\ &-4Prf(\eta)f'(\eta)f''(\eta)+2Prf'(\eta)^3+4Prf(\eta)^2f'''(\eta)=0 \end{aligned} \tag{II.34}$$

The boundary conditions are
(i) at $\eta = 0$: $f(0) = 0$, $f'(0) = 0$, $\theta_1(0) = 1$, $0 \le \theta_2(0) \le 1$,
(ii) at $\eta=\eta_\infty$: $f(\eta_\infty)$=constant, $f'(\eta_\infty) = 0$, $\theta_1(\eta_\infty) = 0$, $\theta_2(\eta_\infty) = 0$.

The values of $\theta_2(0)$ vary from zero to one, representing a constant wall temperature at $\theta_2(0)=0$ and the different shapes of parabolic wall temperature up to $\theta_2(0)=1$. At $\theta_2(0)=1$, the case is similar to that discussed in section II.2.1.1, but the terms of the energy equation are better incorporated than the previous case. Let's set $U_1=f(\eta)$, $U_2=f'(\eta)$, $U_3=f''(\eta)$, $U_4=f'''(\eta)$, $U_5=f^{(4)}(\eta)$, then Eq.(II.34) becomes

$$\begin{aligned} U_1' &= U_2 \\ U_2' &= U_3 \\ U_3' &= U_4 \\ U_4' &= U_5 \\ U_5' &= -2(1+Pr)U_1U_5 - 2(1-Pr)U_2U_4 \\ &\quad + 4PrU_1U_2U_3 - 2PrU_2^3 - 4PrU_1^2U_4 \end{aligned} \tag{II.35}$$

The corresponding boundary conditions for Eq.(II.35) are

(i) $U_1(0) = 0$, $U_1(\eta_\infty) = \text{constant}$,

(ii) $U_2(0) = 0$, $U_2(\eta_\infty) = 0$,

(iii) $U_3(0) = \text{unknown}$, $U_3(\eta_\infty) = 0$,

(iv) $0 \le U_4(0) \le -1$, $U_4(\eta_\infty) = 0$,

(v) $U_5(0) = \text{unknown}$, $U_5(\eta_\infty) = 0$.

After the solution of $f(\eta)$ satisfying the above boundary conditions is determined, Eq.(II.32) can be solved for $\theta_1(\eta)$. Eq.(II.32) is identical with Eq.(I.16) in Part I. Therefore, the solution can be expressed as

$$\theta_1(\eta) = 1 - \frac{\int_0^\eta e^{-2Pr\int_0^t f(s)\,ds}\,dt}{\int_0^\infty e^{-2Pr\int_0^\eta f(s)\,ds}\,d\eta} \tag{II.36}$$

and then

$$\theta_1'(0) = -\frac{1}{\int_0^\infty e^{-2Pr\int_0^\eta f(s)\,ds}\,d\eta} \tag{II.37}$$

II - 3 NUMERICAL SOLUTION

3.1 Numerical Calculation Scheme

The most common method used for solving sets of coupled first-order O.D.E.s like Eq.(II.26), or (II.35) is the Runge-Kutta method. The method applied in this calculation, having truncation error of step size to the order of four, is commonly known as the fourth-order Runge-Kutta method. Its derivation, from series expansion, is shown in "Introduction to Numerical Analysis" [36]. The algorithm of this method is adopted from Burden's book "Numerical Analysis" [29].

In order to start the procedure of calculation, five initial conditions should be given. But in each of the boundary conditions, two initial conditions at $\eta=0$, besides the three conditions given, must be guessed to satisfy the boundary conditions at η_∞. If not satisfied, a criterion is needed to adjust the initial guess to improve the agreement in successive iterations. This method of adjusting guessed initial values to satisfy the boundary conditions at another end is known as the shooting method [29]. The criterion used in this calculation to improve the initial guess in successive iteration is Newton's method [27]. Taking Eq.(II.26) and its boundary conditions as an example, the shooting method is briefly explained as follows:

An error (e) is defined as a selected function value at $\eta=\eta_\infty$, (i.e. $U_1(\eta_\infty)$ or $U_2(\eta_\infty)\cdots U_5(\eta_\infty)$), generated by arbitrary initial values. Therefore, it is obvious that the error (e) is a function of the guessed initial values, g. A series expansion of e(g) from the first guess gives

$$e(g) \approx e_1 + \left(\frac{\partial e}{\partial g}\right)_1 \Delta g \tag{II.38}$$

where Δg denotes the difference between the first guess and the following guess. By this algorithm, the error e(g) is getting close to zero during successive iteration. Therefore, Eq.(II.38) can be solved for Δg by Newton's method

$$\Delta g = \Delta g - \frac{e_1 + \left(\frac{\partial e}{\partial g}\right)_1 \Delta g}{\left(\frac{\partial e}{\partial g}\right)_1} = -e_1 \left(\frac{\partial g}{\partial e}\right)_1 \tag{II.39}$$

The improved guess can be expressed with the above increment as

$$g = g_1 + \Delta g \tag{II.40}$$

The FORTRAN program used to solve Eq.(II.26) along with its boundary conditions, is listed in appendix B. In the program, the error e(g) is defined as

$$\mathrm{ERR} = \mathrm{U2R} - \mathrm{GIVE} \tag{II.41}$$

where U2R represents the value of $f'(\eta_\infty)$, and "GIVE" represents the required boundary condition. The U2R in Eq.(II.41) may be replaced by U3R, U4R, etc.. The algorithm of Eq.(II.39) and (II.40) are written in the FORTRAN program as

$$\begin{aligned} DU3I &= -\frac{ERR}{(ERR-ERR1)*(U3I-U3I1)} \\ DU5I &= -\frac{ERR}{(ERR-ERR1)*(U5I-U5I1)} \end{aligned} \tag{II.42}$$

and

$$\begin{aligned} \mathrm{U3I} &= \mathrm{U3I} + \mathrm{DU3I} \\ \mathrm{U5I} &= \mathrm{U5I} + \mathrm{DU5I} \end{aligned} \tag{II.43}$$

where U3I, U5I represent the guessed initial values of $U_3(0)$ and $U_5(0)$ respectively; U3I1, U5I1 denote the preceding initial values; and ERR1 is their corresponding error value. The iteration can be set to stop at the convergence criterion

$$|ERR| \leq ESP = 10^{-5} \tag{II.44}$$

For the prescribed heat flux boundary condition case, $U_3(0)$ and $U_4(0)$ are the initial values to be determined by the shooting method. Therefore, DU5I, U5I, U5I1 in Eq.(II.42), (II.43) should be changed into DU4I, U4I, U4I1, respectively, in the computer program. It should be mentioned that the FUNCTION SUBROUTINE "E" of FORTRAN listed in appendix B is subject to change for the corresponding differential equations to be solved.

In numerical computation, a proper step size $\Delta\eta$ and an appropriate η_∞ value must be determined, usually by a trial-and-error approach along with the shooting method. Try to use a small value of η_∞ (say, η_∞=5 or smaller) and a comparatively large step size (say, $\Delta\eta$=0.1 or larger) at the beginning. After a trend for the solution is observed, then successively increase η_∞ or reduce step size, if it is necessary, until the boundary conditions along with their respective smooth conditions at $\eta=\eta_\infty$ are satisfied within the range of specified tolerance. The tolerance, ε, is set equal to the order of magnitude at 10^{-3} in this calculation. The formula for this criterion is expressed as

$$\sqrt{f^{I}(\eta)^2+f^{II}(\eta)^2+f^{III}(\eta)^2+f^{(4)}(\eta)^2} \approx \varepsilon \tag{II.45}$$

After η_∞ is determined, a check of the effect of the step size, $\Delta\eta$ on the specified initial values, determined by the shooting scheme, should be made. The procedure is followed by reducing the previous step size by one half until the absolute error between previous and consequent solutions is less than 10^{-4}. Followed by these procedures, the numerical results in this dissertation are calculated at the step size $\Delta\eta=0.01$.

In the case of two assumed functions in the temperature distribution, an additional equation for $\theta_1(\eta)$, Eq.(II.36), should be integrated numerically. The numerical integration algorithm used in this computation is based on the trapezoidal and Simpson's rules [29], which are written into a FORTRAN program listed in appendix C. The step size for integration is adjustable by user to match with that of function $f(\eta)$.

The Convergent Technology's mini computer system is used for numerical computation. The obtained results are checked by a VAX 8800 system along with the Runge-Kutta method in IMSL mathematical software. The maximum deviation of the results obtained from the two computer systems is within 10^{-6}.

The more recent methods for determining guessed initial values are worth referring to. They are the modified Newton-Raphson method [32] and the Nachtsheim-Swigert method [49].

3.2 Heat Transfer Formulas and Numerical Results

3.2.1 One Assumed Function and Prescribed Surface Temperature Case

The heat transfer formula is commonly expressed in relation with the Nusselt number and the Rayleigh number. In this case, the temperature distribution is assumed in Eq.(II.9). By the Fourier law of conduction, the heat flux can be derived as

$$\begin{aligned} q_w &= -K\frac{\partial T}{\partial z}\bigg|_{z=0} = -K\frac{\partial T}{\partial \eta}\bigg|_{\eta=0}\frac{\partial \eta}{\partial z} \\ &= -K(T_{wc}-T_\infty)\left(1-\frac{r^2}{2R^2}\right)\theta'(0)\,\frac{(mGr_R)^{\frac{1}{4}}}{R} \end{aligned} \qquad \text{(II.46)}$$

If r is small, around the stagnation region, then

$$q_{wc}=-K(T_{wc}-T_{\infty})\theta'(0)\,\frac{(mGr_R)^{\frac{1}{4}}}{R} \qquad \text{(II.47)}$$

The Nusselt number around the stagnation region is

$$Nu_R=\frac{q_{wc}R}{(T_{wc}-T_{\infty})K}=-\theta'(0)\,(mGr_R)^{\frac{1}{4}} \qquad \text{(II.48)}$$

The average heat flux over the entire plate, based on the expression in Eq.(II.46), is given by

$$\begin{aligned}\overline{q_w}&=\frac{1}{\pi R^2}\int_0^R 2\pi r q_w dr\\ &=-\theta'(0)\,\frac{2K(T_{wc}-T_{\infty})\,(mGr_R)^{\frac{1}{4}}}{R^3}\int_0^R r(1-\frac{r^2}{2R^2})\,dr \qquad \text{(II.49)}\\ &=-\frac{3}{4}\theta'(0)\,\frac{K(T_{wc}-T_{\infty})\,(mGr_R)^{\frac{1}{4}}}{R}\end{aligned}$$

Therefore, the average Nusselt number formula is

$$\overline{Nu_R}=\frac{\overline{q_w}R}{(T_{wc}-T_{\infty})K}=-\frac{3}{4}\theta'(0)\,(mGr_R)^{\frac{1}{4}} \qquad \text{(II.50)}$$

The numerical solutions of Eq.(II.26) with its boundary conditions, obtained by the numerical method introduced in section II-3.1, are shown from Fig.II-3.1, to Fig.II-3.3, and from Table II-3.1, to Table II-3.3, for Pr=0.72, 1, and 5 respectively.

Differentiating Eq.(II.19) with respect to η, it becomes

$$f^{(4)}(\eta)+2f(\eta)f'''(\eta)+\theta'(\eta)=0 \qquad \text{(II.51)}$$

From the above Eq.(II.51), the following relation at $\eta=0$ is obtained : $f^{(4)}(0)=-\theta'(0)$. The values of $f^{(4)}(0)$ are 0.46202, 0.51854 and 0.86691 for Pr=0.72, 1, and 5, respectively. These results can be summarized and substituted into Eq.(II.48), then the Nusselt number formula at the stagnation region becomes

$$Nu_R = 0.519\,Pr^{0.07}(mRa_R)^{\frac{1}{4}} \tag{II.52}$$

and the average Nusselt number formula becomes

$$\overline{Nu_R} = 0.389\,Pr^{0.07}(mRa_R)^{\frac{1}{4}} \tag{II.53}$$

where " m " should be determined by experiment.

3.2.2 One Assumed Function and Prescribed Constant Surface Flux Case

In this case, the temperature distribution is assumed in Eq.(II.27). According to Newton's law of cooling, the heat flux can be expressed as

$$q_w = h(T_w - T_\infty) \tag{II.54}$$

where q_w=constant, T_w and h are not constant but functions of r. From Eq.(II.27), the wall temperature at the stagnation point can be expressed as

$$T_{wc} - T_\infty = \frac{q_w R}{K(mGr_R^*)^{\frac{1}{5}}}\theta(0) \tag{II.55}$$

Hence, the Nusselt number formula around the stagnation point yields

$$Nu_R = \frac{q_w R}{K(T_{wc} - T_\infty)} = \frac{1}{\theta(0)}(mGr_R^*)^{\frac{1}{5}} \tag{II.56}$$

The average temperature distribution over the entire plate, based on expression in Eq.(II.27), is given by

$$\overline{T_w}-T_\infty=\frac{1}{\pi R^2}\int_0^R 2\pi r\,(T_w-T_\infty)\,dr$$

$$=\frac{2q_w\theta(0)}{K(mGr_R^*)^{\frac{1}{5}}R}\int_0^R r\,(1-\frac{r^2}{2R^2})\,dr \qquad \text{(II.57)}$$

$$=\frac{3}{4}\theta(0)\,\frac{q_wR}{K(mGr_R^*)^{\frac{1}{5}}}$$

The average Nusselt number formula is

$$\overline{Nu_R}=\frac{q_wR}{(\overline{T_w}-T_\infty)\,K}=\frac{4}{3}\,\frac{1}{\theta(0)}\,(mGr_R^*)^{\frac{1}{5}} \qquad \text{(II.58)}$$

The numerical results of Eq.(II.26) and its corresponding boundary conditions in section II-2.1.2, obtained by the numerical method introduced in section II-3.1, are shown from Fig.II-3.4 to Fig.II-3.6, and from Table II-3.4 to Table II-3.6 for Pr=0.72, 1, and 5, respectively. From Eq.(II.19), the following relation at η=0 is obtained : $\theta(0)=-f'''(0)$. The values of $-f'''(0)$ are 1.870963, 1.704898, 1.120025 for Pr=0.72, 1, and 5, respectively. The seven significant digits are for the purpose of obtaining the convergent solutions in the numerical calculation. These results can be summarized and substituted into Eq.(II.56), then the Nusselt number formula, for the vicinity of the stagnation point, can be expressed as

$$Nu_R=0.59\,Pr^{0.12}\,(mRa_R^*)^{\frac{1}{5}} \qquad \text{(II.59)}$$

The average Nusselt number formula becomes

$$\overline{Nu_R}=0.787Pr^{0.12}(mRa_R^*)^{\frac{1}{5}} \tag{II.60}$$

where " m " is to be determined by experiment.

3.2.3 Two Assumed Functions and Prescribed Surface Temperature Case

In this case, the temperature distribution is as in Eq.(II.30). According to Fourier's law of conduction, the heat flux can be expressed as

$$\begin{aligned} q_w &= -K\frac{\partial T}{\partial z}\bigg|_{z=0} \\ &= -K(T_{wc}-T_\infty)\,[\theta_1'(0)-\theta_2'(0)\frac{r^2}{2R^2}]\sqrt{\frac{a}{\nu}} \\ &= -K(T_{wc}-T_\infty)\,[\theta_1'(0)-\theta_2'(0)\frac{r^2}{2R^2}]\frac{(mGr_R)^{\frac{1}{4}}}{R} \end{aligned} \tag{II.61}$$

If r is small, around the stagnation point, then the heat flux is expressed as

$$q_{wc}=-K(T_{wc}-T_\infty)\,\theta_1'(0)\,\frac{(mGr_R)^{\frac{1}{4}}}{R} \tag{II.62}$$

The Nusselt number formula around the stagnation point, gives

$$Nu_R=\frac{q_{wc}R}{(T_{wc}-T_\infty)K}=-\theta_1'(0)\,(mGr_R)^{\frac{1}{4}} \tag{II.63}$$

The average heat flux over the entire plate, based on Eq.(II.61), gives

$$\overline{q_w} = \frac{1}{\pi R^2}\int_0^R 2\pi r q_w dr$$
$$= -\frac{2K(T_{wc}-T_\infty)(mGr_R)^{\frac{1}{4}}}{R^3}\int_0^R r[\theta_1'(0) - \theta_2'(0)\frac{r^2}{2R^2}]dr \qquad \text{(II.64)}$$
$$= \frac{K(T_{wc}-T_\infty)(mGr_R)^{\frac{1}{4}}}{R}[-\theta_1'(0) + \frac{1}{4}\theta_2'(0)]$$

The average Nusselt number formula is

$$\overline{Nu_R} = \frac{\overline{q_w}R}{(T_{wc}-T_\infty)K} = [-\theta_1'(0) + \frac{1}{4}\theta_2'(0)](mGr_R)^{\frac{1}{4}} \qquad \text{(II.65)}$$

The thermal boundary condition of $\theta_2(0)$ varies from zero to one when representing different parabolic wall temperatures in this case. The numerical solutions of Eq.(II.35) and its thermal boundary condition specified at $\theta_2(0)=1$ are shown from Fig.II-3.7 to Fig.II-3.9, for Pr=0.72, 1, and 5 respectively. Then the solutions of $\theta_1(\eta)$ (i.e., Eq.(II.36)), based on the functions of $f(\eta)$ (cf., Table II-3.7), can be obtained by Simpson's rule with step size of 0.1. The curves of $\theta_1(\eta)$ are shown in Fig.II-3.10. The $\theta_1'(0)$ values, expressed by Eq.(II.37), can be obtained by the same method of integration. The values of $-\theta_1'(0)$ are 0.42715, 0.47826, 0.8016 for Pr=0.72, 1, and 5, respectively. Substitute them into Eq.(II.63), and the Nusselt number formula for the vicinity of the stagnation point becomes

$$Nu_R = 0.478 Pr^{0.07}(mRa_R)^{\frac{1}{4}} \qquad \text{(II.66)}$$

From Eq.(II.31), $\theta_2'(0) = -f^{(4)}(0)$; therefore the values of $\theta_2'(0)$ are -0.653482, -0.725941, and -1.176284 for Pr=0.72, 1, and 5 respectively (cf., from Fig.II-3.7 to Fig.II-3.9). By substituting the $\theta_1'(0)$ and $\theta_2'(0)$ values into Eq.(II.65), the average Nusselt number formula becomes

$$\overline{Nu_R}=0.296\,Pr^{0.07}(mRa_R)^{\frac{1}{4}} \qquad \text{(II.67)}$$

If the thermal boundary condition of the wall tends toward the constant wall temperature condition (i.e., isothermal surface condition), then the value of $\theta_2(0)$ should tend toward zero. The solutions of Eq.(II.35) for the values of $\theta_2(0)$ varying from 0.5 to 0.1, at the Prandtl number of one, are shown from Fig.II-3.11 to Fig.II-3.15. The solutions of $\theta_1(\eta)$, the boundary conditions of $f''(0)$ and $f^{(4)}(0)$, and the values of $\theta_1'(0)$ and $\theta_2'(0)$, for the different values of $\theta_2(0)$ are shown in Fig.II-3.16, Fig.II-3.17, and Fig.II-3.18, respectively. The formula of the stagnation point Nusselt number is associated with $-\theta_1'(0)$; its value decreasing with the wall temperature approximates the isothermal surface condition. The coefficient of the average Nusselt number in Eq.(II.65) is shown as a curve in Fig.II-3.18 for the different wall temperature conditions. It shows that the value of curve fits with the coefficient of Eq.(II.67) within ±12%.

In this calculation, the solution for the isothermal surface condition cannot be obtained, because when $\theta_2(0)=0$ the solution becomes a trivial solution.

II-4 DISCUSSIONS

4.1 Streamlines

The mathematical model used for this analysis is based on laminar, axisymmetric, single-plume type stagnation flow (Fig. II-1.1). The order of magnitude for the Rayleigh number is between 10^4 and 10^6. The Prandtl number of the fluid is within the moderate range. According to the above conditions, a downward-facing heated round plate, with Raleigh number of about 10^6, is prepared by using the exterior bottom surface of a tea pot, with a radius of 60 mm, heated by boiling water, hanging in a room with dimensions 3.6x3x2.3 m at a room temperature of about 22 °C. In order to observe streamlines beneath the heated surface, a bundle of incense sticks, with a total diameter of about 20 mm, was used for generating smoke about 180 mm below the heated surface. The photo in Fig.II-4.1.a shows the streamlines beneath the surface without heating; the fluid seems to accumulate beneath the surface and not to flow smoothly toward the edge of the plate. From Fig.II-4.1.b to Fig.II-4.d show streamlines under the surface, heated by boiling water; the fluid flows from the central area toward the edge of the plate smoothly. Although Fig.II-4.1.b does not represent the exact flow pattern of natural convection beneath a heated surface, because the plume-like flow is also partly generated by another hot source (burning incense sticks), it shows that the smoke has the tendency to flow from the center toward the edge of the plate under a heated surface.

The computational streamlines based on the stream function equation, Eq.(II.11), can be plotted as long as $f(\eta)$ is determined. With a modification of Eq.(II.11), the modified stream function, $\overline{\Psi}$, is Ψ/R; and the modified radial coordinate,

$\bar{r}$, is r/R. Therefore, Eq.(II.11) is modified as

$$\bar{\Psi}=\nu\,(mGr_R)^{\frac{1}{4}}\bar{r}^2 f(\eta) \qquad \text{(II.68)}$$

for the prescribed surface temperature condition; and

$$\bar{\Psi}=\nu\,(mGr_R^*)^{\frac{1}{5}}\bar{r}^2 f(\eta) \qquad \text{(II.69)}$$

for the prescribed constant surface flux condition. Fig.II-4.2.a shows the streamlines of the one assumed temperature function case, with the Prandtl number of the fluid at 0.72, for the prescribed surface temperature condition. Fig.II-4.2.b shows the streamlines of the same Prandtl number fluid for the prescribed constant surface flux condition. From observing the two patterns of streamlines, it is seen that the fluid of Prandtl number at 0.72 has a tendency to create a vortex-like pattern for the prescribed constant surface flux condition. This phenomenon is easily explained from the solutions of $f(\eta)$ and $f'(\eta)$, which represent vertical velocity and radial velocity functions, as in Fig.II-3.1 and Fig.II-3.4.

For three-dimensional, axisymmetric, impinging stagnation flow, discussed in section I-2.2 (also cf., p.98, [22]); with the relations of Eq.(I.4) and Eq.(I.26), the modified stream function can be written as

$$\bar{\Psi}=\sqrt{a^*}\,Re_{D,U_{oc}}^{0.5}\frac{R}{D}\nu\bar{r}^2 f(\eta) \qquad \text{(II.70)}$$

Fig.II-4.2.c shows that the streamlines of this impinging stagnation flow are similar to the three-dimensional, axisymmetric, free convective flow for a downward-facing, heated, horizontal plate.

4.2 The Characteristics of Velocity and Temperature Distributions

The comparisons of the vertical velocity, the radial velocity, and the temperature functions, $f(\eta)$, $f'(\eta)$, and $\theta(\eta)$s, for both the prescribed surface temperature and the constant surface flux conditions with different Prandtl numbers, are shown in Fig.II-4.3 to Fig.II-4.14. Some features observed from Fig.II-3.10 to Fig.II-4.14 are summarized as follows:

(1) The maximum value of the functions of the velocity components, $f(\eta)$ and $f'(\eta)$, and the slope of temperature-related functions or the thickness of thermal boundary layer are inversely proportional to the value of the Prandtl number. These phenomena were also found in the free convection of hot vertical plate (cf., p.316, [13], [22]).

(2) The values of $f(\eta_\infty)$ are non-zero constants for the prescribed surface temperature condition (cf., Fig.II-4.3, Fig.II-4.9, Fig.II-4.12), but they are approximately zero for the prescribed constant surface flux condition, with the Prandtl numbers at 0.72 and 1 (cf., Fig.II-4.6).

(3) The maximum values of $f(\eta)$ and $f'(\eta)$ for the prescribed constant surface flux condition are larger than that for the prescribed surface temperature condition.

(4) For the prescribed surface temperature condition, the maximum values of $f(\eta)$ and $f'(\eta)$ in the case of one assumed temperature function (cf., Fig.II-4.3, Fig.II-4.4) are larger than those in the case of two assumed temperature functions, at $\theta_2(0)=1$ (cf., Fig.II-4.9, Fig.II-4.10). Therefore, the thermal boundary layer thicknesses in the case of one assumed temperature function (cf., Fig.II-4.5) are smaller than those in the case of two assumed temperature functions, at $\theta_2(0)=1$ (cf.,

Fig.II-3.10, Fig.II-4.11).

(5) The direction of radial velocity reverses at $\eta \approx 3.8$ for the prescribed constant surface flux condition, with the Prandtl numbers at 0.72 and 1 (cf., Fig.II-4.7).

(6) For the prescribed surface temperature and two assumed temperature functions cases, the thickness of the thermal boundary layer in the central area of the plate increases as the surface temperature gets closer to isothermal condition (Fig.II-3.16).

4.3 The Stagnation Point and the Average Nusselt Numbers

The results of previous research listed in Table II-1.1 show that the free convection investigations of downward-facing heated circular plates [54, 38, 35, 52, 53, 46] are very rare. Most of these results are expressed in terms of average Nusselt number formulas, except Faw's [35] and Schulenberg's [52, 53] investigations of heat transfer around the stagnation point. The results of this dissertation are compared with those of the others as follows.

For the prescribed surface temperature condition:

(1) The Nusselt number is a function of the 1/4 power of the Rayleigh number and 0.07 power of the Prandtl Number. This result based on 1/4 power of the Rayleigh number, is different from Singh's [54] results, where 1/5 power of the Rayleigh number is obtained.

(2) The results for the stagnation point Nusselt number (cf.,Eq.(II.52), (II.66)) are larger than those of the average Nusselt number (cf., Eq.(II.53), (II.67)). This is contradicted by Faw's results [35].

(3) The values of the stagnation point and average Nusselt

number for the one assumed temperature function case (Eq(II.52), (II.53)) are larger than those for the two assumed temperature functions case (Eq.(II.66), (II.67)) by 8% and 24% respectively.

For the prescribed constant surface flux condition:

(4) The Nusselt number formulas show the 1/5 power of the modified Rayleigh number and the 0.12 power of the Prandtl number. This is the same formula as Fujii's [38], but different from Schulenberg's [52, 53], where the 1/6 power of the modified Rayleigh number occurs.

(5) The values of stagnation point Nusselt number are smaller than those of average Nusselt number. This shows the same trend as Faw's results [35].

The "m" in the Nusselt number expressions has not been determined by experiment yet in this investigation. However, from the computational results of the temperature related functions, the thermal boundary layer thickness is approximately at $\eta \approx 6$, for Prandtl numbers at 0.72 and 1 ; and at $\eta \approx 3$, for Prandtl number at 5 (cf., Fig.II-4.5, II-4.8). Substituting Eq.(II.17) and Eq.(II.28) into Eq.(II.10), taking the Rayleigh number and the modified Rayleigh number at an order of magnitude between 10^4 and 10^6, the "m" can be estimated within the range to obtain $0.2<m<0.96$. Comparing Eq.(II.53) with Faw's experimental results [35] at $Ra_R=10^6$, m is 0.53. However, comparing Eq.(II.60) with Fujii's results [38], the constant surface flux case, m is 0.13.

II-5 CONCLUSIONS

The free convection of a downward-facing heated round plate has been analyzed by using the continuity, the Navier-Stokes, and the energy equations. The mathematical model is established by assuming the laminar stagnation flow of axisymmetric single-plume type, and steady state. Through a similarity transformation, the governing partial differential equations are transformed into a fifth-order O.D.E. The similarity solutions are obtained numerically from the Runge-Kutta integration scheme along with the shooting method for both the prescribed surface temperature and the constant surface flux conditions. The present calculations are numerical approximations of the exact solutions of the Navier-Stokes equation and the energy equation.

The heat transfer formulas are derived from the temperature profile solutions. The formulas for the Nusselt number show the 1/4 power dependence on the Rayleigh number, for the prescribed surface temperature condition (this is realized in experimental results by Saunders, Fishenden, Mansion [51], Weise [57], Clifton, and Chapman [33]); and the 1/5 power dependence on the modified Rayleigh number, for the prescribed constant surface flux condition. The 1/5 power dependence (for the constant surface temperature condition) and the 1/6 power dependence (for the constant surface flux condition) of the Nusselt number on the Rayleigh number, derived by Singh et al. [54] and Schulenberg [52, 53], are the results of approximate solutions.

PART III FREE CONVECTION OF A FINITE SIZE UPWARD-FACING HEATED HORIZONTAL ROUND PLATE

III-1 INTRODUCTION

1.1 General Introduction and Research Objectives

In this case, the heated circular plate is facing upward, and the density of the heated medium above the plate is smaller than that of the surrounding medium. Therefore, the unheated fluid flows from the edge of the plate toward the central region along the surface, creating a boundary-layer type flow; then the boundary layer should break down at some distance inward from the edge and an unstable rising plume forms in the central region [64], also known as the stagnation region. A flow pattern of this type is shown in Fig.III-1.1. The differences between this case and the case in Part II are the directions of velocity components, the sign of pressure gradient with respect to radial coordinate, and the stability of the flow. A full understanding of this phenomenon can be very helpful to meteorological research and industrial applications, such as cooling evaluation of more condensed integrated circuit chips.

The purpose of this study is to try to establish a mathematical model for describing the velocity distributions, the temperature profiles, and the heat transfer rate above the central part of the plate by using the Navier-Stokes and the full energy equations. The simplified boundary-layer type equations are not used because the boundary layer breaks down at the stagnation region.

1.2 Previous Studies

Due to the nature of this study, the literature review is limited to the investigations concentrated on the laminar flow regime at steady state. The early heat transfer studies of upward-facing heated horizontal plates started experimentally, such as Weise's [57] investigation of heated square plates in air. McAdam [68] summarized the early experimental results in his book, in which the heat transfer coefficients were shown to be proportional to the 1/4 power of the temperature difference between the heated surface and the surrounding air. Analytical methods based on a differential formulation were then presented by using boundary-layer type momentum and energy equations for a single leading edge plate, which is also known as the semi-infinite plate [73, 61, 72].

Husar and Sparrow [64] observed the flow pattern of the circular plate. They pointed out that the flow in the central region was dominated by a plume.

Torrance and Rockett [75] skillfully formulated the problem of a heated circular plate in a cylindrical enclosure so that the boundary conditions can be well defined. Their analytical solutions, obtained using the finite-difference method, showed streamlines and isothermal lines, from transient to steady state, above the plate at different Grashof numbers . However, the heat transfer correlation indicated the average Nusselt number as a function of the 1/2 power of the Grashof number, which is somewhat larger than the results offered by the others.

Blanc and Gebhart [60] reported an analytical solution for a heated disk by using a similarity analysis. However, this did not yield physically meaningful solutions.

Goldstein et al. [62], and Lloyd and Moran [67] investigated the problem by using mass transfer experiments. Goldstein et al. recommended the use of a characteristic length evaluated as the ratio of the heated area to the encompassing perimeter for correlating experimental data of different geometric surfaces. Their results commonly showed the 1/4 power of the Rayleigh number in the expression of the average Sherwood and Nusslet numbers.

Al-Arabi and El-Riedy [59] tested plates, with diameter ranging from 10 cm to 50 cm, heated by steam on the bottom. They reported a 1/4 power of the Rayleigh number in heat transfer correlation and chose the diameter as the characteristic length. They also found the average heat transfer rates were close between square and circular plates, if the side length was equal to the diameter.

Zakerullah and Ackroyd [77] formulated the problem by using boundary-layer type equations in the differential forms. The solutions were not valid in the central region. Their analytical results showed the 1/5 power of the Rayleigh number in heat transfer correlation. However, the power was increased to 1/4 when the analysis included fluid property variation.

Yousef et al. [76] investigated three heated square plates, 10x10 cm, 20x20 cm, 40x40 cm ,respectively, in air using a Mach-Zehnder interferometer. The 1/4 power of the Rayleigh number in average heat transfer correlation was shown to apply. The distributions of local heat transfer coefficients at different temperature-difference conditions showed that the coefficients at the edges were larger than those at the center.

Merkin [69, 70] extended the method reported by Zakerullah and Ackroyd [77] to simulate the characteristics of heat transfer and fluid flow around the stagnation area. However, the boundary-layer type equations were still used in the formulation; this was pointed out as inadequate by Zakerullah and Ackroyd.

Hrycak and Sandman [63] formulated the heat transfer expression at the stagnation point by the integral method. The reports indicated that the Nusselt number is a function of the 1/4 power of the Rayleigh number.

Liburdy et al. [65, 66] formulated the problem including the central plume-type flow by using boundary-layer type equations. However, the solutions were obtained from the edge up to midway to the center. Their investigation indicated that the heat transfer in the central area contributed much less than that of the peripheral area in overall heat transfer of the plate. The 1/5 power of the Rayleigh number in heat transfer correlation was obtained.

Sahraoui et al. [74] reported results based on both analytical and experimental methods. The 1/5 power of the Rayleigh number in heat transfer correlation was shown to apply.

A view of previous research suggests that the stagnation flow in the central region has not been well formulated. The 1/5 power of the Rayleigh number in heat transfer correlation usually appeared in analytical results, but the 1/4 power dependency was often reported in experimental results.

III-2 MATHEMATICAL MODEL OF DIFFERENTIAL FORMULATION

The continuity, the Navier-Stokes, and the full energy equations are used to formulate this problem. The assumptions for the flow are that it be laminar, axisymmetric, of steady state and of single plume. Adopting the Boussinesq approximation, the governing equations in cylindrical coordinates with the gravitational vector at 180 degrees with respect to the z-axis are written as follows.

$$\frac{\partial u}{\partial r}+\frac{u}{r}+\frac{\partial w}{\partial z}=0 \tag{III.1}$$

$$u\frac{\partial u}{\partial r}+w\frac{\partial u}{\partial z}=-\frac{1}{\rho}\frac{\partial p}{\partial r}+\nu\left(\frac{\partial^2 u}{\partial r^2}+\frac{1}{r}\frac{\partial u}{\partial r}+\frac{\partial^2 u}{\partial z^2}-\frac{u}{r^2}\right) \tag{III.2}$$

$$u\frac{\partial w}{\partial r}+w\frac{\partial w}{\partial z}=-\frac{1}{\rho}\frac{\partial p}{\partial z}+g\beta(T-T_\infty)+\nu\left(\frac{\partial^2 w}{\partial r^2}+\frac{1}{r}\frac{\partial w}{\partial r}+\frac{\partial^2 w}{\partial z^2}\right) \tag{III.3}$$

$$u\frac{\partial T}{\partial r}+w\frac{\partial T}{\partial z}=\alpha\left(\frac{\partial^2 T}{\partial r^2}+\frac{1}{r}\frac{\partial T}{\partial r}+\frac{\partial^2 T}{\partial z^2}\right)+\frac{\nu}{C_p}\Phi \tag{III.4}$$

The temperature distribution above the plate is assumed to be of a parabolic shape, such as

$$\frac{T-T_\infty}{T_{wc}-T_\infty}=\theta(\eta)\left(1-\frac{r^2}{R^2}\right) \tag{III.5}$$

where η denotes the same expression as in Eq.(II.10). Let's choose the same Stokes stream function, Ψ, as in Eq.(II.11); however, the directions of velocity components are opposite those in Eq. (II.12) and Eq.(II.13). Therefore, they should be expressed as

$$u=-\frac{1}{r}\frac{\partial\Psi}{\partial z}=-arf'(\eta) \qquad \text{(III.6)}$$

$$w=\frac{1}{r}\frac{\partial\Psi}{\partial r}=2\sqrt{a\nu}\,f(\eta) \qquad \text{(III.7)}$$

The partial derivative terms in the Navier-Stokes equation can be derived from Eq.(III.6) and (III.7). They are

$$\begin{aligned}&\frac{\partial u}{\partial r}=-af'(\eta)\,;\ \frac{\partial^2 u}{\partial r^2}=0\,;\ \frac{\partial u}{\partial z}=-a\sqrt{\frac{a}{\nu}}\,rf''(\eta)\,;\ \frac{\partial^2 u}{\partial z^2}=-\frac{a^2}{\nu}rf'''(\eta)\\&\frac{\partial w}{\partial r}=0\,;\ \frac{\partial^2 w}{\partial r^2}=0\,;\ \frac{\partial w}{\partial z}=2af'(\eta)\,;\ \frac{\partial^2 w}{\partial z^2}=2a\sqrt{\frac{a}{\nu}}\,f''(\eta)\end{aligned} \qquad \text{(III.8)}$$

With relations in Eq.(III.6), (III.7) and (III.8), the continuity equation, Eq.(III.1), is satisfied. By substituting Eq.(III.8) into Eq.(III.3), integrating Eq.(III.3) from z=0 to $z=z_0$, the pressure near the central region surface of the plate can be approximately expressed as

$$P_s \approx P_\infty-\rho g\beta\,(T-T_\infty)\,Z_0 \qquad \text{(III.9)}$$

By substituting Eq.(III.5) into Eq.(III.9), and differentiating with respect to r, the pressure derivative term in Eq.(III.2) becomes

$$-\frac{1}{\rho}\frac{\partial P}{\partial r}=-2g\beta\,(T_{wc}-T_\infty)\,\theta(\eta)\,\frac{r}{R^2}Z_0 \qquad \text{(III.10)}$$

By substituting Eq.(II.8) and multiplying $(R^2\nu^2)$ in both the numerator and denominator of Eq.(III.10), it becomes

$$-\frac{1}{\rho}\frac{\partial P}{\partial r}=-2r\frac{mGr_R\nu^2}{R^4}\theta(\eta) \qquad \text{(III.11)}$$

Set $a^2=(m\ Gr_R\ \nu^2)/R^4$, hence

$$\sqrt{\frac{a}{\nu}}=\frac{(m\ Gr_R)^{\frac{1}{4}}}{R} \tag{III.12}$$

$$-\frac{1}{\rho}\frac{\partial p}{\partial r}=-2a^2 r\theta(\eta) \tag{III.13}$$

With the relations in Eq.(III.8), and (III.13), the Navier-Stokes equation in radial coordinates (i.e. Eq.(III.2)) can be transformed into

$$f'''(\eta)-2f(\eta)f''(\eta)+f'(\eta)^2+2\theta(\eta)=0 \tag{III.14}$$

With the temperature distribution in Eq.(III.5), the partial derivative terms of temperature in the energy equation are expressed as

$$\begin{aligned}
&\frac{\partial T}{\partial r}=-(T_{wc}-T_\infty)\theta(\eta)\frac{2r}{R^2}\\
&\frac{\partial^2 T}{\partial r^2}=-(T_{wc}-T_\infty)\theta(\eta)\frac{2}{R^2}\\
&\frac{\partial T}{\partial z}=(T_{wc}-T_\infty)\ (1-\frac{r^2}{R^2})\theta'(\eta)\sqrt{\frac{a}{\nu}}\\
&\frac{\partial^2 T}{\partial z^2}=(T_{wc}-T_\infty)\ (1-\frac{r^2}{R^2})\theta''(\eta)\frac{a}{\nu}
\end{aligned} \tag{III.15}$$

With the relation in Eq.(III.6), (III.7), (III.15),the energy equation, Eq.(III.4), is then transformed into

$$\begin{aligned}
&2arf'(\eta)\theta(\eta)\frac{r}{R^2}+2af(\eta)\theta'(\eta)\ (1-\frac{r^2}{R^2})\\
&=\alpha\left[-\frac{4}{R^2}\theta(\eta)+(1-\frac{r^2}{R^2})\theta''(\eta)\frac{a}{\nu}\right]\\
&+\frac{\nu}{C_p(T_{wc}-T_\infty)}\left[12a^2 f'(\eta)^2+r^2\frac{a^3}{\nu}f''(\eta)^2\right]
\end{aligned} \tag{III.16}$$

Around the stagnation point (i.e. r close to zero), the r^2 terms can be neglected. Therefore, Eq.(III.16) becomes

$$2af(\eta)\theta'(\eta)=\alpha\left[-\frac{4}{R^2}\theta(\eta)+\theta''(\eta)\frac{a}{\nu}\right]+\frac{\nu}{C_p(T_{wc}-T_\infty)}[12a^2f'(\eta)^2] \quad \text{(III.17)}$$

By rearranging Eq.(III.17), it becomes

$$\theta''(\eta)-2Prf(\eta)\theta'(\eta)-\frac{4}{\sqrt{mGr_R}}\theta(\eta)+12PrEcf'(\eta)^2=0 \quad \text{(III.18)}$$

The last two terms can be neglected for the same reasons indicated in section II-2.1.1; therefore, it becomes

$$\theta''(\eta)-2Prf(\eta)\theta'(\eta)=0 \quad \text{(III.19)}$$

By substituting Eq.(III.14) into Eq.(III.19), the fifth order, nonlinear, ordinary differential equation can be obtained as follows.

$$f^{(5)}(\eta)-2(1+Pr)f(\eta)f^{(4)}(\eta)-2f'(\eta)f'''(\eta)+4Prf(\eta)^2f'''(\eta)=0 \quad \text{(III.20)}$$

The boundary conditions are

(i) at $\eta=0$: w=0; u=0; T=Surface Temperature;

(ii) at $\eta=\eta_\infty$: u=Finite Constant; $T=T_\infty$.

With the relations in Eq.(III.6), (III.7), and (III.5), the boundary conditions for $f(\eta)$ and $\theta(\eta)$ are

(i) at $\eta=0$: $f(0)=0$; $f'(0)=0$; $\theta(0)=1$;

(ii) at $\theta=\eta_\infty$: $f'(\eta_\infty)$=Finite Constant; $f''(\eta_\infty)=0$; $\theta(\eta_\infty)=0$.

The boundary conditions for $\theta(\eta)$ can be converted into $f(\eta)$ associated conditions by using Eq.(III.14). Hence, $\theta(0)=1$ is equivalent to $f'''(0)=-2$, and $\theta(\eta_\infty)=0$ is equivalent to $f'''(\eta_\infty)=0$.

Set $U_1=f(\eta)$, $U_2=f'(\eta)$, $U_3=f''(\eta)$, $U_4=f'''(\eta)$, $U_5=f^{(4)}(\eta)$, then Eq.(III.20) becomes

$$
\begin{aligned}
U_1' &= U_2 \\
U_2' &= U_3 \\
U_3' &= U_4 \\
U_4' &= U_5 \\
U_5' &= 2(1+Pr)U_1U_5 + 2U_2U_4 - 4PrU_1^2U_4
\end{aligned}
\tag{III.21}
$$

The boundary conditions for Eq.(III.21) are

(i) $U_1(0)=0$; $U_1(\eta_\infty)$=Finite Value;

(ii) $U_2(0)=0$; $U_2(\eta_\infty)$=Finite Constant;

(iii) $U_3(0)$=Unknown ; $U_3(\eta_\infty)=0$;

(iv) $U_4(0)=-2$; $U_4(\eta_\infty)=0$;

(v) $U_5(0)$=Unknown ; $U_5(\eta_\infty)=0$.

The $U_3(0)$ should be a positive value which forces an inward flow in the radial direction near the surface of the plate (i.e., it ensures that $f'(\eta)$ is positive within $\eta=0$ and η=certain positive value). Following the derivation of Nusselt number in section II-3.2.1, the Nusselt number around the stagnation point region becomes

$$Nu_R = -\theta'(0)\,(mGr_R)^{\frac{1}{4}} \tag{III.22}$$

III-3 DISCUSSIONS

The solution of $f'(\eta)$ is allowed to have two possible properties. (1) The $f'(\eta)$ is positive to $f'(\eta_\infty)$ which is a finite constant. If this condition can be achieved, the flow pattern can be interpreted as a thermal jet which has the radial velocity component constant above the boundary layer attached on the surface of the plate. (2) The $f'(\eta)$ is an oscillating function and its amplitude is decreasing to zero as η approaches η_∞. This can be interpreted as the consecutive vortices occurring above the plate. However, none of these conditions are satisfied so as to produce a physically applicable solution when the numerical method introduced in section II-3.1 is used. Two assumed functions in temperature profile, similar to Eq.(II.30), have been put into the energy equation, thereby gaining an extra equation in the mathematical model. Unfortunately, a meaningful solution still cannot be obtained. The exact reasons still remain veiled. Probably, the formulation is not valid for this unstable flow pattern or the numerical method is not effective. However, the Nusselt number expression derived from the mathematical formulation shows the 1/4 power dependence on the Rayleigh number; this is in line with the experimental results by Goldstein et al. [62], Lloyd and Moran [67], Al-Arabi and El-Riedy [59], and Yousef et al. [76].

APPENDIX A

```
C     -------------------------------------------------------------------
C     THIS PROGRAM IS DESIGNED FOR PROCESSING THE EXPERIMENTAL DATA
C      OF THE FORCED CONVECTION BY AN ARRAY OF AIR JETS IMPINGING
C      NORMAL TO A HORIZONTAL ROUND PLATE
C     -------------------------------------------------------------------
      REAL TGIVEN(50),TAC(50),TAF(100)
      REAL TAVE(20),TWALL(6),TAVER(6),TCONF(6),H(6),RAD(20),T(200)
      REAL XNU(6),HP(6),XNUP(6),CXNU(6),CXNUP(6)
      INTEGER IREDUE,IDATE1,IDATE2,IDATE3,ITIME1,ITIME2,ITIME3
      INTEGER N,NCN,NZN,K,I,J,L,NRE*4
      CHARACTER*20 FNAME1,FNAME2
C     TGIVEN:ARRAY FOR INPUTING TEMP. MEASUREMENT FROM THERMOCOUPLES
C     TAC   :ARRAY FOR CONVERTED TEMP. IN DEGREES CELSIUS
C     TAF   :ARRAY FOR CONVERTED TEMP. IN DEGREES FAHRENHEIT
C     TAVE  :ARRAY FOR RING AVERAGED TEMP. BOTH TOP AND BOTTOM
C     TWALL :ARRAY FOR RING AVERAGED WALL TEMP.
C     TAVER :ARRAY FOR RING AVERAGED TEMP. IN DEGREES RANKINE
C     TCONF :ARRAY FOR THERMAL CONDUCTIVITY OF INVAR OF EACH RING
C     H     :ARRAY FOR HEAT TRANSFER COEFFICIENT OF EACH RING
C     RAD   :ARRAY FOR THE DIMENSIONLESS RING RADIUS
C     T     :ARRAY FOR CONVERTING TEMP. READINGS (mV.) TO  C
C     XNU   :ARRAY FOR NUSSELT NUMBER OF EACH RING
C      ARRAY NAMES START WITH "C" DENOTE THE CORRECTED VALUES WITH
C     RESPECT TO NOMINAL REYNOLDS NUMBERS; ENDED WITH "P" DENOTE THE
C     VALUES ARE CALCULATED BASED ON THE AIR TEMP. OF PLENUM CHAMBER
C     N     :NUMBER OF NOZZLES
C     NCN   :Cn/D VALUES       ;    NZN  :Zn/D VALUES
C     NRE   :NOMINAL REYNOLDS NUMBER OF THE SPECIFIED TEST
C     CONA  :THERMAL CONDUCTIVITY OF AIR
      DATA T /.039,.078,.117,.156,.195,.234,.273,.312,.351,.391,.43,
     &.47,.51,.549,.589,.629,.669,.709,.749,.789,.83,.87,.911,
     &.951,.992,1.032,1.073,1.114,1.155,1.196,1.237,1.279,1.32,
     &1.361,1.403,1.444,1.486,1.528,1.569,1.611,1.653,1.695,
     &1.738,1.78,1.822,1.865,1.907,1.95,1.992,2.035,2.078,2.121,
     &2.164,2.207,2.25,2.294,2.337,2.38,2.424,2.467,2.511,2.555,
     &2.599,2.643,2.687,2.731,2.775,2.819,2.864,2.908,2.953,2.997,
     &3.042,3.087,3.131,3.176,3.221,3.266,3.312,3.357,3.402,3.447,
     &3.493,3.538,3.584,3.63,3.676,3.721,3.767,3.813,3.859,3.906,
     &3.952,3.998,4.044,4.091,4.137,4.184,4.231,4.277,4.324,4.371,
     &4.418,4.465,4.512,4.559,4.607,4.654,4.701,4.749,4.796,4.844,
     &4.891,4.939,4.987,5.035,5.083,5.131,5.179,5.227,5.275,5.324,
     &5.372,5.42,5.469,5.517,5.566,5.615,5.663,5.712,5.761,5.810,
     &5.859,5.908,5.957,6.007,6.056,6.105,6.155,6.204,6.254,6.303,
     &6.353,6.502,6.552,6.602,6.652/
      WRITE(*,448)
448   FORMAT(//)
      WRITE(*,'(A\)')' Input the name of the DATA file....'
      READ(*,'(A)') FNAME1
      WRITE(*,'(/A\)')' Input the name of the OUT file...'
      READ(*,'(A)') FNAME2
      OPEN(2,FILE=FNAME1,STATUS='OLD')
      OPEN(3,FILE=FNAME2,STATUS='NEW')
C      ----------------
C      INPUTING THE DATA
C      ----------------
9090   CONTINUE
4      FORMAT(F6.4)
5      FORMAT(A2,1X,I2,1X,I2,1X,I2)
6      FORMAT(I2,1X,I1,I1,1X,A2)
9000   FORMAT(I1)
       READ(2,9000) IREDUE
       IF(IREDUE.EQ.2) GOTO 3300
       READ(2,5) NAME,IDATE1,IDATE2,IDATE3
```

```
      READ(2,6) ITIME1,ITIME2,ITIME3,ITIME4
9001  FORMAT(F6.4,1X,I1,1X,I1,1X,I2,1X,I6)
      READ(2,9001) D,N,NCN,NZN,NRE
9002  FORMAT(F5.2,1X,F5.2)
      READ(2,*) PBAR,PPLEN
9003  FORMAT(F5.2,1X,F5.2)
      READ(2,*) P1P2,P2
      READ(2,4) (TGIVEN(K),K=1,33)
      WRITE(3,17) NAME
17    FORMAT(' DATA RECORDED BY : ',A2)
      WRITE(3,18) IDATE1,IDATE2,IDATE3
18    FORMAT(' DATE OF READING : ',I2,'/',I2,'/'I2)
      WRITE(3,19) ITIME1,ITIME2,ITIME3,ITIME4
19    FORMAT(' TIME OF READING : ',I2,':',I1,I1,1X,A2)
      IF (REDUE.EQ.1) GOTO 1122
      GOTO 1123
1122  WRITE(3,29)
29    FORMAT(//,' THIS IS A REDO')
      GOTO 1123
1123  CONTINUE
      WRITE(3,111) D,N,NCN,NZN,NRE,PBAR,PPLEN,P1P2,P2
111   FORMAT(//,' DIAMETER OF NOZZLES = ',F7.4,/,
     %' NUMBER OF NOZZLES    = ',I7,/,
     %' CN/D                 = ',I7,/,
     %' ZN/D                 = ',I7,/,
     %' REYNOLDS NUMBER      = ',I7,/,
     %' BAROMETRIC PRESSURE = ',F7.2,/,
     %' P3-P0                = ',F7.2,/,
     %' P1-P2                = ',F7.2,/,
     %' P2-P0                = ',F7.2,/)
C     ---------------------------------
C     SEARCHING THE TEMPERATURE RANGE
C     ---------------------------------
      DO 40 I=1,33
      K=I
      DO 20 J=1,150
      DIFF=TGIVEN(I)-T(J)
      IF(DIFF.LE.0)GO TO 30
   20 CONTINUE
   30 DIFF1=T(J)-T(J-1)
      DIFF2=TGIVEN(I)-T(J-1)
      EK=DIFF2/DIFF1
      TAC(K)=J-1+EK
      TAF(K)=1.8*TAC(K)+32.
   40 CONTINUE
C     ------------------------------
C     PRINTING OUT THE TEMPERATURES
C     ------------------------------
      DO 70 L=1,33
      WRITE(3,60) L,TGIVEN(L),TAC(L),TAF(L)
   60 FORMAT(' TEMP.',I4,' :',F6.4,' MILIVOLTS    ',F6.2,
     #' C',F8.2,'  F')
   70 CONTINUE
C     ------------------------------------
C     CALCULATING THE AVERAGE TERMPERATURES
C     ------------------------------------
      TAVE(1)=(TAF(1)+TAF(2)+TAF(3))/3
      TAVE(2)=(TAF(4)+TAF(5)+TAF(6))/3
      TAVE(3)=(TAF(7)+TAF(8)+TAF(9))/3
      TAVE(4)=(TAF(10)+TAF(11))/2
      TAVE(5)=(TAF(12)+TAF(13))/2
      TAVE(6)=TAF(14)
      TAVE(7)=(TAF(15)+TAF(16)+TAF(17))/3
      TAVE(8)=(TAF(18)+TAF(19)+TAF(20))/3
      TAVE(9)=(TAF(21)+TAF(22)+TAF(23))/3
```

```
      TAVE(10)=(TAF(24)+TAF(25))/2
      TAVE(11)=(TAF(26)+TAF(27))/2
      TAVE(12)=TAF(28)
      WRITE(3,99)
99    FORMAT(//,' AVERAGE TEMPERATURE OF THE RINGS',/)
      DO 120 K=1,6
      WRITE(3,100) K,TAVE(K),TAVE(K+6)
100   FORMAT('RING#',I3,'BOTTOM TEMP.=',F6.2,'F',3X,'TOP
     &TEMP.=',F6.2,'F')
120   CONTINUE
      TAVE(13)=(TAF(29)+TAF(30))/2
      TAVE(14)=(TAF(31)+TAF(32))/2
      WRITE(3,160) TAVE(13),TAVE(14)
160   FORMAT('AMBIENT TEMP.=',F6.2,'F',5X,'JET TEMP.=',F6.2,'F')
      TPLENF=TAVE(14)
      TPLENR=TPLENF+459.7
      PBARPS=PBAR*0.491
      PLENPS=PPLEN*0.03617
      TREFR=TPLENR*((PBARPS+PLENPS)/PBARPS)**(-0.2857)
      TREF=TREFR-459.7
C     -------------------------------------------------------
C     LOCAL HEAT TRANSFER COEFFICIENT
C     PARAMETERS ENDING WITH "P" ARE BASED ON THE PLENUM TEMP.
C     -------------------------------------------------------
      DO 200 I=1,6
      TWALL(I)=TAVE(I+6)+(TAVE(I+6)-TAVE(I))*0.08642
      TAVER(I)=((TAVE(I)+TAVE(I+6))/2)+459.7
      TCONF(I)=7.856+0.005478*(TAVER(I)-491.7)+0.0000034568*
     & ((TAVER(I)-491.7)**2)
      H(I)=-(TCONF(I)/0.0531)*(TAVE(I+6)-TAVE(I))/(TWALL(I)-TREF)
      HP(I)=-(TCONF(I)/0.0531)*(TAVE(I+6)-TAVE(I))/(TWALL(I)
     & -TAVE(14))
      TAVAF=(TREF+TWALL(I))/2
      TAVAFP=(TAVE(14)+TWALL(I))/2
      CONA=(1.33+0.41*(TAVAF/200))*0.01
      CONAP=(1.33+0.41*(TAVAFP/200))*0.01
C     ------------------
C     LOCAL NUSSELT NUMBER
C     ------------------
      XNU(I)=(H(I)*D*0.08333333)/CONA
      XNUP(I)=(HP(I)*D*0.08333333)/CONAP
200   CONTINUE
C     ---------------------------------------
C     OUTPUT BASED ON THE REFERENCE TEMPERATURE
C     ---------------------------------------
      WRITE(3,333)
333   FORMAT(//,' HEAT TRANSFER CHARACTERISTICS BASED ON TREF',
     %/,' RING NO.',4X,'H(ENG.UNITS)',
     %3X,'NUSSELT NUMBER',/)
      DO 400 K=1,6
      WRITE(3,444) K,H(K),XNU(K)
444   FORMAT(I6,F15.2,F15.2)
400   CONTINUE
C     -------------------------------------
C     OUTPUT BASED ON THE PLENUM TEMPERATURE
C     -------------------------------------
      WRITE(3,555)
555   FORMAT(//,' HEAT TRANSFER CHARACTERISTICS BASED ON TPLEN',
     %/,' RING NO.',4X,'H(ENG.UNITS)',
     %4X,'NUSSELT NUMBER',/)
      DO 600 K=1,6
      WRITE(3,666) K,HP(K),XNUP(K)
666   FORMAT(I6,F15.2,F15.2)
600   CONTINUE
```

```
C     -----------------------------------------------------
C     CALCULATE THE AVERAGE HEAT TRANSFER COEFFICIENT AND
C     AVERAGE NUSSELT NUMBER
C     -----------------------------------------------------
      RAD(1)=0
      RAD(2)=0.563/D
      RAD(3)=0.689/D
      RAD(4)=1.13/D
      RAD(5)=1.84/D
      RAD(6)=2.63/D
      RAD(7)=3.00/D
      CALL SUB1(RAD,XNU,AVNU)
      CALL SUB1(RAD,XNUP,AVNUP)
      WRITE(3,777) AVNU
777   FORMAT(//,' AVERAGE NUSSELT NUMBER BASED ON TREF = ',F7.2)
      WRITE(3,888) AVNUP
888   FORMAT(//,' AVERAGE NUSSELT NUMBER BASED ON TPLEN= ',F7.2)
C     -------------------------------------------------
C     CALCULATION OF REYNOLDS NUMBER BY USING THE DATA
C     FROM THE ORIFICE PLATE
C     -------------------------------------------------
      P1=P1P2+P2
      P1PS=P1*0.03617
      P1PSA=P1PS+PBARPS
      P2PSA=(P2*0.03617)+PBARPS
C     -------------------------
C     DENSITY OF AIR IN THE PIPE
C     -------------------------
      RO1=(P1PSA*144)/(53.35*TPLENR)
C     ----------------
C     EXPANSION FACTOR
C     ----------------
      Y=1-0.322215*(1-P2PSA/P1PSA)
C     ---------------------------------
C     VISCOSITY OF AIR AT THE NOZZLE EXIT
C     ---------------------------------
      VISNOZ=0.00001165*((TREFR/491.7)**1.5)*(689.7/(TREFR+198))
C     ----------------------------
C     VISCOSITY OF AIR IN THE PIPE
C     ----------------------------
      VISPIP=0.00001165*((TAVE(14)+459.7)/491.7)**1.5*
     %(689.7/(TAVE(14)+657.7))
C     ----------------------------
C     PIPE RYNOLDS NUMBER
C     ----------------------------
      REPIP=N*NRE*(D/2.067)*(VISNOZ/VISPIP)
C     ----------------------------
C     VELOCITY APPROACH FACTOR
C     ----------------------------
      F=1.06445046
C     -------------------------
C     COEFFICIENT OF DISCHARGE
C     -------------------------
      C=0.605305+0.0007603432*(1000000/REPIP)**0.68
C     ----------------
C     MASS FLOWW RATE
C     ----------------
      FLOW=359.2*1.4641*C*F*Y*(P1P2*RO1)**0.5/3600
C     ---------------
C     REYNOLDS NUMBER
C     ---------------
      REYNOL=FLOW*48/(N*3.14159265*D*VISNOZ)
      WRITE(3,999) REYNOL
999   FORMAT('REYNOLDS NUMBER CALCULATED FROM THE ORIFICE PLATE:'
     &,//,' RE= ',F10.2)
```

```
C      ------------------------------
C      CORRECTION FOR REYNOLDS NUMBER
C      ------------------------------
       IF(REYNOL.NE.NRE) GO TO 2220
       GOTO 3300
2220   CONTINUE
       DO 2221 L=1,6
       CXNU(L)=XNU(L)*(NRE/REYNOL)**0.5
       CXNUP(L)=XNUP(L)*(NRE/REYNOL)**0.5
2221   CONTINUE
       CAVNU=AVNU*(NRE/REYNOL)**0.65
       CAVNUP=AVNUP*(NRE/REYNOL)**0.65
       WRITE(3,2230)
2230   FORMAT(///,
      %' CORRECTED LOCAL NUSSELT NUMBER BASED ON TREF.',/,
      %' RING NO.',3X,'NUSSELT NUMBER',/)
       DO 2300 L=1,6
       WRITE(3,2231) L,CXNU(L)
2231   FORMAT(I6,F15.2)
2300   CONTINUE
       WRITE(3,2232)
2232   FORMAT(//,' CORRECTED LOCAL NUSSELT NUMBER BASED ON TPLEN.'
      &,/,' RING NO.',3X,'NUSSELT NUMBER',/)
       DO 2301 L=1,6
       WRITE(3,2233) L,CXNUP(L)
2233   FORMAT(I6,F15.2)
2301   CONTINUE
       WRITE(3,2234) CAVNU
2234   FORMAT('CORRECTED AVERAGE NUSSELT NO. BASED ON TREF=',F6.2)
       WRITE(3,2235) CAVNUP
2235   FORMAT('CORRECTED AVERAGE NUSSELT NO. BASED ONTPLEN=',F6.2)
       GOTO 9090
3300   CONTINUE
       STOP
       END
C      ---------------------------------------------------------
C       SUBROUTINE USED FOR CALCULATING AVERAGE NUSSELT NUMBER BY
C      CUBIC SPLINE METHOD; REFER TO GERALD'S PAGE 215 [5]
C      ---------------------------------------------------------
       SUBROUTINE SUB1(XXX,YYY,AVGVOL)
       REAL X(10),Y(10),S(10),A(8,4)
       REAL AA,BB,CC,DD,DRAD(20)
       REAL XXX(20),YYY(20)
       INTEGER N,I,K,J,NM1,NM2
C      N  : NUMBER OF PAIRS OF X-Y POINTS
C      X  : ARRAY FOR DIMENSIONLESS RING RADIUS
C      Y  : ARRAY FOR NUSSELT NUMBER CORRESPONDENT TO X ARRAY
C      S  : ARRAY OF SECOND DERIVATIVE AT THE POINTS
C      A  : AUGMENTED MATRIX OF COEFFICIENTS FOR FINDING S
C     TVOL:TOTAL VOLUMN UNDER THE CURVE CONNECTED BY 8 CUBIC POLY.
C      DRAD:ARRAY OF THE VALUE OF EACH X INTERVAL
C    AA,BB,CC,DD:THE COEFFICIENTS OF CUBIC POLY. FOR EACH INTERVAL
C     AI,BI,CI,DI:THE SUBTOTAL RELATED TO ai,bi,ci,di IN Eq.(I-44)
C      SI : THE SUBTOTAL OF EACH INTERVAL
C      AVGVOL: THE AVERAGE NUSSELT NO. VALUE OF THE PLATE
       N=9
       X(1)=XXX(1)
       X(2)=(XXX(1)+XXX(2))/2
       X(3)=XXX(2)
       X(4)=XXX(3)
       X(5)=XXX(4)
       X(6)=XXX(5)
       X(7)=(XXX(6)-XXX(5))/2+XXX(5)
       X(8)=XXX(6)
       X(9)=XXX(7)
```

```
      Y(1)=YYY(6)
      Y(2)=(2*YYY(6)+YYY(5))/3
      Y(3)=YYY(5)
      Y(4)=YYY(4)
      Y(5)=YYY(3)
      Y(6)=YYY(2)
      Y(7)=(YYY(2)+2*YYY(1))/3
      Y(8)=YYY(1)
      Y(9)=((Y(8)-Y(7))/(X(8)-X(7))*(X(9)-X(8)))+Y(8)
      NM2=N-2
      NM1=N-1
      DX1=X(2)-X(1)
      DY1=(Y(2)-Y(1))/DX1*6.
      DO 10 I=1,NM2
      DX2=X(I+2)-X(I+1)
      DY2=(Y(I+2)-Y(I+1))/DX2*6.
      A(I,1)=DX1
      A(I,2)=2.*(DX1+DX2)
      A(I,3)=DX2
      A(I,4)=DY2-DY1
      DX1=DX2
      DY1=DY2
10    CONTINUE
C     START TO SOLVE TRIDIAGONAL SYSTEM
100   DO 110 I=2,NM2
      A(I,2)=A(I,2)-A(I,1)/A(I-1,2)*A(I-1,3)
      A(I,4)=A(I,4)-A(I,1)/A(I-1,2)*A(I-1,4)
110   CONTINUE
C     START TO DO BACK SUBSTITUTION
      A(NM2,4)=A(NM2,4)/A(NM2,2)
      DO 120 I=2,NM2
      J=NM1-I
      A(J,4)=(A(J,4)-A(J,3)*A(J+1,4))/A(J,2)
120   CONTINUE
C     PUT THE VALUES INTO S VECTOR
      DO 130 I=1,NM2
      S(I+1)=A(I,4)
130   CONTINUE
C     THE LINEAR ENDS ARE THE TYPE OF END CONDITION USED
150   S(1)=0
      S(N)=0
      TVOL=0
      DO 5500 K=1,NM1
      DRAD(K)=X(K+1)-X(K)
      AA=(S(K+1)-S(K))/(6.*DRAD(K))
      BB=S(K)/2.
      CC=(Y(K+1)-Y(K))/DRAD(K)-(2.*DRAD(K)*S(K)+DRAD(K)*S(K+1))/6
      DD=Y(K)
      AI=AA*((X(K+1)**5)/5.+(X(K)*X(K+1)**2)*(X(K+1)*X(K)
     & -(3*X(K+1)**2)/4.-(X(K)**2)/2)+(X(K)**5)/20.)
      BI=BB*((X(K+1)**4)/4.-(2*X(K)*X(K+1)**3)/3.
     & +((X(K+1)*X(K))**2)/2.-(X(K)**4)/12.)
      CI=CC*((X(K+1)**3)/3.-(X(K)*X(K+1)**2)/2.+(X(K)**3)/6.)
      DI=(DD/2.)*(X(K+1)**2-X(K)**2)
      SI=AI+BI+CI+DI
      TVOL=TVOL+SI
5500  CONTINUE
      AVGVOL=2*TVOL/X(9)**2
      RETURN
      END
```

APPENDIX B

```
C     ---------------------------------------------------------------
C     THIS PROGRAM IS DESIGNED TO SOLVE A FIFTH-ORDER O.D.E.
C     BY USING FOURTH-ORDER RUNGE-KUTTA METHOD.
C     THE EQ(II.26) WITH ITS PRESCRIBED SURFACE TEMP. BOUNDARY
C     CONDITION ARE SOLVED IN THIS PROGRAM
C     ---------------------------------------------------------------
      REAL*8 L,ET,EMAX,HH,Pr
      REAL*8 U1,U2,U3,U4,U5,U6
      REAL*8 U1I,U2I,U3I,U4I,U5I
      REAL*8 U1R,U2R,U3R,U4R,U5R,U6R
      REAL*8 U3I1,DU3I,U5I1,DU5I
      REAL*8 ERR1,ERR,EPS,GIVE
C     L : TWO TIMES THE LENGTH OF STEP SIZE
C     ET: INDEPENDENT VARIABLE
C     EMAX : MAX. VALUE OF INDEPENDENT VARIABLE IN CALCULATION
C     MAXIT: MAX. NUMBER OF ITERATIONS
C     HH : STEP SIZE
C     Pr : PRANDTL NUMBER VALUE
C     U1,U2,U3,U4,U5,U6 :INPUT VALUES IN RUNGE-KUTTA SUBROUTINE
C     U1I,U2I,U3I,U4I,U5I :INITIAL VALUES (LEFT END B. C.)
C     U1R,U2R ...U6R :OUTPUT VALUES FROM RUNGE-KUTTA SUBROUTINE
C     ERR : DEVIATION BETWEEN THE REQUIRED AND THE SHOT VALUES
C     IP,IPP: SET-UP INTERVAL FOR PRINTOUT; PRINT CONTROL INDEX
      CHARACTER*40 DATA
      CHARACTER*40 FNAME
      EXTERNAL A,B,C,D,E
1     FORMAT('"USINGD RUNGE-KUTTA METHOD TO SOLVE FIFTH ORDER
     &O.D.E."')
3     FORMAT(2X,'T',3X,'F',8X,'F1',5X,'F2',6X,'F3',6X,
     &'F4',6X,'F5',6X,'THETA')
4     FORMAT(F4.1,7(1X,F9.6))
5     FORMAT(2X,'Pr = ',F5.3)
      WRITE(*,'(A\)') 'Enter INTput filename : '
      READ(*,'(a)') DATA
      WRITE(*,'(A\)') 'Enter OUTput filename : '
      READ(*,'(a)') FNAME
      WRITE(*,'(A\)') 'MAX NUMBER OF ITERATION : '
      READ(*,*) MAXIT
      OPEN(2,FILE=DATA,STATUS='OLD')
      OPEN(3,FILE=FNAME,STATUS='NEW')
      WRITE(3,1)
      READ(2,*) HH,EMAX,U1I,U2I,U3I,U4I,U5I,Pr,IP
      READ(2,*) DU3I,DU5I,GIVE,EPS
      WRITE(3,5) Pr
      L=HH/2.
      IT=0
      IPP=0
10    I=0
      IT=IT+1
      IF(IT.GE.MAXIT) GOTO 70
      WRITE(*,4)ET,U1R,U2R,U3R,U4R,U5R,U6R,THETA
      U1=U1I
      U2=U2I
      U3=U3I
      U4=U4I
      U5=U5I
      U6=E(U1I,U2I,U3I,U4I,U5I,Pr)
      THETA=U2**2-2.*U1*U3-U4
      ET=0.
      IF(IPP.EQ.0) GOTO 20
```

```
      WRITE(3,3)
      WRITE(3,4) ET,U1,U2,U3,U4,U5,U6,THETA
 20   I=I+1
      CALL RK(U1,U2,U3,U4,U5,U1R,U2R,U3R,U4R,U5R,Pr,L)
      U6R=E(U1R,U2R,U3R,U4R,U5R,Pr)
      THETA=U2R**2-2.*U1R*U3R-U4R
      ET=ET+HH
      IF(IPP.EQ.0) GOTO 30
      IF((I/IP)*IP.NE.I) GO TO 30
      WRITE(3,4) ET,U1R,U2R,U3R,U4R,U5R,U6R,THETA
 30   U1=U1R
      U2=U2R
      U3=U3R
      U4=U4R
      U5=U5R
      IF(ET.LT.EMAX) GO TO 20
      ERR=U2R-GIVE
      IF(ABS(ERR).LE.EPS) GOTO 40
      IF(IT.GT.1) GOTO 100
      ERR1=ERR
      U3I1=U3I
      U3I=U3I+DU3I
      U5I1=U5I
      U5I=U5I+DU5I
      GOTO 10
100   DU3I=-ERR/(ERR-ERR1)*(U3I-U3I1)
      DU5I=-ERR/(ERR-ERR1)*(U5I-U5I1)
      ERR1=ERR
      U3I1=U3I
      U3I=U3I+DU3I
      U5I1=U5I
      U5I=U5I+DU5I
      GOTO 10
40    IF(IPP) 50,50,60
50    IPP=1
      GOTO 10
60    IT=IT-1
      WRITE(3,6)IT
6     FORMAT(/,6X,'NO. OF ITERATION = ',I4)
      CLOSE(2)
      CLOSE(3)
70    STOP
      END

C     --------------------------------------------------------
C     SUBROUTINE OF FOURTH-ORDER RUNGE-KUTTA METHOD
C     --------------------------------------------------------
      SUBROUTINE RK(U1,U2,U3,U4,U5,U1R,U2R,U3R,U4R,U5R,Pr,L)
      EXTERNAL A,B,C,D,E
      REAL*8 M11,M12,M13,M14
      REAL*8 M21,M22,M23,M24
      REAL*8 M31,M32,M33,M34
      REAL*8 M41,M42,M43,M44
      REAL*8 M51,M52,M53,M54
      REAL*8 U1,U2,U3,U4,U5
      REAL*8 U1R,U2R,U3R,U4R,U5R,L,Pr
      M11=L*A(U2)
      M21=L*B(U3)
      M31=L*C(U4)
      M41=L*D(U5)
      M51=L*E(U1,U2,U3,U4,U5,Pr)
```

```
      M12=L*A(U2+M21)
      M22=L*B(U3+M31)
      M32=L*C(U4+M41)
      M42=L*D(U5+M51)
      M52=L*E(U1+M11,U2+M21,U3+M31,U4+M41,U5+M51,Pr)
      M13=L*A(U2+M22)
      M23=L*B(U3+M32)
      M33=L*C(U4+M42)
      M43=L*D(U5+M52)
      M53=L*E(U1+M12,U2+M22,U3+M32,U4+M42,U5+M52,Pr)
      M14=L*A(U2+2.*M23)
      M24=L*B(U3+2.*M33)
      M34=L*C(U4+2.*M43)
      M44=L*D(U5+2.*M53)
      M54=L*E(U1+2.*M13,U2+2.*M23,U3+2.*M33,U4+2.*M43
     &,U5+2.*M53,Pr)
      U1R=U1+(M11+2.*(M12+M13)+M14)/3.
      U2R=U2+(M21+2.*(M22+M23)+M24)/3.
      U3R=U3+(M31+2.*(M32+M33)+M34)/3.
      U4R=U4+(M41+2.*(M42+M43)+M44)/3.
      U5R=U5+(M51+2.*(M52+M53)+M54)/3.
      RETURN
      END
C     ---------------------------------------------
      REAL FUNCTION A(U2)
      REAL*8 U2
      A=U2
      RETURN
      END
C
      REAL FUNCTION B(U3)
      REAL*8 U3
      B=U3
      RETURN
      END
C
      REAL FUNCTION C(U4)
      REAL*8 U4
      C=U4
      RETURN
      END
C
      REAL FUNCTION D(U5)
      REAL*8 U5
      D=U5
      RETURN
      END
C
      REAL FUNCTION E(U1,U2,U3,U4,U5,Pr)
      REAL*8 U1,U2,U3,U4,U5,Pr
      E=-2.*(1.+Pr)*U1*U5-2.*U2*U4-4.*Pr*U1*U1*U4
      RETURN
      END
```

APPENDIX C

```
C     -----------------------------------------------------------
C     THIS PROGRAM IS DESIGNED FOR SOLVING EQ.(II.36) BY USING
C     TRAPEZOID AND SIMPSON'S RULE
C     -----------------------------------------------------------
      IMPLICIT REAL*8 (A-H,O-Z)
      REAL*8 X(2000),Y(2000),INCR,IND(2000),THETA(2000)
      REAL*8 ST(2000),TOTAL,SI,PR
      CHARACTER*40 DATA
      CHARACTER*40 FNAME
C     X :ARRAY FOR INDEPENDENT VARIABLE
C     Y :ARRAY FOR DEPENDENT VARIABLE
C     INCR: INCREMENTAL VALUE
C     IND: ARRAY FOR THE INTEGRAL OF f(eta) IN EQ.(II.36)
C     ST: ARRAY FOR THE EXPONENTIAL FUNC. OF f(eta) INTEGRAL
C     NP; NPD: NUMBER OF POINTS; NUMBER OF DIVISION
C     PR: PRANDTL NUMBER
C     H: STEP SIZE
C     TOTAL:INTEGRAL OF EXPONENTIAL FUNC. IN THE NUMERATOR
C            OF EQ.(II.36)
C     THETA : ARRAY FOR THETA1 IN EQ.(II.36)
      WRITE(*,'(A\)') 'ENTER INPut Filename : '
      READ (*,'(A)') DATA
      WRITE(*,'(A\)') 'ENTER  OUTput Filename : '
      READ (*,'(A)') FNAME
      OPEN(2,FILE=DATA,STATUS='OLD')
      OPEN(3,FILE=FNAME,STATUS='NEW')
      READ(2,*) PR,NP,H
      READ(2,*) (X(K),Y(K),K=1,NP)
4     FORMAT(F6.2,1X,F10.6,1X,F10.6)
      IND(1)=0.
      ST(1)=1.
      WRITE(3,5)
5     FORMAT('ETA',3X,'INTEGRAL OF F(ETA)',1X,'EXPONENTIAL
     &FUNC. OF F(ETA) INTEGRAL')
      WRITE(3,6) X(1),IND(1),ST(1)
C     -----------------------------------------------------------
C     BY USING TRAPEZOID RULE TO INTEGRATE INTERMIATE AVLUES OF
C     F(ETA) INTEGRAL IN THE NUMERATOR OF EQ.(II.36)
C     -----------------------------------------------------------
      NPD=NP-1
      DO 10 I=1,NPD
      INCR=(Y(I)+Y(I+1))*H/2.
      IND(I+1)=IND(I)+INCR
      ST(I+1)=EXP(-2*PR*IND(I+1))
      WRITE(3,6) X(I+1),IND(I+1),ST(I+1)
6     FORMAT(F6.2,1X,F12.7,2X,F11.9)
10    CONTINUE
C     -----------------------------------------------------------
C     BY USING SIMPSOM'S RULE TO CALCULATE THE DENOMINATOR OF
C     EQ.(II.36) BASED ON THE EXPONENTIAL FUNC. OF FINTEGRAL
C     EVALUATED BY TRAPEZOID RULE
```

```
C     -------------------------------------------------------------
      SI=H*(ST(1)+ST(NP))/3.
      OI=0.
      EI=0.
      N=NP-1
      NI=N/2
      DO 50 I=1,NI
      J=2*I
      M=2*I+1
      OI=ST(J)*4*H/3.+OI
      IF(J.EQ.N) GOTO 30
      EI=ST(M)*2*H/3.+EI
50    CONTINUE
30    SI=SI+OI+EI
      WRITE (3,8) X(1),X(NP)
8     FORMAT(/,2X,'THE INTEGRAL LIMITS ARE
     &FROM',F6.2,'TO',F6.2)
      WRITE (3,9) SI
9     FORMAT(2X,'USING SIMPSON'S RULE, THE INTEGRAL
     &VALUE=',F11.7)
      TOTAL=0.
      THETA(1)=1.0
      WRITE(3,7)
7     FORMAT('ETA',1X,'INTEGRATION OF EXPONENTIAL
     &FUNC',2X,'THETA1')
      WRITE(3,4) X(1),TOTAL,THETA(1)
      DO 20 I=1,N
      INCR=(ST(I)+ST(I+1))*H/2.
      TOTAL=TOTAL+INCR
      THETA(I+1)=1.0-(TOTAL/SI)
      WRITE(3,4) X(I+1),TOTAL,THETA(I+1)
20    CONTINUE
      CLOSE(2)
      CLOSE(3)
      STOP
      END
```

BIBLIOGRAPHY

(PART I)

[1] Behbahani, A. I., and Goldstein, R. J., "Local Heat Transfer to Staggered Arrays of Impinging Circular Jets," *J. of Eng. Power (ASME)*, Vol. 105, pp. 354-360, (1983).

[2] Datta, C. S.,"Cooling Characteristics of a Turbulent Round Jet Impinging Normally on a Heated Flat Plate," M.S. thesis, Mech. Eng. Dept., N.J.I.T., Newark, N.J. (1970).

[3] Flynn, D. R., "Calculation of the Thermal Conductivity of an Invar Sample from Electrical Resistivity Data," N.B.S. Report 9655 (1967).

[4] Freidman, S. J., and Mueller, A. C., "Heat Transfer to Flat Surfaces," Proc. Gen. Disc. on Heat Transfer, Institution of Mech. Engineers, London, pp. 138-142, (1951).

[5] Gerald, C. F., and Wheatley, P.O., *Applied Numerical Analysis*, 3rd ed., Addison-Wesley, Reading, MA (1984).

[6] Gardon, R., and Conbonpue, J. A., "Heat Transfer between a Flat Plate and Jets of Air Impinging on It," *International Developments in Heat Transfer (ASME)*, pp. 454-460, (1961).

[7] Guyer, E. C., *Handbook of Applied Thermal Design*, McGraw-Hill, N.Y., pp. 1-72, (1989).

[8] Hilgeroth, E., "Heat Transfer in Jet Flow Perpendicular to Heat Transfer Surface," *Chemei-Ing.-Tech.*, Vol. 37, pp. 1264-1272, (1965).

[9] Hrycak, P., "Heat Transfer from Impinging Jets -- a Literature Review," AFWAL-TR-81-3054, Air Force Wright Aeronautical Lab., Wright-Patterson AFB, OH (1980).

[10] Hrycak, P., "Heat Transfer from Round Impinging Jets to a Flat Plate," *Int. J. Heat Mass Transfer*, Vol. 26, No. 12, pp. 1857-1865, (1983).

[11] Hrycak, P., Kaya, D. M., Sethi, S., Wei, C. H., "Heat Transfer and Fluid Flow of Arrays of Impinging Jets," *Proc. 10th Symposium on Engineering Applications of Mechanics*, Queen's University, Kingston, Ontario, Canada, pp. 175-180, (1990).

[12] Jachna, S., "Axisymmetric Air Jet impinging on a Hemispherical Concave Plate," Sc. D. Dissertation,

Mech. Eng. Dept., N.J.I.T., Newark, N.J. (1977).

[13] Kays, W. M., and Crawford M. E., *Convective Heat and Mass Transfer*, (2nd ed.) McGraw-Hill, N.Y., (1980).

[14] Kaya, D. M., "Experimental Investigation of Heat Transfer from an Array of Jets Impinging Normally on a Flat Plate," Mech. Eng. Dept., M.S. Thesis, N.J.I.T., Newark, N.J., (1985).

[15] Kercher, D. M., and Tabakoff, W., "Heat Transfer by a Square Array of Round Air Jets Impinging Perpendicular to a Flat Surface Including the Effect of Spent Air," *J. Eng. Power (ASME)*, Vol. 92, pp. 73-82, (1970).

[16] Kezios, S.P., "Heat Transfer in the Flow of a Cylindrical Air Jet Normal to an Infinite Plane," Ph. D. Dissertation, Illinois Institute of Technology (1956).

[17] Kiper, A. M., "Impinging Water Jet Cooling of VLSI Circuits," *Int. Comm. Heat Mass Transfer*, Vol. 11, pp. 517-526, (1984).

[18] Krotzsch, P., *Chem.-Ing.-Tech.*, Vol. 40, p. 339, (1968). (cited by Martin, H.)

[19] Martin, H., "Heat and Mass Transfer between Impinging Gas and Solid Surfaces," in *Advances in Heat Transfer*, ed. by Hartnett, J. P., and Irvine, Jr., T. F., Academic Press, N.Y., (1977).

[20] Omega Engineering, Inc., *The Omega Complete Temperature Measurement Handbook and Encyclopedia*, p. Z-53 (1990).

[21] Ott, H. H., "Heat Transfer to a Plate Cooled by Air," *Schweiz Bauzeitung*, Vol. 79, pp. 834-840 (1961).

[22] Schlichting, H., *Boundary Layer Theory*, (7th ed.) McGraw-Hill, N.Y., (1979).

[23] Sethi, S., "Experimental Investigation of Submerged, Turbulent, Array of Air Jets Impinging on a Flat Plate," Mech. Eng. Dept., M.S. Thesis, N.J.I.T., Newark, N.J. (1984).

[24] Sibulkin, M., "Heat Transfer Near the Forward Stagnation Point of a Body of Revolution," *J. of Aeron. Science*, Vol. 19, pp. 570-571, (1952).

[25] Wang, X. S., Dagan, Z., and Jiji, L. M., "Heat Transfer between a Circular Free Impinging Jet and a Solid Surface with Non-Uniform Wall Temperature or Wall Heat Flux - 1. Solution for the Stagnation Region," *Int. J. Heat Mass Transfer*, Vol.32, No.7, pp. 1351-1360, (1989).

(PART II)

[26] Aihara, T., Yamada, Y., and Endo, S., "Free Convection along the Downward-Facing Surface of a Heated Horizontal Plate," *Int. J. Heat Mass Transfer*, Vol. 15, pp. 2535-2549, (1972).

[27] Arpaci, V. S., and Larsen, P. S., *Convection Heat Transfer*, p. 53, p. 283, Prentice-Hall, N.J., (1984).

[28] Birkebak, R. C., and Abdulkadir, A., "Heat Transfer by Natural Convection from the Lower Side of Finite Horizontal, Heated Surface," *Proc. 4th Int. Heat Transfer Conference*, Vol. 4, NC 2.2, (1970).

[29] Burden, R. L., Faires, J. D., and Reynolds, A. C., *Numerical Analysis*, (2nd ed.), p. 236, p. 469, Prindle, Weber & Schmidt, Boston, MA (1981).

[30] Chang, K. S., Choi, C. J., and Cho, C. H., "Laminar Natural Convection Heat Transfer from Sharp-Edged Horizontal Bars with Flow Separation," *Int. J. Heat Mass Transfer* ,Vol. 31, No. 6, pp. 1177-1187, (1988).

[31] Chen, C. J., "Free Convection from a Two-Dimensional Finite Horizontal Plate," *Trans. ASME*, Vol. 92C, pp. 548-550, (1970).

[32] Chen, T. S., "Parabolic Systems - Local Nonsimilarity Method," in *Handbook of Numerical Heat Transfer*, pp. 199-203, John Wiley & Sons, (1988).

[33] Clifton, J. V., and Chapman A. J., "Natural Convection on a Finite Size Horizontal Plate," *Int. J. Heat Mass Transfer*, Vol. 12, pp. 1573-1584, (1969).

[34] Faw, R. E., and Dullforce, T. A., "Holographic Interferometry Measurement of Convective Heat Transport beneath a Heated Horizontal Late in Air," *Int. J. Heat Mass Transfer*, Vol. 24, No .5, pp. 859-869 (1981).

[35] Faw, R. E., and Dullforce, T. A., "Holographic Interferometry Measurement of Convective Heat Transport beneath a Heated Horizontal Circular Plate in Air," *Int. J. Heat Mass Transfer*, Vol. 25, No. 8, pp. 1157-1166, (1982).

[36] Fröberg, C. E., *Introduction to Numerical Analysis*, p. 244 Addison-Wesley, Reading, MA (1969).

[37] Fujii, T., and Imura H., "Natural Convection Heat Transfer from a Plate with Arbitrary Inclination," *Int. J. Heat Mass Transfer*, Vol. 15, pp. 755-767, (1972).

[38] Fujii, T., Honda, H., and Morioka, I., "A Theoretical Study of Natural Convection Heat Transfer from Downward-Facing Horizontal Surfaces with Uniform Heat Flux," *Int. J. Heat Mass Transfer*, Vol. 16, pp. 611-627, (1973).

[39] Goldstein, R. J., and Lau, K. S., "Laminar Natural Convection from a Horizontal Plate and Influence of Plate Edge Extensions," *J. Fluid Mech.*, Vol. 129, pp. 55-75 (1983).

[40] Gryzagoridis, J., "Natural Convection from an Isothermal Downward-Facing Horizontal Plate," *Int. Comm. Heat Mass Transfer*, Vol. 11, pp. 183-190, (1984).

[41] Guceri, S. I., and Farouk, B., "Numerical Solutions in Laminar and Turbulent Natural Convection," in *Natural Convection Fundamentals and Applications*, pp. 615-620, edited by KaKac, S., Aung, W., and VisKanta, R., Hemisphere, N.Y., (1985).

[42] Hassan, K. E., and Mohamed, S. A., "Natural Convection from Isothermal Flat Surface," *Int. J. Heat Mass Transfer*, Vol. 13, pp. 1873-1886, (1970).

[43] Hatfield, D. W., and Edward, D. K., "Edge and Aspect Ratio Effects on Natural Convection from Horizontal Heated Plate Facing Downward," *Int. J. Heat Mass Transfer*, Vol. 24, No. 6, pp. 1019-1024, (1981).

[44] Hrycak, P., "Calculation of Heat Transfer for a Downward-Facing Heated Horizontal Plate," *Proc. 12th Canadian Congress of Applied Mechanics*, Vol. 2, pp. 700-701, (1989).

[45] Hrycak, P., "Free Convection Heat Transfer from a Finite Horizontal Plate," CSME Mechanical Engineering Forum, Vol.1, pp. 471-476 (1990).

[46] Hrycak, P., "Free Convection Heat Transfer from a Finite Horizontal Plate," *Proc. 10th Symposium on Engineering Applications of mechanics*, pp. 225-230, (1990).

[47] Karvinen, R., Kuumola, V., and Kunttu, H., "Simultaneous Natural Convection from Upward and Downward Surfaces of Horizontal Plate," *Proc. of Int. Heat Transfer Conference*, 2-NC-14, pp. 241-245, (1990).

[48] Levy, S., "Integral Methods in Natural Convection Flow," *(ASME) J. Appl. Mech.*, Vol. 22, pp. 515-522, (1955).

[49] Nachtsheim, P. R., and Swigert P., "Satisfaction of Asymptotic Boundary Conditions in Numerical Solution of Systems of Nonlinear Equations of boundary-layer type," NASA TN D-3004, (1965).

[50] Restrepo, F., and Glicksman, L. R., "The Effect of Edge Conditions on Natural Convection from a Horizontal Plate," *Int. J. Heat Mass Transfer*, Vol. 17, pp. 135-142, (1974).

[51] Saunders, O. A., Fishenden, M., Mansion, H. D., "Some Measurements for Convection by an Optical Method," *Engineering*, pp. 483-485, (May 1935).

[52] Schulenberg, T., "Natural Convection Heat Transfer to Liquid Metals below Downward-Facing Horizontal Surface," *Int. J. Heat Mass Transfer*, Vol. 27, pp. 433-441, (1984).

[53] Schulenberg, T., "Natural Convection Heat Transfer below Downward-Facing Horizontal Surfaces," *Int. J. Heat Mass Transfer*, Vol. 28, pp. 467-477, (1985).

[54] Singh, S. N., Birkebak, R. C., and Drake, Jr., R. M., "Laminar Free Convection Heat Transfer from Downward-Facing Horizontal Surfaces of Finite Dimensions," *Progress in Heat and Mass Transfer*, Vol. 2, pp. 87-98 (1969).

[55] Sugawara, S., and Michiyoshi, I., "Heat Transfer from a Horizontal Flat Plate by Natural Convection," *Trans. (JSME)*, Vol. 21, 109, pp. 651-657, (1955).

[56] Wagner, C., "Discussion on Integral Methods in Natural Convection Flow," *(ASME) J. appl. Mech.*, Vol. 23, pp. 320-321 (1956).

[57] Weise, R., "Warmeubergang durch freie Konvektion an quadratischen Platten," *Forsch Geb. Ing. Wes.*, Vol. 6, pp. 281-292 (1935).

[58] Yuan, S. W., *Foundations of Fluid Mechanics*, p .207, Prentice-Hall, Englewood Cliffs, NJ, (1967).

(PART III)

[59] Al-Arabi, M., and El-Riedy, M. K., "Natural Convection Heat Transfer from Isothermal Horizontal Plates of Different Shapes," *Int. J. Heat Mass Transfer*, Vol. 19, pp. 1399-1404, (1976).

[60] Blanc, P., and Gebhart, B., "Buoyancy Induced Flows Adjacent to Horizontal Surfaces," *Proc. of the 5th International Heat Transfer Conference*, Tokyo, Japan, Vol. III, pp. 20-24, (1974).

[61] Gill, W. N., Zen, D. W., and Casal, E. D., "Free Convection on a Horizontal Plate," *J. of Applied Mathematics and Physics (ZAMP)*, Vol. 16, pp. 539-541, (1965).

[62] Goldstein, R. J., Sparrow, E. M., and Jones, D.C., "Natural Convection Mass Transfer Adjacent to Horizontal Plates," *Int. J. Heat Mass Transfer*, Vol. 16, pp.1025-1035, (1973).

[63] Hrycak, H., Sandman, D. J., "Radiative and Free Convective Heat Transfer from a Finite Horizontal Plate Inside an Enclosure," *Proc. of Symposium 14th Space Simulation Conference*, pp. 42-45, NASA Conference Publication 2444 (1986).

[64] Husar, R. B., and Sparrow E. M., "Patterns of Free Convection Flow Adjacent to Horizontal Heated Surfaces," *Int. J. Heat Mass Transfer*, Vol. 11, pp. 1206-1208, (1968).

[65] Liburty, J. A., and Tsai, B. J., "Numerical Prediction of Natural Convection from a Horizontal Disk," *Proc. of 8th International Heat Transfer Conference*, San Francisco, CA, Vol. 2, pp. 441-446, (1986).

[66] Liburdy, J. A., and Robinson, S. B., "Prediction of the Natural Convection Heat Transfer from a Horizontal Heated Disk," *J. of Heat Transfer (ASME)*, Vol. 109, pp. 906-911, (1987).

[67] Lloyd, J. R., and Moran, W. R., "Natural Convection Adjacent to Horizontal Surface of Various Planforms," *J. of Heat Transfer, (ASME)*, pp. 443-447, (1974).

[68] McAdam, W. H., *Heat Transmission*, p. 240, McGraw-Hill, New York (1942).

[69] Merkin, J. H., "Free Convection above a Heated Horizontal Circular Disk," *J. of Applied Mathematics and Physics (ZAMP)*, Vol. 34, pp. 596-608, (1983).

[70] Merkin, J. H., "Free Convection above a Uniformly Heated Horizontal Circular Disk," *Int. J. Heat Mass Transfer*, Vol. 28, No. 6, pp. 1157-1163, (1985).

[71] Pera, L., and Gebhart, B., "Natural Convection Boundary Layer Flow over Horizontal and Slightly Inclined Surfaces," *Int. J. Heat Mass Transfer*, Vol. 16, pp. 1131-1146, (1973).

[72] Rotem, Z., and Claassen, L., "Natural Convection above Unconfined Horizontal Surfaces," *J. Fluid Mech.*, Vol. 36, Part 1, pp. 173-192, (1969).

[73] Stewartson, K., "On Free Convection from a Horizontal Plate," *J. of Applied Mathematics and Physics (ZAMP)*, 9a, pp. 276-282, (1958).

[74] Sahraoui, M., Kaviany, M., and Marshall H., "Natural Convection from Horizontal Disks and Rings," *J. of Heat Transfer (ASME)*, Vol. 112, pp. 110-116, (1990).

[75] Torrance, K. E., and Rockett, J. A., "Numerical Study of Natural Convection in an Enclosure with Localized Heating from below - Creeping Flow to the Onset of Laminar Instability," *J. Fluid Mech.*, Vol. 36, Part 1, pp. 33-54, (1969).

[76] Yousef, W. W., Tarasuk, J. D., and Mckeen, W. J., "Free Convection Heat Transfer from Upward-Facing Isothermal Horizontal Surface," *J. of Heat Transfer (ASME)*, Vol. 104, pp. 493-500, (1982).

[77] Zakerullah, M., and Ackroyd, J. A. D., "Laminar Natural Convection Boundary Layers on Horizontal Circular Discs," *J. of Applied mathematics and Physics (ZAMP)*, Vol. 30, 427-435, (1979).

Table II-1.1 Previous Studies of Downward-Facing Heated Horizontal plate (two pages)

Researchers	Analytical Results	Experimental Results
O.A. Saunders et al. (1935)		Rectangular plate in air; Pr=0.7; $Nu=CRa^{1/4}$.
R. Weise (1935)		Square plate in air; $Nu=0.56Ra^{1/4}$.
J.V. Clifton et al. (1969)	Use integral method; boundary layer equation; Two-dimensional flow; $T_w=C$; $0.72<Pr<5$; $Nu_L=0.58Ra_L^{1/5}$.	$1.25\times10^4<Gr_L<1.25\times10^6$ $Nu_L=0.297Ra_L^{1/4}$.
S.N. Singh et al. (1969)	Use integral method; boundary layer equation Two-dimensional flow. Circular plate: * $Nu_R=0.638Ra_R^{1/5}$. Square plate: * $Nu_L=0.945Ra_L^{1/5}$. Infinite strip: * $Nu_L=0.66Ra_L^{1/5}$.	Circular plate: * $Nu_R=0.818Ra_R^{1/5}Pr^{-.016}$ Square plate: * $Nu_L=1.08Ra_L^{1/5}$.
C.J. Chen (1970)	Differential formulation; Two-dimensional boundary layer equation. $Nu_L=CGr_L^{1/4}$.	
R.C. Birkebak et al. (1970)		Square plate in water: * $Nu_L=0.898Ra_L^{1/5}$.
K.E. Hassan et al. (1970)		Rectangular plate in air: $Nu_L=0.06Gr_L^{1/3}$.
T. Aihara et al. (1972)		Square plate in air: $*Nu_L=0.66Ra_L^{1/5}$; $Ra\sim10^7$
T. Fujii et al. (1972)		Rectangular plate: $Nu_L=0.58Ra_L^{1/5}$; $10^6<Ra_L<10^{11}$.
T. Fujii et al. (1973)	Use Integral method; Two-dimensional boundary layer equation; $q_w=C$. Circular plate: $Nu_R=0.528Ra_R^{1/5}$; Pr=1. $Nu_R=0.506Ra_R^{1/5}$; Pr=0.7.	
F. Restrepo et al. (1974)		Square plate in air; $1.7\times10^6<Ra_L<7\times10^6$; $Nu_L=0.167Ra_L^{0.276}$.

Researchers	Analytical Results	Experimental Results
R.E. Faw et al. (1981)		Square plate in air; $T_w=C$; * $Nu_L=0.87Ra_L^{1/5}$.
D.W. Hatfield et al. (1981)		Rectangular and square plates; Pr=0.72; 6; 4800. $Nu_L=1.01Ra_L^{0.19}$.
R.E. Faw et al. (1982)		Circular plate; $T_w=C$. $1.07\times10^6<Ra_R<1.6\times10^6$ $Nu_{0,R}=0.487Ra_R^{1/5}$. $Nu_R=0.65Ra_R^{1/5}$.
R.J. Goldstein et al. (1983)	Finite difference methods; Two-dimensional infinite strip; Pr=0.72; * $Nu_L=0.975Ra_L^{0.19}$.	Square plate in air; * $Sh_L=0.861Ra_L^{1/5}$. 1/5 power is imposed; the power from experiment is 0.914.
T. Schulenberg (1984)	Differential formulation; for very small Prandtl number. Circular plate: $Nu_R=0.705Pr^{0.2}Ra_R^{1/5}$; $T_w=C$. $Nu_R=0.776Pr^{0.167}Ra_R^{*1/6}$; $q_w=C$	
J. Gryzagoridis (1984)		Rectangular plate: $Nu_x(T_w-T_\infty)=0.4Ra_x^{0.34}$. x:distance measured from the center.
T. Schulenberg (1985)	Differential formulation; for very large Prandtl number. Circular plate: $Nu_R=0.619Ra_R^{1/5}$; $T_w=C$ $Nu_R=0.693Ra_R^{*1/6}$; $q_w=C$.	
K.S. Chang et al. (1988)	Finite difference method. Square plate in air; Pr=0.7: $Nu_L=0.27Ra_L^{1/4}$.	
R. Karvinen et al. (1990)		Rectangular plate in air: $Nu_L=0.5Ra_L^{1/3}$; $T_w=C$.
P. Hrycak et al. (1990)	Differential formulation; for axisymmetric flow. Circular plate: $Nu_R=0.519Pr^{0.07}(mRa_R)^{1/4}$; $0.3<m<0.9$.	

TABLE II-3.1 : FREE CONVECTION OF DOWNWARD-FACING HEATED PLATE, ONE ASSUMED FUNCTION IN TEMPERATURE DISTRIBUTION AND PRESCRIBED SURFACE TEMPERATURE CASE.

Pr = 0.720

η	$f(\eta)$	$f'(\eta)$	$f''(\eta)$	$f'''(\eta)$	$f^{(4)}(\eta)$	$f^{(5)}(\eta)$	$\theta(\eta)$
.0	.000000	.000000	.763593	-1.000000	.462024	.000000	1.000000
.1	.003653	.071436	.665909	-.953562	.468909	.130382	.953800
.2	.013969	.133338	.572923	-.905855	.486699	.218691	.907627
.3	.030019	.186183	.484810	-.855994	.511353	.268160	.861551
.4	.050921	.230471	.401813	-.803481	.539140	.281918	.815676
.5	.075845	.266726	.324208	-.748175	.566668	.263662	.770138
.6	.104017	.295501	.252266	-.690256	.590958	.217996	.725097
.7	.134716	.317376	.186229	-.630174	.609538	.150469	.680726
.8	.167282	.332950	.126281	-.568602	.620532	.067372	.637208
.9	.201116	.342839	.072531	-.506363	.622715	-.024632	.594727
1.0	.235681	.347664	.025000	-.444372	.615529	-.118965	.553458
1.1	.270501	.348044	-.016383	-.383567	.599047	-.209600	.513565
1.2	.305162	.344587	-.051783	-.324852	.573903	-.291455	.475196
1.3	.339310	.337878	-.081450	-.269040	.541179	-.360664	.438475
1.4	.372648	.328477	-.105711	-.216822	.502277	-.414716	.403505
1.5	.404933	.316903	-.124953	-.168738	.458781	-.452437	.370360
1.6	.435972	.303639	-.139609	-.125164	.412333	-.473869	.339092
1.7	.465619	.289119	-.150143	-.086316	.364517	-.480050	.309725
1.8	.493767	.273732	-.157032	-.052258	.316773	-.472754	.282262
1.9	.520347	.257818	-.160752	-.022918	.270341	-.454220	.256682
2.0	.545323	.241672	-.161767	.001887	.226222	-.426901	.232948
2.1	.568682	.225540	-.160517	.022429	.185171	-.393252	.211006
2.2	.590438	.209630	-.157412	.039041	.147705	-.355572	.190788
2.3	.610621	.194107	-.152827	.052100	.114123	-.315892	.172217
2.4	.629277	.179103	-.147098	.061999	.084537	-.275913	.155209
2.5	.646463	.164716	-.140519	.069139	.058905	-.236987	.139673
2.6	.662243	.151019	-.133349	.073907	.037070	-.200123	.125518
2.7	.676691	.138059	-.125805	.076672	.018788	-.166019	.112650
2.8	.689881	.125864	-.118070	.077773	.003760	-.135104	.100977
2.9	.701890	.114446	-.110295	.077521	-.008346	-.107582	.090407
3.0	.712796	.103802	-.102602	.076190	-.017871	-.083484	.080853
3.1	.722675	.093920	-.095085	.074022	-.025153	-.062709	.072230
3.2	.731604	.084777	-.087818	.071223	-.030517	-.045064	.064460
3.3	.739654	.076346	-.080855	.067972	-.034262	-.030299	.057467
3.4	.746896	.068594	-.074234	.064416	-.036663	-.018128	.051180
3.5	.753395	.061487	-.067978	.060676	-.037965	-.008256	.045534
3.6	.759214	.054986	-.062102	.056852	-.038381	-.000389	.040468
3.7	.764411	.049054	-.056608	.053023	-.038100	.005755	.035927
3.8	.769042	.043652	-.051495	.049250	-.037279	.010435	.031859
3.9	.773158	.038742	-.046755	.045581	-.036054	.013888	.028218
4.0	.776806	.034289	-.042374	.042049	-.034535	.016326	.024960
4.1	.780030	.030256	-.038339	.038680	-.032816	.017935	.022047
4.2	.782870	.026610	-.034632	.035490	-.030971	.018874	.019443
4.3	.785363	.023319	-.031235	.032488	-.029059	.019281	.017117
4.4	.787544	.020353	-.028128	.029679	-.027128	.019273	.015040
4.5	.789444	.017685	-.025293	.027062	-.025215	.018946	.013185
4.6	.791090	.015286	-.022710	.024634	-.023347	.018382	.011530

4.7	.792510	.013135	-.020360	.022390	-.021544	.017646	.010053
4.8	.793725	.011207	-.018226	.020323	-.019822	.016792	.008735
4.9	.794758	.009483	-.016290	.018423	-.018188	.015863	.007560
5.0	.795628	.007943	-.014536	.016682	-.016650	.014893	.006511
5.1	.796352	.006570	-.012948	.015090	-.015210	.013909	.005576
5.2	.796947	.005349	-.011513	.013637	-.013868	.012931	.004743
5.3	.797426	.004263	-.010217	.012313	-.012623	.011974	.003999
5.4	.797803	.003301	-.009047	.011109	-.011473	.011049	.003337
5.5	.798090	.002450	-.007991	.010015	-.010412	.010165	.002746
5.6	.798297	.001699	-.007040	.009023	-.009438	.009326	.002220
5.7	.798433	.001039	-.006183	.008125	-.008545	.008537	.001750
5.8	.798507	.000460	-.005412	.007312	-.007729	.007797	.001332
5.9	.798527	-.000046	-.004718	.006577	-.006984	.007108	.000959
6.0	.798500	-.000486	-.004095	.005913	-.006306	.006469	.000626
6.1	.798432	-.000867	-.003534	.005314	-.005689	.005879	.000330
6.2	.798329	-.001195	-.003030	.004773	-.005129	.005334	.000066
6.3	.798195	-.001475	-.002577	.004286	-.004620	.004835	-.000169
6.4	.798035	-.001712	-.002171	.003847	-.004160	.004377	-.000379
6.5	.797854	-.001910	-.001806	.003453	-.003744	.003958	-.000566
6.6	.797654	-.002074	-.001479	.003097	-.003367	.003577	-.000733
6.7	.797440	-.002207	-.001186	.002778	-.003027	.003229	-.000882
6.8	.797214	-.002313	-.000923	.002491	-.002720	.002913	-.001015
6.9	.796978	-.002393	-.000687	.002233	-.002444	.002626	-.001133
7.0	.796736	-.002451	-.000475	.002001	-.002194	.002365	-.001238
7.1	.796489	-.002489	-.000286	.001793	-.001970	.002130	-.001332
7.2	.796239	-.002508	-.000116	.001606	-.001768	.001916	-.001416
7.3	.795988	-.002512	.000036	.001439	-.001586	.001724	-.001491
7.4	.795737	-.002502	.000173	.001289	-.001422	.001550	-.001557
7.5	.795488	-.002478	.000295	.001154	-.001275	.001393	-.001617
7.6	.795241	-.002443	.000404	.001033	-.001143	.001251	-.001670
7.7	.794999	-.002398	.000502	.000925	-.001025	.001123	-.001717
7.8	.794762	-.002343	.000589	.000828	-.000918	.001008	-.001759
7.9	.794531	-.002280	.000668	.000741	-.000823	.000905	-.001796
8.0	.794306	-.002210	.000738	.000663	-.000737	.000812	-.001830
8.1	.794089	-.002133	.000800	.000593	-.000660	.000728	-.001860
8.2	.793880	-.002050	.000857	.000531	-.000591	.000653	-.001887
8.3	.793679	-.001962	.000907	.000475	-.000529	.000585	-.001910
8.4	.793488	-.001869	.000952	.000425	-.000474	.000525	-.001931
8.5	.793306	-.001772	.000992	.000380	-.000424	.000470	-.001950
8.6	.793134	-.001671	.001028	.000340	-.000379	.000421	-.001967
8.7	.792972	-.001566	.001060	.000304	-.000340	.000377	-.001982
8.8	.792820	-.001459	.001089	.000272	-.000304	.000338	-.001996
8.9	.792680	-.001349	.001114	.000243	-.000272	.000303	-.002008
9.0	.792551	-.001236	.001137	.000217	-.000243	.000271	-.002018
9.1	.792433	-.001121	.001158	.000194	-.000218	.000243	-.002028
9.2	.792327	-.001005	.001176	.000174	-.000195	.000217	-.002036
9.3	.792232	-.000886	.001193	.000155	-.000174	.000194	-.002044
9.4	.792149	-.000766	.001207	.000139	-.000156	.000174	-.002051
9.5	.792079	-.000645	.001220	.000124	-.000139	.000156	-.002057
9.6	.792020	-.000522	.001232	.000111	-.000124	.000139	-.002062
9.7	.791974	-.000398	.001243	.000099	-.000111	.000125	-.002067
9.8	.791941	-.000274	.001252	.000088	-.000100	.000111	-.002071
9.9	.791920	-.000148	.001260	.000079	-.000089	.000100	-.002075
10.0	.791911	-.000021	.001268	.000071	-.000080	.000089	-.002079

TABLE II-3.2 : FREE CONVECTION OF DOWNWARD-FACING HEATED PLATE, ONE ASSUMED FUNCTION IN TEMPERATURE DISTRIBUTION AND PRESCRIBED SURFACE TEMPERATURE CASE.

Pr = 1.0

η	$f(\eta)$	$f'(\eta)$	$f''(\eta)$	$f'''(\eta)$	$f^{(4)}(\eta)$	$f^{(5)}(\eta)$	$\theta(\eta)$
.0	.000000	.000000	.723457	-1.000000	.518540	.000000	1.000000
.1	.003453	.067432	.626056	-.947925	.524966	.120636	.948149
.2	.013171	.125386	.533912	-.894681	.541175	.196472	.896339
.3	.028232	.174395	.447184	-.839506	.562914	.231920	.844670
.4	.047770	.215011	.366087	-.782042	.586359	.231392	.793296
.5	.070973	.247808	.290852	-.722290	.608158	.199880	.742413
.6	.097091	.273384	.221696	-.660560	.625494	.143162	.692250
.7	.125430	.292356	.158788	-.597414	.636167	.067733	.643052
.8	.155363	.305353	.102235	-.533600	.638648	-.019495	.595074
.9	.186323	.313015	.052061	-.469986	.632105	-.111612	.548564
1.0	.217809	.315976	.008201	-.407486	.616378	-.202173	.503755
1.1	.249382	.314861	-.029503	-.347002	.591909	-.285610	.460855
1.2	.280665	.310273	-.061295	-.289365	.559641	-.357547	.420040
1.3	.311340	.302788	-.087495	-.235291	.520885	-.414974	.381453
1.4	.341145	.292947	-.108491	-.185353	.477185	-.456274	.345193
1.5	.369868	.281249	-.124717	-.139964	.430180	-.481120	.311323
1.6	.397348	.268147	-.136644	-.099373	.381485	-.490278	.279866
1.7	.423464	.254048	-.144755	-.063673	.332595	-.485344	.250810
1.8	.448136	.239307	-.149540	-.032817	.284814	-.468474	.224113
1.9	.471314	.224235	-.151475	-.006637	.239217	-.442111	.199702
2.0	.492980	.209092	-.151015	.015127	.196625	-.408760	.177487
2.1	.513138	.194097	-.148585	.032808	.157618	-.370808	.157355
2.2	.531811	.179427	-.144577	.046782	.122545	-.330395	.139187
2.3	.549039	.165223	-.139339	.057453	.091560	-.289340	.122851
2.4	.564874	.151590	-.133182	.065230	.064649	-.249106	.108212
2.5	.579379	.138608	-.126376	.070514	.041673	-.210807	.095137
2.6	.592619	.126329	-.119150	.073688	.022397	-.175226	.083492
2.7	.604669	.114786	-.111697	.075107	.006521	-.142858	.073148
2.8	.615602	.103992	-.104176	.075094	-.006291	-.113961	.063982
2.9	.625492	.093948	-.096716	.073939	-.016389	-.088600	.055877
3.0	.634416	.084643	-.089418	.071895	-.024126	-.066694	.048725
3.1	.642445	.076057	-.082359	.069182	-.029837	-.048063	.042426
3.2	.649650	.068161	-.075598	.065985	-.033839	-.032455	.036885
3.3	.656099	.060926	-.069173	.062461	-.036420	-.019581	.032020
3.4	.661856	.054315	-.063112	.058740	-.037836	-.009136	.027753
3.5	.666982	.048291	-.057428	.054925	-.038317	-.000813	.024014
3.6	.671533	.042816	-.052127	.051101	-.038060	.005682	.020743
3.7	.675562	.037853	-.047206	.047332	-.037233	.010623	.017883
3.8	.679119	.033363	-.042657	.043668	-.035979	.014262	.015384
3.9	.682249	.029309	-.038468	.040146	-.034416	.016822	.013202
4.0	.684994	.025658	-.034623	.036792	-.032644	.018501	.011299
4.1	.687393	.022374	-.031103	.033622	-.030740	.019470	.009639
4.2	.689480	.019427	-.027892	.030646	-.028768	.019875	.008193
4.3	.691288	.016786	-.024968	.027869	-.026779	.019842	.006932
4.4	.692847	.014424	-.022311	.025290	-.024811	.019472	.005835
4.5	.694182	.012315	-.019903	.022905	-.022893	.018854	.004879
4.6	.695317	.010436	-.017724	.020709	-.021047	.018056	.004048

4.7	.696276	.008764	-.015755	.018693	-.019286	.017137	.003324
4.8	.697076	.007278	-.013980	.016848	-.017622	.016142	.002695
4.9	.697737	.005962	-.012380	.015165	-.016059	.015107	.002147
5.0	.698274	.004797	-.010942	.013633	-.014601	.014061	.001671
5.1	.698701	.003769	-.009649	.012241	-.013246	.013025	.001256
5.2	.699032	.002863	-.008489	.010980	-.011995	.012014	.000896
5.3	.699277	.002067	-.007449	.009839	-.010842	.011041	.000583
5.4	.699448	.001369	-.006517	.008809	-.009785	.010114	.000311
5.5	.699554	.000760	-.005684	.007879	-.008818	.009238	.000074
5.6	.699603	.000230	-.004939	.007042	-.007935	.008416	-.000132
5.7	.699602	-.000230	-.004273	.006289	-.007133	.007650	-.000311
5.8	.699559	-.000627	-.003678	.005613	-.006404	.006938	-.000467
5.9	.699479	-.000968	-.003148	.005006	-.005743	.006281	-.000602
6.0	.699367	-.001259	-.002675	.004463	-.005146	.005676	-.000720
6.1	.699229	-.001505	-.002253	.003975	-.004606	.005121	-.000822
6.2	.699067	-.001711	-.001878	.003539	-.004120	.004614	-.000911
6.3	.698888	-.001882	-.001544	.003150	-.003682	.004151	-.000988
6.4	.698692	-.002021	-.001247	.002802	-.003288	.003731	-.001055
6.5	.698484	-.002132	-.000982	.002491	-.002935	.003349	-.001114
6.6	.698267	-.002218	-.000747	.002213	-.002617	.003003	-.001165
6.7	.698041	-.002282	-.000539	.001966	-.002333	.002691	-.001209
6.8	.697811	-.002327	-.000353	.001746	-.002078	.002408	-.001248
6.9	.697577	-.002354	-.000189	.001550	-.001850	.002154	-.001281
7.0	.697340	-.002365	-.000043	.001375	-.001647	.001925	-.001310
7.1	.697104	-.002363	.000087	.001220	-.001465	.001719	-.001335
7.2	.696868	-.002348	.000202	.001081	-.001302	.001534	-.001357
7.3	.696635	-.002323	.000304	.000959	-.001157	.001368	-.001377
7.4	.696404	-.002288	.000394	.000849	-.001028	.001219	-.001393
7.5	.696177	-.002244	.000474	.000753	-.000913	.001086	-.001408
7.6	.695955	-.002193	.000545	.000667	-.000810	.000967	-.001420
7.7	.695739	-.002136	.000608	.000590	-.000719	.000861	-.001431
7.8	.695529	-.002072	.000663	.000522	-.000638	.000765	-.001441
7.9	.695325	-.002003	.000712	.000462	-.000565	.000681	-.001449
8.0	.695128	-.001930	.000756	.000409	-.000501	.000605	-.001456
8.1	.694939	-.001852	.000794	.000362	-.000444	.000537	-.001463
8.2	.694758	-.001771	.000829	.000320	-.000394	.000477	-.001468
8.3	.694585	-.001687	.000859	.000283	-.000349	.000424	-.001473
8.4	.694420	-.001599	.000885	.000250	-.000309	.000376	-.001477
8.5	.694265	-.001510	.000909	.000221	-.000273	.000333	-.001481
8.6	.694119	-.001418	.000930	.000195	-.000242	.000296	-.001484
8.7	.693982	-.001324	.000948	.000173	-.000214	.000262	-.001486
8.8	.693854	-.001228	.000964	.000152	-.000189	.000232	-.001489
8.9	.693736	-.001131	.000978	.000135	-.000167	.000206	-.001491
9.0	.693628	-.001033	.000991	.000119	-.000148	.000182	-.001493
9.1	.693529	-.000933	.001002	.000105	-.000131	.000161	-.001494
9.2	.693441	-.000832	.001012	.000093	-.000116	.000143	-.001496
9.3	.693363	-.000730	.001021	.000082	-.000102	.000126	-.001497
9.4	.693295	-.000628	.001029	.000072	-.000090	.000112	-.001498
9.5	.693237	-.000525	.001035	.000064	-.000080	.000099	-.001499
9.6	.693190	-.000421	.001041	.000056	-.000070	.000088	-.001500
9.7	.693153	-.000317	.001047	.000049	-.000062	.000077	-.001500
9.8	.693127	-.000212	.001051	.000044	-.000055	.000068	-.001501
9.9	.693111	-.000106	.001055	.000038	-.000048	.000061	-.001501
10.0	.693106	-.000001	.001059	.000034	-.000043	.000053	-.001502

TABLE II-3.3 : FREE CONVECTION OF DOWNWARD-FACING HEATED PLATE, ONE ASSUMED FUNCTION IN TEMPERATURE DISTRIBUTION AND PRESCRIBED SURFACE TEMPERATURE CASE.

Pr = 5.0

η	$f(\eta)$	$f'(\eta)$	$f''(\eta)$	$f'''(\eta)$	$f^{(4)}(\eta)$	$f^{(5)}(\eta)$	$\theta(\eta)$
.0	.000000	.000000	.537160	-1.000000	.866912	.000000	1.000000
.1	.002523	.048861	.441499	-.913168	.870779	.062991	.913328
.2	.009468	.088590	.354547	-.825771	.876915	.048162	.826905
.3	.019966	.120062	.276360	-.737942	.878386	-.027368	.741322
.4	.033234	.144155	.206948	-.650423	.870034	-.145088	.657448
.5	.048580	.161742	.146226	-.564373	.848613	-.285500	.576327
.6	.065394	.173682	.093978	-.481182	.812816	-.429542	.499056
.7	.083156	.180808	.049847	-.402274	.763148	-.560418	.426676
.8	.101422	.183906	.013337	-.328949	.701607	-.665233	.360065
.9	.119827	.183709	-.016164	-.262248	.631242	-.736014	.299871
1.0	.138076	.180884	-.039357	-.202875	.555639	-.769896	.246463
1.1	.155936	.176023	-.056995	-.151173	.478441	-.768536	.199932
1.2	.173230	.169644	-.069847	-.107130	.402941	-.736974	.160108
1.3	.189829	.162188	-.078666	-.070438	.331819	-.682253	.126609
1.4	.205644	.154022	-.084162	-.040555	.267004	-.612101	.098893
1.5	.220620	.145445	-.086981	-.016787	.209667	-.533856	.076321
1.6	.234727	.136695	-.087697	.001644	.160293	-.453764	.058211
1.7	.247959	.127959	-.086804	.015535	.118815	-.376614	.043886
1.8	.260324	.119374	-.084716	.025655	.084762	-.305683	.032702
1.9	.271843	.111044	-.081775	.032711	.057406	-.242876	.024079
2.0	.282544	.103039	-.078255	.037331	.035889	-.188978	.017507
2.1	.292463	.095405	-.074372	.040054	.019315	-.143947	.012550
2.2	.301638	.088171	-.070292	.041330	.006823	-.107194	.008850
2.3	.310111	.081349	-.066142	.041528	-.002370	-.077811	.006112
2.4	.317922	.074942	-.062013	.040943	-.008950	-.054757	.004104
2.5	.325113	.068943	-.057971	.039806	-.013497	-.036980	.002642
2.6	.331724	.063343	-.054064	.038295	-.016489	-.023495	.001586
2.7	.337794	.058125	-.050320	.036547	-.018310	-.013432	.000828
2.8	.343361	.053273	-.046759	.034662	-.019264	-.006048	.000287
2.9	.348460	.048767	-.043390	.032715	-.019588	-.000730	-.000097
3.0	.353125	.044588	-.040216	.030759	-.019462	.003018	-.000368
3.1	.357388	.040717	-.037237	.028833	-.019024	.005585	-.000559
3.2	.361278	.037135	-.034448	.026961	-.018375	.007277	-.000692
3.3	.364824	.033822	-.031842	.025162	-.017590	.008325	-.000785
3.4	.368051	.030760	-.029413	.023446	-.016725	.008905	-.000849
3.5	.370984	.027933	-.027150	.021819	-.015820	.009151	-.000894
3.6	.373645	.025325	-.025046	.020282	-.014903	.009160	-.000925
3.7	.376056	.022919	-.023091	.018838	-.013993	.009004	-.000946
3.8	.378235	.020702	-.021275	.017483	-.013106	.008737	-.000960
3.9	.380202	.018660	-.019591	.016216	-.012248	.008397	-.000970
4.0	.381972	.016780	-.018029	.015032	-.011428	.008012	-.000977
4.1	.383563	.015050	-.016582	.013929	-.010647	.007602	-.000982
4.2	.384987	.013460	-.015241	.012901	-.009908	.007181	-.000985
4.3	.386259	.011999	-.013999	.011946	-.009211	.006760	-.000987
4.4	.387391	.010657	-.012850	.011058	-.008555	.006346	-.000988
4.5	.388394	.009426	-.011786	.010233	-.007941	.005944	-.000989
4.6	.389279	.008297	-.010801	.009468	-.007366	.005556	-.000990

4.7	.390057	.007263	-.009890	.008759	-.006829	.005186	-.000991
4.8	.390735	.006317	-.009048	.008101	-.006328	.004833	-.000991
4.9	.391323	.005451	-.008268	.007492	-.005862	.004499	-.000991
5.0	.391828	.004661	-.007548	.006928	-.005428	.004184	-.000991
5.1	.392257	.003940	-.006881	.006405	-.005024	.003888	-.000991
5.2	.392618	.003283	-.006265	.005922	-.004650	.003610	-.000991
5.3	.392916	.002685	-.005696	.005475	-.004302	.003350	-.000991
5.4	.393157	.002143	-.005169	.005061	-.003979	.003106	-.000992
5.5	.393346	.001650	-.004683	.004678	-.003680	.002879	-.000992
5.6	.393488	.001205	-.004233	.004324	-.003403	.002667	-.000992
5.7	.393588	.000803	-.003817	.003997	-.003146	.002470	-.000992
5.8	.393650	.000440	-.003433	.003694	-.002908	.002286	-.000992
5.9	.393678	.000115	-.003077	.003415	-.002688	.002116	-.000992
6.0	.393674	-.000176	-.002749	.003156	-.002485	.001957	-.000992
6.1	.393644	-.000435	-.002445	.002917	-.002297	.001811	-.000992
6.2	.393588	-.000666	-.002165	.002696	-.002122	.001674	-.000992
6.3	.393511	-.000869	-.001906	.002492	-.001961	.001548	-.000992
6.4	.393415	-.001048	-.001666	.002304	-.001812	.001431	-.000992
6.5	.393303	-.001203	-.001444	.002129	-.001675	.001323	-.000992
6.6	.393175	-.001337	-.001240	.001968	-.001548	.001222	-.000992
6.7	.393036	-.001451	-.001050	.001819	-.001430	.001129	-.000992
6.8	.392886	-.001548	-.000875	.001682	-.001322	.001044	-.000992
6.9	.392727	-.001627	-.000714	.001555	-.001221	.000964	-.000992
7.0	.392561	-.001691	-.000564	.001437	-.001129	.000891	-.000992
7.1	.392389	-.001740	-.000426	.001329	-.001043	.000823	-.000992
7.2	.392213	-.001776	-.000298	.001229	-.000964	.000760	-.000992
7.3	.392034	-.001800	-.000180	.001136	-.000891	.000702	-.000992
7.4	.391854	-.001813	-.000071	.001050	-.000823	.000649	-.000992
7.5	.391672	-.001815	.000030	.000971	-.000761	.000599	-.000992
7.6	.391491	-.001807	.000124	.000898	-.000703	.000554	-.000992
7.7	.391311	-.001790	.000210	.000830	-.000650	.000512	-.000992
7.8	.391133	-.001765	.000290	.000768	-.000601	.000473	-.000992
7.9	.390958	-.001732	.000364	.000710	-.000555	.000437	-.000992
8.0	.390787	-.001692	.000432	.000657	-.000513	.000403	-.000992
8.1	.390620	-.001646	.000495	.000607	-.000474	.000373	-.000992
8.2	.390458	-.001593	.000554	.000562	-.000439	.000344	-.000992
8.3	.390302	-.001535	.000608	.000520	-.000406	.000318	-.000992
8.4	.390151	-.001472	.000658	.000481	-.000375	.000294	-.000992
8.5	.390007	-.001404	.000704	.000444	-.000347	.000272	-.000992
8.6	.389871	-.001331	.000747	.000411	-.000321	.000251	-.000992
8.7	.389741	-.001255	.000786	.000380	-.000296	.000232	-.000992
8.8	.389620	-.001174	.000823	.000352	-.000274	.000214	-.000992
8.9	.389507	-.001090	.000857	.000325	-.000253	.000198	-.000992
9.0	.389402	-.001003	.000888	.000301	-.000234	.000183	-.000992
9.1	.389306	-.000913	.000917	.000278	-.000217	.000169	-.000992
9.2	.389219	-.000820	.000944	.000258	-.000201	.000157	-.000992
9.3	.389142	-.000724	.000969	.000238	-.000185	.000145	-.000992
9.4	.389075	-.000626	.000991	.000220	-.000172	.000134	-.000992
9.5	.389017	-.000526	.001013	.000204	-.000159	.000124	-.000992
9.6	.388970	-.000424	.001032	.000189	-.000147	.000114	-.000992
9.7	.388932	-.000319	.001050	.000175	-.000136	.000106	-.000992
9.8	.388906	-.000213	.001067	.000162	-.000126	.000098	-.000992
9.9	.388890	-.000106	.001083	.000149	-.000116	.000090	-.000992
10.0	.388885	.000003	.001097	.000138	-.000108	.000084	-.000992

TABLE II-3.4 : FREE CONVECTION OF DOWNWARD-FACING HEATED PLATE, ONE ASSUMED FUNCTION IN TEMPERATURE DISTRIBUTION AND PRESCRIBED CONSTANT SURFACE FLUX CASE.

Pr = 0.72

η	$f(\eta)$	$f'(\eta)$	$f''(\eta)$	$f'''(\eta)$	$f^{(4)}(\eta)$	$f^{(5)}(\eta)$	$\theta(\eta)$
.0	.000000	.000000	1.219610	-1.870963	1.000000	.000000	1.870963
.2	.021965	.207847	.865680	-1.665901	1.071018	.613895	1.671073
.4	.078700	.349137	.554816	-1.438038	1.210489	.702085	1.472607
.6	.157788	.432998	.292284	-1.183436	1.325040	.390486	1.278685
.8	.248745	.469572	.082454	-.913935	1.352299	-.135961	1.093413
1.0	.343179	.469571	-.073653	-.649886	1.270338	-.668916	.920935
1.2	.434837	.443486	-.179262	-.412065	1.095189	-1.048343	.764644
1.4	.519469	.400779	-.241245	-.215427	.865905	-1.207252	.626689
1.6	.594567	.349296	-.268625	-.066403	.625750	-1.165859	.507842
1.8	.659004	.295001	-.270897	.036426	.408352	-.992774	.407645
2.0	.712660	.242031	-.256695	.099727	.232327	-.763706	.324725
2.2	.756078	.192949	-.233044	.132470	.102699	-.536322	.257158
2.4	.790189	.149093	-.205142	.143642	.015468	-.343184	.202790
2.6	.816097	.110937	-.176508	.140932	-.037659	-.195870	.159471
2.8	.834939	.078393	-.149298	.130238	-.065842	-.092790	.125216
3.0	.847801	.051045	-.124665	.115712	-.077208	-.026169	.098276
3.2	.855666	.028322	-.103087	.100048	-.078117	.013306	.077169
3.4	.859397	.009603	-.084613	.084855	-.073129	.034073	.060670
3.6	.859733	-.005718	-.069055	.070984	-.065287	.042792	.047787
3.8	.857299	-.018193	-.056106	.058802	-.056491	.044274	.037729
4.0	.852613	-.028311	-.045417	.048377	-.047841	.041773	.029871
4.2	.846104	-.036488	-.036644	.039617	-.039908	.037365	.023724
4.4	.838124	-.043075	-.029471	.032349	-.032937	.032304	.018907
4.6	.828960	-.048364	-.023618	.026374	-.026982	.027296	.015122
4.8	.818848	-.052595	-.018848	.021492	-.021990	.022701	.012142
5.0	.807980	-.055962	-.014961	.017520	-.017863	.018670	.009788
5.2	.796510	-.058627	-.011790	.014297	-.014483	.015235	.007922
5.4	.784567	-.060717	-.009201	.011685	-.011731	.012366	.006439
5.6	.772255	-.062339	-.007083	.009570	-.009503	.010001	.005256
5.8	.759658	-.063576	-.005347	.007856	-.007702	.008070	.004309
6.0	.746845	-.064498	-.003919	.006466	-.006250	.006505	.003548
6.2	.733876	-.065160	-.002743	.005337	-.005080	.005242	.002935
6.4	.720796	-.065608	-.001771	.004419	-.004137	.004226	.002438
6.6	.707644	-.065879	-.000964	.003670	-.003376	.003410	.002035
6.8	.694454	-.066003	-.000293	.003058	-.002762	.002755	.001706
7.0	.681251	-.066004	.000267	.002557	-.002266	.002229	.001436
7.2	.668059	-.065903	.000735	.002146	-.001864	.001808	.001215
7.4	.654896	-.065715	.001130	.001807	-.001537	.001469	.001032
7.6	.641778	-.065455	.001462	.001527	-.001272	.001196	.000881
7.8	.628718	-.065134	.001744	.001295	-.001055	.000977	.000755
8.0	.615728	-.064760	.001983	.001102	-.000878	.000799	.000650
8.2	.602817	-.064343	.002187	.000941	-.000733	.000656	.000562
8.4	.589993	-.063888	.002361	.000807	-.000614	.000540	.000489
8.6	.577264	-.063400	.002511	.000694	-.000516	.000446	.000426
8.8	.564635	-.062885	.002640	.000600	-.000435	.000369	.000374
9.0	.552112	-.062345	.002752	.000520	-.000367	.000306	.000329
9.2	.539698	-.061785	.002849	.000452	-.000311	.000255	.000290
9.4	.527399	-.061207	.002933	.000395	-.000265	.000213	.000258
9.6	.515217	-.060612	.003007	.000346	-.000226	.000178	.000230
9.8	.503155	-.060004	.003072	.000304	-.000193	.000149	.000205
10.0	.491216	-.059384	.003129	.000268	-.000166	.000126	.000184
10.2	.479402	-.058753	.003179	.000237	-.000143	.000106	.000166
10.4	.467715	-.058113	.003224	.000211	-.000123	.000090	.000150
10.6	.456157	-.057464	.003264	.000188	-.000107	.000076	.000136
10.8	.444730	-.056807	.003300	.000168	-.000092	.000065	.000124
11.0	.433435	-.056144	.003331	.000151	-.000080	.000055	.000114
11.2	.422273	-.055475	.003360	.000136	-.000070	.000047	.000104
11.4	.411245	-.054800	.003386	.000122	-.000061	.000041	.000096
11.6	.400353	-.054121	.003409	.000111	-.000054	.000035	.000088
11.8	.389597	-.053437	.003430	.000101	-.000047	.000030	.000082
12.0	.378978	-.052749	.003449	.000092	-.000042	.000026	.000076

12.2	.368498	-.052057	.003467	.000084	-.000037	.000023	.000071
12.4	.358156	-.051362	.003483	.000077	-.000033	.000020	.000066
12.6	.347953	-.050664	.003498	.000071	-.000029	.000017	.000062
12.8	.337890	-.049963	.003512	.000066	-.000026	.000015	.000058
13.0	.327968	-.049260	.003524	.000061	-.000023	.000013	.000054
13.2	.318187	-.048553	.003536	.000056	-.000021	.000012	.000051
13.4	.308547	-.047845	.003547	.000052	-.000018	.000010	.000048
13.6	.299049	-.047135	.003557	.000049	-.000016	.000009	.000045
13.8	.289693	-.046422	.003566	.000046	-.000015	.000008	.000043
14.0	.280480	-.045708	.003575	.000043	-.000013	.000007	.000041
14.2	.271410	-.044992	.003584	.000041	-.000012	.000006	.000039
14.4	.262483	-.044275	.003592	.000038	-.000011	.000006	.000037
14.6	.253700	-.043556	.003599	.000036	-.000010	.000005	.000035
14.8	.245061	-.042835	.003606	.000034	-.000009	.000004	.000033
15.0	.236566	-.042113	.003613	.000033	-.000008	.000004	.000032
15.2	.228215	-.041390	.003619	.000031	-.000007	.000004	.000030
15.4	.220010	-.040666	.003625	.000030	-.000007	.000003	.000029
15.6	.211949	-.039940	.003631	.000029	-.000006	.000003	.000028
15.8	.204034	-.039213	.003637	.000027	-.000005	.000003	.000026
16.0	.196264	-.038486	.003642	.000026	-.000005	.000002	.000025
16.2	.188640	-.037757	.003647	.000025	-.000004	.000002	.000024
16.4	.181161	-.037027	.003652	.000025	-.000004	.000002	.000023
16.6	.173829	-.036296	.003657	.000024	-.000004	.000002	.000022
16.8	.166643	-.035564	.003662	.000023	-.000003	.000002	.000021
17.0	.159604	-.034831	.003666	.000023	-.000003	.000002	.000020
17.2	.152711	-.034097	.003671	.000022	-.000003	.000001	.000020
17.4	.145965	-.033363	.003675	.000021	-.000002	.000001	.000019
17.6	.139366	-.032627	.003679	.000021	-.000002	.000001	.000018
17.8	.132914	-.031891	.003683	.000021	-.000002	.000001	.000017
18.0	.126609	-.031154	.003688	.000020	-.000002	.000001	.000017
18.2	.120452	-.030416	.003692	.000020	-.000001	.000001	.000016
18.4	.114443	-.029677	.003696	.000020	-.000001	.000001	.000015
18.6	.108581	-.028938	.003699	.000019	-.000001	.000001	.000015
18.8	.102868	-.028198	.003703	.000019	-.000001	.000001	.000014
19.0	.097302	-.027457	.003707	.000019	-.000001	.000001	.000013
19.2	.091885	-.026715	.003711	.000019	-.000001	.000001	.000013
19.4	.086617	-.025972	.003715	.000019	.000000	.000001	.000012
19.6	.081496	-.025229	.003718	.000019	.000000	.000001	.000012
19.8	.076525	-.024485	.003722	.000019	.000000	.000001	.000011
20.0	.071703	-.023740	.003726	.000019	.000000	.000001	.000011
20.2	.067029	-.022994	.003730	.000019	.000000	.000001	.000010
20.4	.062505	-.022248	.003733	.000019	.000000	.000001	.000010
20.6	.058130	-.021501	.003737	.000019	.000000	.000001	.000009
20.8	.053904	-.020753	.003741	.000019	.000000	.000001	.000009
21.0	.049829	-.020005	.003745	.000019	.000001	.000001	.000008
21.2	.045903	-.019255	.003748	.000019	.000001	.000001	.000008
21.4	.042127	-.018505	.003752	.000019	.000001	.000001	.000007
21.6	.038501	-.017755	.003756	.000019	.000001	.000000	.000007
21.8	.035025	-.017003	.003760	.000019	.000001	.000000	.000006
22.0	.031699	-.016251	.003764	.000020	.000001	.000000	.000006
22.2	.028525	-.015497	.003768	.000020	.000001	.000000	.000005
22.4	.025501	-.014743	.003772	.000020	.000001	.000000	.000005
22.6	.022627	-.013989	.003776	.000020	.000001	.000000	.000004
22.8	.019905	-.013233	.003780	.000021	.000001	.000000	.000004
23.0	.017334	-.012477	.003784	.000021	.000001	.000000	.000004
23.2	.014915	-.011719	.003788	.000021	.000002	.000000	.000003
23.4	.012646	-.010961	.003793	.000021	.000002	.000000	.000003
23.6	.010530	-.010202	.003797	.000022	.000002	.000000	.000002
23.8	.008566	-.009443	.003801	.000022	.000002	.000000	.000002
24.0	.006753	-.008682	.003806	.000023	.000002	.000000	.000001
24.2	.005093	-.007920	.003810	.000023	.000002	.000000	.000001
24.4	.003585	-.007158	.003815	.000023	.000002	.000000	.000001
24.6	.002230	-.006394	.003820	.000024	.000002	.000000	.000000
24.8	.001027	-.005630	.003824	.000024	.000002	.000000	.000000
25.0	-.000022	-.004865	.003829	.000025	.000002	.000000	-.000001

TABLE II-3.5 : FREE CONVECTION OF DOWNWARD-FACING HEATED PLATE, ONE ASSUMED FUNCTION IN TEMPERATURE DISTRIBUTION AND PRESCRIBED CONSTANT SURFACE FLUX CASE.
Pr = 1.0

η	$f(\eta)$	$f'(\eta)$	$f''(\eta)$	$f'''(\eta)$	$f^{(4)}(\eta)$	$f^{(5)}(\eta)$	$\theta(\eta)$
.0	.000000	.000000	1.076521	-1.704898	1.000000	.000000	1.704898
.2	.019324	.182548	.755749	-1.500917	1.055363	.468645	1.505033
.4	.069019	.305120	.477344	-1.279697	1.157335	.485793	1.306904
.6	.137962	.376567	.245123	-1.040114	1.228360	.184666	1.114282
.8	.216874	.406434	.061770	-.793641	1.221289	-.265023	.932037
1.0	.298418	.404520	-.073037	-.557682	1.123998	-.691844	.764910
1.2	.377191	.380207	-.163128	-.348908	.954256	-.975871	.616526
1.4	.449565	.341809	-.215177	-.178541	.746110	-1.075307	.488847
1.6	.513432	.296126	-.237390	-.050649	.534854	-1.015042	.382107
1.8	.567875	.248282	-.238130	.036977	.346822	-.853866	.295123
2.0	.612839	.201804	-.224871	.090579	.195921	-.652908	.225765
2.2	.648835	.158861	-.203640	.118043	.085241	-.457511	.171452
2.4	.676696	.120580	-.178878	.127101	.010835	-.292786	.129531
2.6	.697404	.087343	-.153586	.124315	-.034512	-.167295	.097537
2.8	.711964	.059056	-.129603	.114712	-.058591	-.079275	.073322
3.0	.721332	.035347	-.107917	.101834	-.068282	-.022128	.055103
3.2	.726374	.015709	-.088932	.087995	-.068979	.011942	.041447
3.4	.727850	-.000409	-.072689	.074580	-.064569	.030007	.031233
3.6	.726410	-.013539	-.059021	.062331	-.057666	.037681	.023599
3.8	.722601	-.024171	-.047657	.051569	-.049914	.039056	.017889
4.0	.716879	-.032735	-.038290	.042357	-.042275	.036924	.013612
4.2	.709620	-.039600	-.030616	.034617	-.035256	.033088	.010402
4.4	.701132	-.045075	-.024355	.028199	-.029079	.028647	.007985
4.6	.691665	-.049419	-.019260	.022926	-.023795	.024228	.006159
4.8	.681425	-.052843	-.015120	.018624	-.019364	.020158	.004774
5.0	.670578	-.055519	-.011756	.015129	-.015699	.016577	.003720
5.2	.659258	-.057587	-.009024	.012300	-.012698	.013519	.002914
5.4	.647576	-.059162	-.006801	.010013	-.010258	.010961	.002295
5.6	.635620	-.060335	-.004989	.008165	-.008284	.008851	.001818
5.8	.623464	-.061180	-.003511	.006674	-.006692	.007129	.001447
6.0	.611166	-.061757	-.002301	.005468	-.005411	.005733	.001158
6.2	.598776	-.062115	-.001308	.004493	-.004381	.004607	.000932
6.4	.586332	-.062292	-.000491	.003702	-.003553	.003703	.000754
6.6	.573869	-.062321	.000183	.003061	-.002888	.002978	.000614
6.8	.561412	-.062227	.000741	.002539	-.002352	.002398	.000502
7.0	.548985	-.062031	.001204	.002113	-.001921	.001933	.000413
7.2	.536606	-.061750	.001591	.001765	-.001573	.001561	.000341
7.4	.524290	-.061398	.001914	.001479	-.001291	.001263	.000283
7.6	.512050	-.060988	.002186	.001245	-.001063	.001025	.000236
7.8	.499898	-.060527	.002415	.001051	-.000878	.000833	.000198
8.0	.487842	-.060024	.002609	.000891	-.000728	.000679	.000167
8.2	.475891	-.059485	.002773	.000758	-.000605	.000555	.000141
8.4	.464050	-.058916	.002913	.000648	-.000504	.000455	.000120
8.6	.452326	-.058321	.003033	.000555	-.000422	.000373	.000102
8.8	.440723	-.057704	.003137	.000478	-.000354	.000308	.000087
9.0	.429246	-.057068	.003225	.000413	-.000298	.000254	.000075
9.2	.417897	-.056415	.003302	.000358	-.000252	.000211	.000064
9.4	.406681	-.055747	.003369	.000312	-.000213	.000175	.000056
9.6	.395599	-.055068	.003428	.000272	-.000181	.000146	.000048
9.8	.384654	-.054377	.003479	.000239	-.000154	.000122	.000042
10.0	.373849	-.053677	.003523	.000210	-.000132	.000102	.000036
10.2	.363184	-.052968	.003563	.000186	-.000113	.000086	.000032
10.4	.352662	-.052252	.003598	.000165	-.000097	.000073	.000027
10.6	.342284	-.051529	.003629	.000147	-.000084	.000061	.000024
10.8	.332051	-.050800	.003657	.000131	-.000073	.000052	.000021
11.0	.321964	-.050066	.003682	.000118	-.000063	.000044	.000018
11.2	.312025	-.049328	.003704	.000106	-.000055	.000038	.000016
11.4	.302234	-.048585	.003724	.000096	-.000048	.000032	.000014
11.6	.292591	-.047838	.003742	.000087	-.000042	.000028	.000012
11.8	.283099	-.047088	.003759	.000079	-.000037	.000024	.000010
12.0	.273756	-.046335	.003774	.000072	-.000032	.000021	.000009

12.2	.264565	-.045578	.003788	.000066	-.000029	.000018	.000007
12.4	.255525	-.044820	.003800	.000060	-.000025	.000015	.000006
12.6	.246637	-.044058	.003812	.000056	-.000022	.000013	.000005
12.8	.237902	-.043295	.003823	.000051	-.000020	.000012	.000004
13.0	.229320	-.042529	.003833	.000048	-.000018	.000010	.000003
13.2	.220891	-.041762	.003842	.000044	-.000016	.000009	.000002
13.4	.212615	-.040993	.003850	.000041	-.000014	.000008	.000002
13.6	.204494	-.040222	.003858	.000039	-.000013	.000007	.000001
13.8	.196527	-.039449	.003866	.000036	-.000011	.000006	.000000
14.0	.188714	-.038675	.003873	.000034	-.000010	.000005	.000000
14.2	.181056	-.037900	.003880	.000032	-.000009	.000005	-.000001
14.4	.173554	-.037124	.003886	.000031	-.000008	.000004	-.000001
14.6	.166207	-.036346	.003892	.000029	-.000007	.000004	-.000002
14.8	.159016	-.035567	.003897	.000028	-.000007	.000003	-.000002
15.0	.151980	-.034787	.003903	.000026	-.000006	.000003	-.000003
15.2	.145101	-.034006	.003908	.000025	-.000005	.000003	-.000003
15.4	.138378	-.033224	.003913	.000024	-.000005	.000002	-.000003
15.6	.131812	-.032441	.003918	.000023	-.000004	.000002	-.000004
15.8	.125402	-.031657	.003922	.000022	-.000004	.000002	-.000004
16.0	.119149	-.030872	.003927	.000022	-.000004	.000002	-.000004
16.2	.113054	-.030086	.003931	.000021	-.000003	.000002	-.000005
16.4	.107115	-.029299	.003935	.000020	-.000003	.000002	-.000005
16.6	.101334	-.028512	.003939	.000020	-.000003	.000001	-.000005
16.8	.095710	-.027724	.003943	.000019	-.000002	.000001	-.000005
17.0	.090244	-.026935	.003947	.000019	-.000002	.000001	-.000006
17.2	.084936	-.026145	.003950	.000018	-.000002	.000001	-.000006
17.4	.079786	-.025355	.003954	.000018	-.000002	.000001	-.000006
17.6	.074795	-.024563	.003958	.000018	-.000002	.000001	-.000006
17.8	.069961	-.023772	.003961	.000017	-.000001	.000001	-.000007
18.0	.065286	-.022979	.003965	.000017	-.000001	.000001	-.000007
18.2	.060769	-.022186	.003968	.000017	-.000001	.000001	-.000007
18.4	.056412	-.021392	.003971	.000017	-.000001	.000001	-.000007
18.6	.052213	-.020597	.003975	.000017	-.000001	.000001	-.000007
18.8	.048173	-.019802	.003978	.000016	-.000001	.000001	-.000008
19.0	.044292	-.019006	.003981	.000016	-.000001	.000001	-.000008
19.2	.040570	-.018210	.003984	.000016	.000000	.000001	-.000008
19.4	.037008	-.017412	.003988	.000016	.000000	.000001	-.000008
19.6	.033606	-.016615	.003991	.000016	.000000	.000000	-.000008
19.8	.030362	-.015816	.003994	.000016	.000000	.000000	-.000008
20.0	.027279	-.015017	.003997	.000016	.000000	.000000	-.000009
20.2	.024356	-.014217	.004001	.000016	.000000	.000000	-.000009
20.4	.021592	-.013417	.004004	.000016	.000000	.000000	-.000009
20.6	.018989	-.012616	.004007	.000016	.000000	.000000	-.000009
20.8	.016546	-.011814	.004010	.000016	.000000	.000000	-.000009
21.0	.014264	-.011012	.004013	.000016	.000000	.000000	-.000009
21.2	.012142	-.010209	.004017	.000016	.000000	.000000	-.000010
21.4	.010180	-.009405	.004020	.000016	.000000	.000000	-.000010
21.6	.008380	-.008601	.004023	.000017	.000001	.000000	-.000010
21.8	.006740	-.007796	.004027	.000017	.000001	.000000	-.000010
22.0	.005262	-.006990	.004030	.000017	.000001	.000000	-.000010
22.2	.003944	-.006184	.004033	.000017	.000001	.000000	-.000010
22.4	.002788	-.005377	.004037	.000017	.000001	.000000	-.000011
22.6	.001794	-.004569	.004040	.000017	.000001	.000000	-.000011
22.8	.000961	-.003761	.004044	.000017	.000001	.000000	-.000011
23.0	.000289	-.002951	.004047	.000018	.000001	.000000	-.000011
23.2	-.000220	-.002142	.004051	.000018	.000001	.000000	-.000011
23.4	-.000567	-.001331	.004054	.000018	.000001	.000000	-.000011
23.6	-.000752	-.000520	.004058	.000018	.000001	.000000	-.000012
23.8	-.000775	.000292	.004061	.000018	.000001	.000000	-.000012
24.0	-.000636	.001104	.004065	.000018	.000001	.000000	-.000012
24.2	-.000333	.001918	.004069	.000019	.000001	.000000	-.000012
24.4	.000132	.002732	.004072	.000019	.000001	.000000	-.000012
24.6	.000760	.003547	.004076	.000019	.000001	.000000	-.000012
24.8	.001550	.004362	.004080	.000019	.000001	.000000	-.000013
25.0	.002505	.005179	.004084	.000019	.000001	.000000	-.000013

TABLE II-3.6 : FREE CONVECTION OF DOWNWARD-FACING HEATED PLATE, ONE ASSUMED FUNCTION IN TEMPERATURE DISTRIBUTION AND PRESCRIBED CONSTANT SURFACE FLUX CASE.
Pr = 5.0

η	$f(\eta)$	$f'(\eta)$	$f''(\eta)$	$f'''(\eta)$	$f^{(4)}(\eta)$	$f^{(5)}(\eta)$	$\theta(\eta)$
.0	.000000	.000000	.586085	-1.120025	1.000000	.000000	1.120025
.2	.010295	.096152	.382138	-.919009	1.011853	.053672	.920386
.4	.036010	.155550	.218584	-.716846	1.001503	-.191173	.725299
.6	.070603	.186248	.094876	-.522674	.928492	-.539845	.543965
.8	.109113	.195968	.008086	-.349836	.790670	-.814857	.386474
1.0	.148052	.191586	-.047208	-.209005	.614152	-.919408	.259689
1.2	.185185	.178722	-.077945	-.104381	.434242	-.856079	.165191
1.4	.219258	.161569	-.091229	-.033656	.278598	-.689784	.099766
1.6	.249719	.142978	-.093243	.009570	.160187	-.494694	.057442
1.8	.276472	.124704	-.088724	.032930	.079203	-.321323	.031681
2.0	.299687	.107704	-.080934	.043291	.028772	-.190557	.016818
2.2	.319668	.092410	-.071921	.045886	.000103	-.102657	.008635
2.4	.336773	.078938	-.062858	.044262	-.014549	-.048592	.004306
2.6	.351361	.067229	-.054349	.040617	-.020876	-.017731	.002095
2.8	.363773	.057143	-.046660	.036216	-.022599	-.001334	.000997
3.0	.374315	.048505	-.039867	.031733	-.021964	.006659	.000466
3.2	.383259	.041138	-.033950	.027501	-.020240	.010034	.000214
3.4	.390843	.034871	-.028840	.023663	-.018110	.010993	.000097
3.6	.397271	.029553	-.024455	.020261	-.015922	.010754	.000044
3.8	.402718	.025047	-.020708	.017287	-.013844	.009966	.000019
4.0	.407336	.021233	-.017514	.014711	-.011949	.008967	.000009
4.2	.411251	.018009	-.014800	.012493	-.010260	.007925	.000004
4.4	.414573	.015286	-.012496	.010593	-.008776	.006925	.000002
4.6	.417393	.012987	-.010544	.008970	-.007485	.006003	.000001
4.8	.419791	.011048	-.008892	.007587	-.006369	.005174	.000000
5.0	.421833	.009413	-.007495	.006412	-.005409	.004440	.000000
5.2	.423574	.008036	-.006315	.005414	-.004587	.003798	.000000
5.4	.425062	.006875	-.005319	.004569	-.003884	.003239	.000000
5.6	.426336	.005898	-.004479	.003854	-.003286	.002756	.000000
5.8	.427431	.005075	-.003770	.003249	-.002777	.002341	.000000
6.0	.428375	.004382	-.003173	.002738	-.002346	.001986	.000000
6.2	.429191	.003799	-.002670	.002306	-.001980	.001682	.000000
6.4	.429901	.003309	-.002246	.001942	-.001670	.001423	.000000
6.6	.430520	.002896	-.001889	.001635	-.001408	.001203	.000000
6.8	.431064	.002549	-.001589	.001376	-.001187	.001016	.000000
7.0	.431543	.002258	-.001336	.001158	-.001000	.000858	.000000
7.2	.431970	.002012	-.001123	.000974	-.000842	.000723	.000000
7.4	.432351	.001806	-.000944	.000820	-.000709	.000610	.000000
7.6	.432694	.001633	-.000794	.000690	-.000597	.000514	.000000
7.8	.433006	.001487	-.000667	.000580	-.000502	.000433	.000000
8.0	.433291	.001364	-.000561	.000488	-.000423	.000365	.000000
8.2	.433553	.001261	-.000471	.000410	-.000356	.000307	.000000
8.4	.433796	.001175	-.000396	.000345	-.000299	.000259	.000000
8.6	.434024	.001102	-.000333	.000290	-.000252	.000218	.000000
8.8	.434238	.001041	-.000279	.000244	-.000212	.000183	.000000
9.0	.434441	.000990	-.000235	.000205	-.000178	.000154	.000000
9.2	.434634	.000947	-.000197	.000172	-.000150	.000130	.000000
9.4	.434820	.000911	-.000165	.000145	-.000126	.000109	.000000
9.6	.434999	.000880	-.000139	.000122	-.000106	.000092	.000000
9.8	.435173	.000855	-.000117	.000102	-.000089	.000077	.000000
10.0	.435341	.000834	-.000098	.000086	-.000075	.000065	.000000
10.2	.435506	.000816	-.000082	.000072	-.000063	.000055	.000000
10.4	.435668	.000801	-.000069	.000061	-.000053	.000046	.000000
10.6	.435827	.000788	-.000058	.000051	-.000044	.000039	.000000
10.8	.435983	.000777	-.000048	.000043	-.000037	.000032	.000000
11.0	.436138	.000769	-.000041	.000036	-.000031	.000027	.000000
11.2	.436291	.000761	-.000034	.000030	-.000026	.000023	.000000
11.4	.436442	.000755	-.000028	.000025	-.000022	.000019	.000000
11.6	.436593	.000750	-.000024	.000021	-.000019	.000016	.000000
11.8	.436742	.000745	-.000020	.000018	-.000016	.000014	.000000
12.0	.436891	.000742	-.000017	.000015	-.000013	.000011	.000000

12.2	.437039	.000739	-.000014	.000013	-.000011	.000010	.000000
12.4	.437186	.000736	-.000012	.000011	-.000009	.000008	.000000
12.6	.437333	.000734	-.000010	.000009	-.000008	.000007	.000000
12.8	.437480	.000732	-.000008	.000007	-.000007	.000006	.000000
13.0	.437626	.000731	-.000007	.000006	-.000005	.000005	.000000
13.2	.437772	.000730	-.000005	.000005	-.000005	.000004	.000000
13.4	.437918	.000729	-.000004	.000004	-.000004	.000003	.000000
13.6	.438064	.000728	-.000004	.000004	-.000003	.000003	.000000
13.8	.438209	.000727	-.000003	.000003	-.000003	.000002	.000000
14.0	.438355	.000727	-.000002	.000003	-.000002	.000002	.000000
14.2	.438500	.000726	-.000002	.000002	-.000002	.000002	.000000
14.4	.438645	.000726	-.000002	.000002	-.000002	.000001	.000000
14.6	.438790	.000726	-.000001	.000002	-.000001	.000001	.000000
14.8	.438935	.000725	-.000001	.000001	-.000001	.000001	.000000
15.0	.439080	.000725	-.000001	.000001	-.000001	.000001	.000000
15.2	.439225	.000725	.000000	.000001	-.000001	.000001	.000000
15.4	.439370	.000725	.000000	.000001	-.000001	.000001	.000000
15.6	.439515	.000725	.000000	.000001	-.000001	.000000	.000000
15.8	.439660	.000725	.000000	.000001	.000000	.000000	.000000
16.0	.439805	.000725	.000000	.000000	.000000	.000000	.000000
16.2	.439950	.000725	.000000	.000000	.000000	.000000	.000000
16.4	.440095	.000725	.000000	.000000	.000000	.000000	.000000
16.6	.440240	.000725	.000000	.000000	.000000	.000000	.000000
16.8	.440385	.000725	.000000	.000000	.000000	.000000	.000000
17.0	.440530	.000725	.000000	.000000	.000000	.000000	.000000
17.2	.440675	.000725	.000000	.000000	.000000	.000000	.000000
17.4	.440820	.000725	.000000	.000000	.000000	.000000	.000000
17.6	.440965	.000725	.000000	.000000	.000000	.000000	.000000
17.8	.441111	.000725	.000000	.000000	.000000	.000000	.000000
18.0	.441256	.000725	.000000	.000000	.000000	.000000	.000000
18.2	.441401	.000726	.000000	.000000	.000000	.000000	.000000
18.4	.441546	.000726	.000000	.000000	.000000	.000000	.000000
18.6	.441691	.000726	.000000	.000000	.000000	.000000	.000000
18.8	.441836	.000726	.000000	.000000	.000000	.000000	.000000
19.0	.441981	.000726	.000000	.000000	.000000	.000000	.000000
19.2	.442127	.000726	.000001	.000000	.000000	.000000	.000000
19.4	.442272	.000726	.000001	.000000	.000000	.000000	.000000
19.6	.442417	.000726	.000001	.000000	.000000	.000000	.000000
19.8	.442562	.000726	.000001	.000000	.000000	.000000	.000000
20.0	.442708	.000726	.000001	.000000	.000000	.000000	.000000
20.2	.442853	.000727	.000001	.000000	.000000	.000000	.000000
20.4	.442998	.000727	.000001	.000000	.000000	.000000	.000000
20.6	.443143	.000727	.000001	.000000	.000000	.000000	.000000
20.8	.443289	.000727	.000001	.000000	.000000	.000000	.000000
21.0	.443434	.000727	.000001	.000000	.000000	.000000	.000000
21.2	.443580	.000727	.000001	.000000	.000000	.000000	.000000
21.4	.443725	.000727	.000001	.000000	.000000	.000000	.000000
21.6	.443871	.000727	.000001	.000000	.000000	.000000	.000000
21.8	.444016	.000727	.000001	.000000	.000000	.000000	.000000
22.0	.444161	.000728	.000001	.000000	.000000	.000000	.000000
22.2	.444307	.000728	.000001	.000000	.000000	.000000	.000000
22.4	.444453	.000728	.000001	.000000	.000000	.000000	.000000
22.6	.444598	.000728	.000001	.000000	.000000	.000000	.000000
22.8	.444744	.000728	.000001	.000000	.000000	.000000	.000000
23.0	.444889	.000728	.000001	.000000	.000000	.000000	.000000
23.2	.445035	.000728	.000001	.000000	.000000	.000000	.000000
23.4	.445180	.000728	.000001	.000000	.000000	.000000	.000000
23.6	.445326	.000728	.000001	.000000	.000000	.000000	.000000
23.8	.445472	.000728	.000001	.000000	.000000	.000000	.000000
24.0	.445618	.000729	.000001	.000000	.000000	.000000	.000000
24.2	.445763	.000729	.000001	.000000	.000000	.000000	.000000
24.4	.445909	.000729	.000001	.000000	.000000	.000000	.000000
24.6	.446055	.000729	.000001	.000000	.000000	.000000	.000000
24.8	.446201	.000729	.000001	.000000	.000000	.000000	.000000
25.0	.446346	.000729	.000001	.000000	.000000	.000000	.000000

TABLE II-3.7 :SOLUTIONS OF f(η) FOR THE PRANDTL NUMBERS OF 0.72, 1.0, AND 5.0 IN FREE CONVECTION OF DOWNWARD-FACING HEATED PLATE, TWO ASSUMED FUNCTIONS IN TEMPERATURE DISTRIBUTION AND PRESCRIBED SURFACE TEMPERATURE CASE.

η	Pr=0.72	Pr=1.0	Pr=5.0
.0	.00000	.00000	.00000
.1	.00327	.00307	.00220
.2	.01246	.01167	.00819
.3	.02666	.02489	.01715
.4	.04503	.04192	.02836
.5	.06681	.06201	.04121
.6	.09129	.08448	.05519
.7	.11783	.10873	.06986
.8	.14586	.13423	.08489
.9	.17487	.16048	.09998
1.0	.20441	.18709	.11492
1.1	.23408	.21369	.12954
1.2	.26356	.24000	.14371
1.3	.29257	.26575	.15733
1.4	.32086	.29075	.17033
1.5	.34825	.31483	.18269
1.6	.37459	.33788	.19438
1.7	.39977	.35980	.20538
1.8	.42370	.38052	.21571
1.9	.44634	.40002	.22537
2.0	.46766	.41827	.23439
2.1	.48765	.43528	.24277
2.2	.50631	.45106	.25056
2.3	.52367	.46564	.25778
2.4	.53976	.47906	.26445
2.5	.55462	.49136	.27060
2.6	.56831	.50259	.27626
2.7	.58088	.51280	.28147
2.8	.59238	.52205	.28624
2.9	.60287	.53039	.29060
3.0	.61242	.53789	.29458
3.1	.62107	.54458	.29821
3.2	.62889	.55054	.30150
3.3	.63594	.55581	.30447
3.4	.64227	.56045	.30716
3.5	.64794	.56449	.30957
3.6	.65298	.56800	.31173
3.7	.65746	.57100	.31366
3.8	.66141	.57355	.31536
3.9	.66489	.57569	.31686
4.0	.66792	.57744	.31817
4.1	.67055	.57884	.31930
4.2	.67281	.57993	.32027
4.3	.67474	.58074	.32109
4.4	.67636	.58128	.32177
4.5	.67770	.58160	.32233
4.6	.67879	.58170	.32276
4.7	.67966	.58162	.32309

4.8	.68031	.58136	.32331
4.9	.68078	.58096	.32344
5.0	.68109	.58043	.32349
5.1	.68124	.57977	.32346
5.2	.68127	.57902	.32336
5.3	.68117	.57817	.32320
5.4	.68097	.57725	.32297
5.5	.68067	.57626	.32270
5.6	.68029	.57521	.32238
5.7	.67984	.57411	.32202
5.8	.67933	.57298	.32162
5.9	.67877	.57181	.32119
6.0	.67816	.57062	.32072
6.1	.67751	.56941	.32024
6.2	.67683	.56818	.31973
6.3	.67612	.56695	.31920
6.4	.67540	.56572	.31866
6.5	.67465	.56449	.31811
6.6	.67390	.56327	.31755
6.7	.67315	.56205	.31698
6.8	.67239	.56085	.31641
6.9	.67163	.55967	.31583
7.0	.67087	.55850	.31526
7.1	.67013	.55736	.31469
7.2	.66939	.55624	.31412
7.3	.66867	.55515	.31356
7.4	.66796	.55408	.31300
7.5	.66727	.55305	.31245
7.6	.66660	.55205	.31192
7.7	.66595	.55107	.31140
7.8	.66532	.55014	.31088
7.9	.66471	.54923	.31039
8.0	.66413	.54837	.30991
8.1	.66358	.54754	.30944
8.2	.66305	.54675	.30900
8.3	.66255	.54600	.30857
8.4	.66208	.54528	.30816
8.5	.66164	.54461	.30777
8.6	.66122	.54398	.30740
8.7	.66084	.54339	.30705
8.8	.66050	.54284	.30673
8.9	.66018	.54233	.30643
9.0	.65990	.54186	.30615
9.1	.65965	.54144	.30589
9.2	.65943	.54106	.30566
9.3	.65925	.54073	.30545
9.4	.65910	.54043	.30527
9.5	.65899	.54018	.30512
9.6	.65891	.53998	.30499
9.7	.65887	.53982	.30489
9.8	.65886	.53970	.30481
9.9	.65888	.53963	.30476
10.0	.65895	.53960	.30474

I Free Jet Zone
II Deflection Zone
III Wall Jet Zone

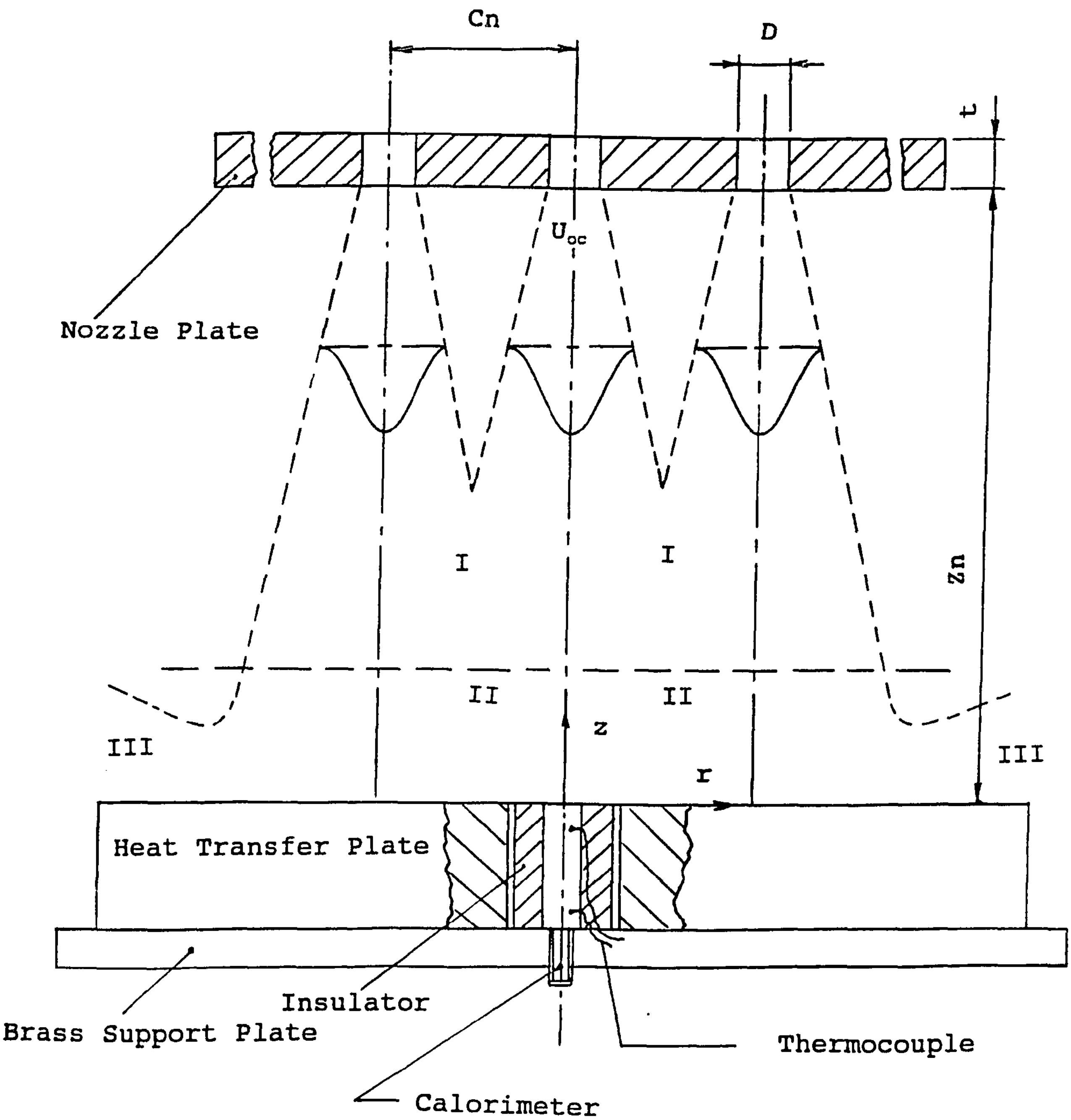

Fig.I-1.1 Flow Pattern Under Impinging Jets and Experimental Outline

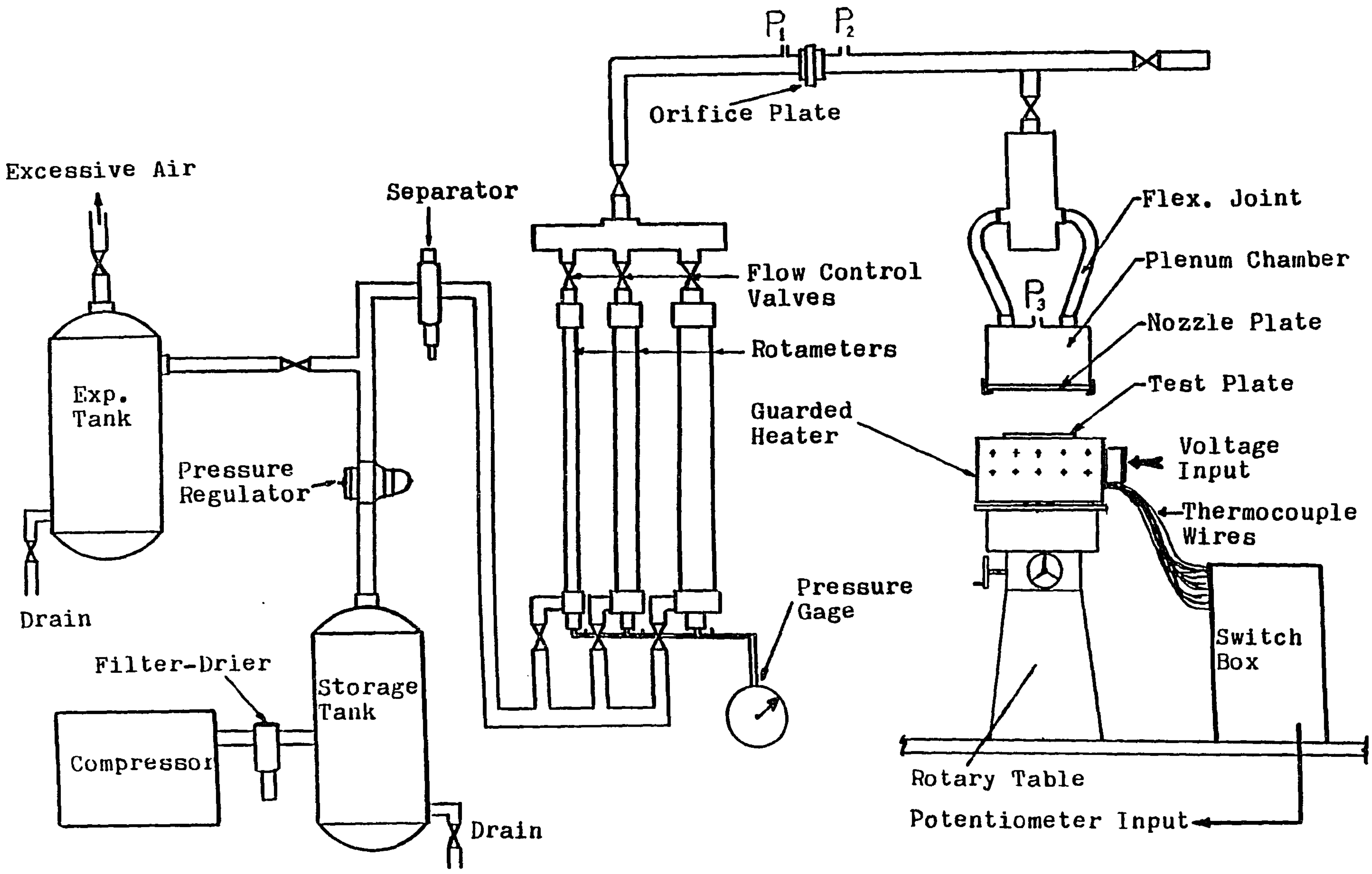

Fig.I-3.1 Experimental Piping System and Test Set-Up

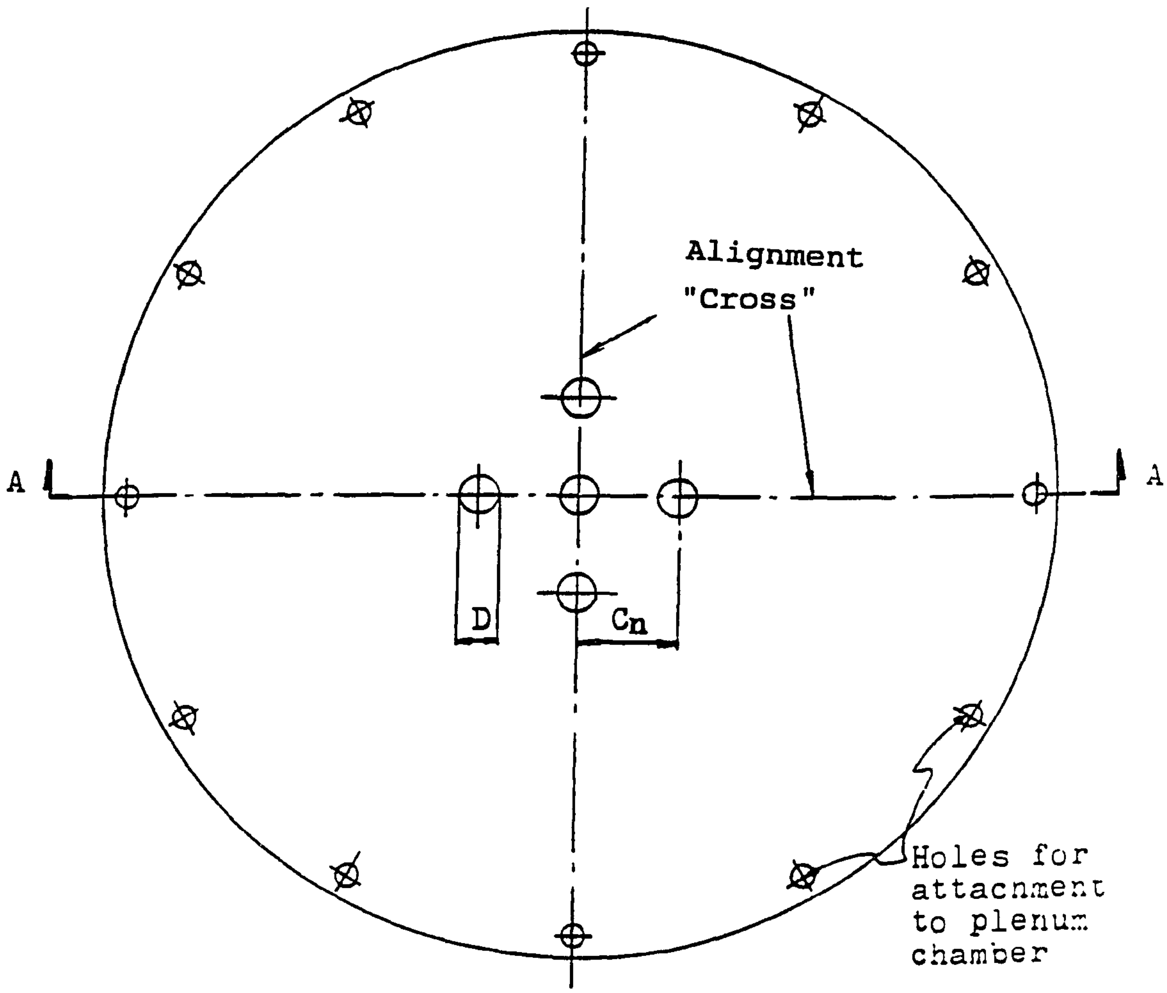

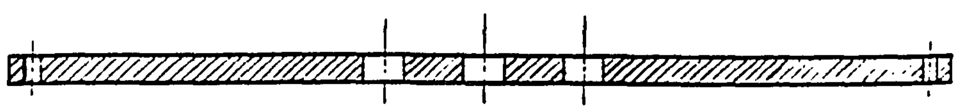

SECTION A-A

Fig.I-3.2 Nozzle Plate

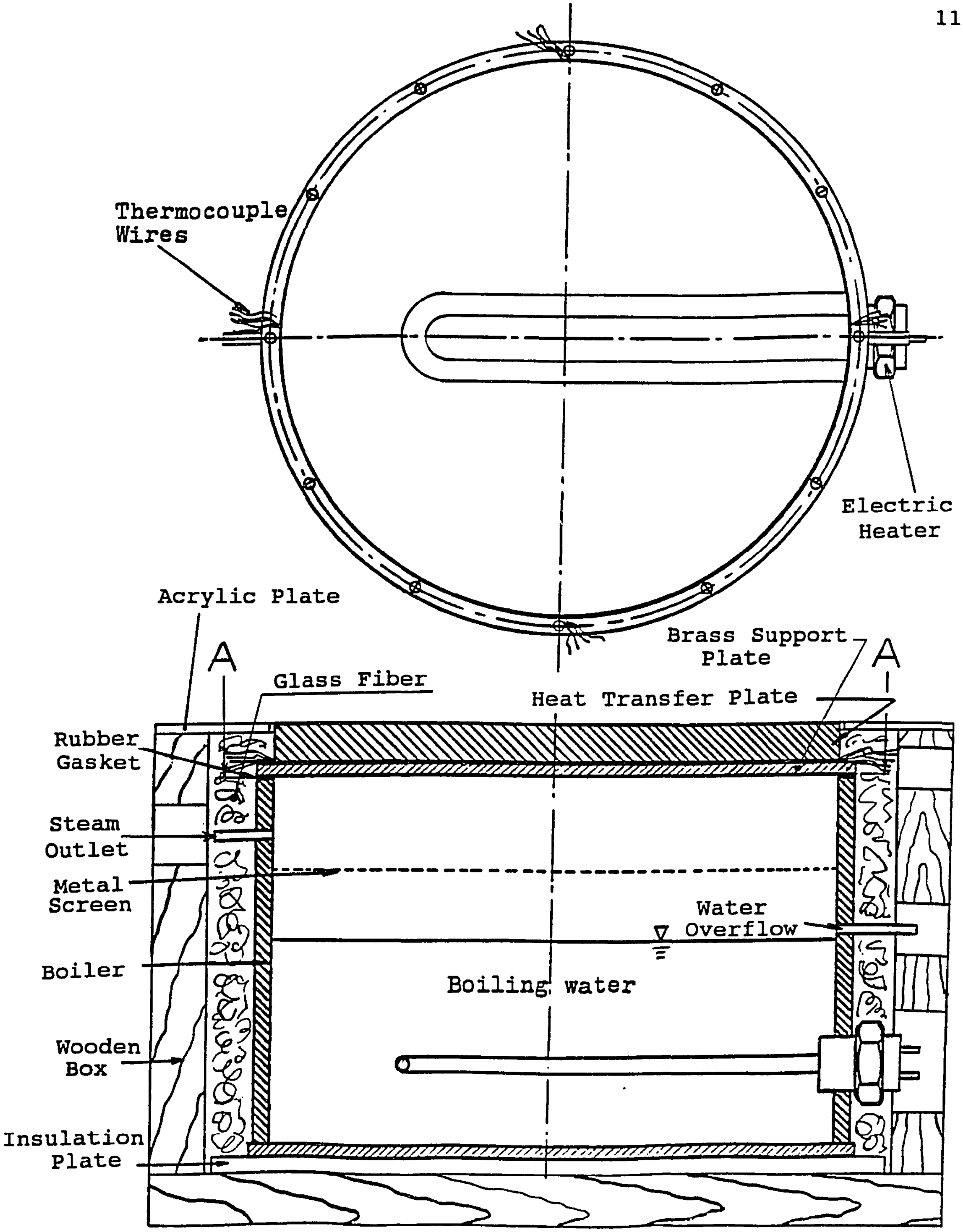

Fig.I-3.3 Test Plate and Box Assembly

Number Indicates the Position of Calorimeter
Center is Ring #1
(all dimensions in mm)

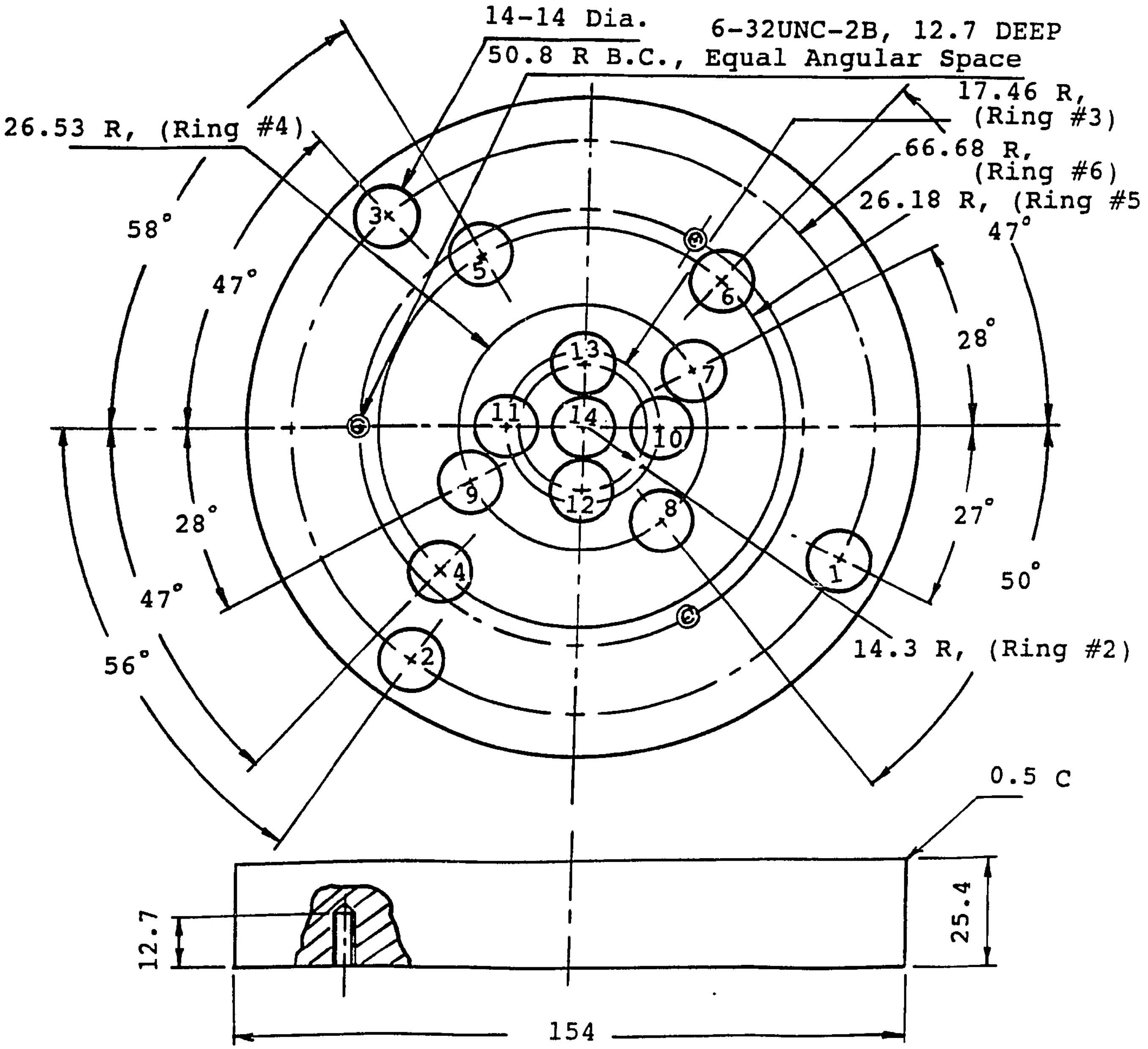

Fig.I-3.4 Heat Transfer Plate Configuration

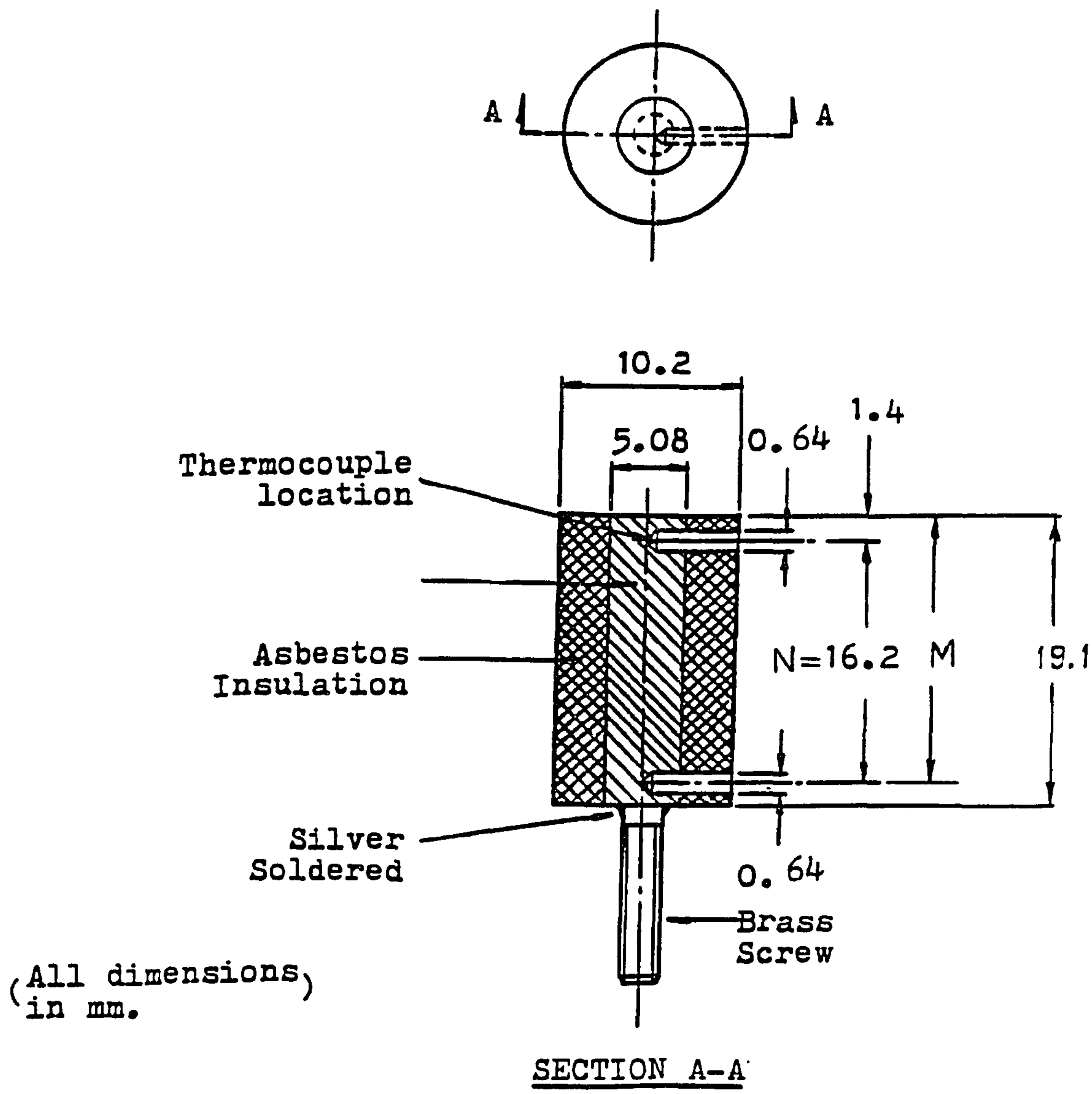

Fig.I-3.5 Calorimeter Configuration

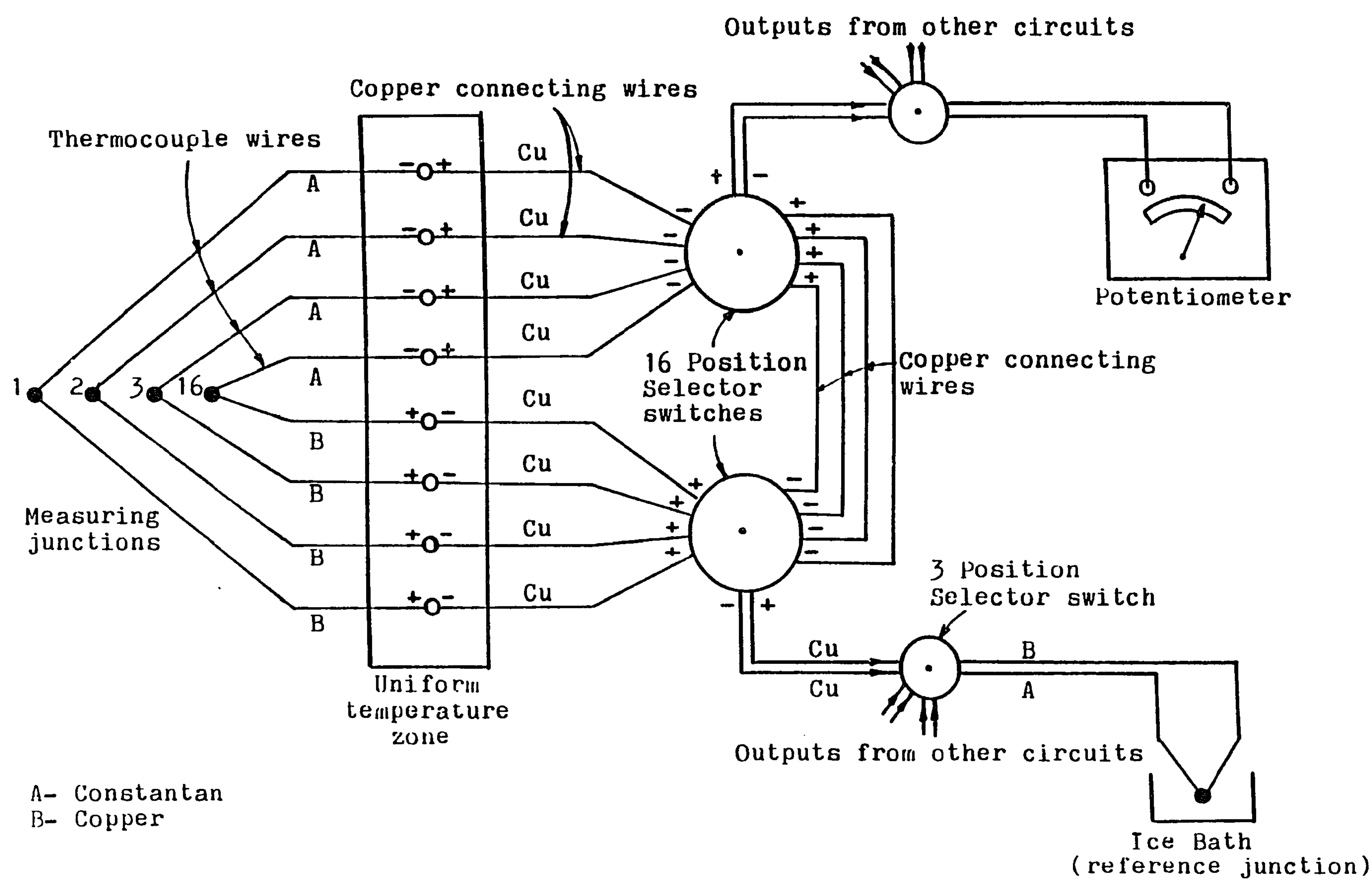

Fig.I-3.6 Temperature Measurement System

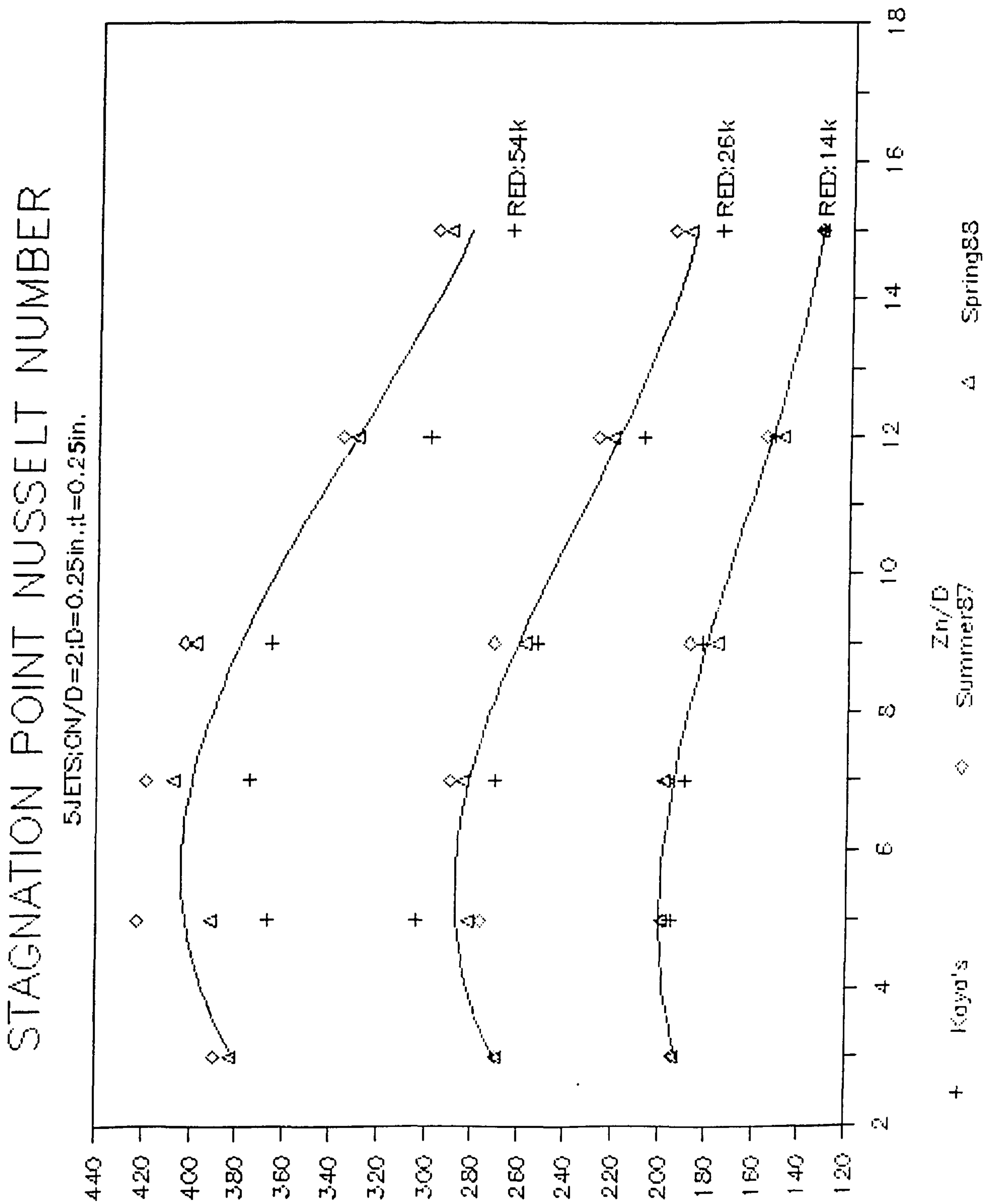

Fig.I-4.1 Stagnation Point Nusselt Number vs. Zn/D for Five Jets, D=6.35 mm, Cn/D=2

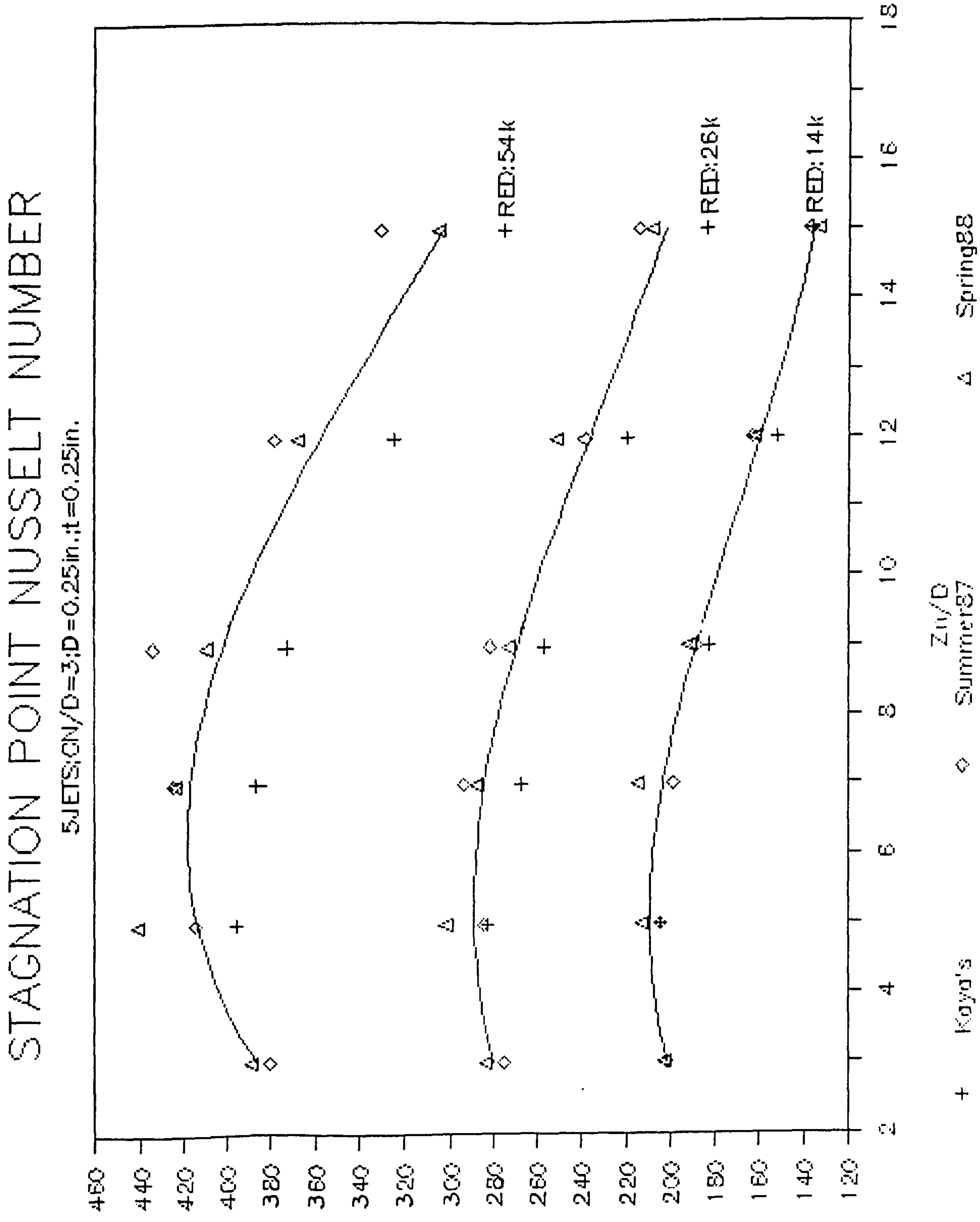

Fig.I-4.2 Stagnation Point Nusselt Number vs. Zn/D for Five Jets, D=6.35 mm, Cn/D=3

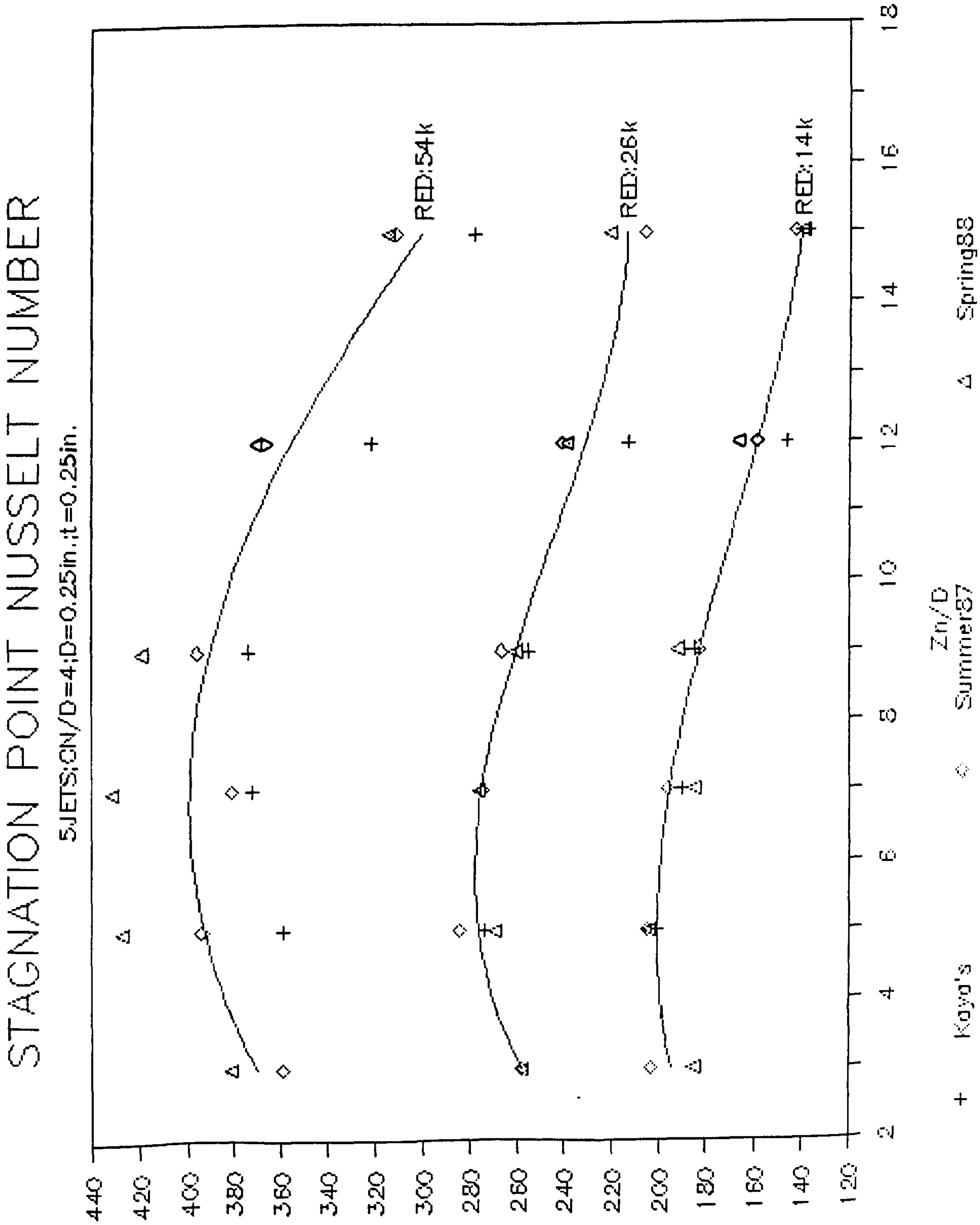

Fig.I-4.3 Stagnation Point Nusselt Number vs. Zn/D for Five Jets, D=6.35 mm, Cn/D=4

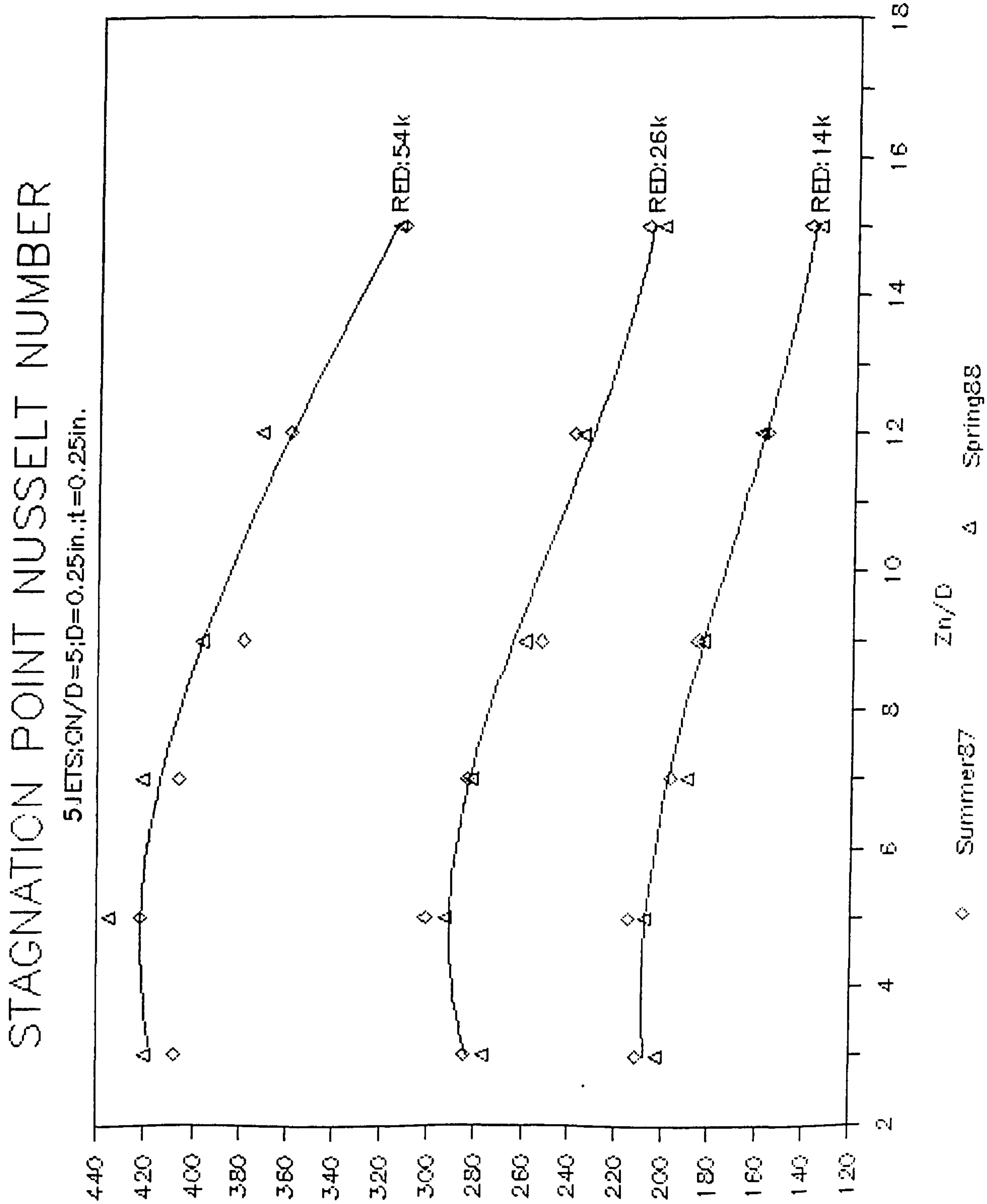

Fig.I-4.4 Stagnation Point Nusselt Number vs. Zn/D for Five Jets, D=6.35 mm, Cn/D=5

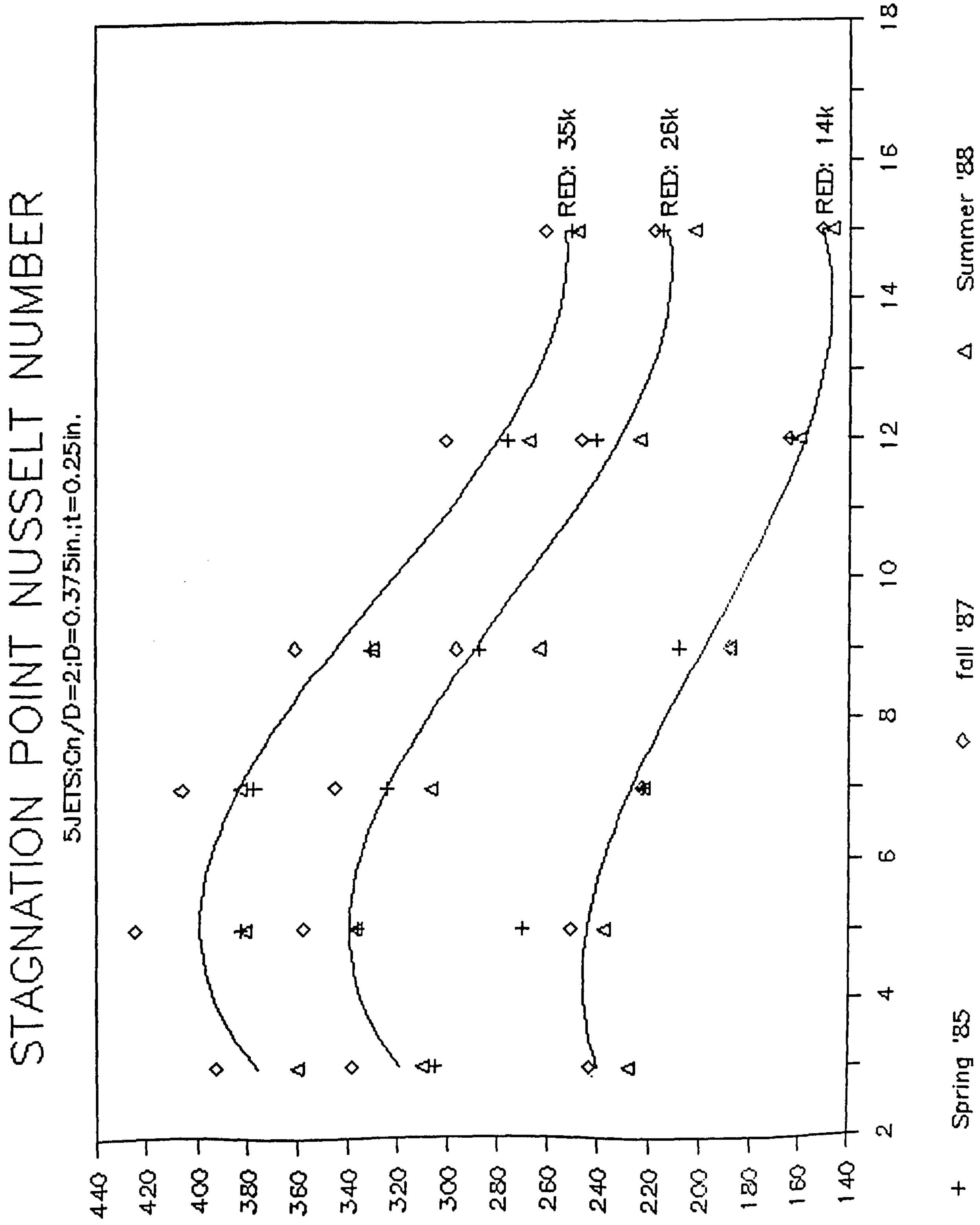

Fig.I-4.5 Stagnation Point Nusselt Number vs. Zn/D for Five Jets, D=9.53 mm, Cn/D=2

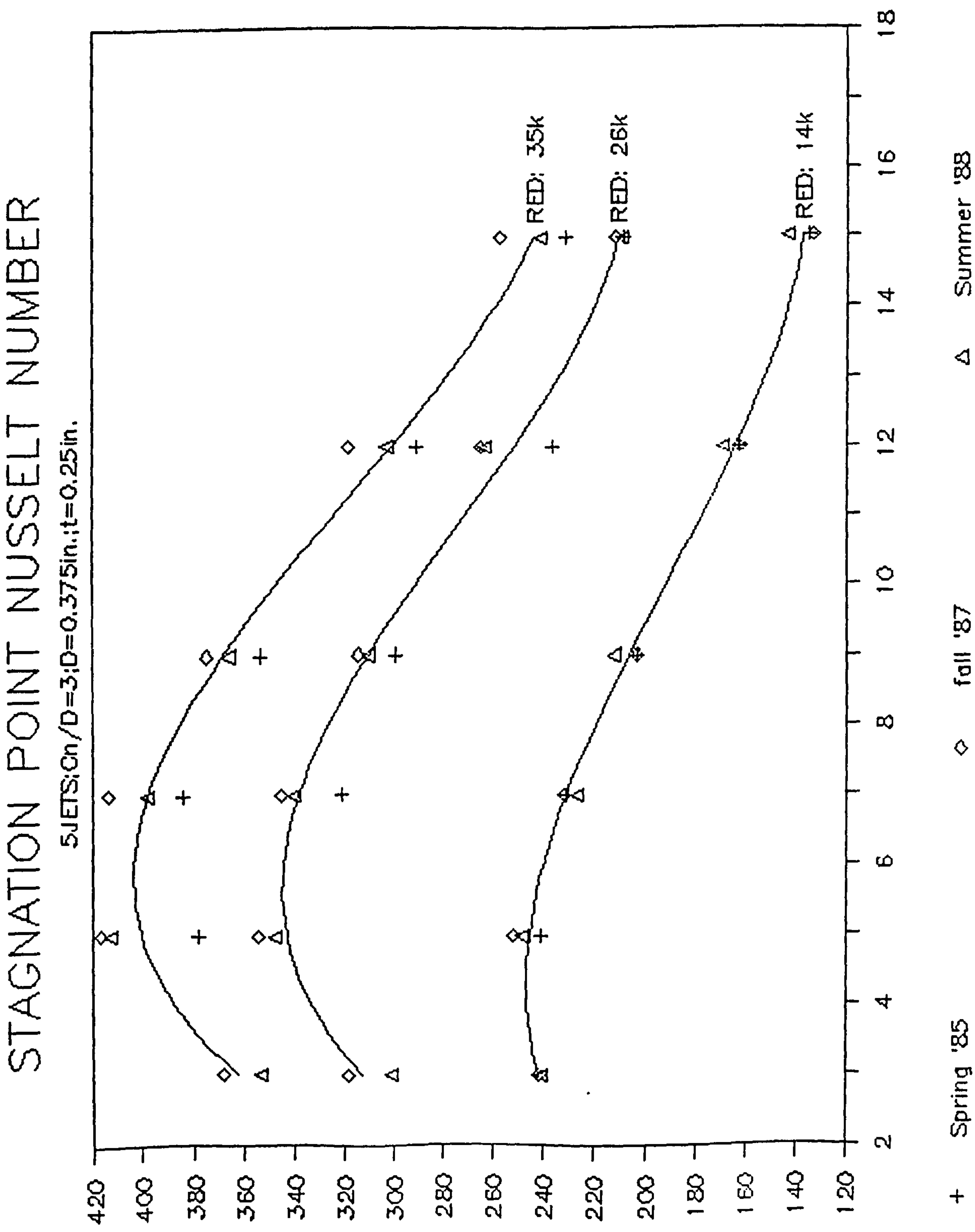

Fig.I-4.6 Stagnation Point Nusselt Number vs. Zn/D for Five Jets, D=9.53 mm, Cn/D=3

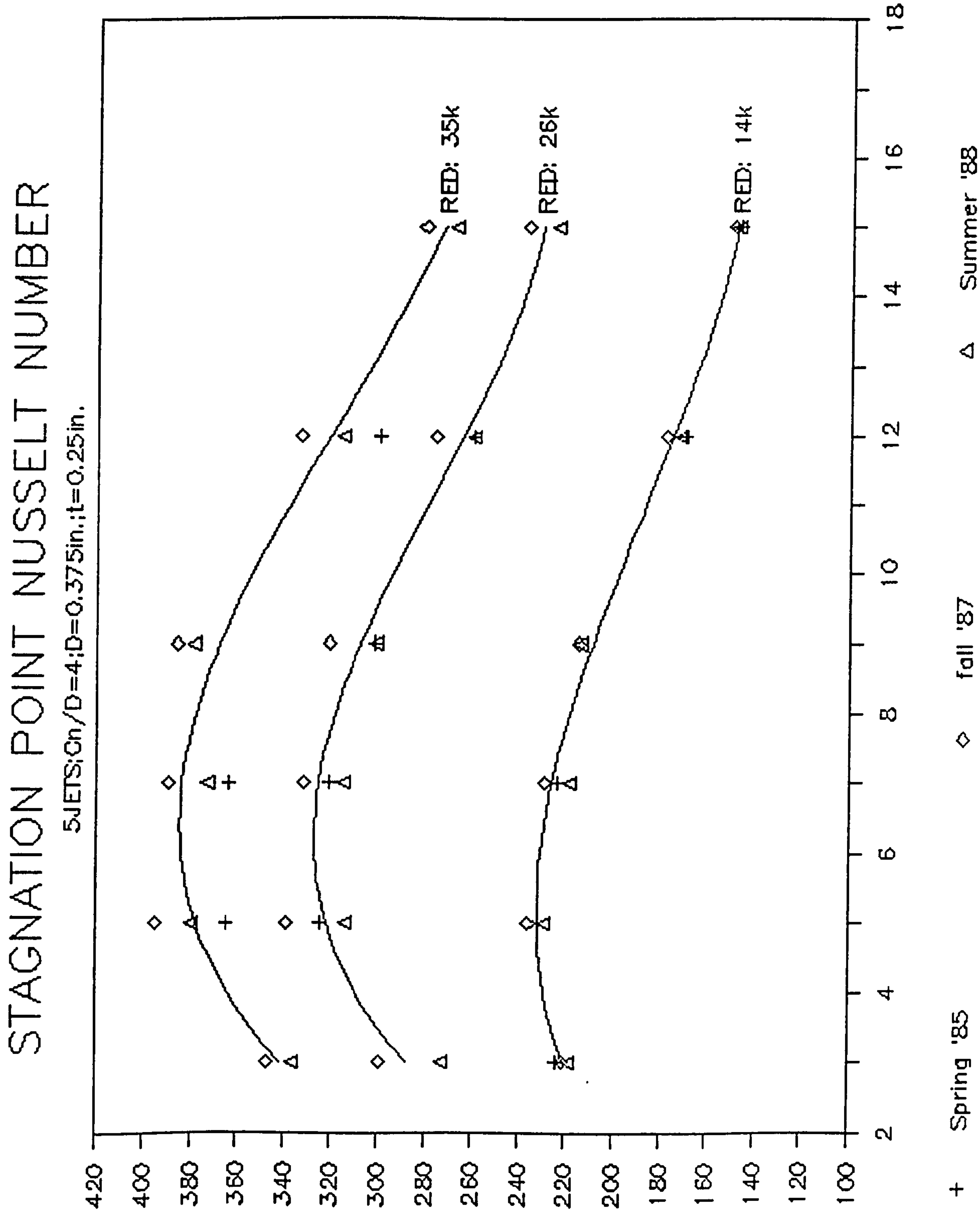

Fig.I-4.7 Stagnation Point Nusselt Number vs. Zn/D for Five Jets, D=9.53 mm, Cn/D=4

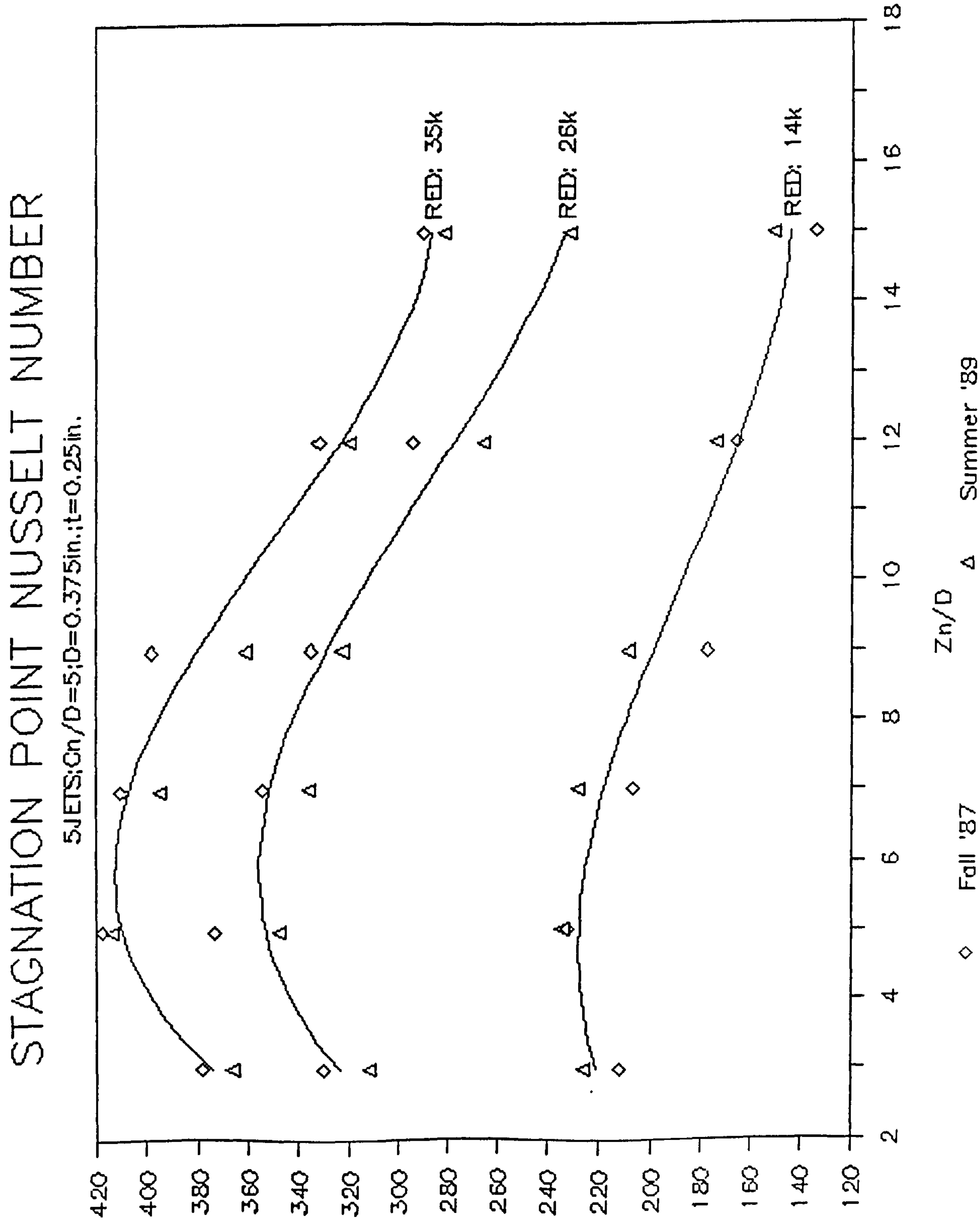

Fig.I-4.8 Stagnation Point Nusselt Number vs. Zn/D for Five Jets, D=9.53 mm, Cn/D=5

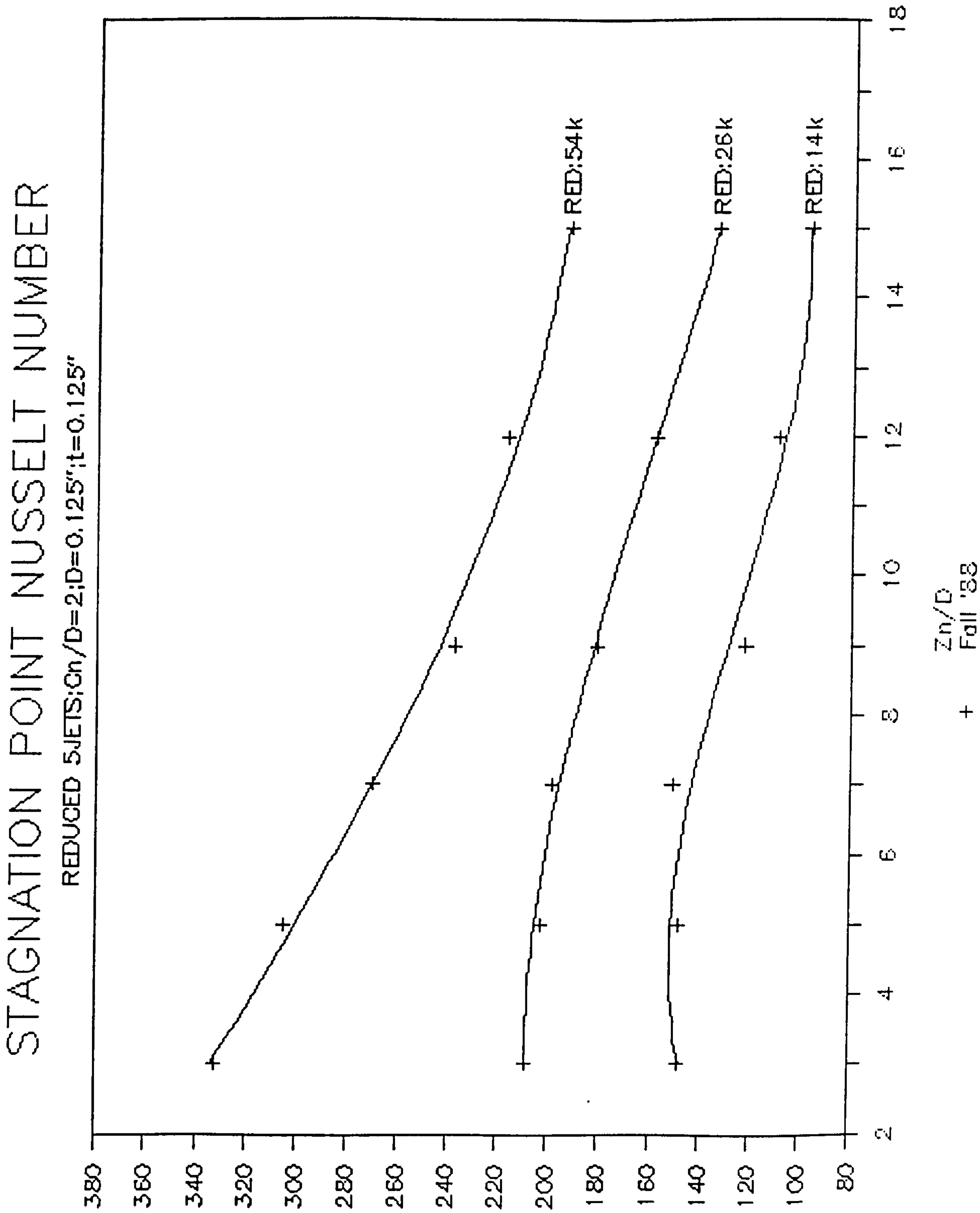

Fig.I-4.9 Stagnation Point Nusselt Number vs. Zn/D for Reduced Five Jets, D=3.18 mm, Cn/D=2

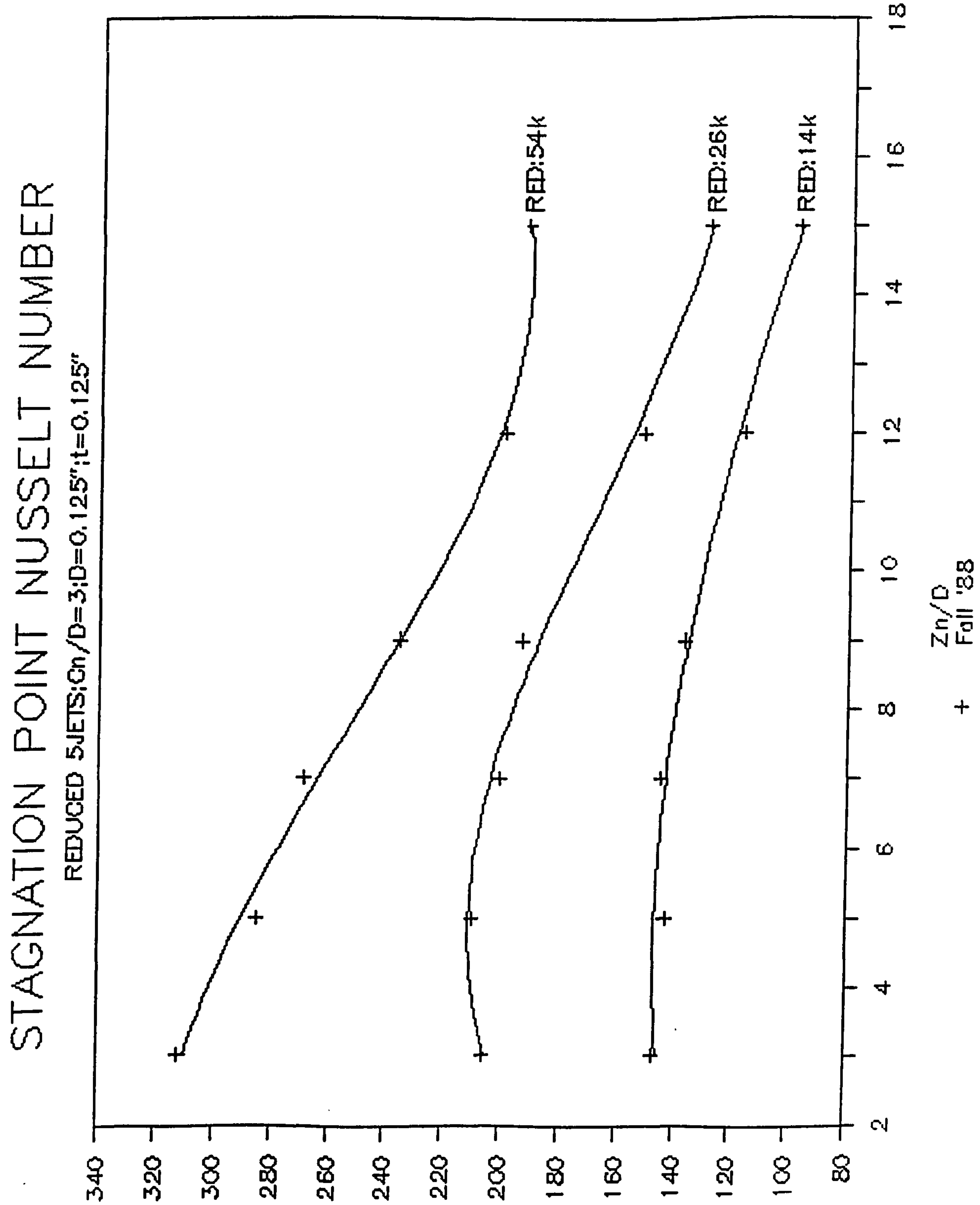

Fig.I-4.10 Stagnation Point Nusselt Number vs. Zn/D for Reduced Five Jets, D=3.18 mm, Cn/D=3

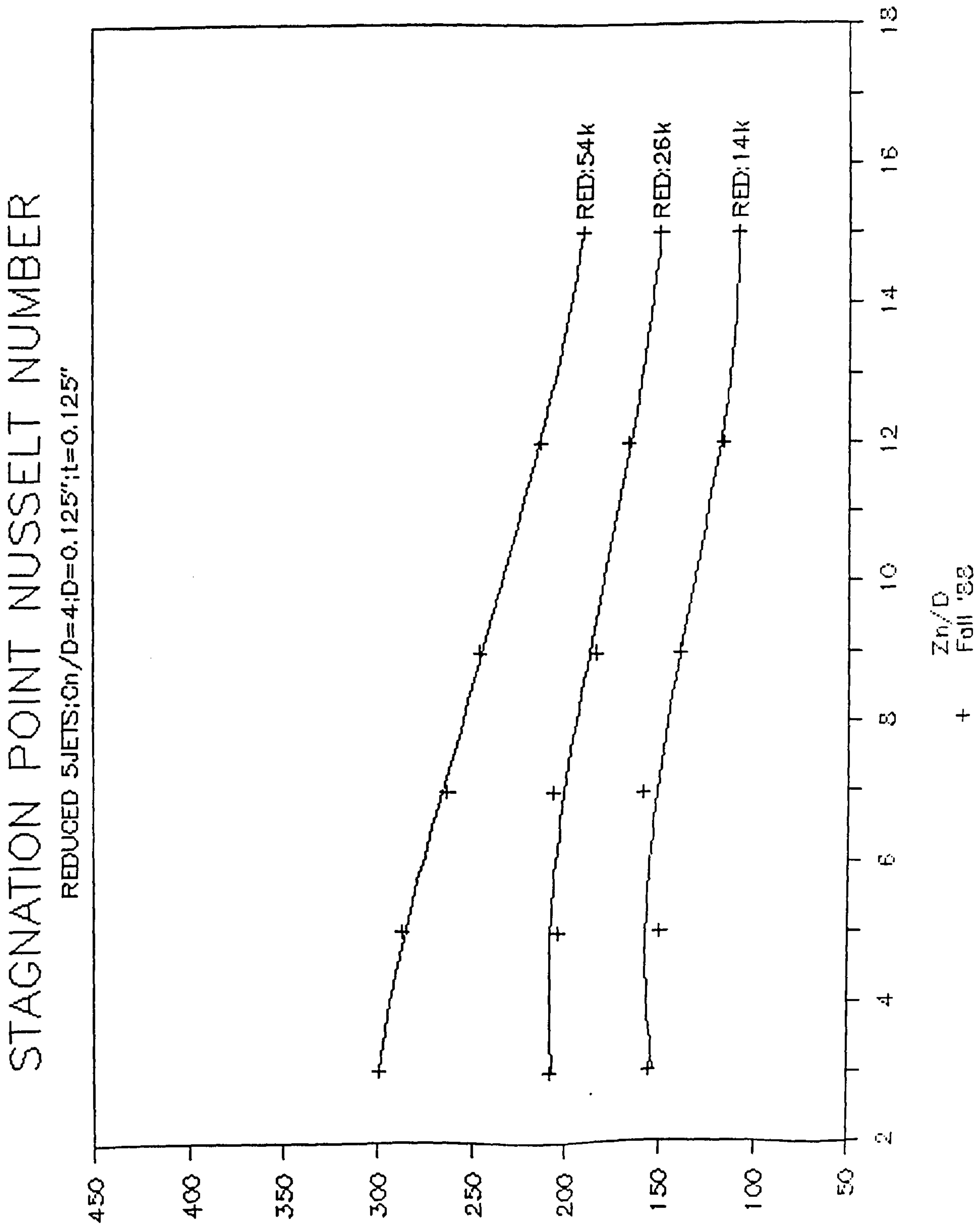

Fig.I-4.11 Stagnation Point Nusselt Number vs. Zn/D for Reduced Five Jets, D=3.18 mm, Cn/D=4

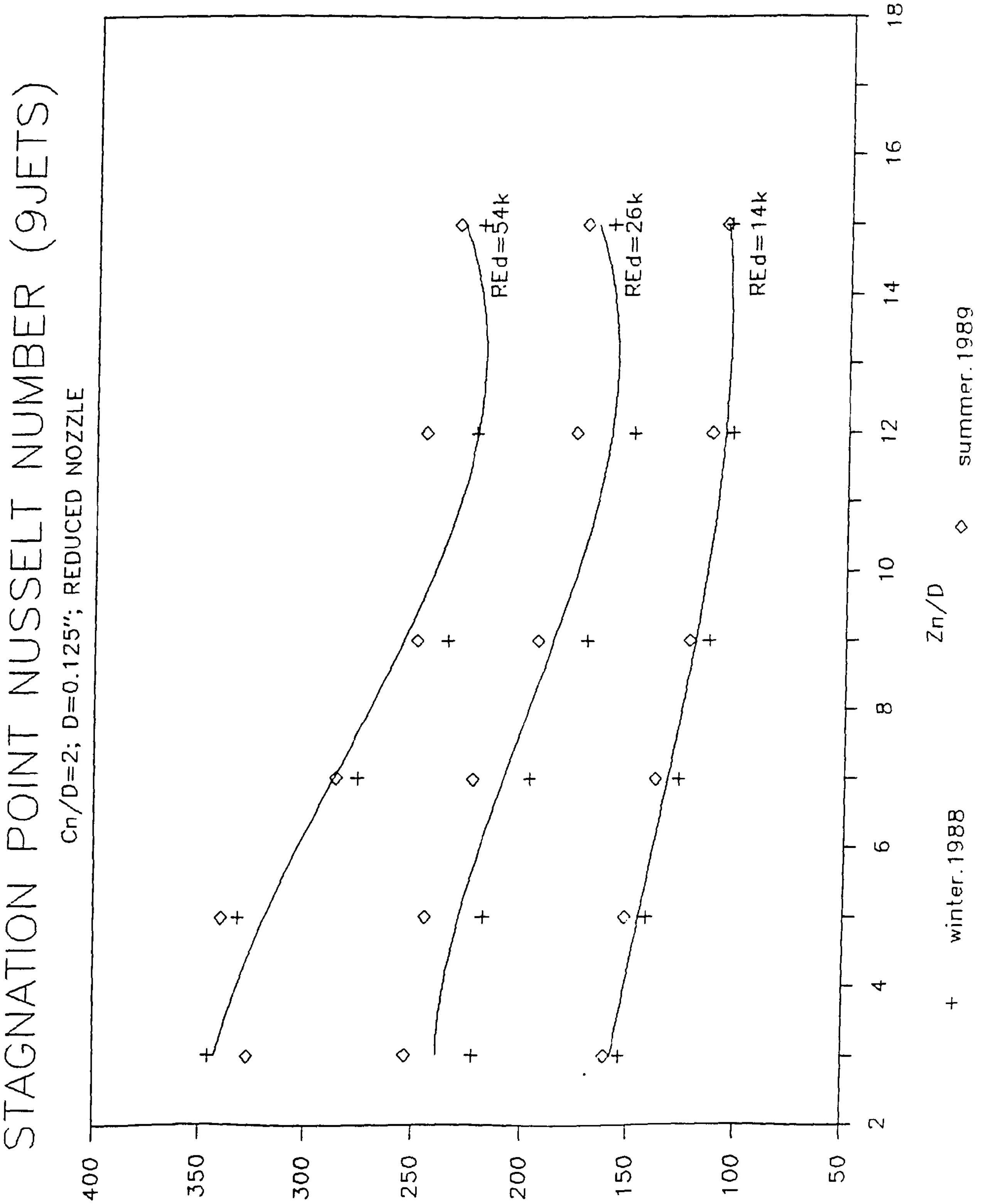

Fig. I-4.12 Stagnation Point Nusselt Number vs. Zn/D for Reduced Nine Jets, D=3.18 mm, Cn/D=2

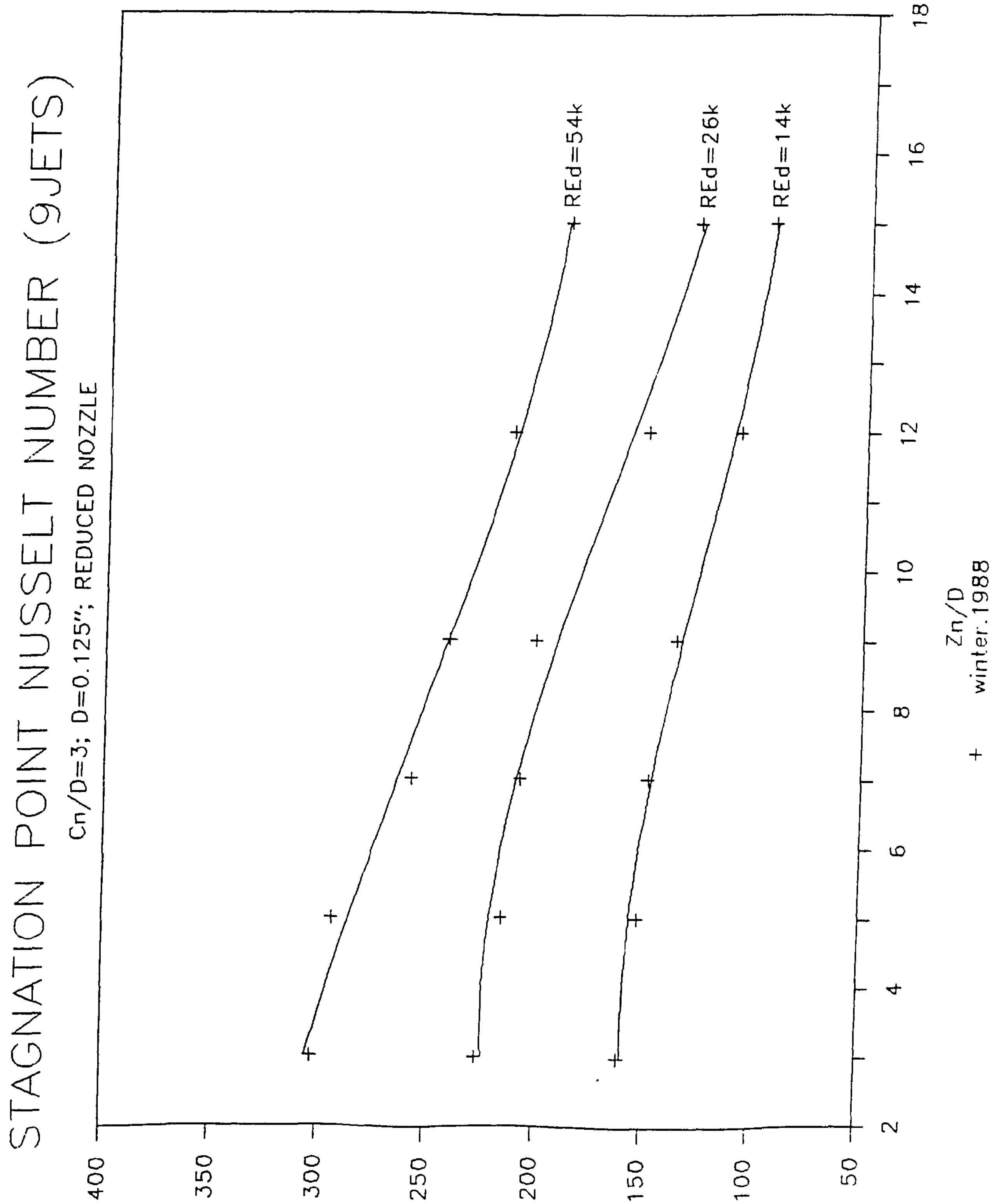

Fig.I-4.13 Stagnation Point Nusselt Number vs. Zn/D for Reduced Nine Jets, D=3.18 mm, Cn/D=3

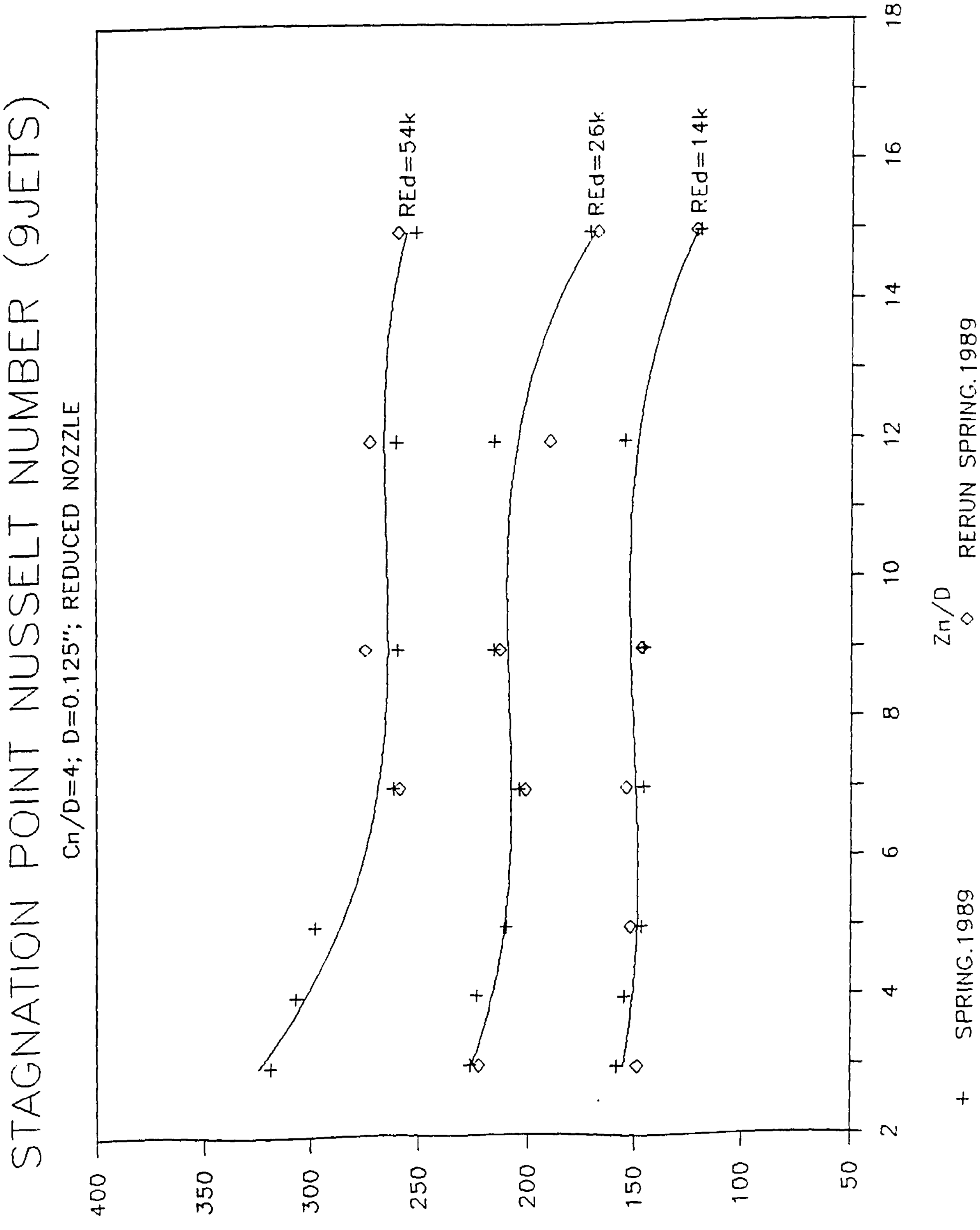

Fig.I-4.14 Stagnation Point Nusselt Number vs. Zn/D for Reduced Nine Jets, D=3.18 mm, Cn/D=4

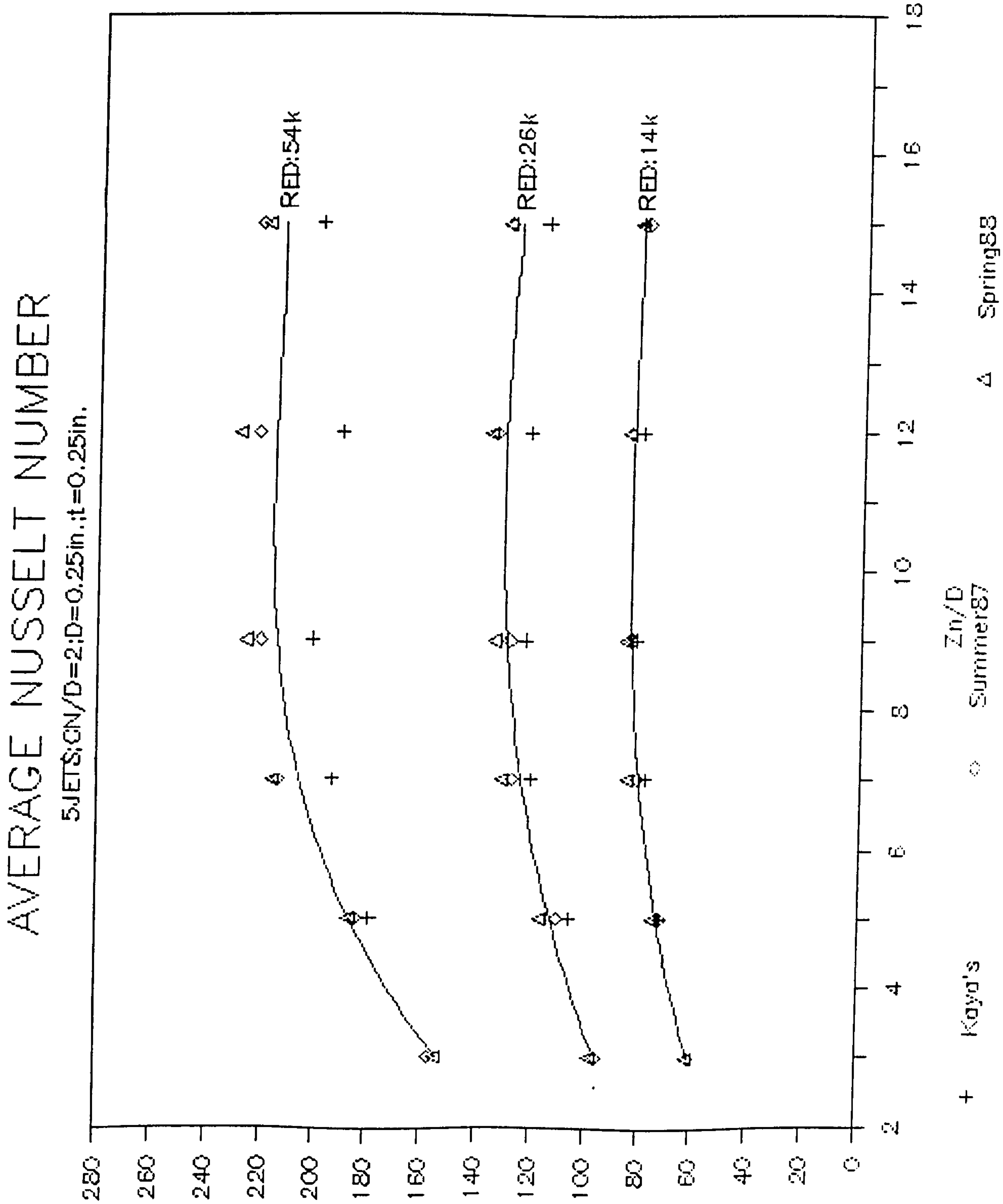

Fig.I-4.15 Average Nusselt Number vs. Zn/D for Five Jets, D=6.35 mm, Cn/D=2

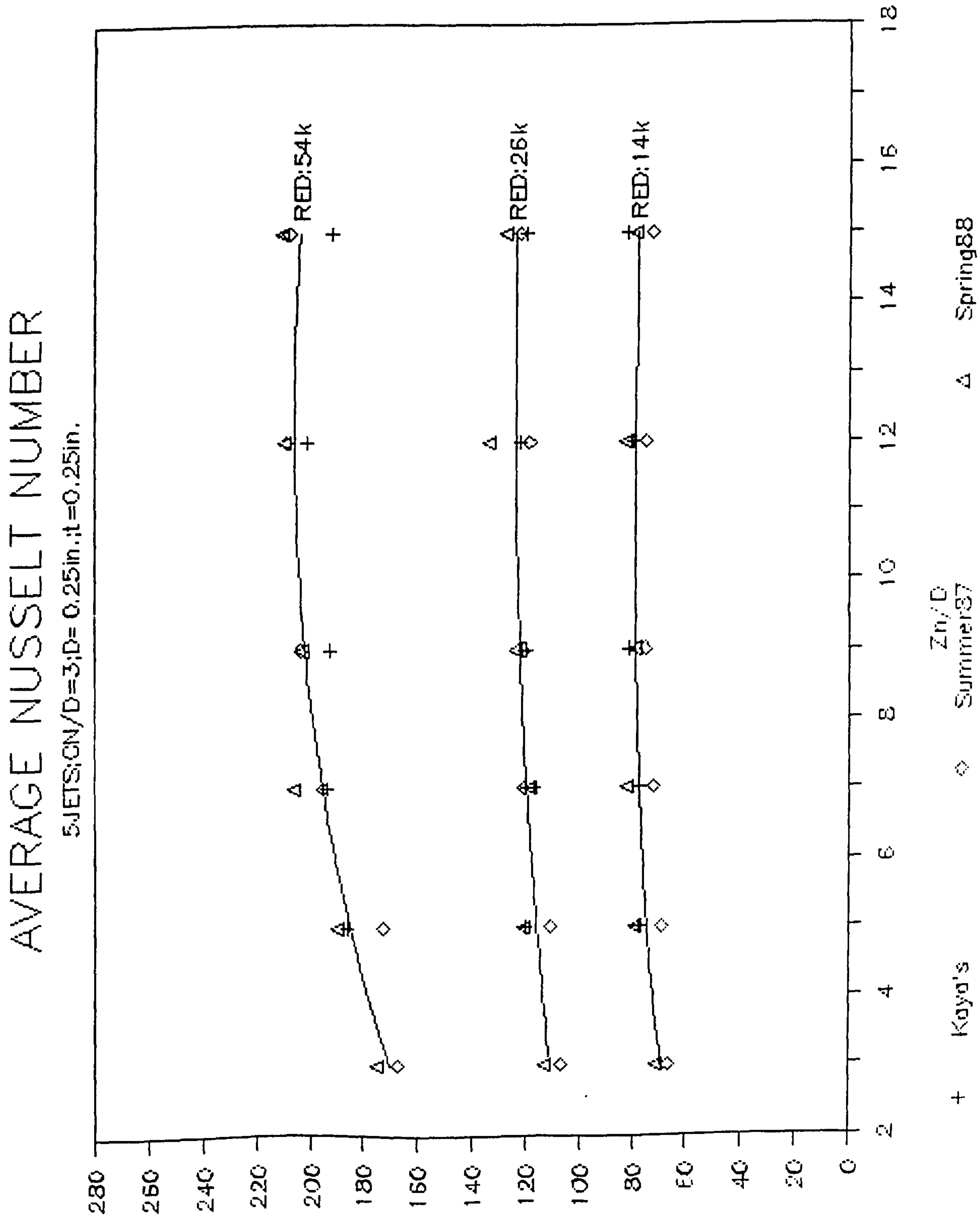

Fig.I-4.16 Average Nusselt Number vs. Zn/D for Five Jets, D=6.35 mm, Cn/D=3

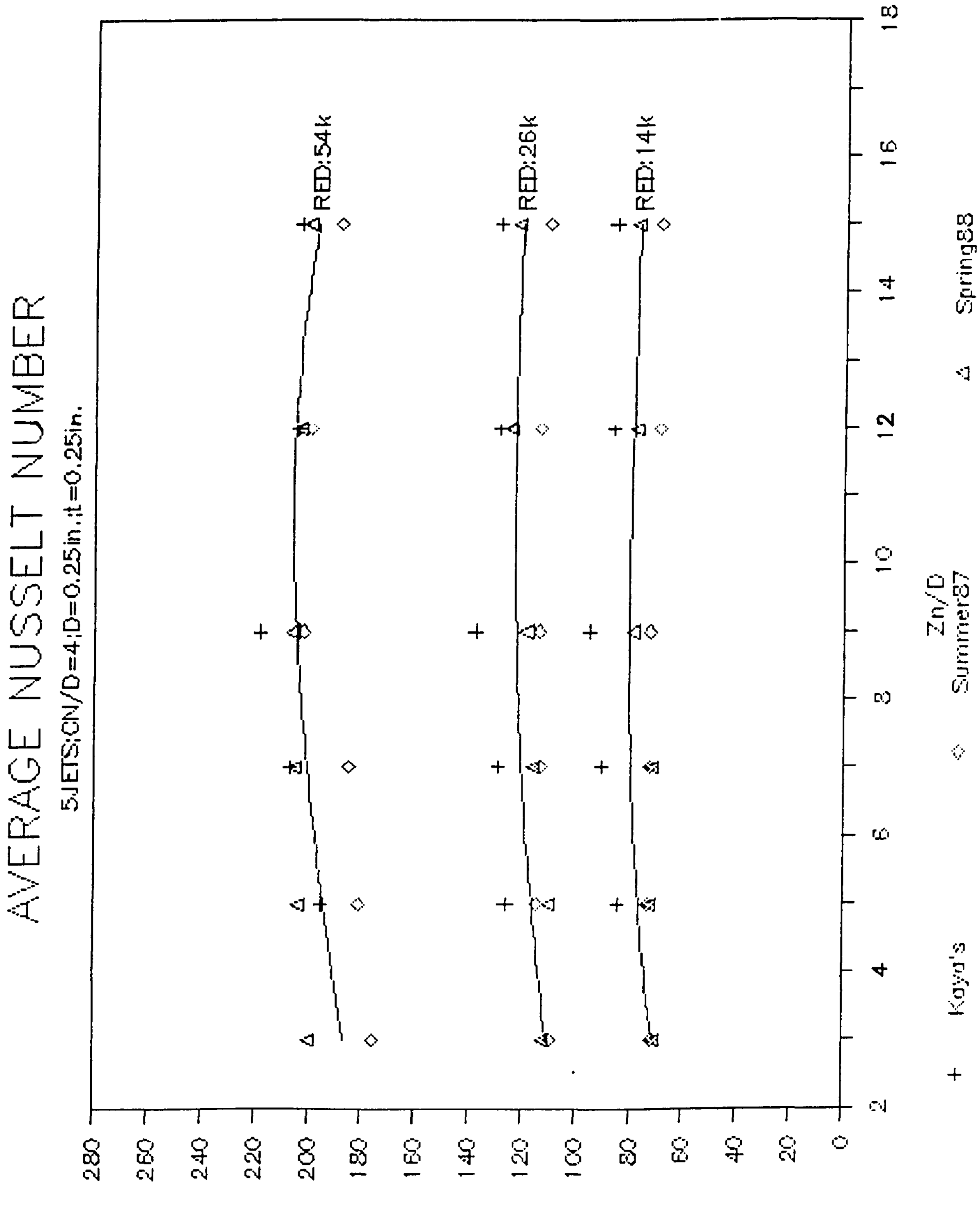

Fig.I-4.17 Average Nusselt Number vs. Zn/D for Five Jets, D=6.35 mm, Cn/D=4

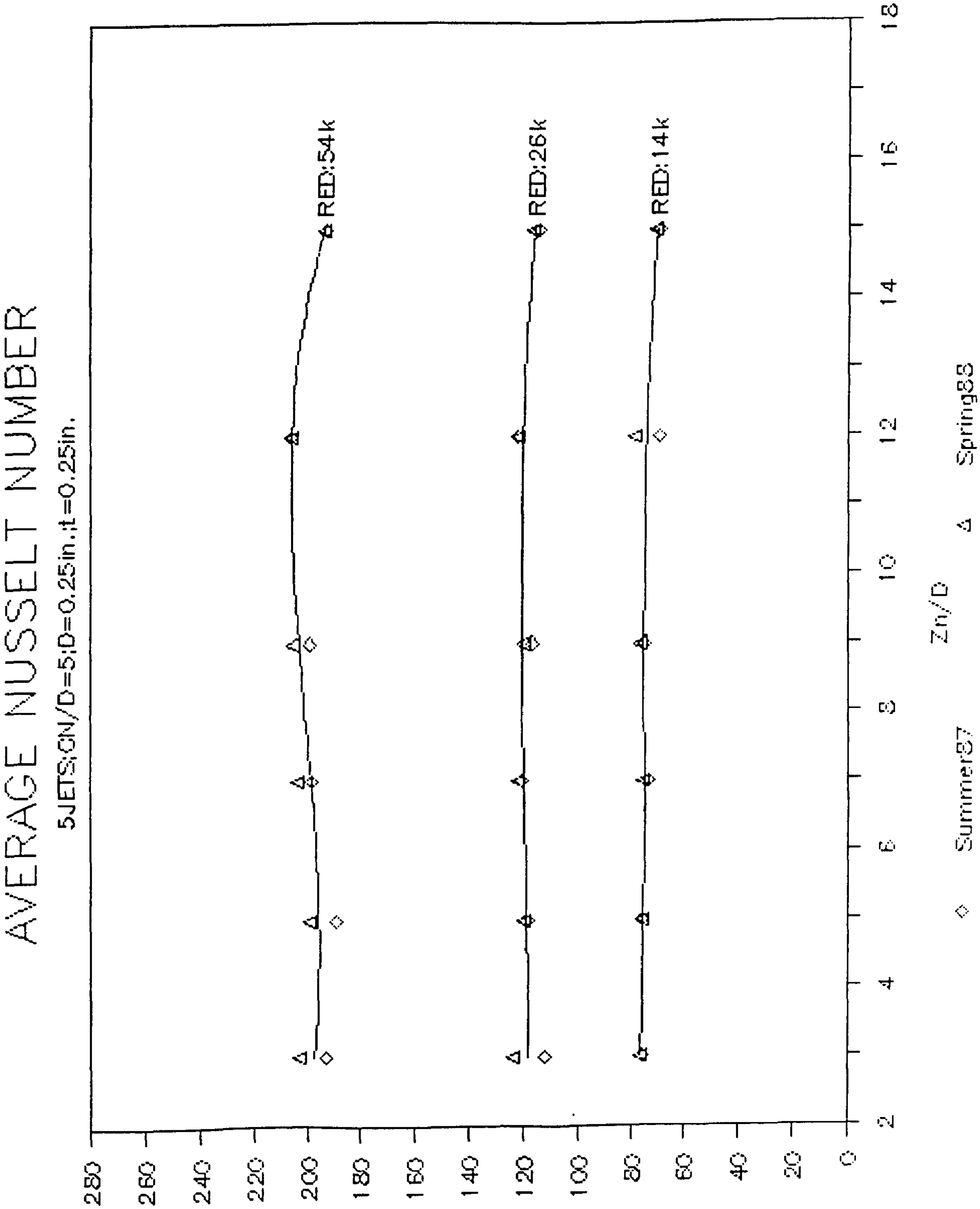

Fig.I-4.18 Average Nusselt number vs. Zn/D for Five Jets, D=6.35 mm, Cn/D=5

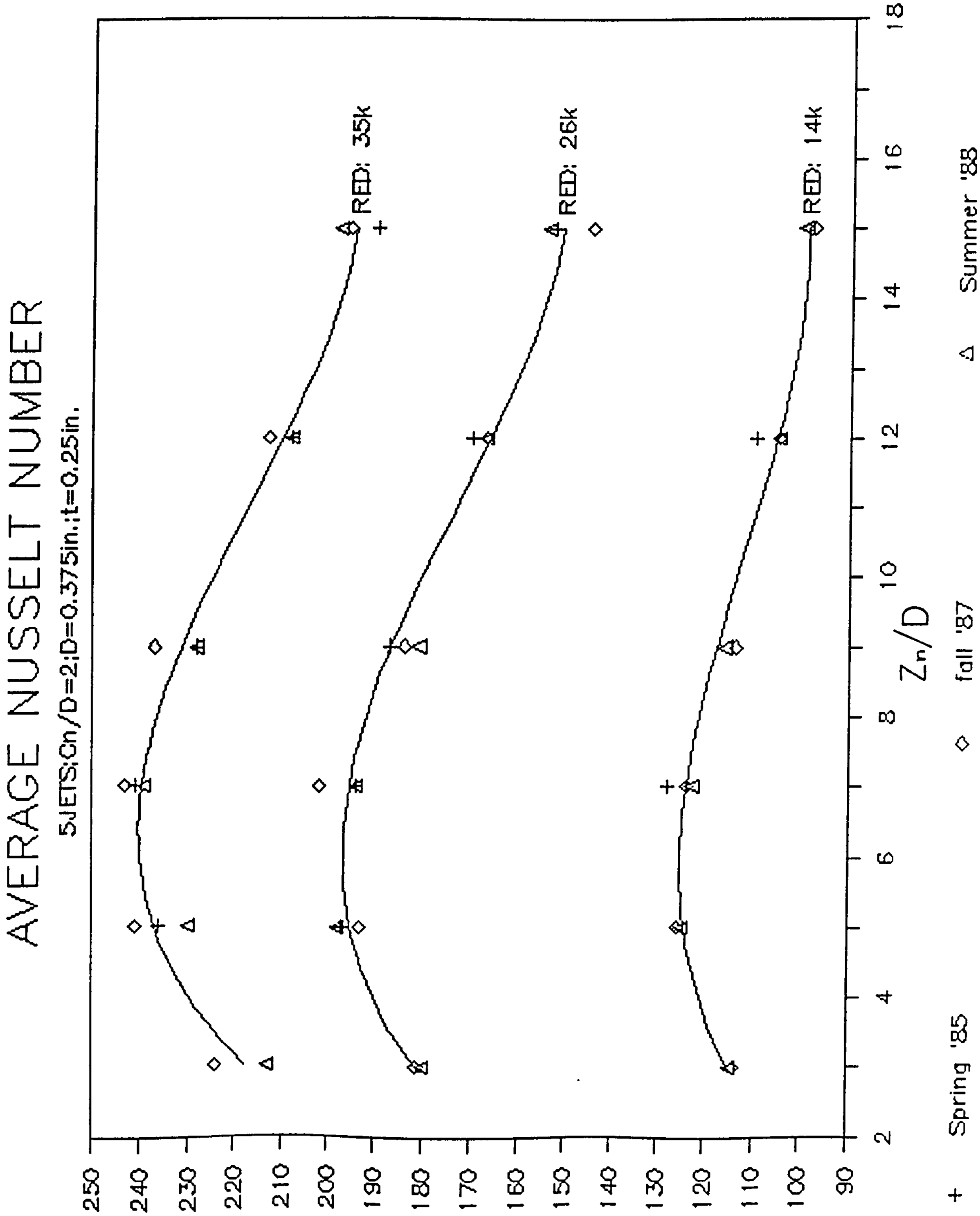

Fig.I-4.19 Average Nusselt number vs. Zn/D for Five Jets, D=9.53 mm, Cn/D=2

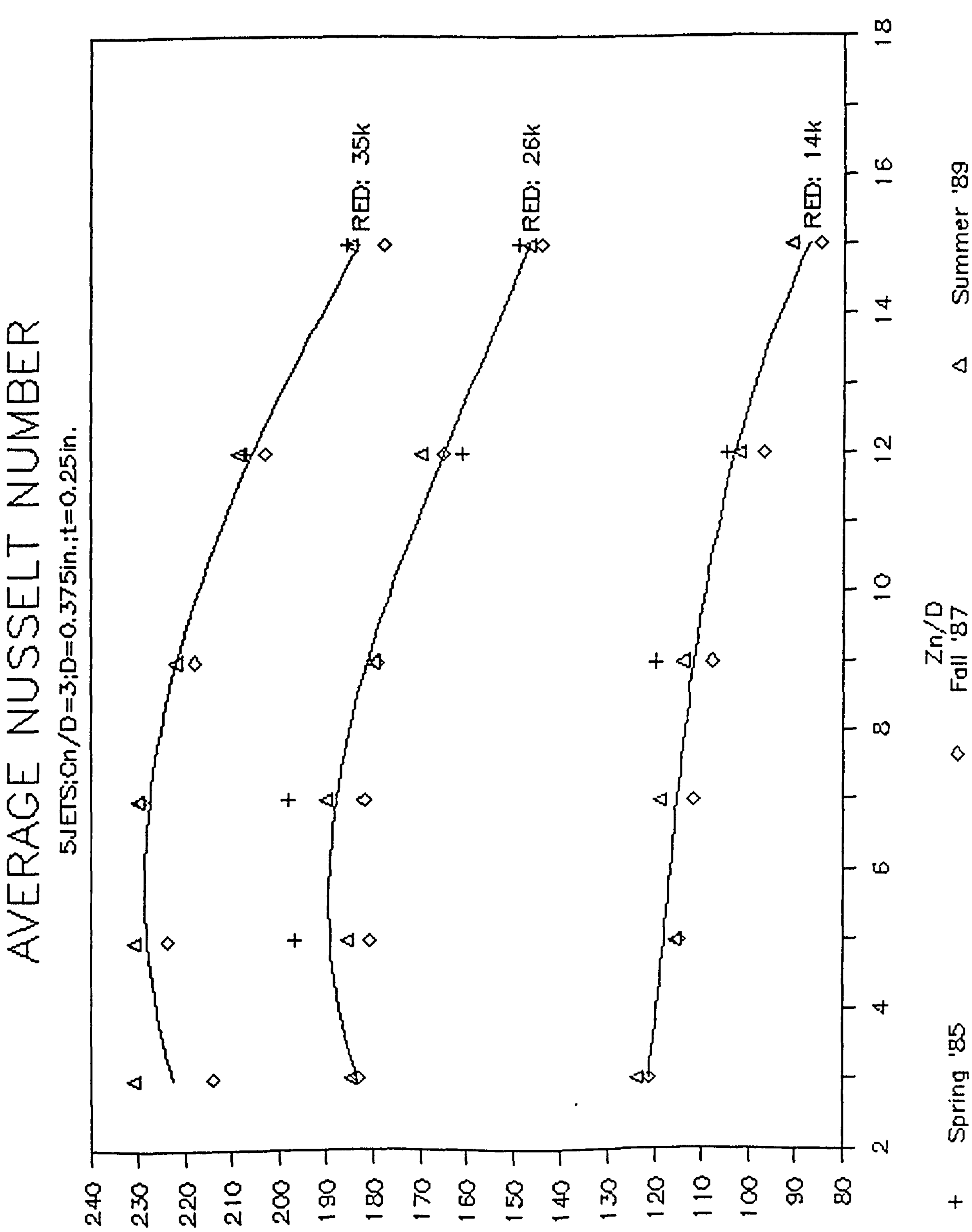

Fig.I-4.20 Average Nusselt Number vs. Zn/D for Five Jets, D=9.53 mm, Cn/D=3

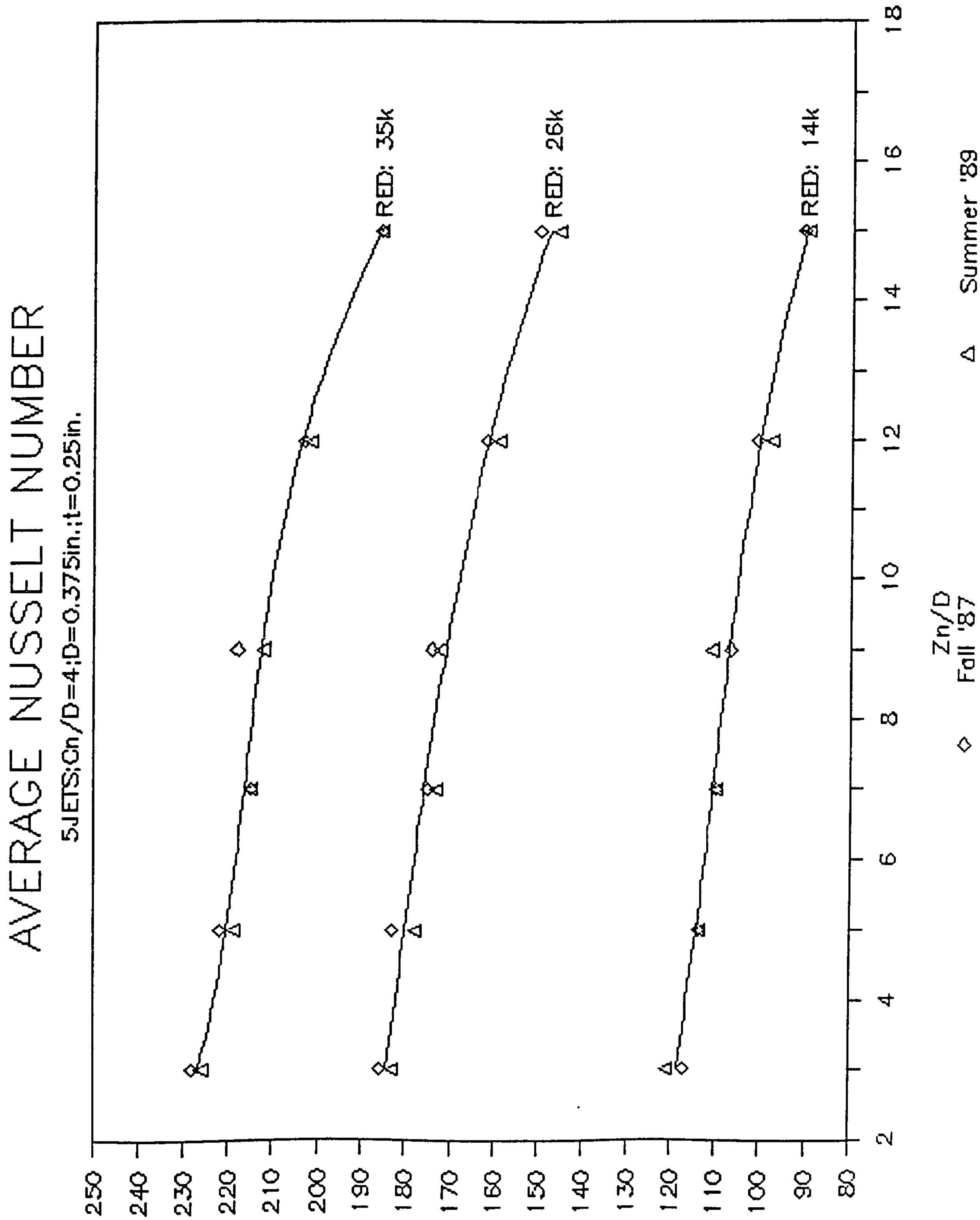

Fig.I-4.21 Average Nusselt Number vs. Zn/D for Five Jets, D=9.53 mm, Cn/D=4

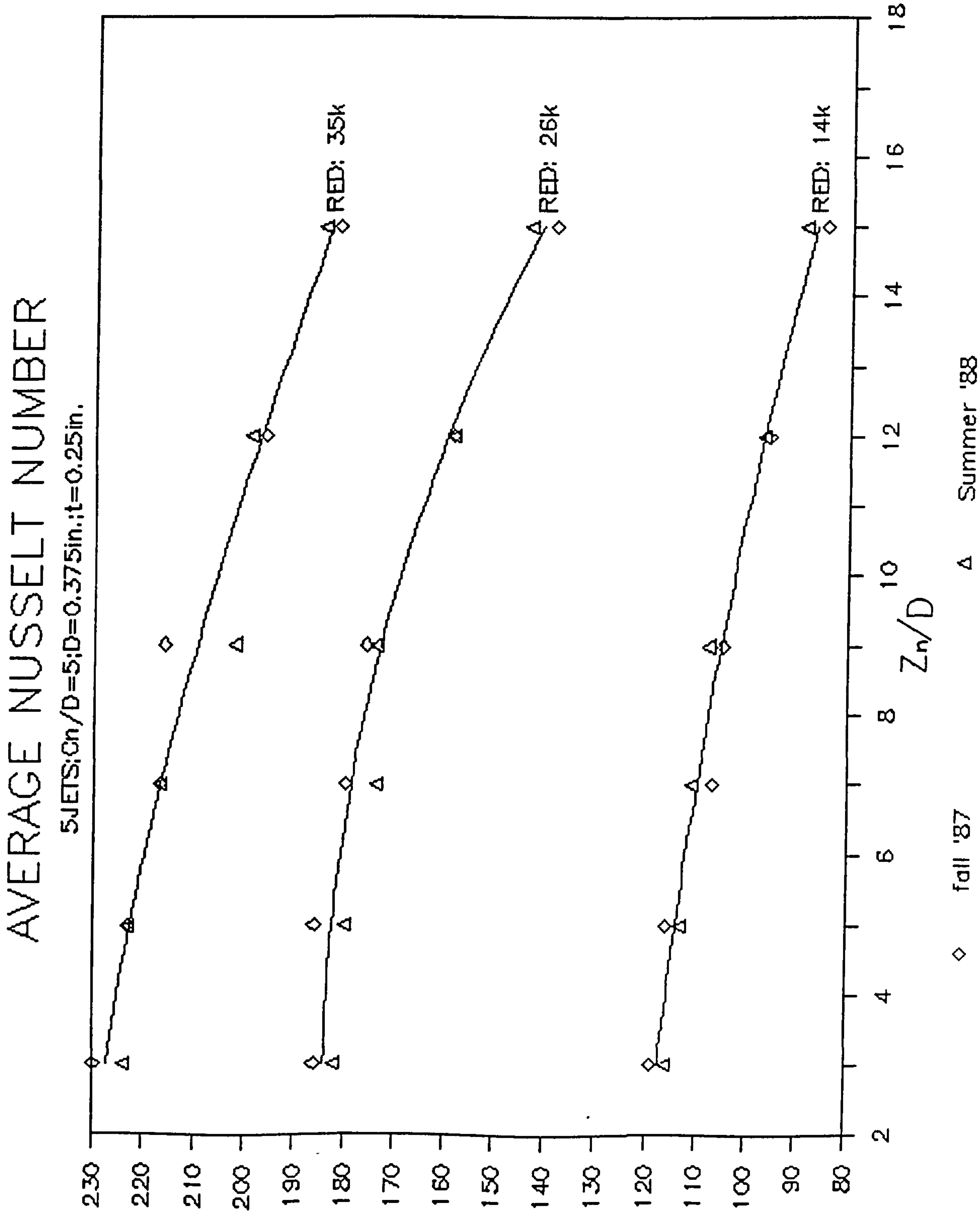

Fig.I-4.22 Average Nusselt Number vs. Zn/D for Five Jets,
D=9.53 mm, Cn/D=5

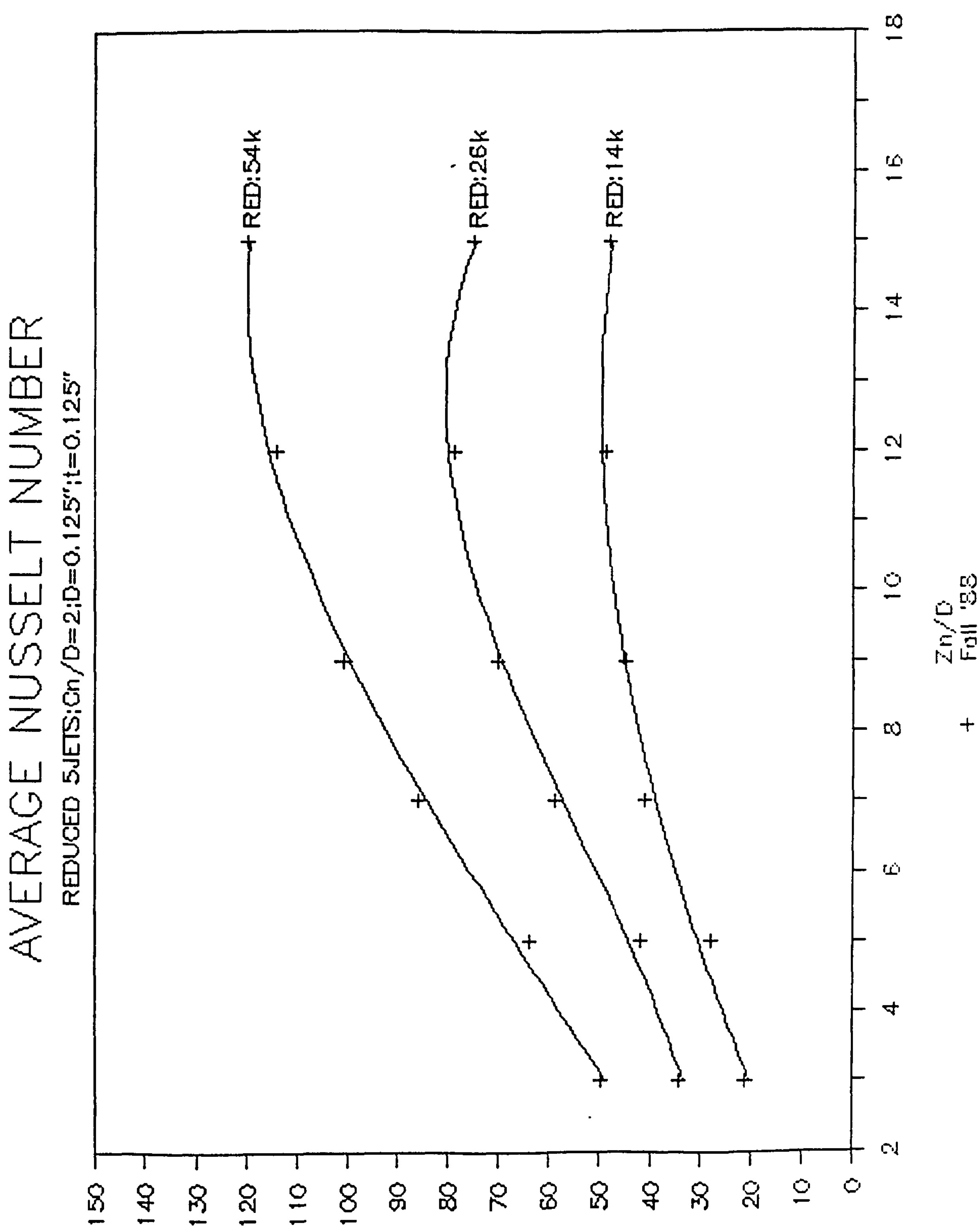

Fig.I-4.23 Average Nusselt Number vs. Zn/D for Reduced Five Jets, D=3.18 mm, Cn/D=2

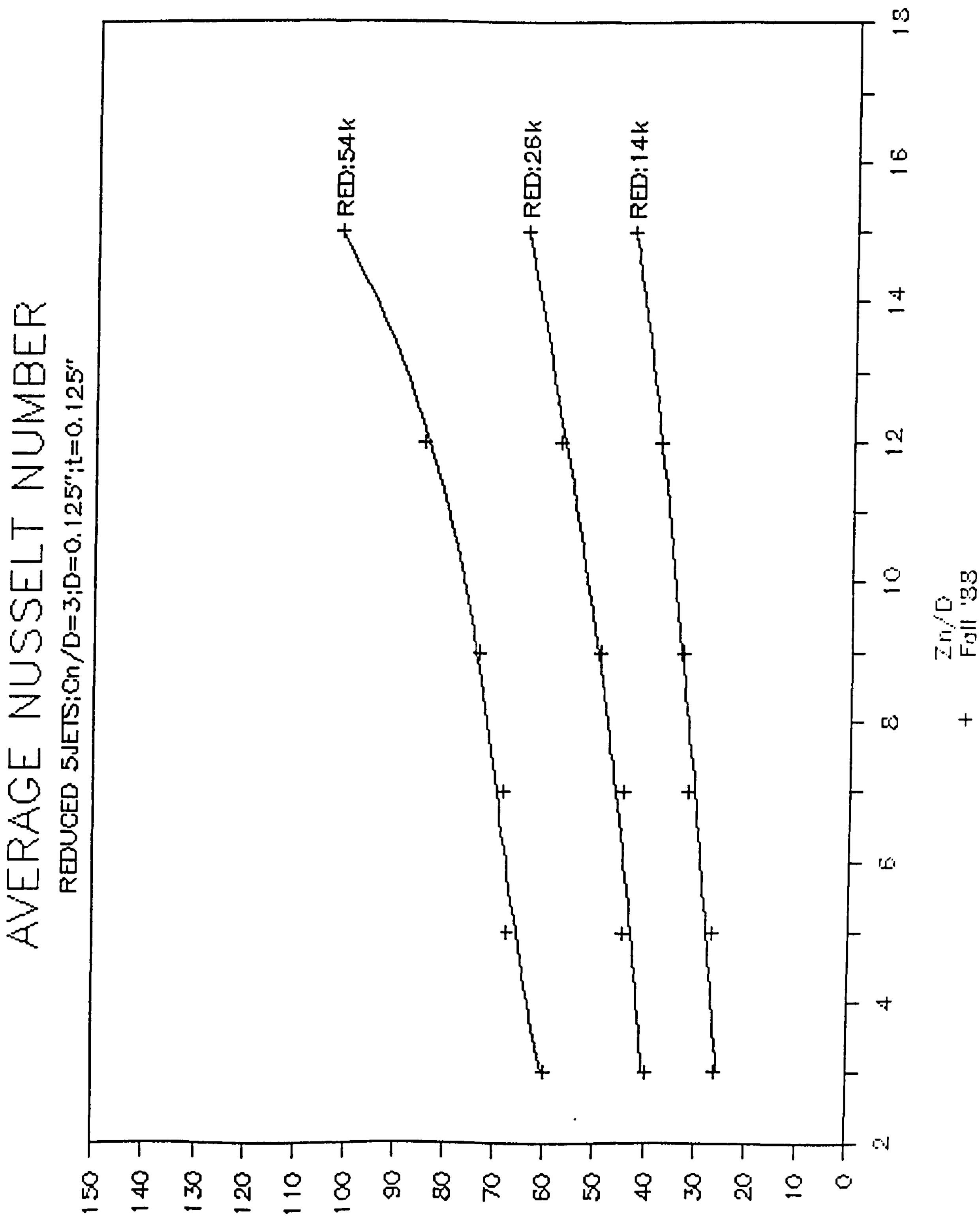

Fig.I-4.24 Average Nusselt Number vs. Zn/D for Reduced Five Jets, D=3.18 mm, Cn/D=3

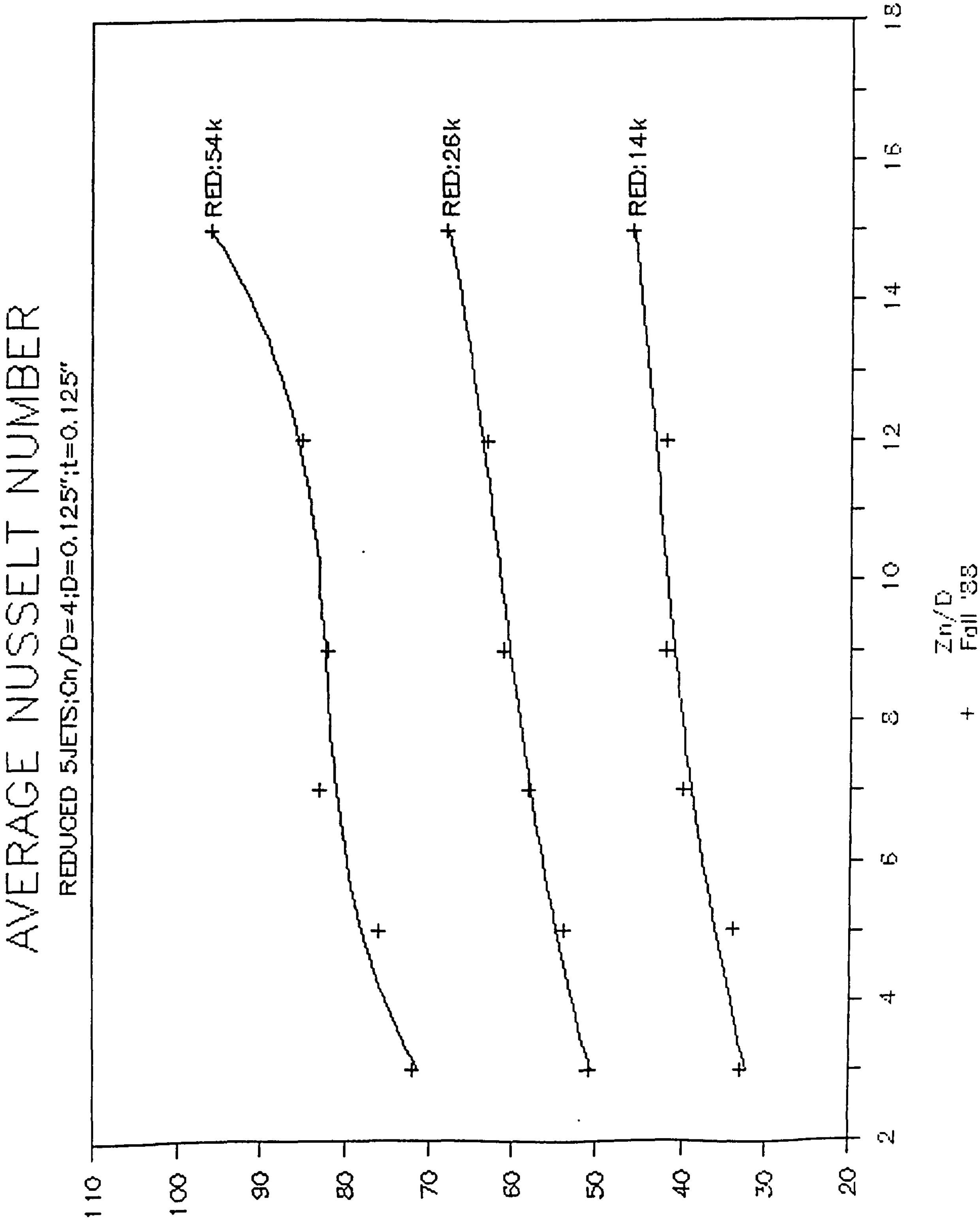

Fig.I-4.25 Average Nusselt Number vs. Zn/D for Reduced Five Jets, D=3.18 mm, Cn/D=4

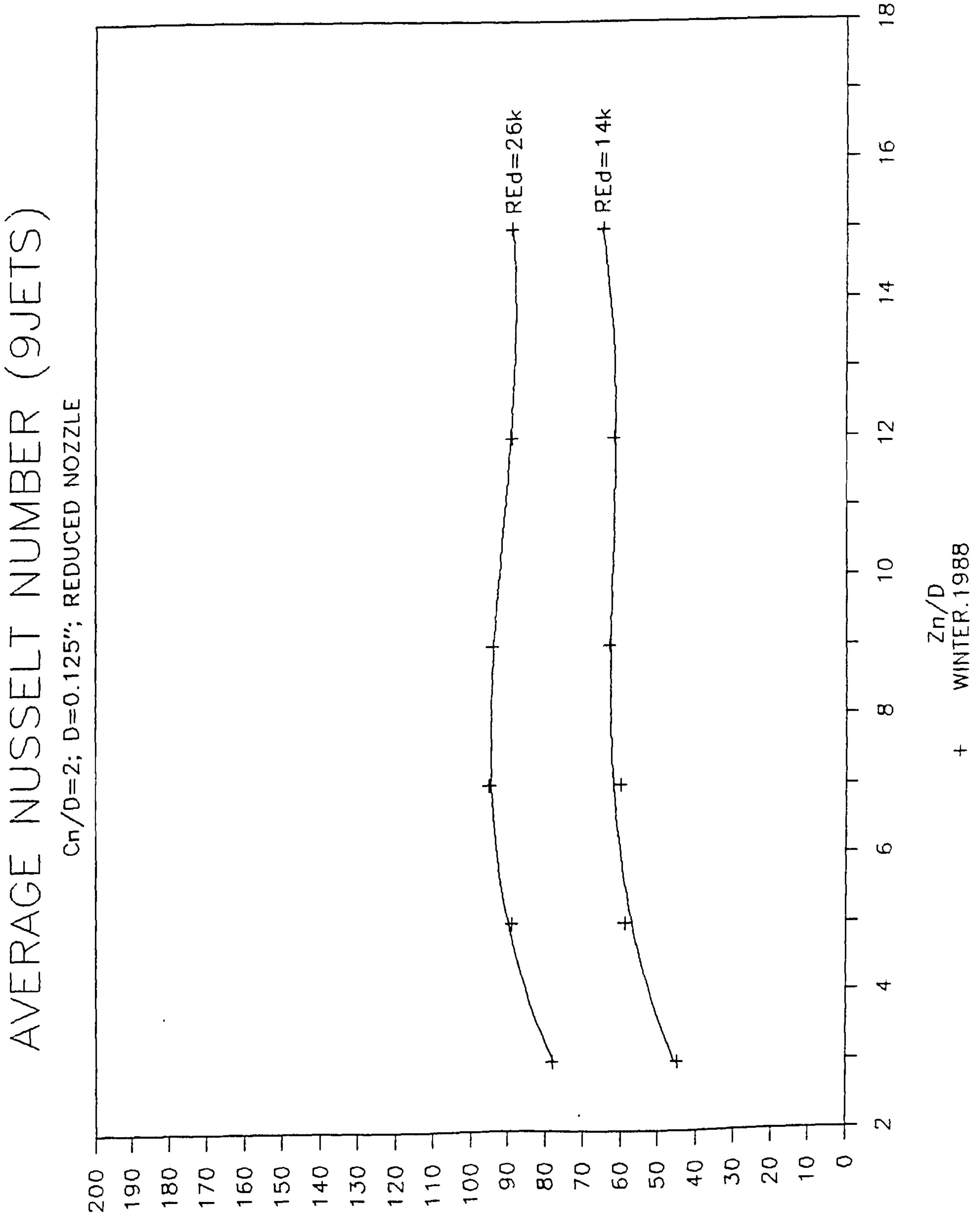

Fig.I-4.26 Average Nusselt Number vs. Zn/D for Reduced Nine Jets, D=3.18 mm, Cn/D=2

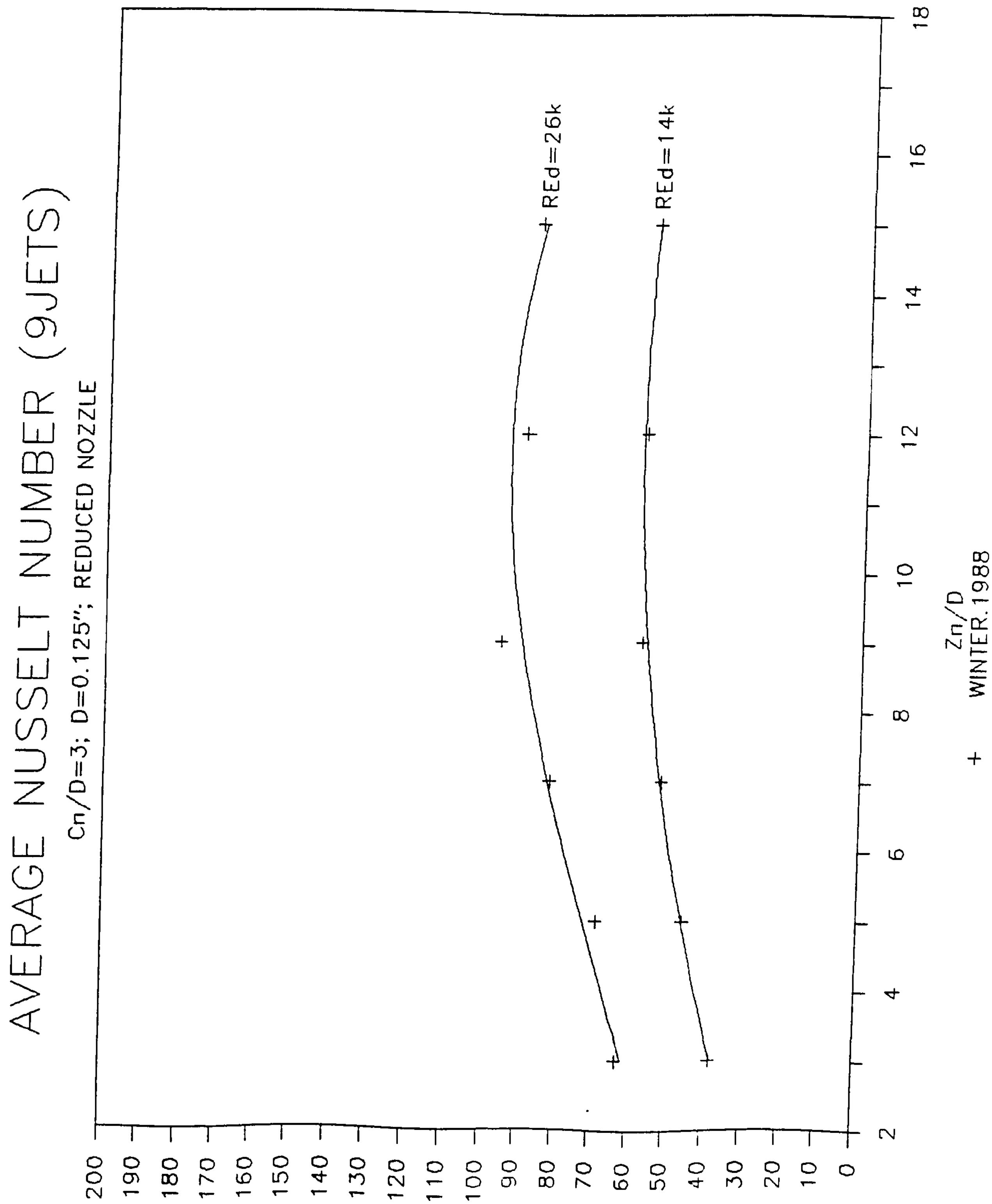

Fig.I-4.27 Average Nusselt Number vs. Zn/D for Reduced Nine Jets, D=3.18 mm, Cn/D=3

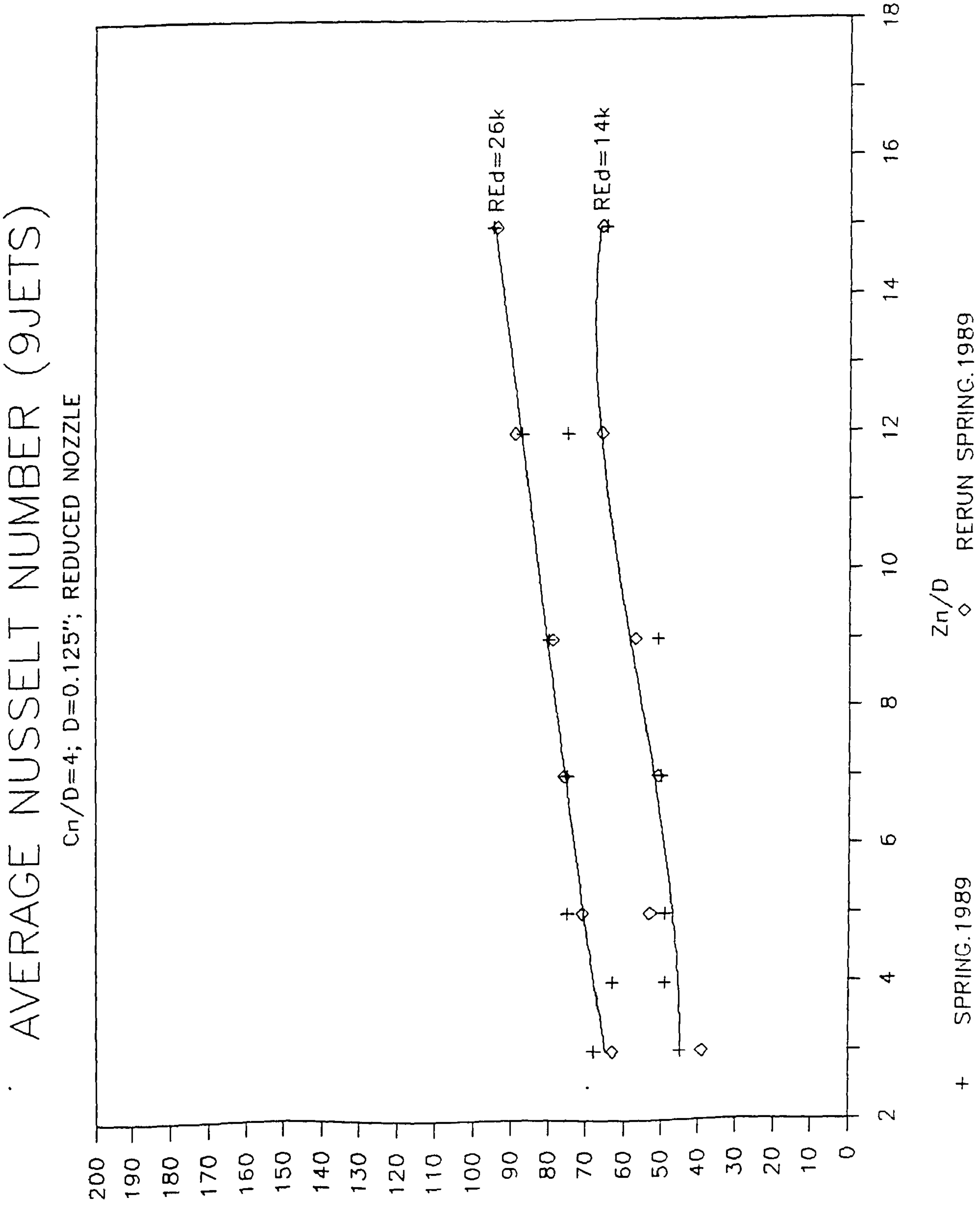

Fig.I-4.28 Average Nusselt Number vs. Zn/D for Reduced Nine Jets, D=3.18 mm, Cn/D=4

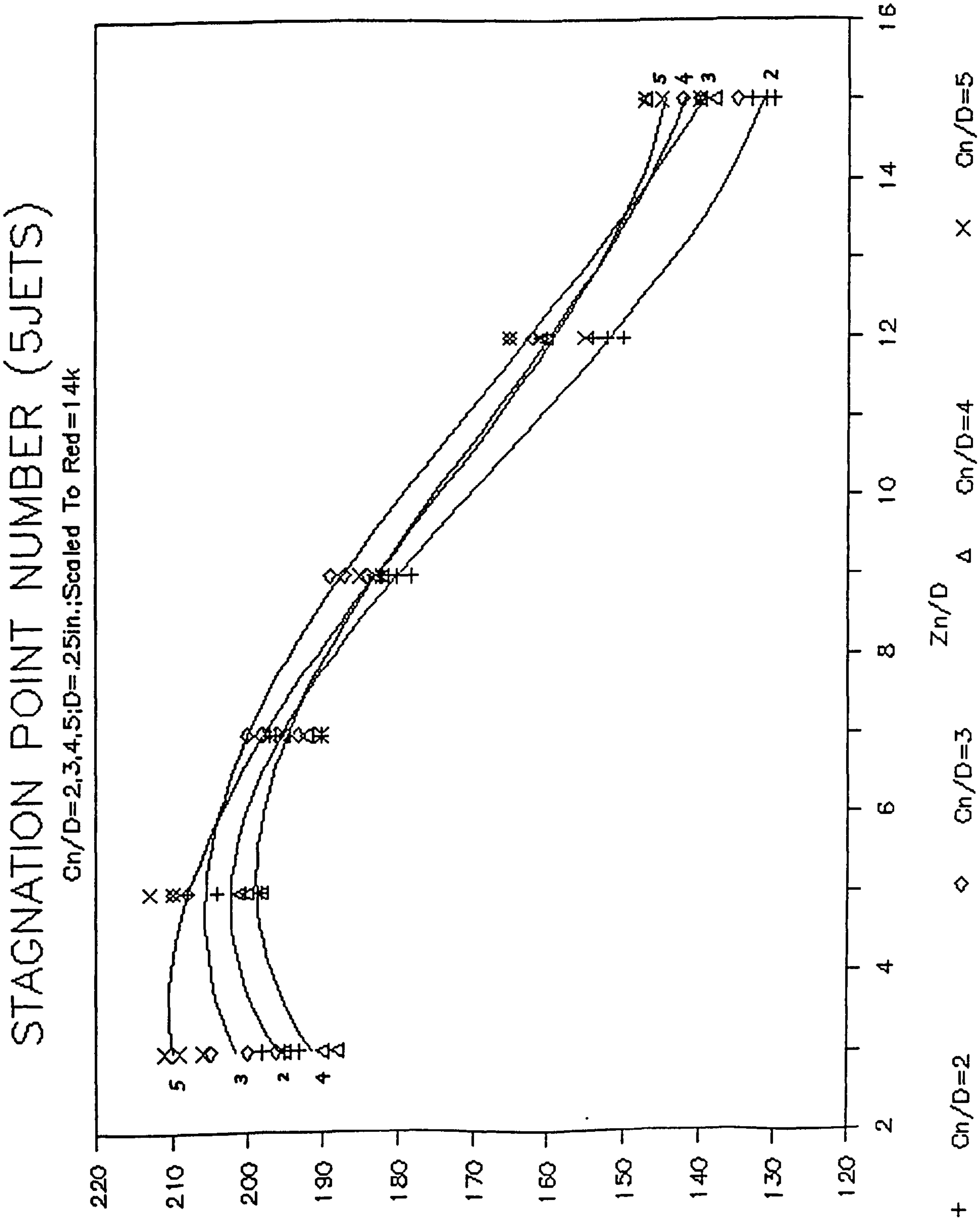

Fig.I-5.1 Comparison with Cn/D=2, 3, 4, 5 of Stagnation Point Nusselt Number at Re_D Scaled to 14,000, for Five Jets, D=6.35 mm

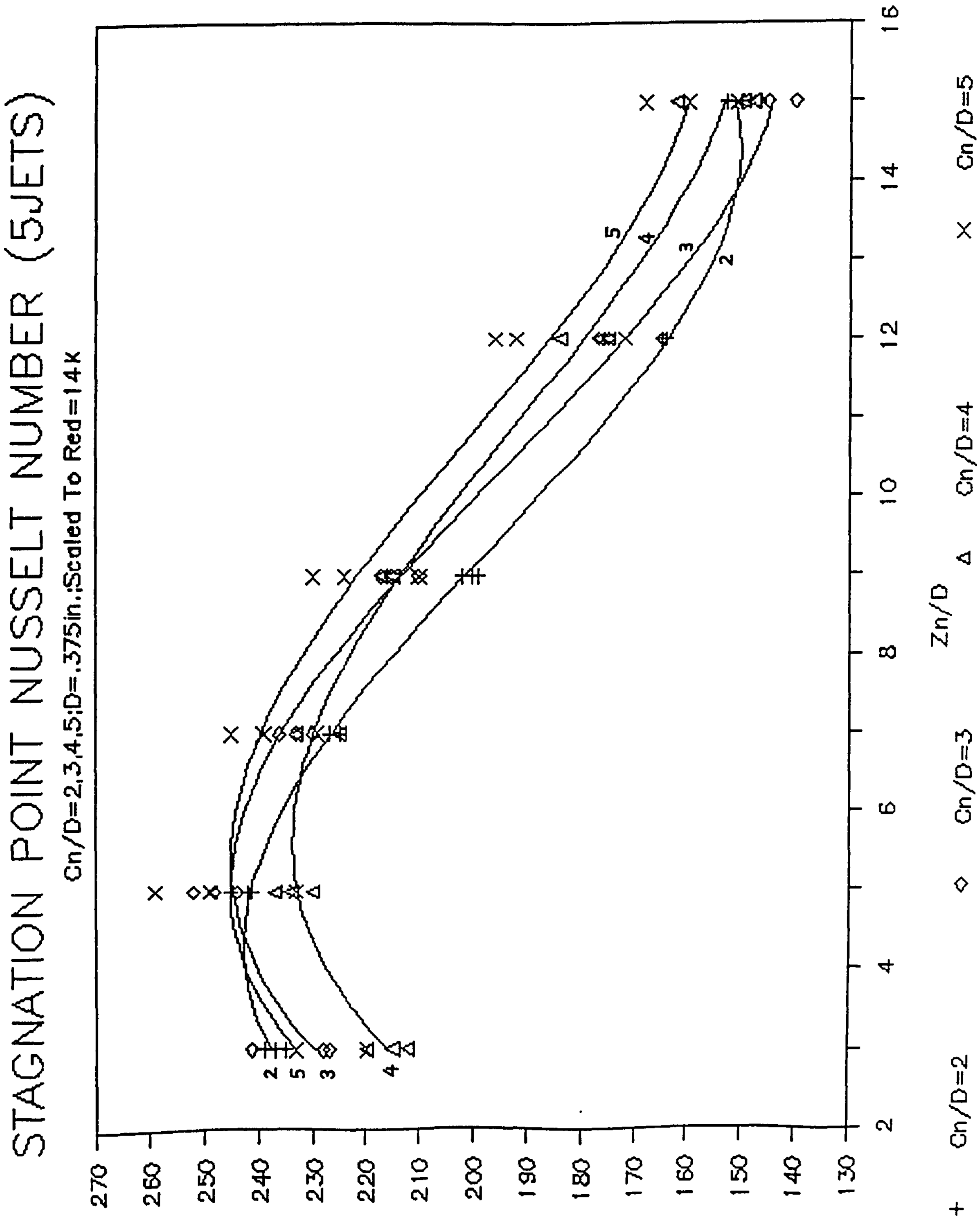

Fig.I-5.2 Comparison with Cn/D=2, 3, 4, 5 of Stagnation Point Nusselt Number at Re_D Scaled to 14,000, for Five Jets, D=9.53 mm

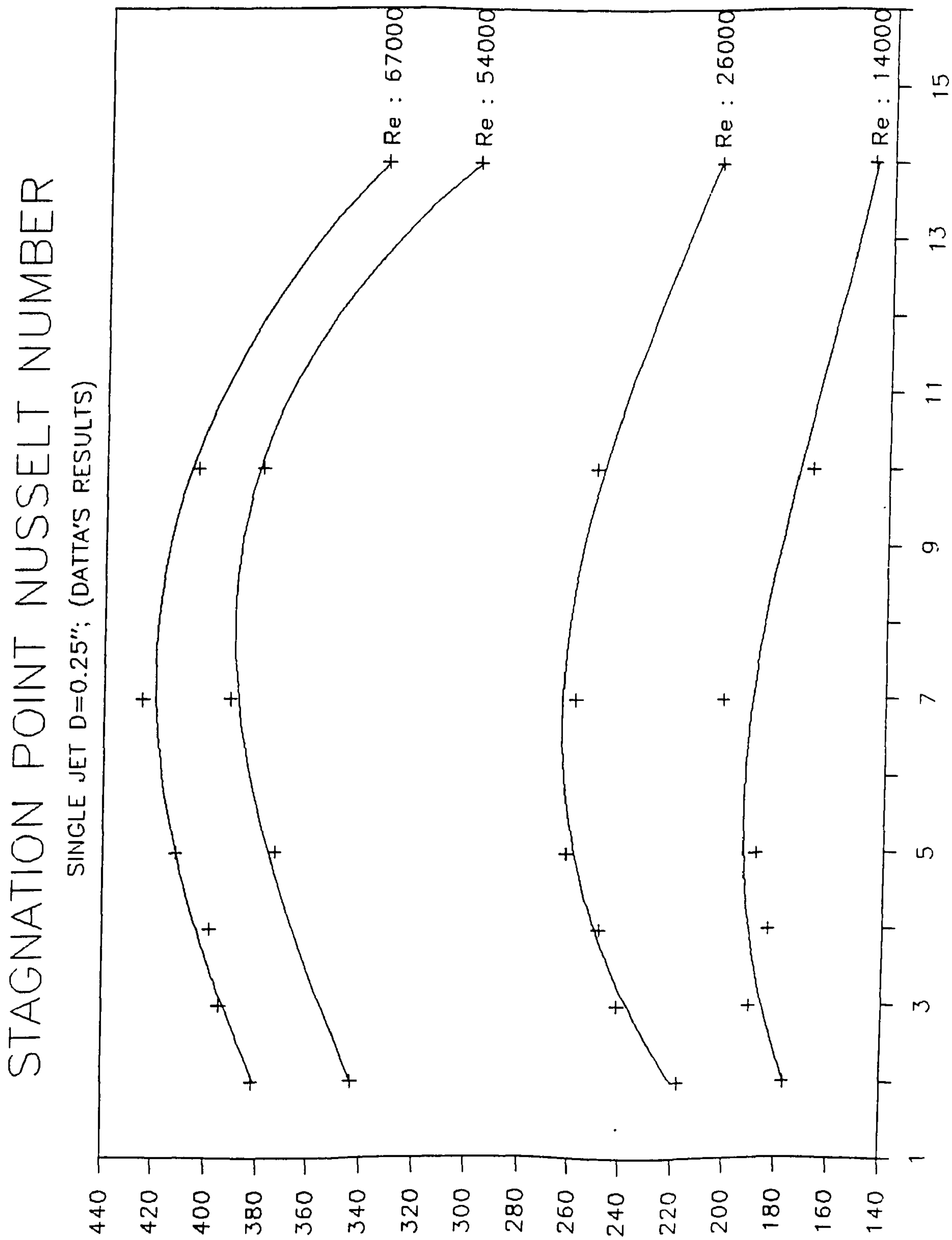

Fig.I-5.3 Stagnation Point Nusselt Number vs. Zn/D for Single Jet, D=6.35 mm

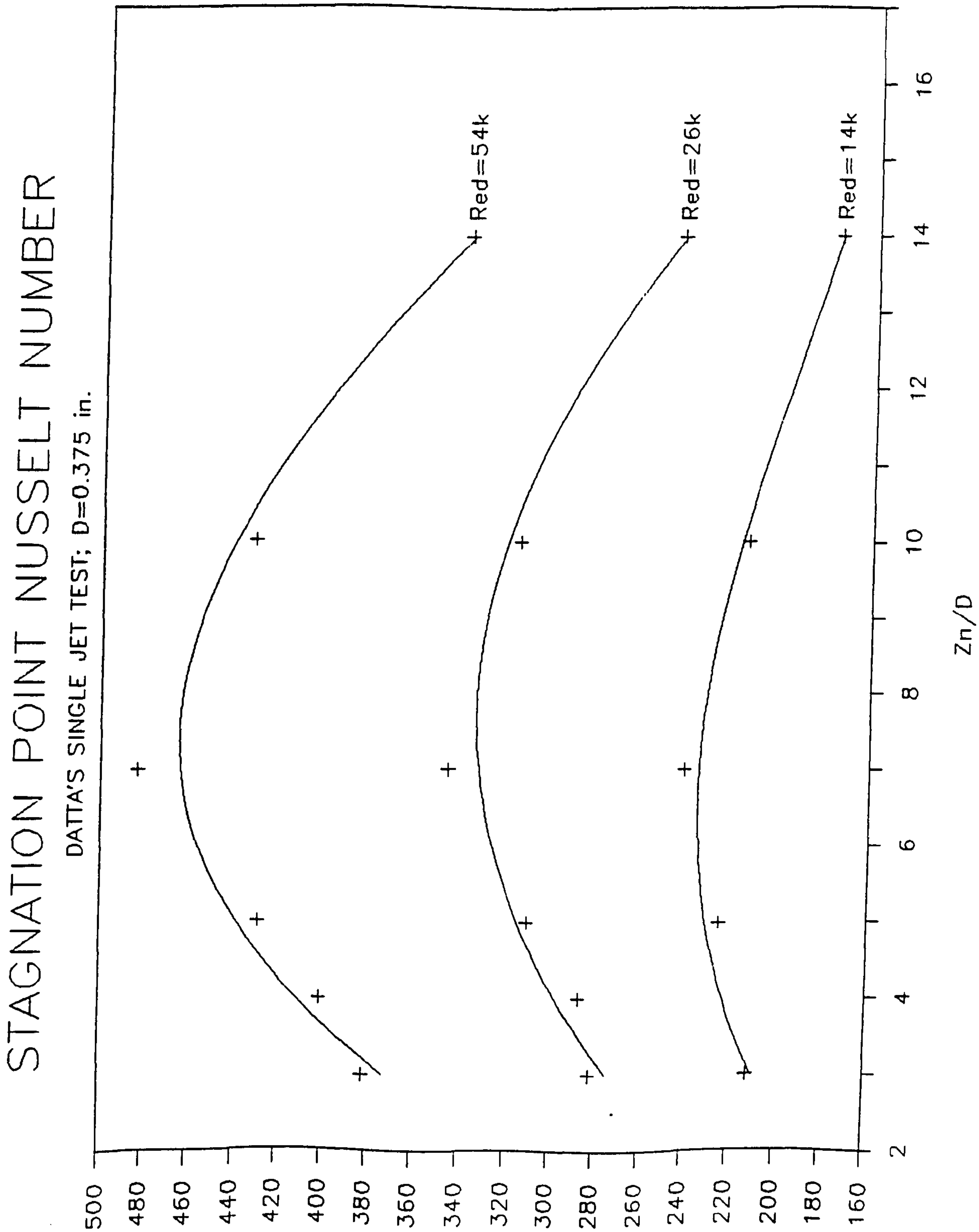

Fig.I-5.4 Stagnation Point Nusselt Number vs. Zn/D for Single Jet, D=9.53 mm

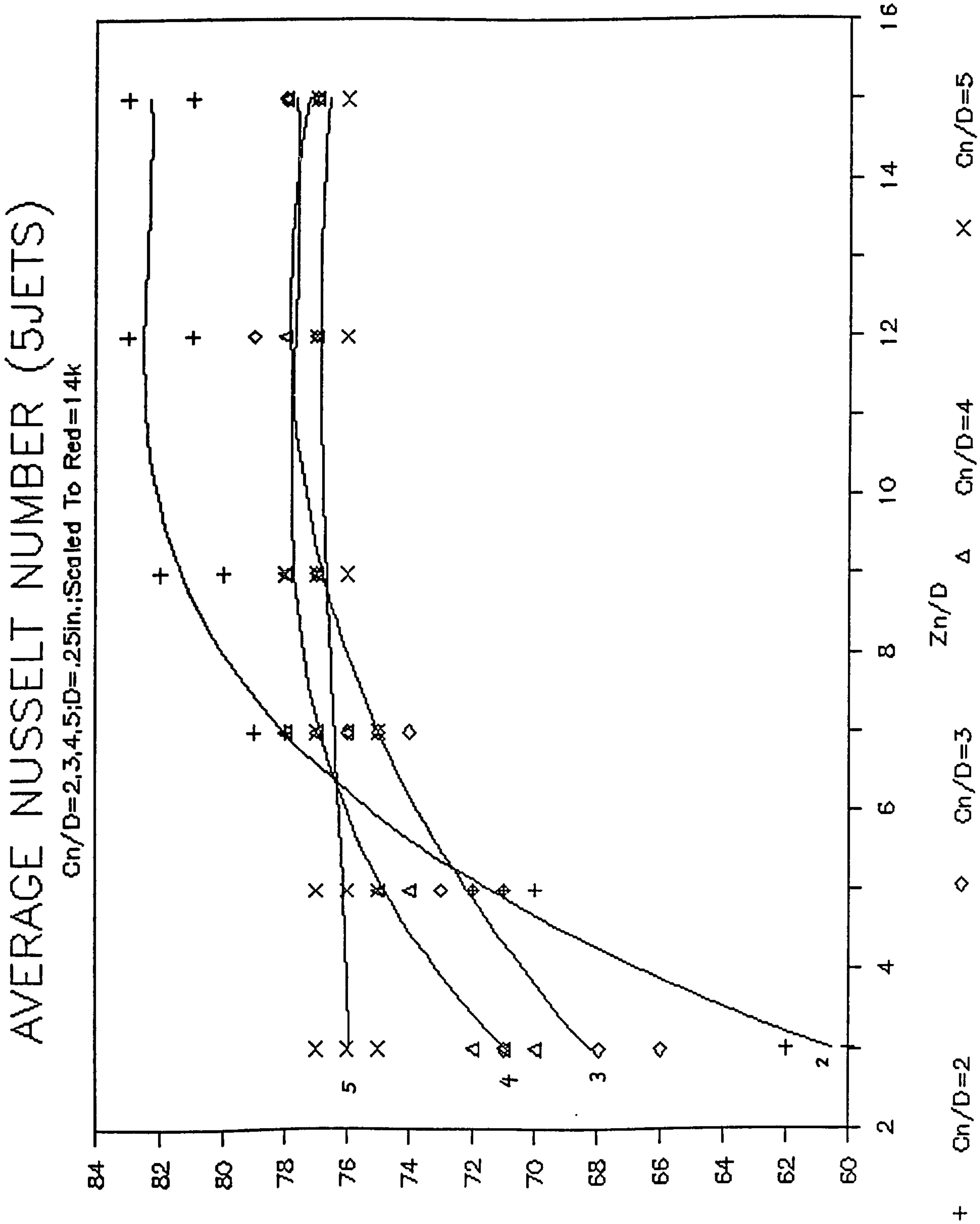

Fig.I-5.5 Comparison with Cn/D=2,3,4,5 of Average Nusselt Number at Re_D Scaled to 14,000, for Five Jets, D=6.35 mm

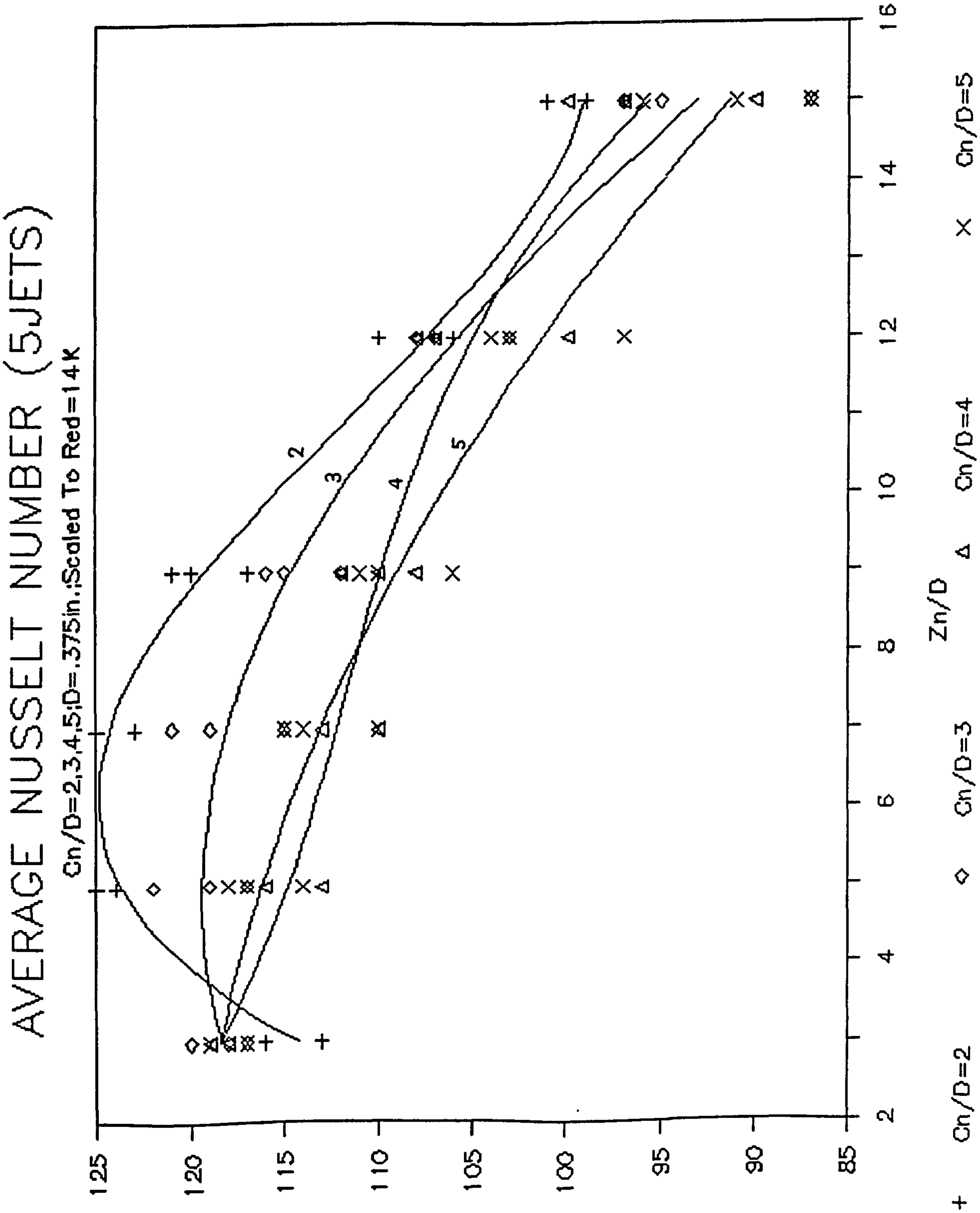

Fig.I-5.6 Comparison with Cn/D=2,3,4,5 of Average Nusselt Number at Re_D scaled to 14,000, for Five Jets, D=9.53 mm

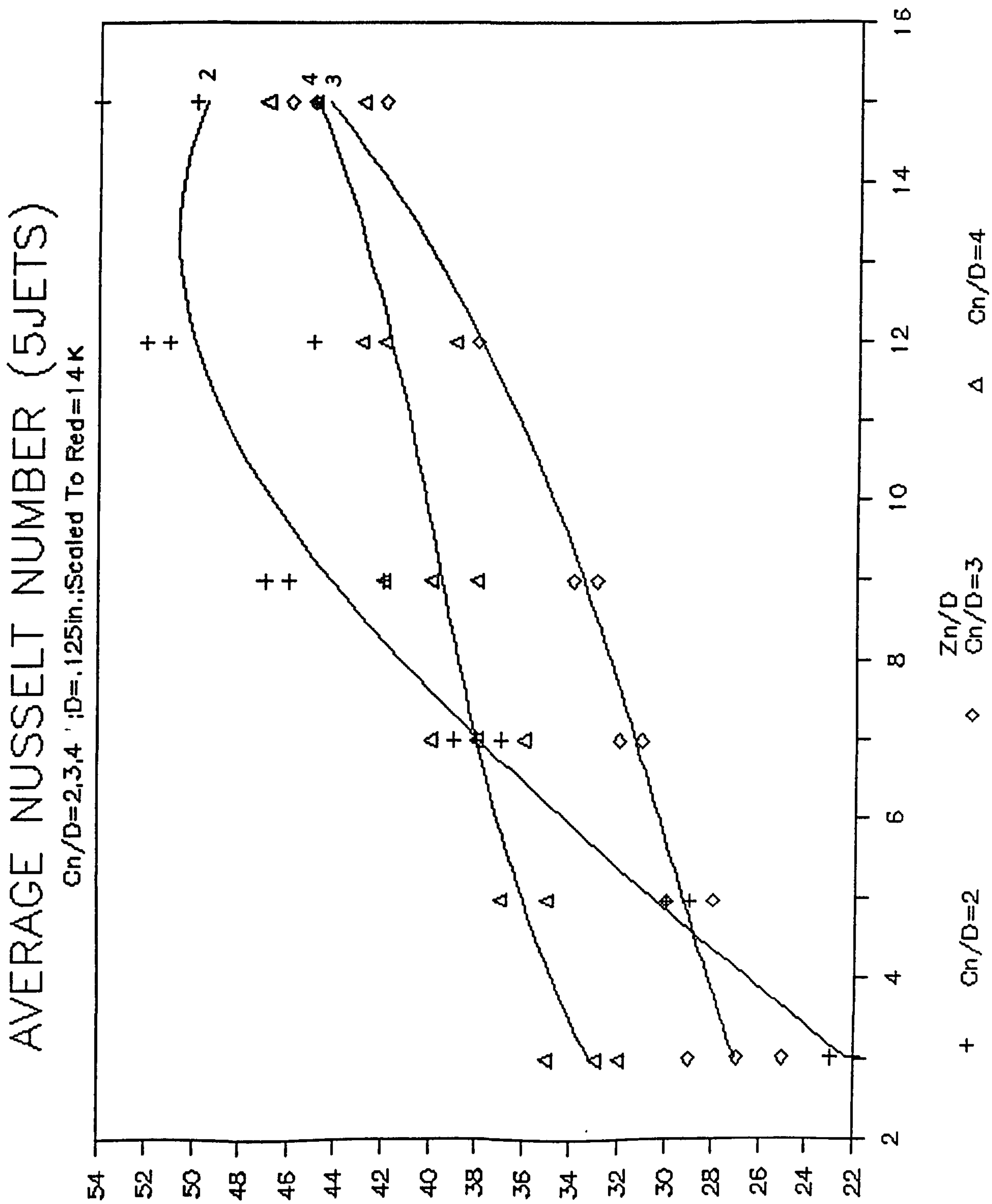

Fig.I-5.7 Comparison with Cn/D=2, 3, 4 of Average nusselt Number at Re_D scaled to 14,000, for Reduced Five Jets, D=3.18 mm

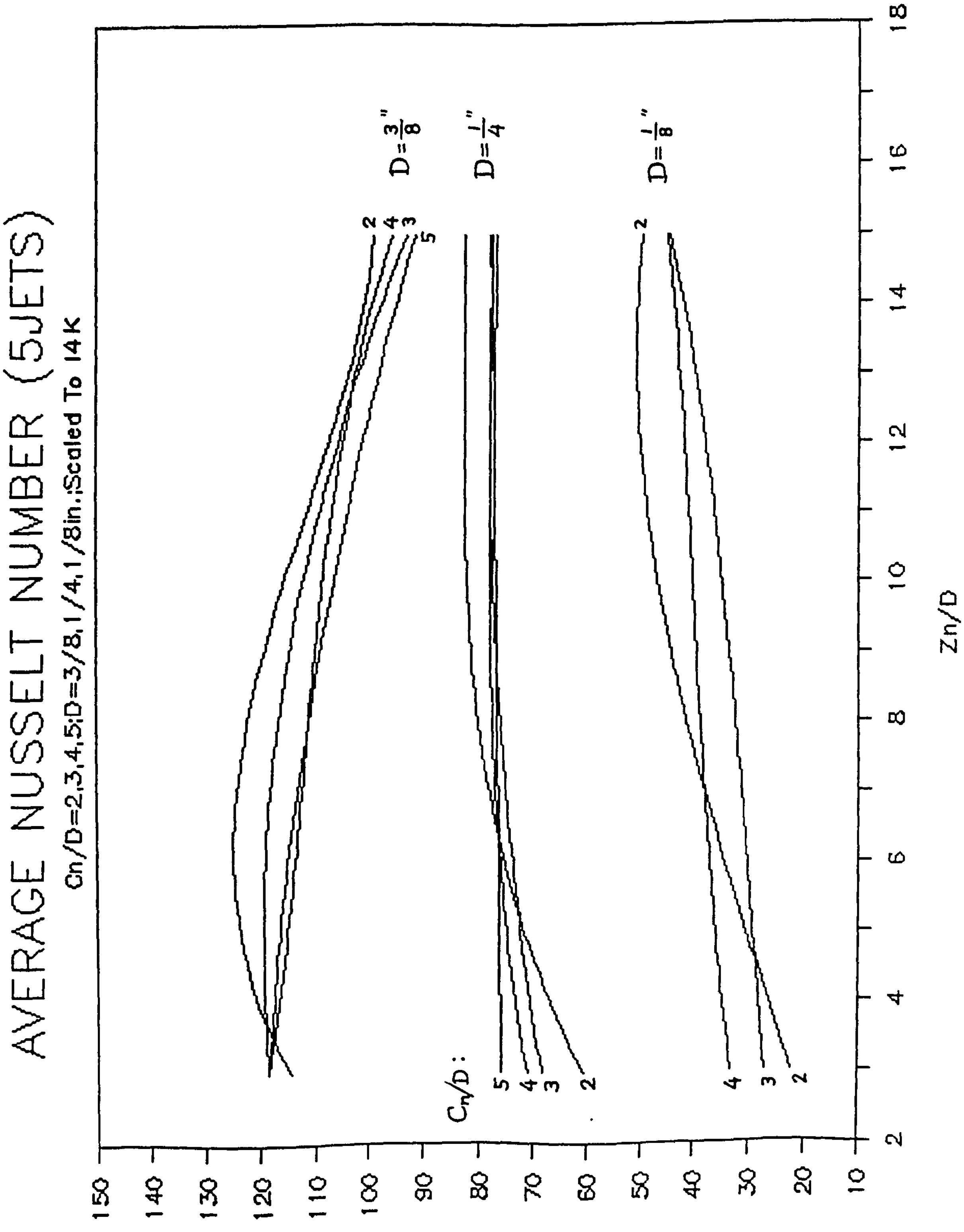

Fig.I-5.8 Comparison with Cn/D=2, 3, 4, 5 of Average Nusselt Number at Re_D Scaled to 14,000, for Five Jets, D=3.18, 6.35, 9.53 mm

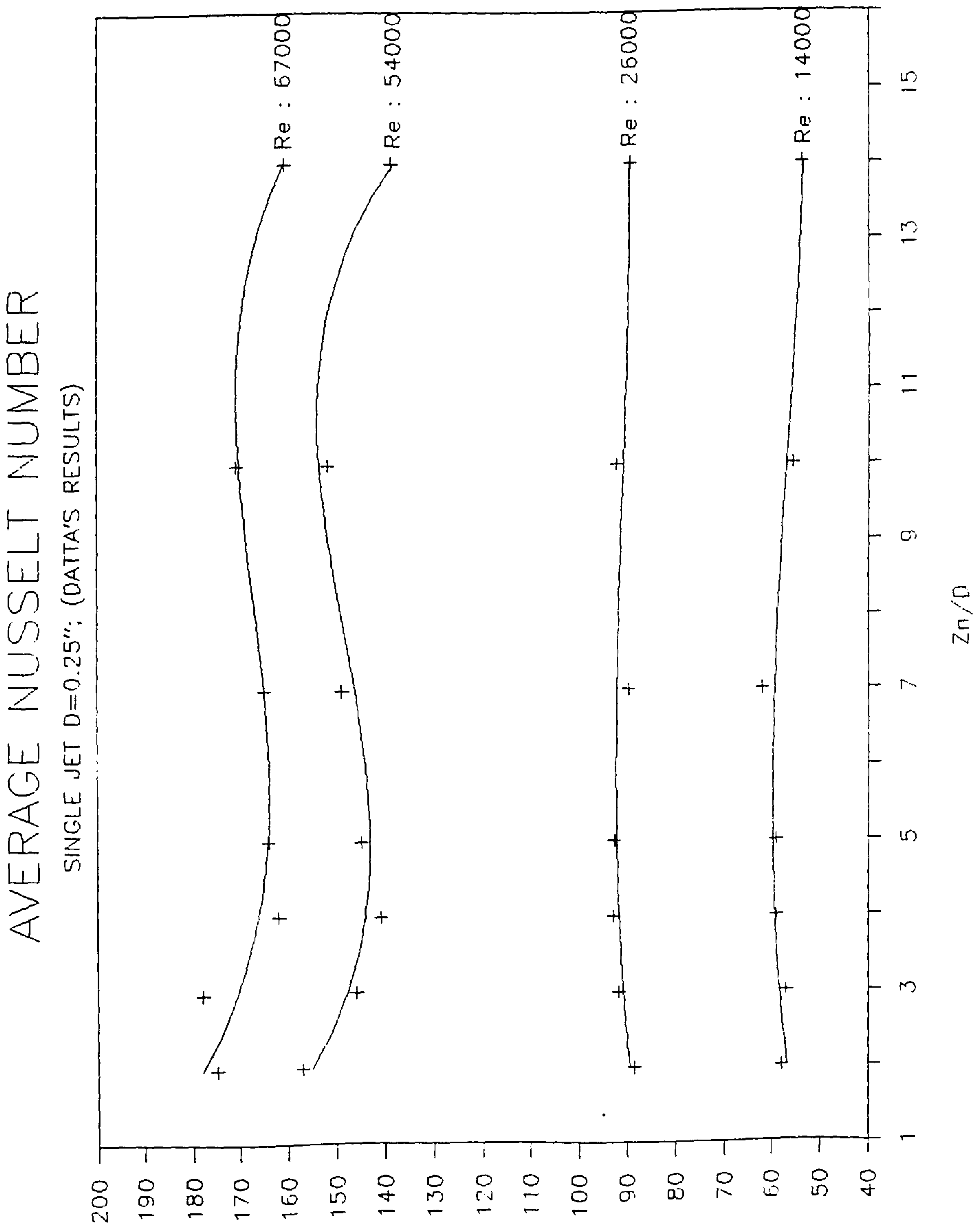

Fig.I-5.9 Average Nusselt Number vs. Zn/D, for single Jet, D=6.35 mm

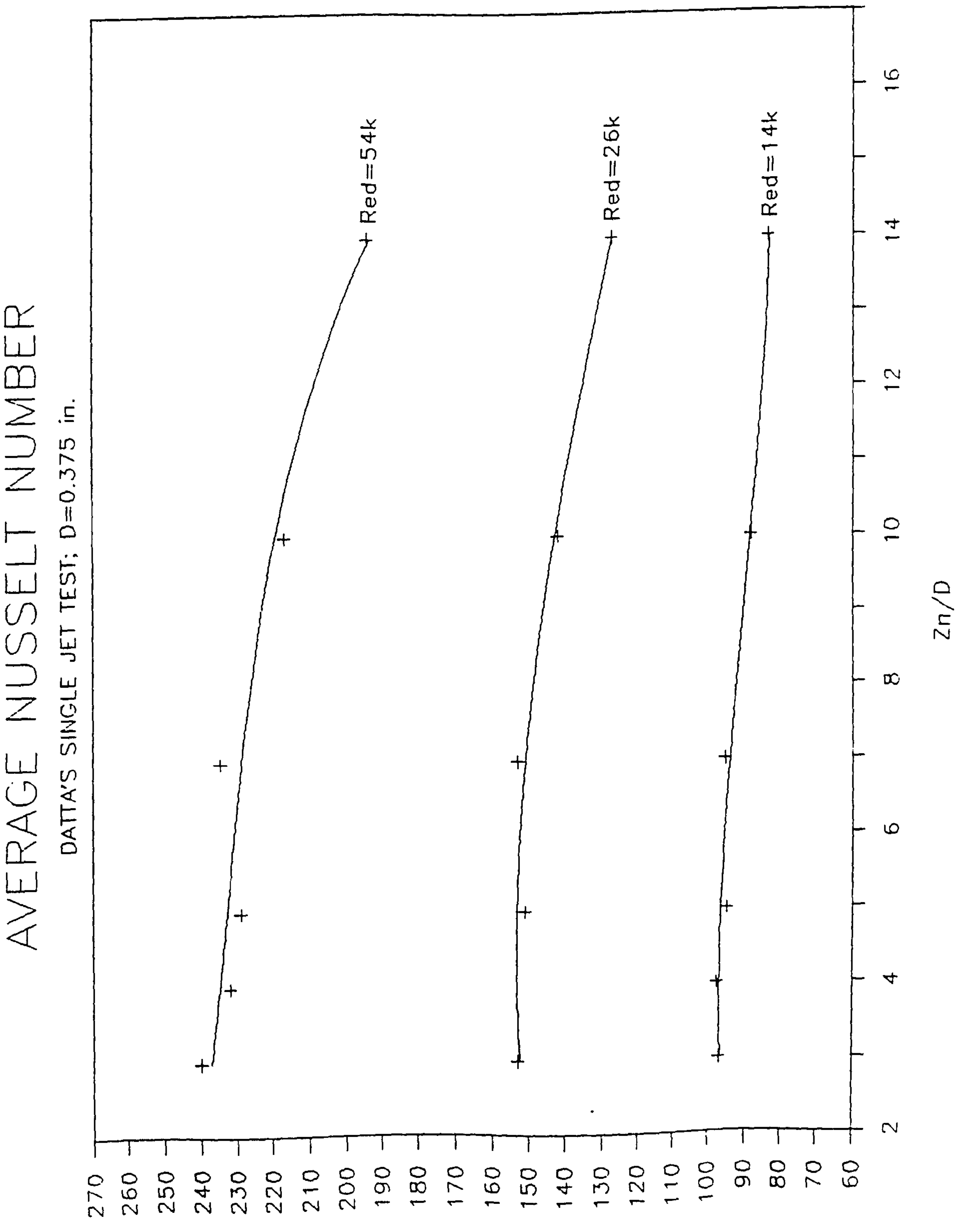

Fig.I-5.10 Average Nusselt Number vs. Zn/D, for Single Jet, D=9.53 mm

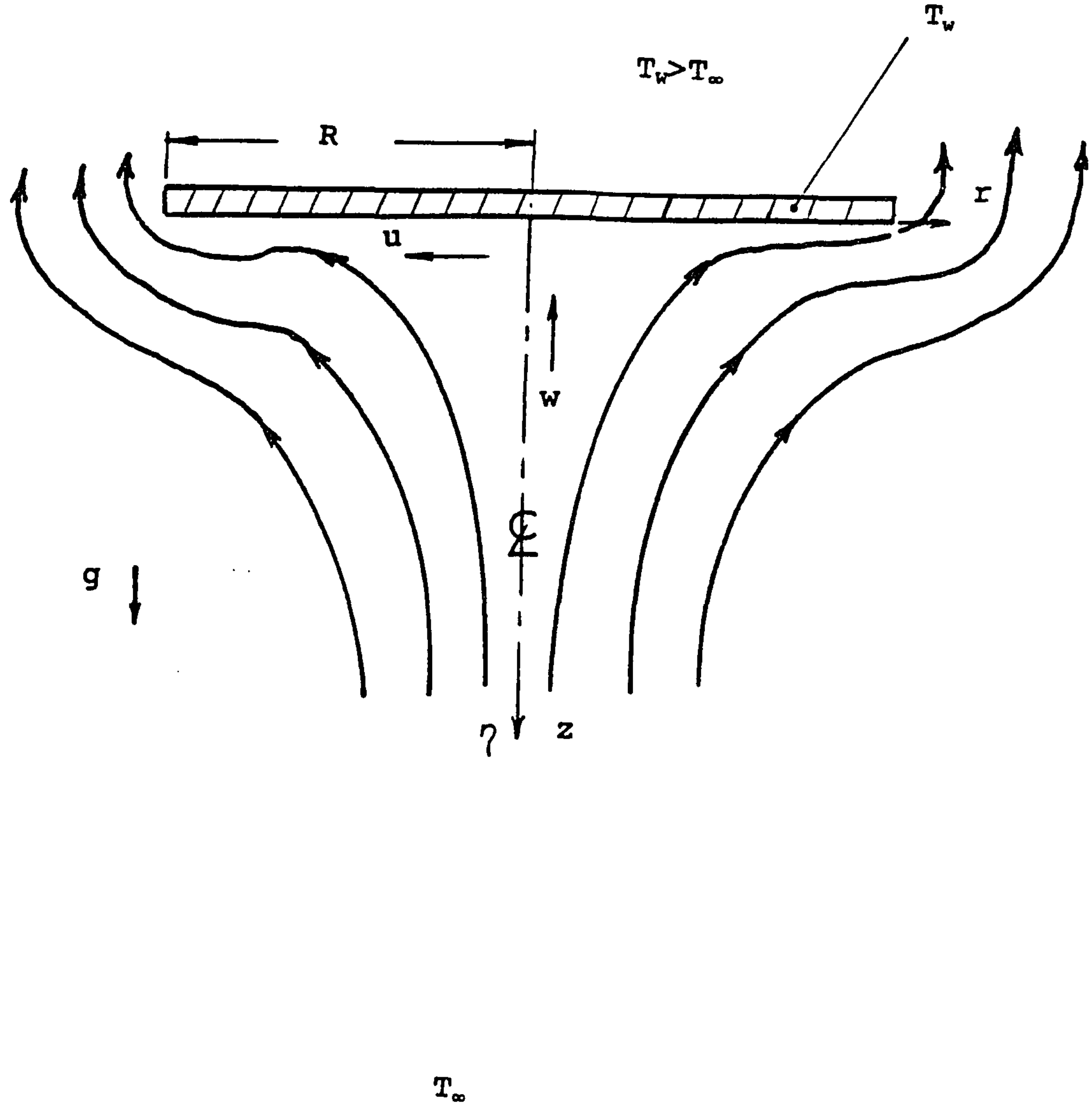

Fig.II-1.1 Flow Pattern and Coordinate System of Downward-Facing Heated Round Plate

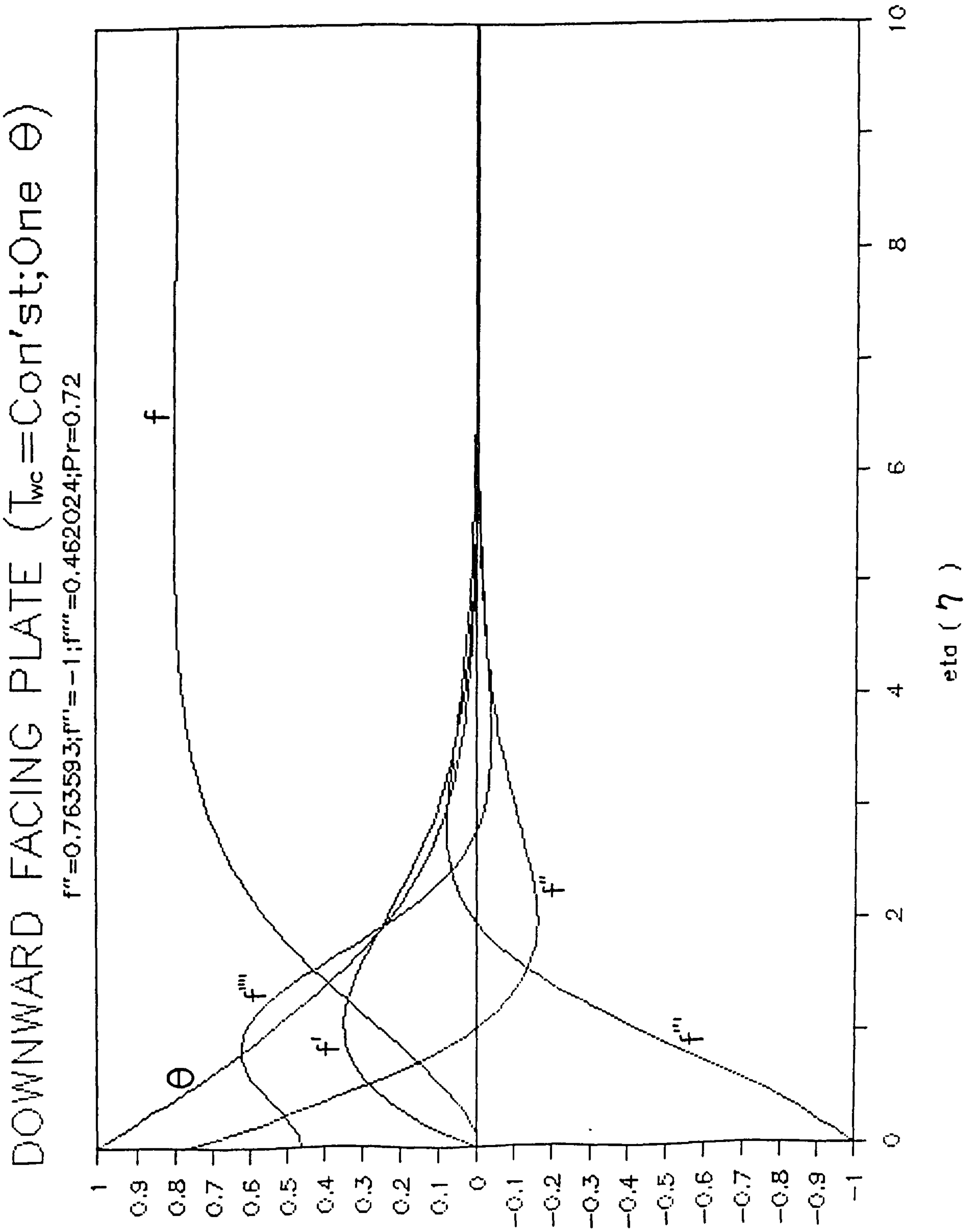

Fig.II-3.1 Solution of Downward-Facing Heated Plate, One Assumed Temperature Function, and Prescribed Surface Temperature Case at Pr=0.72

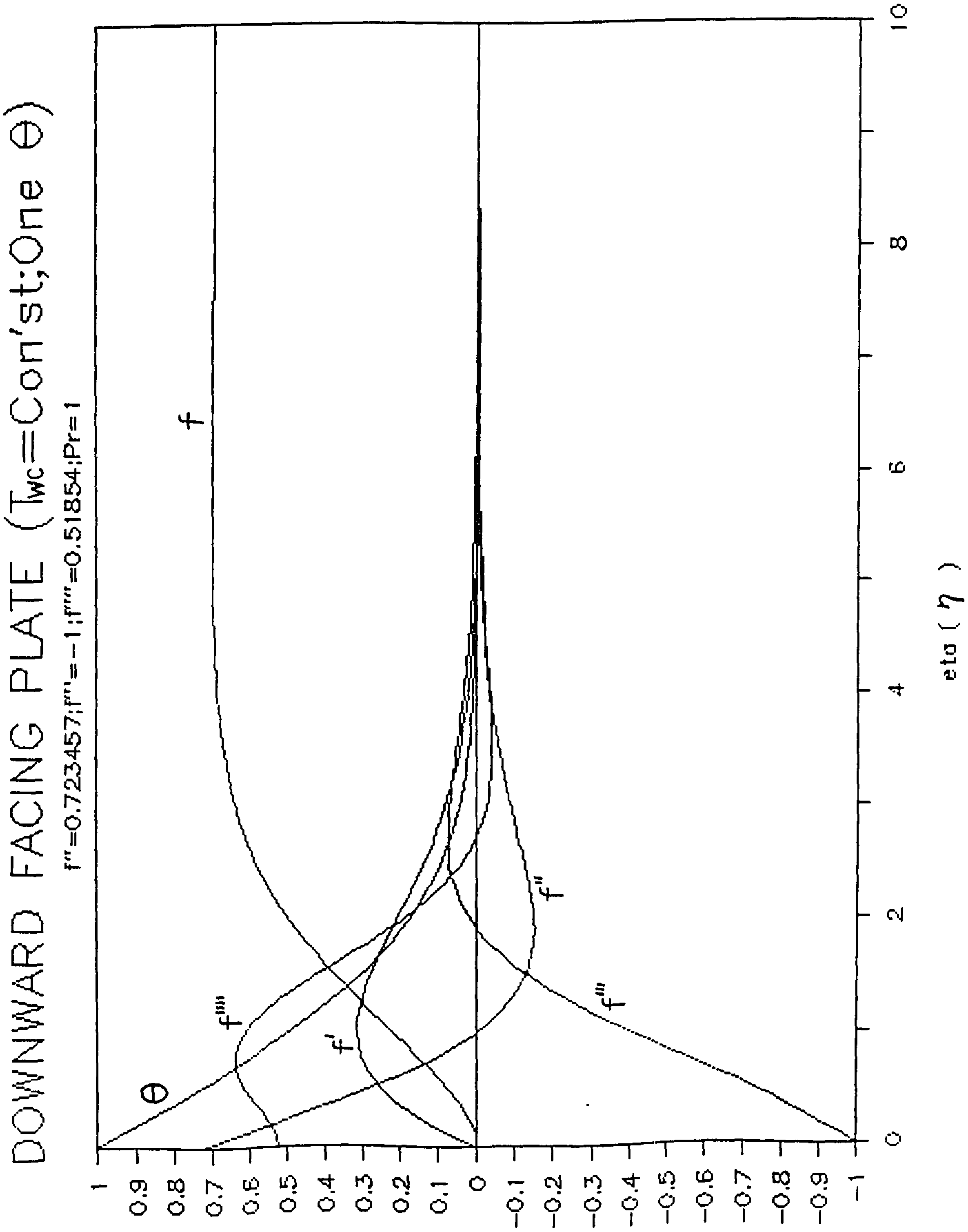

Fig.II-3.2 Solution of Downward-Facing Heated Plate, One Assumed Temperature Function, and Prescribed Surface Temperature Case at Pr=1.0

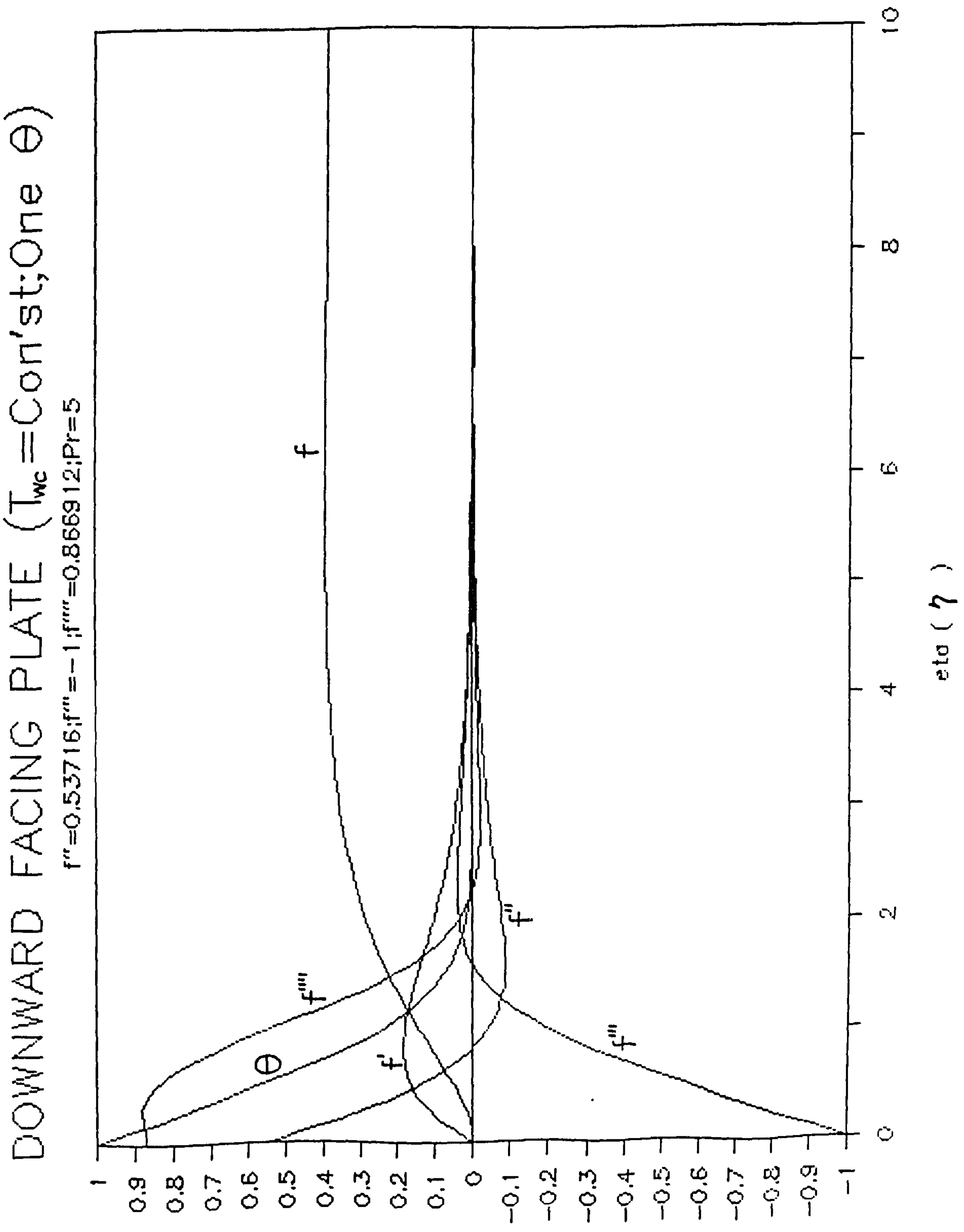

Fig.II-3.3 Solution of Downward-Facing Heated Plate, One Assumed Temperature Function, and Prescribed Surface Temperature case at Pr=5.0

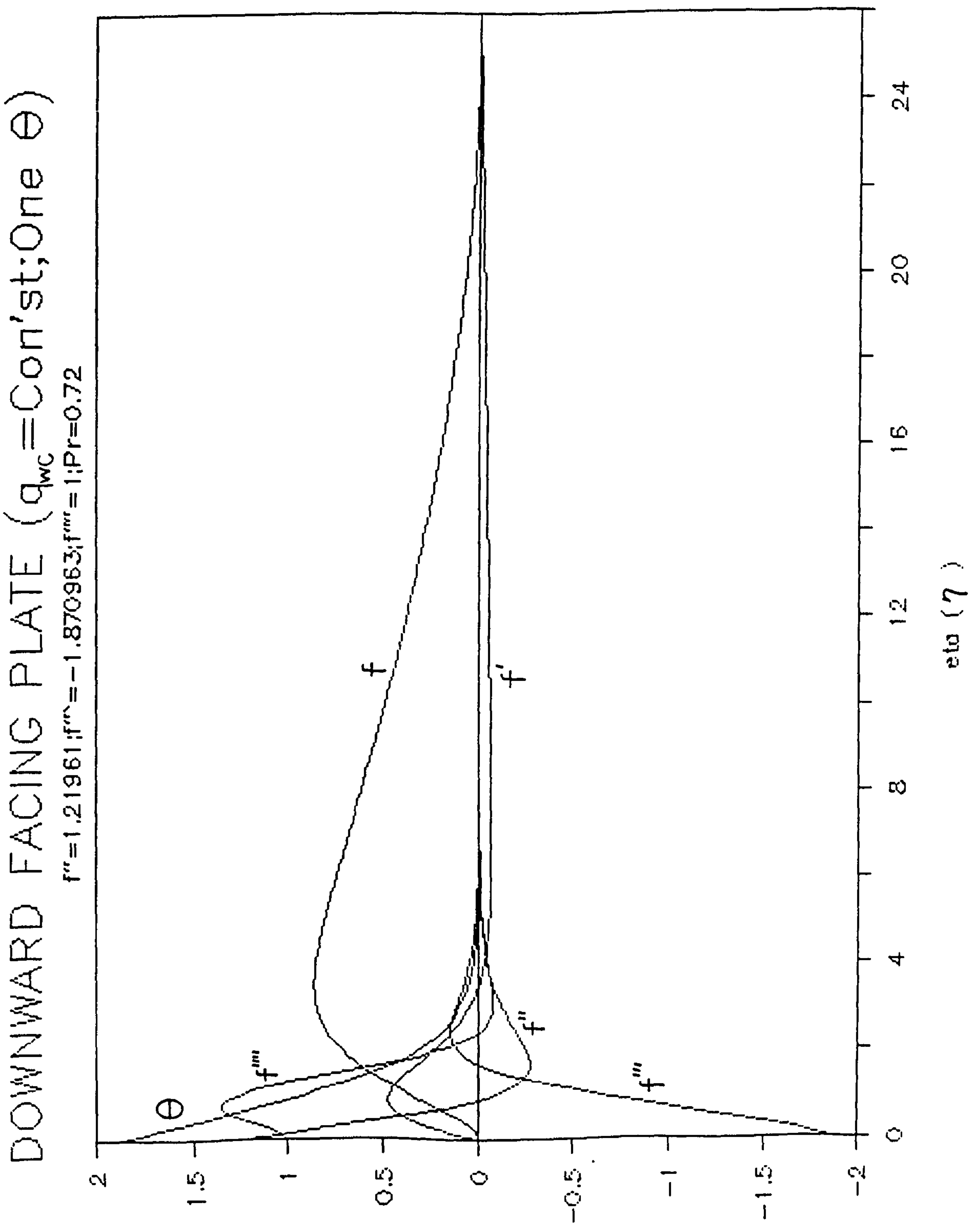

Fig.II-3.4 Solution of Downward-Facing Heated Plate, One Assumed Temperature Function, and Prescribed Constant Surface Flux Case at Pr=0.72

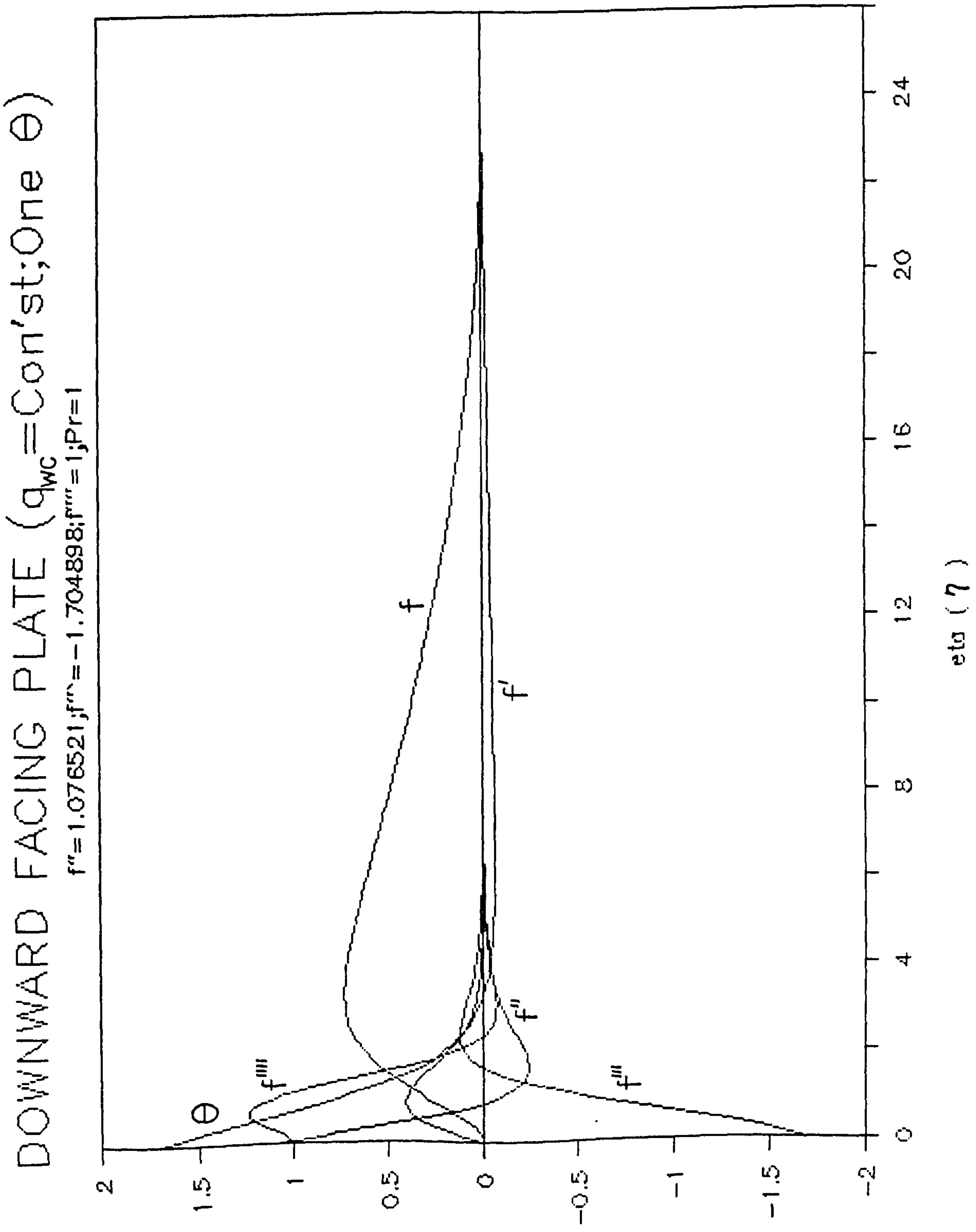

Fig.II-3.5 Solution of Downward-Facing Heated Plate, One Assumed Temperature Function, and Prescribed Constant Surface Flux Case at Pr=1.0

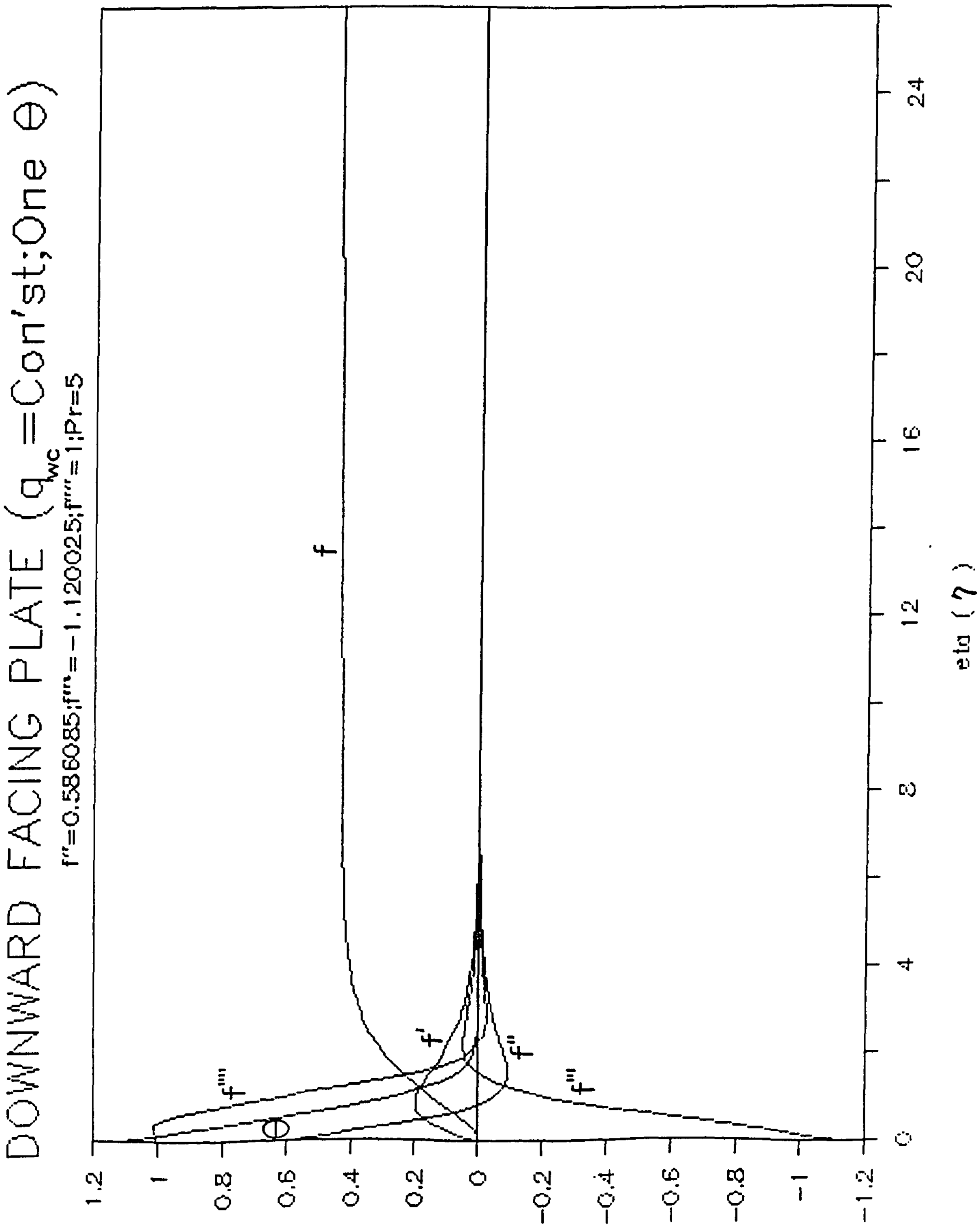

Fig.II-3.6 Solution of Downward-Facing Heated Plate, One Assumed Temperature Function, and Prescribed Constant Surface Flux Case at Pr=5.0

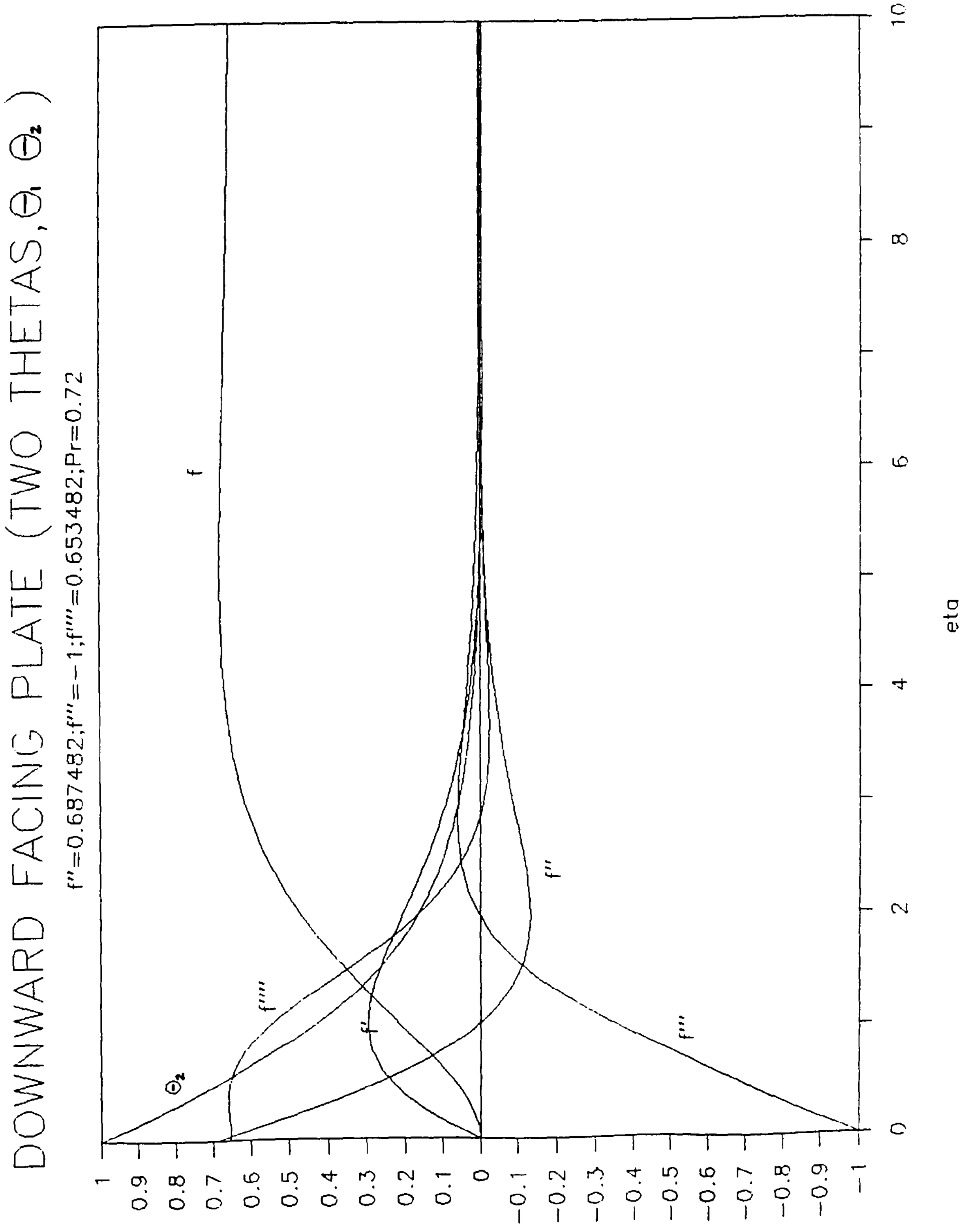

Fig.II-3.7 Solution of Downward-Facing Heated Plate, Two Assumed Temperature Functions, and Prescribed Surface Temperature Case at $\theta_2(0)=1$, Pr=0.72

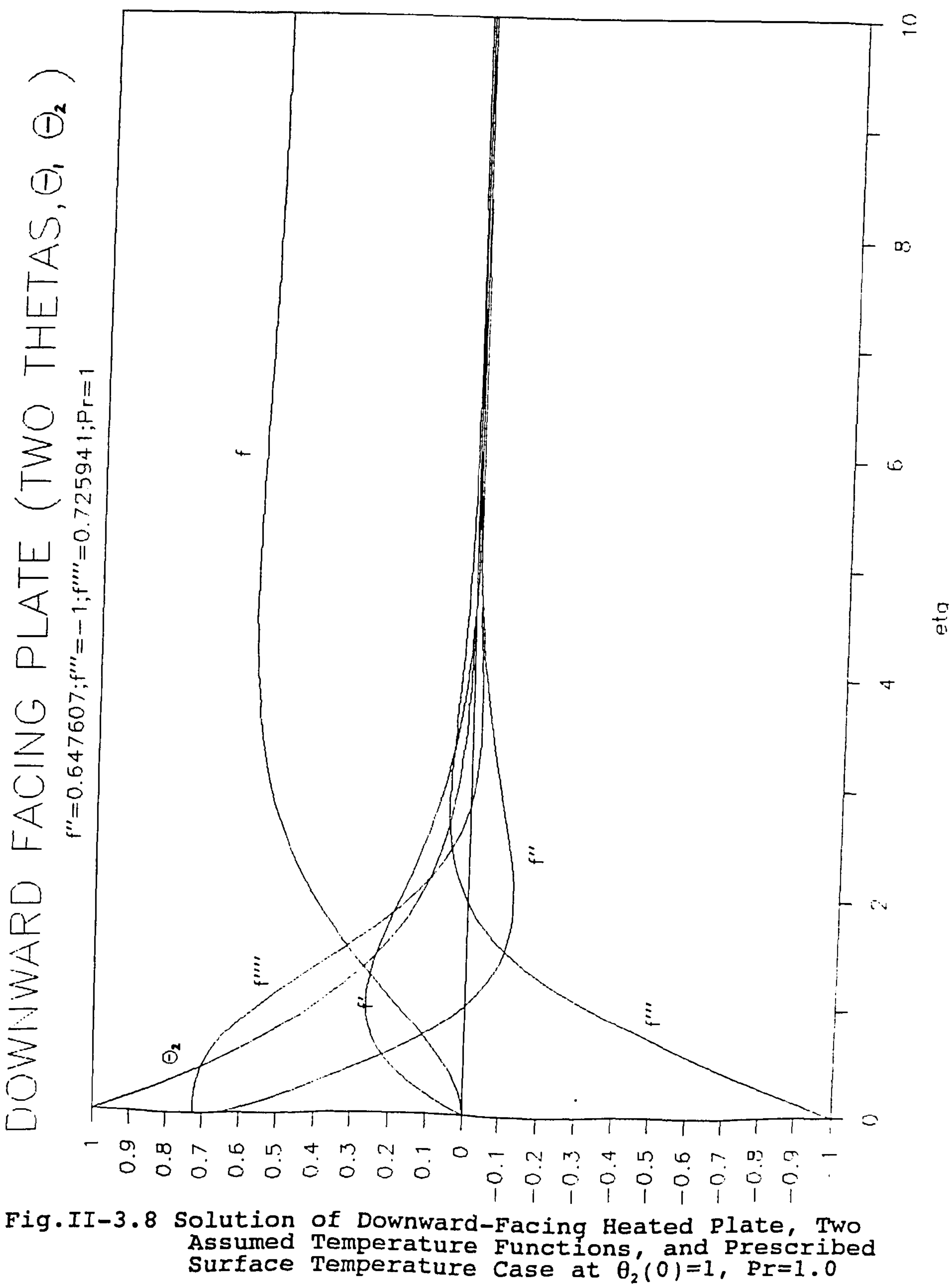

Fig.II-3.8 Solution of Downward-Facing Heated Plate, Two Assumed Temperature Functions, and Prescribed Surface Temperature Case at $\theta_2(0)=1$, Pr=1.0

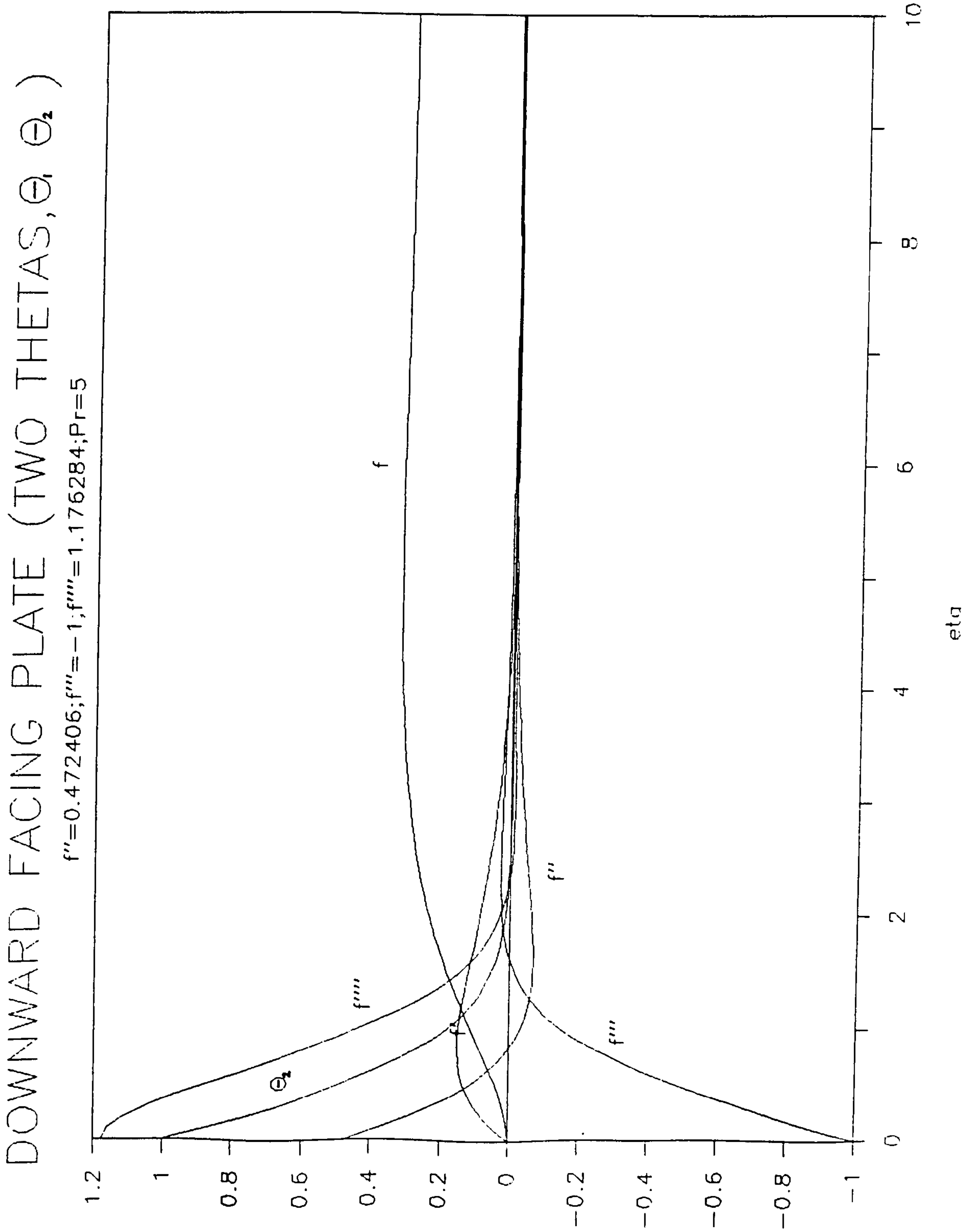

Fig.II-3.9 Solution of Downward-Facing Heated Plate, Two Assumed Temperature Functions, and Prescribed Surface Temperature Case at $\theta_2(0)=1$, Pr=5.0

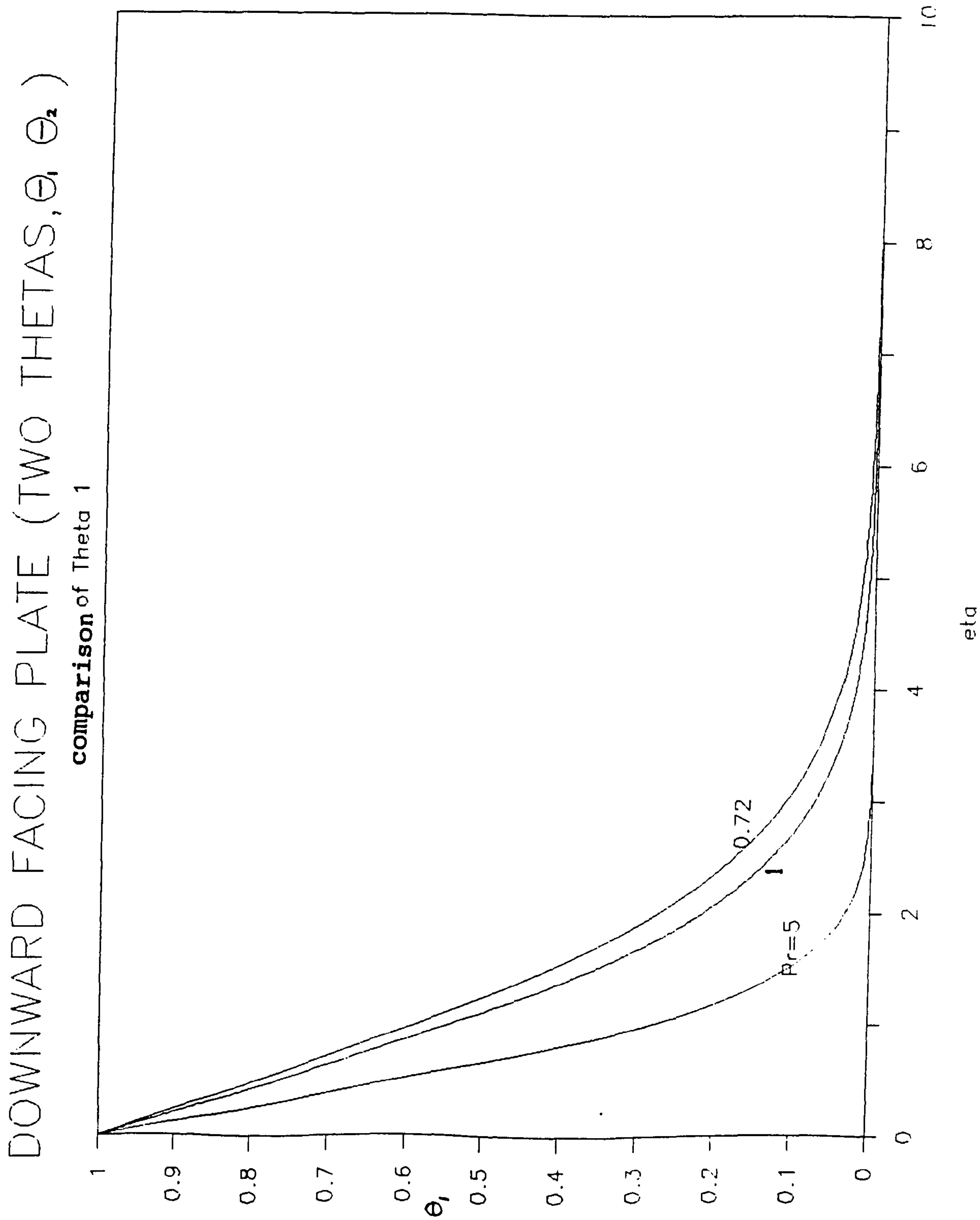

Fig.II-3.10 Solution of $\theta_1(\eta)$ of Pr=0.72, 1, 5 for Downward-Facing Heated Plate, Two Assumed Temperature Functions, and Prescribed Surface Temperature Case at $\theta_2(0)=1$

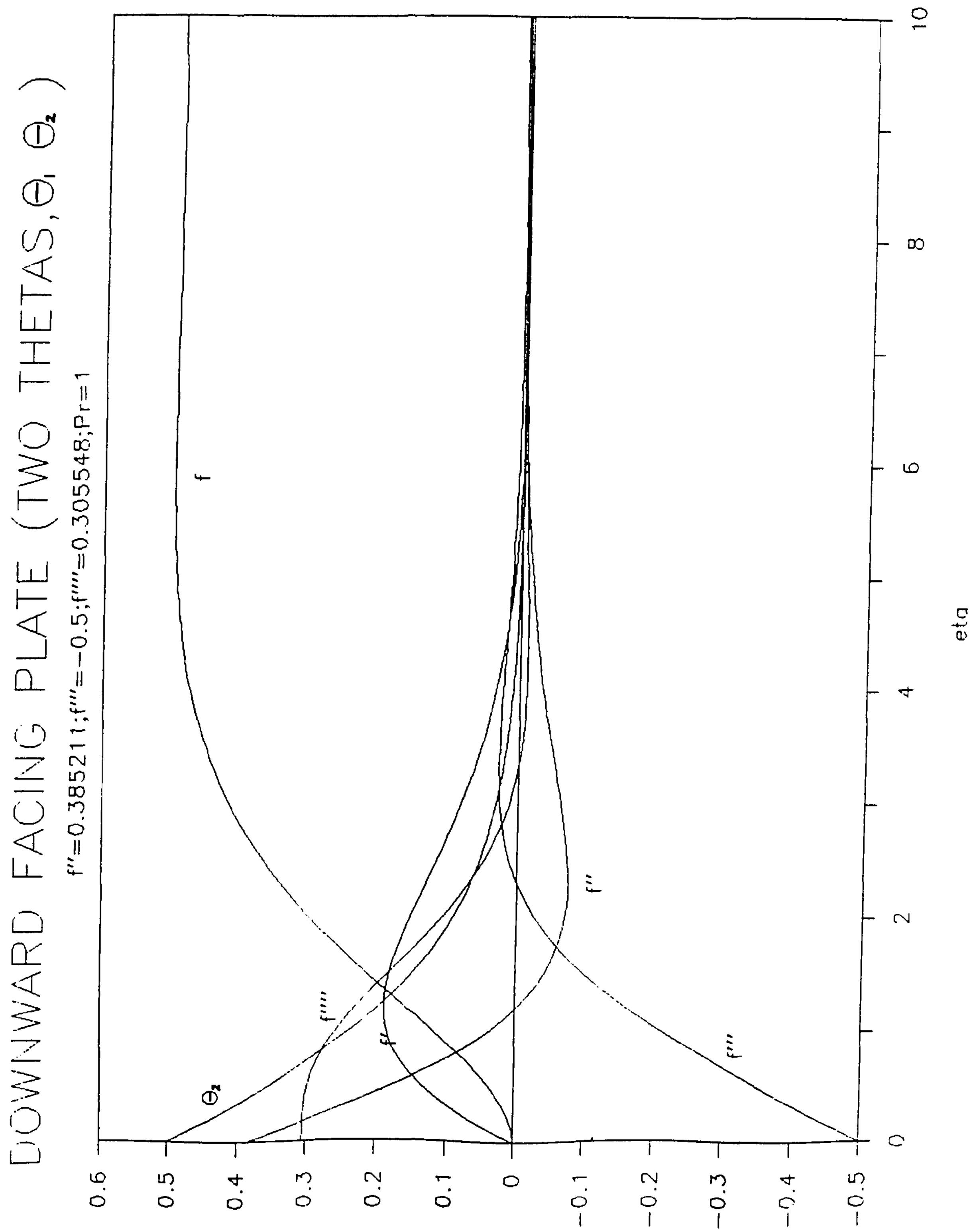

Fig.II-3.11 Solution of Downward-Facing Heated Plate, Two Assumed Temperature Functions, and Prescribed Surface Temperature Case at $\theta_2(0)=0.5$, Pr=1.0

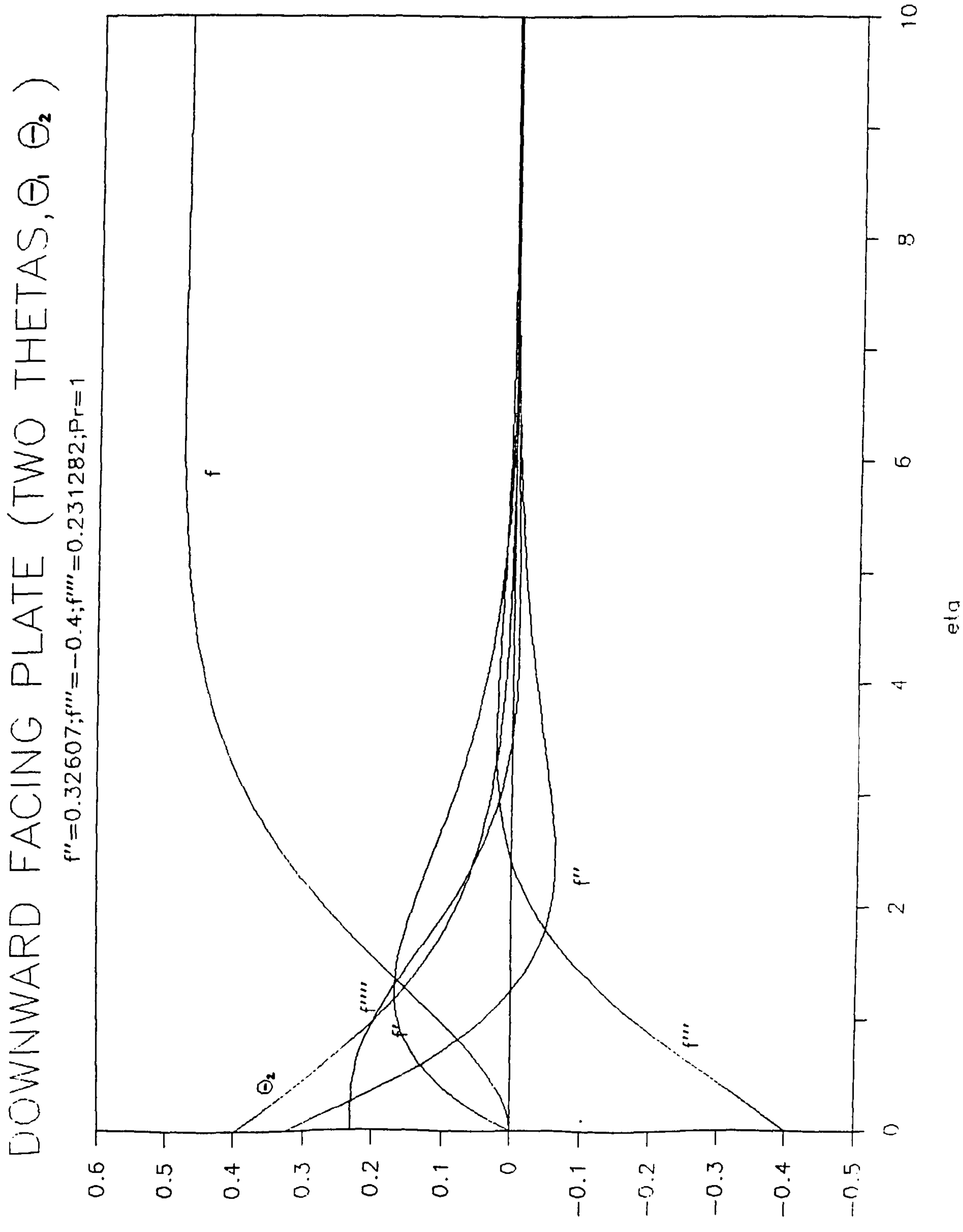

Fig.II-3.12 Solution of Downward-Facing Heated Plate, Two Assumed Temperature Functions, and Prescribed Surface Temperature Case at $\theta_2(0)=0.4$, Pr=1.0

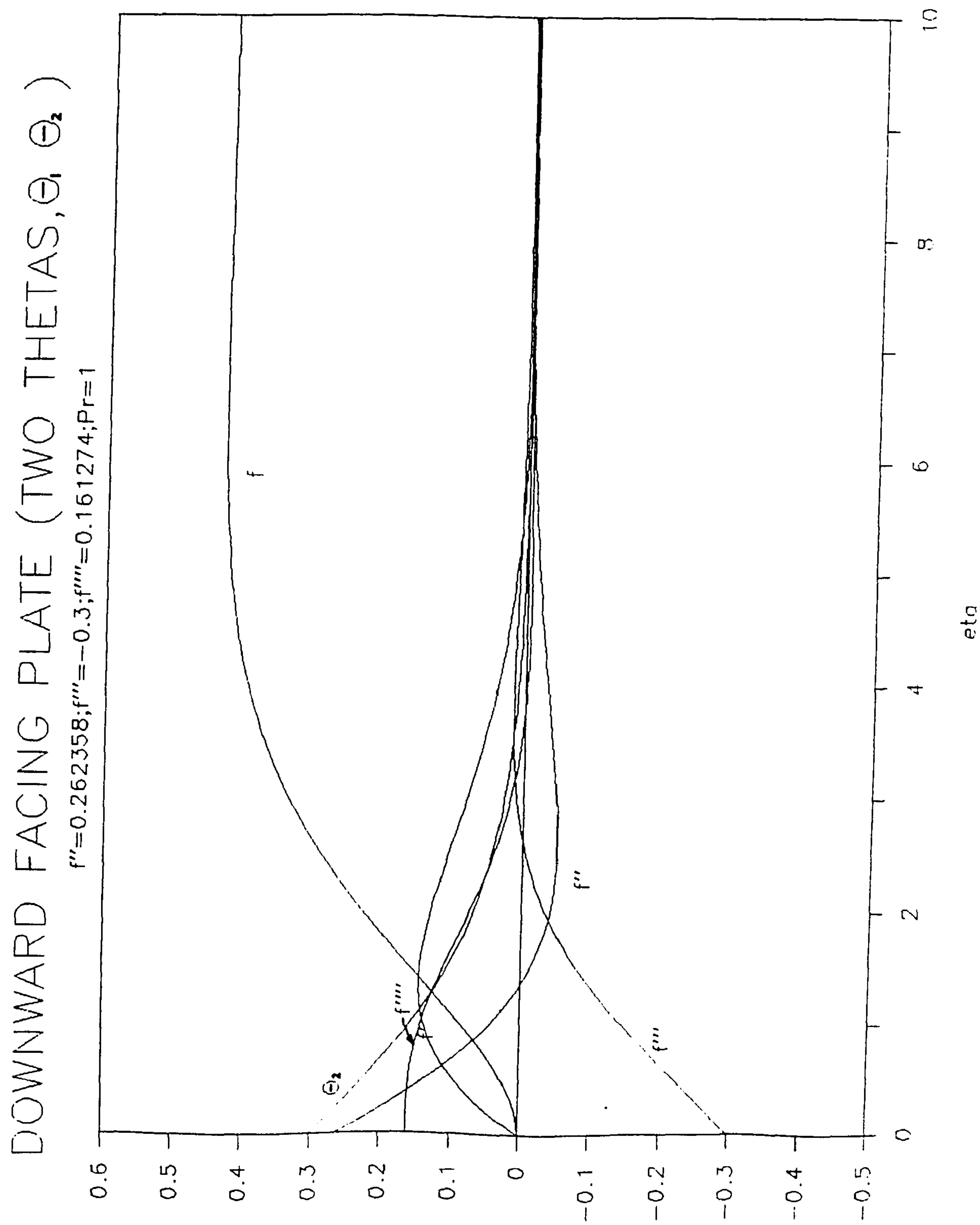

Fig.II-3.13 Solution of Downward-Facing Heated Plate, Two Assumed Temperature Functions, and Prescribed Surface Temperature Case at $\theta_2(0)=0.3$, Pr=1.0

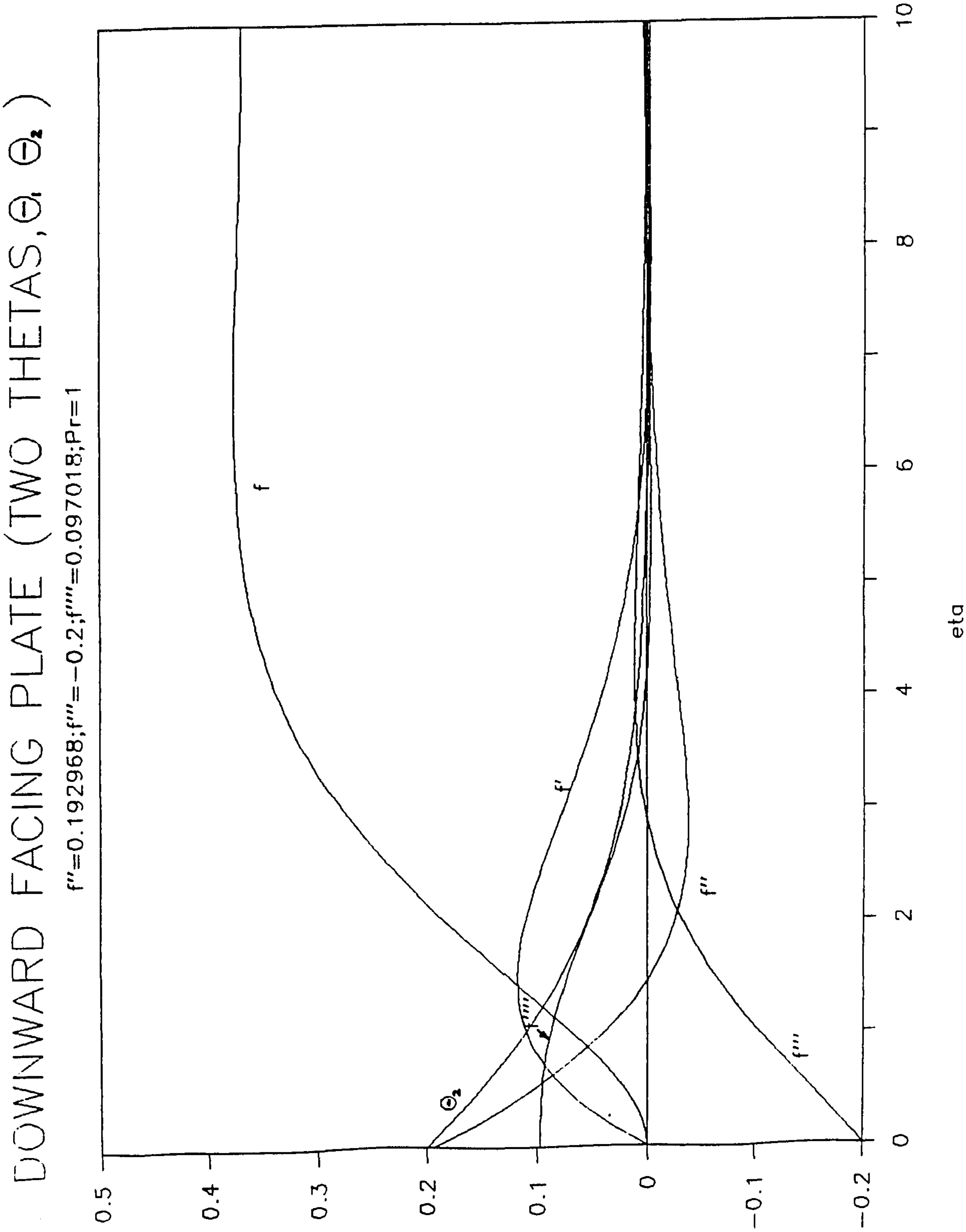

Fig.II-3.14 Solution of Downward-Facing Heated Plate, Two Assumed Temperature Functions, and Prescribed Surface Temperature Case at $\theta_2(0)=0.2$, Pr=1.0

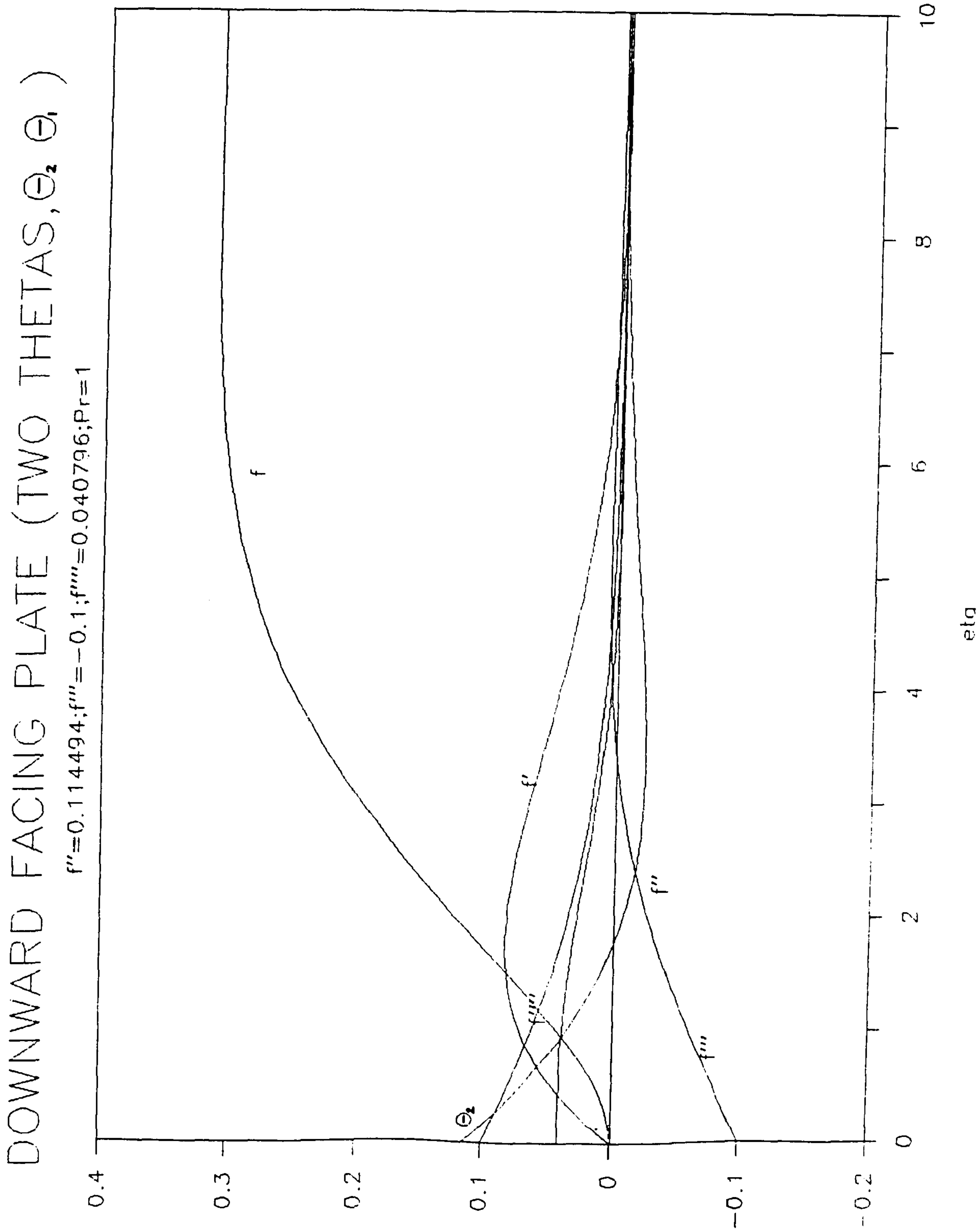

Fig.II-3.15 Solution of Downward-Facing Heated Plate, Two Assumed Temperature Functions, and Prescribed Surface Temperature Case at $\theta_2(0)=0.1$, Pr=1.0

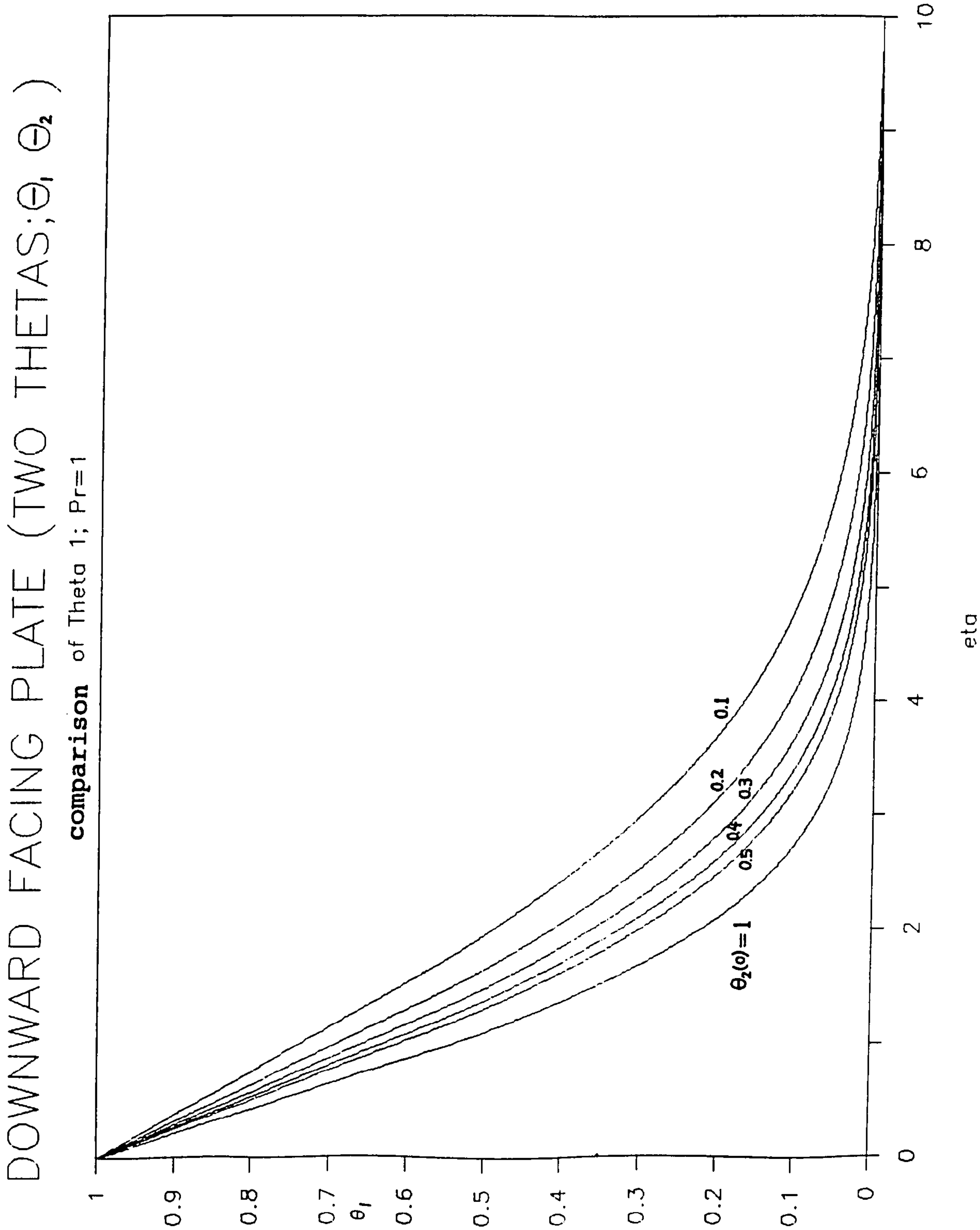

Fig.II-3.16 Solution of $\theta_1(\eta)$ of Pr=1 for Downward-Facing Heated Plate, Two Assumed Temperature Functions, and Prescribed Surface Temperature Case at $\theta_2(0)=1$, 0.5, 0.4, 0.3, 0.2, 0.1

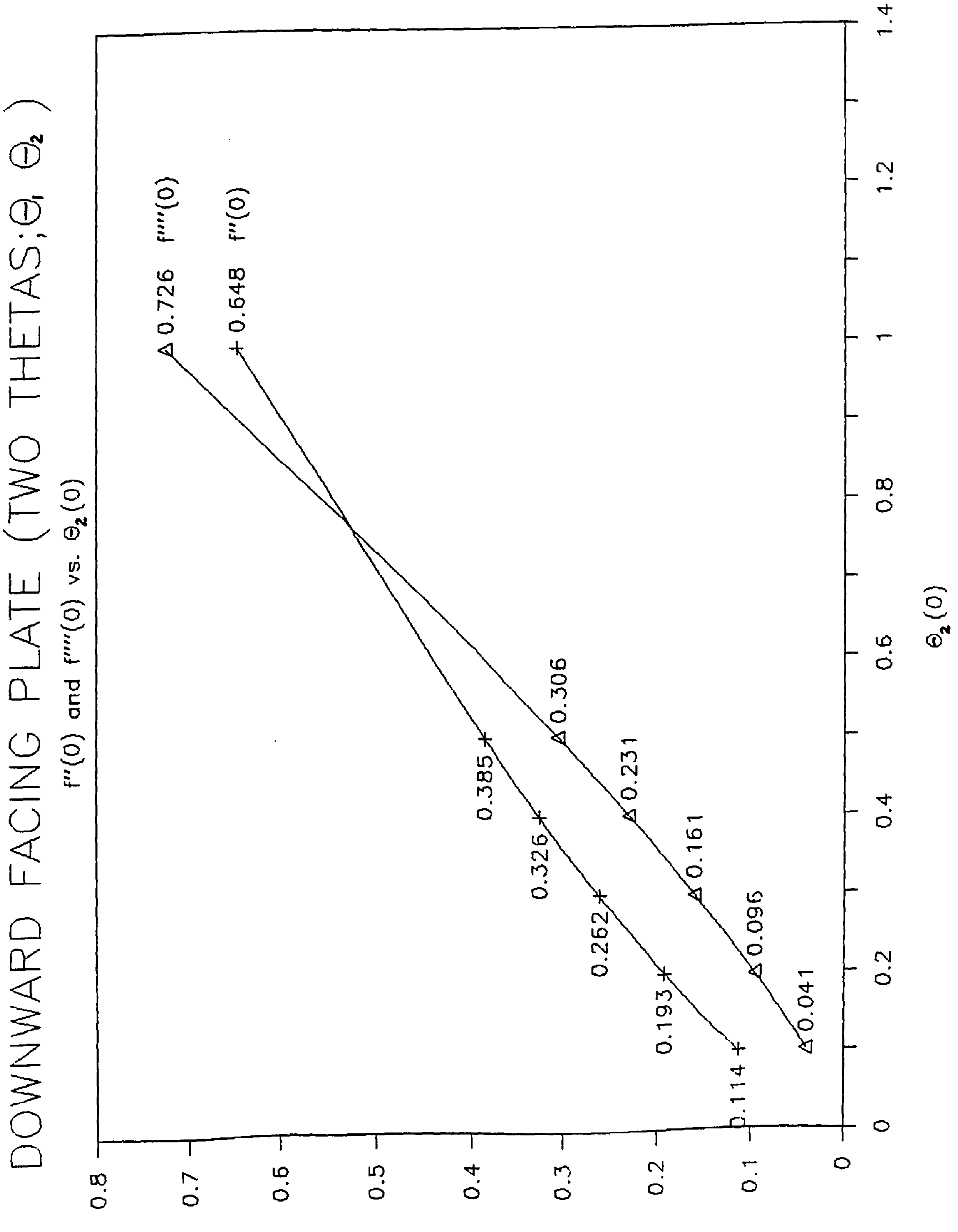

Fig.II-3.17 Trend of f"(0) and f""(0) vs. $\theta_2(0)$ for Downward-Facing Heated Plate, Two Assumed Temperature Functions, and Prescribed Surface Temp. Case at Pr=1.0

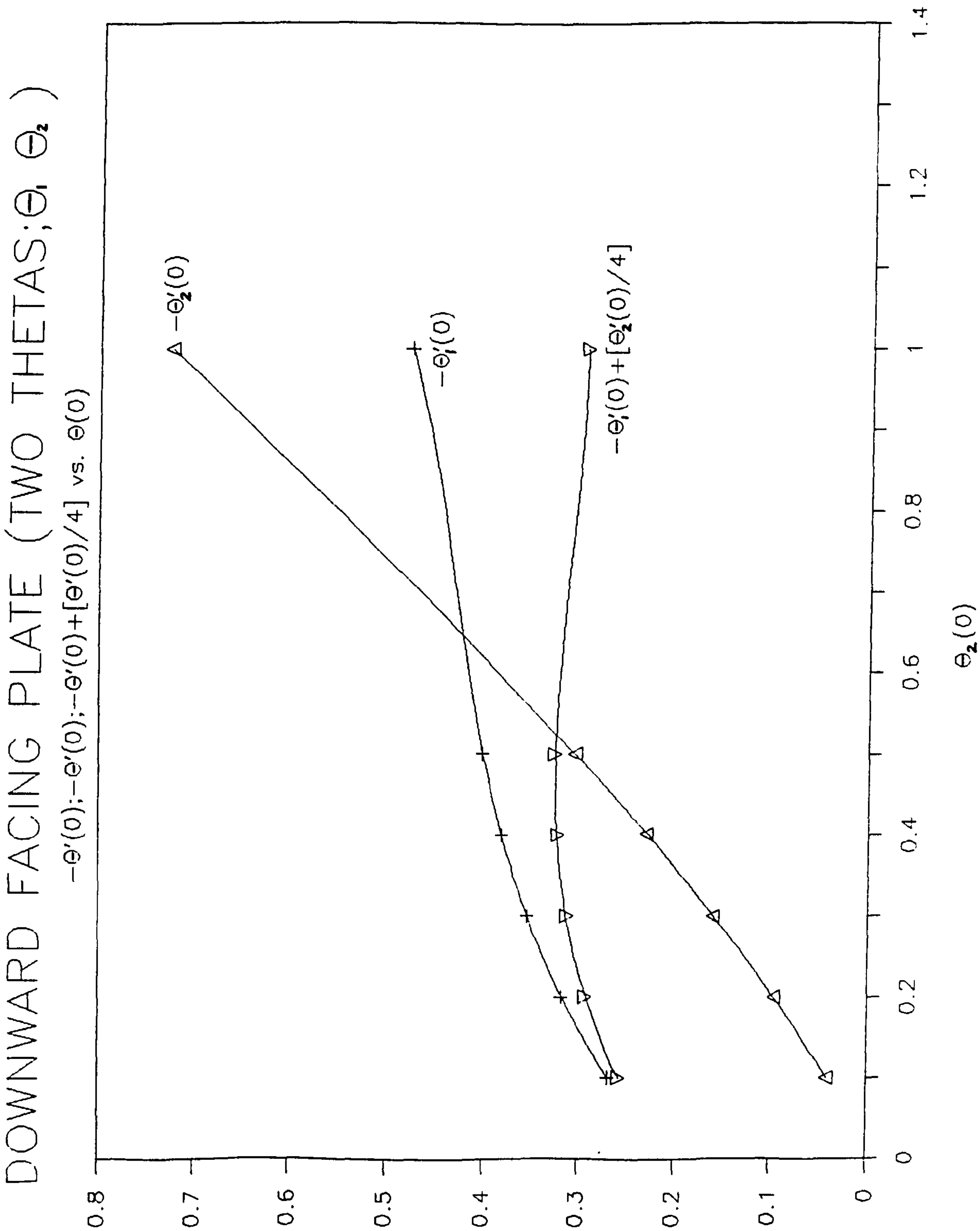

Fig.II-3.18 Trend of the Coefficient in Eq.(II.65) vs. $\theta_2(0)$ for Downward-Facing Heated Plate, Two Assumed Temperature Functions, Prescribed Surface Temp. Case at Pr=1.0

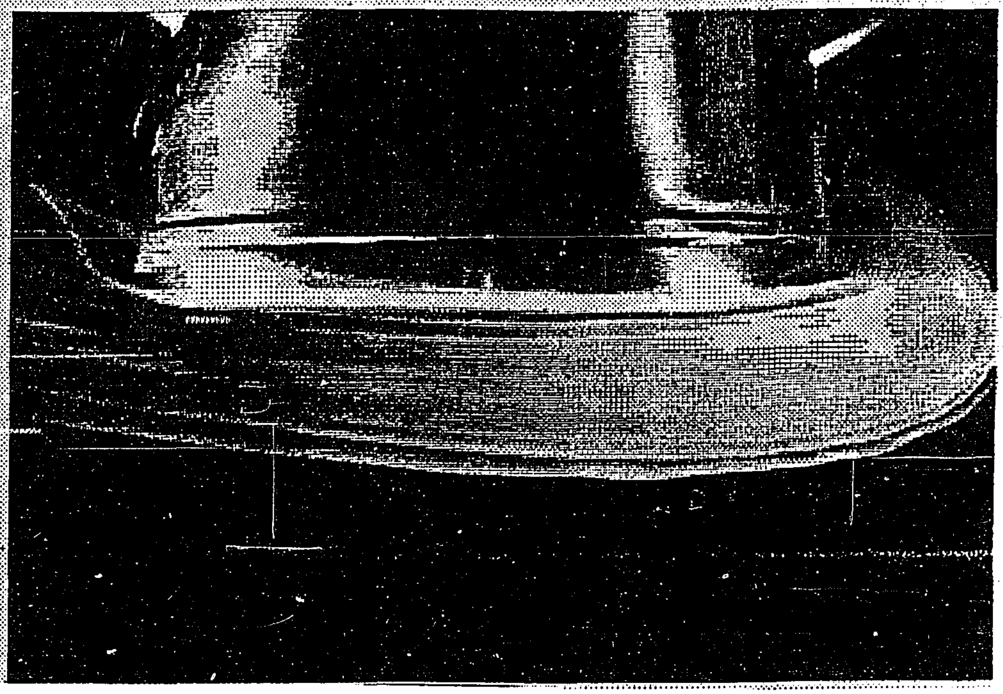

Fig.II-4.1.a Smoke beneath a Round Surface (R=60 mm) without Heating at T_∞=22 °C

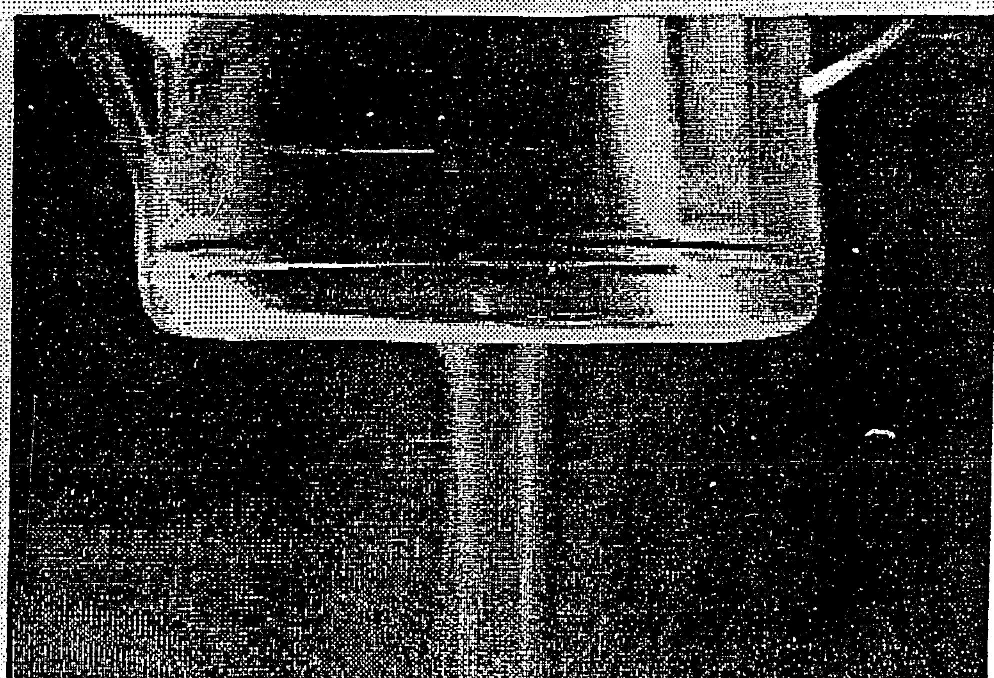

Fig.II-4.1.b Smoke beneath a Round Surface (R=60 mm) at T_w=100 °C and T_∞=22 °C

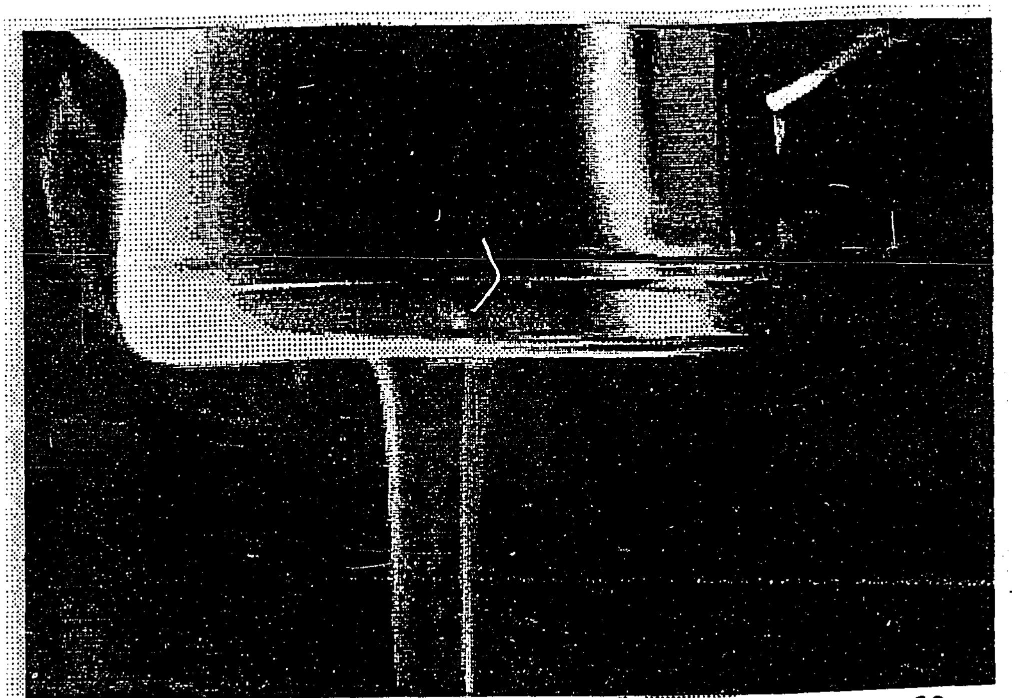

Fig.II-4.1.c Smoke beneath a Round Surface (R=60 mm) at T_w=100 °C and T_∞=22 °C

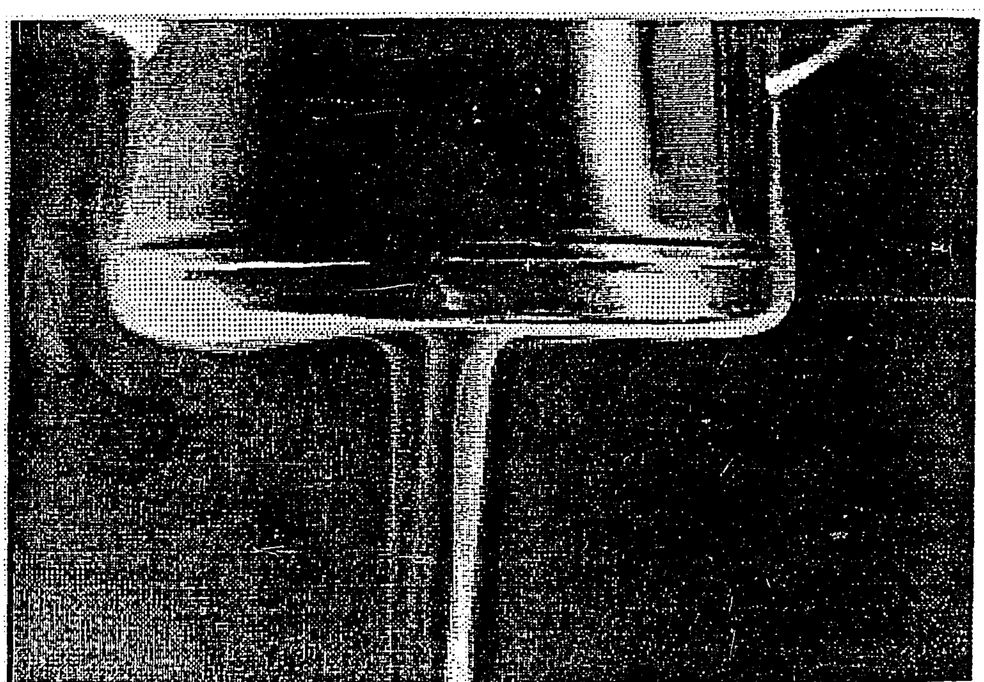

Fig.II-4.1.d Smoke beneath a Round Surface (R=60 mm) at T_w=100 °C and T_∞=22 °C

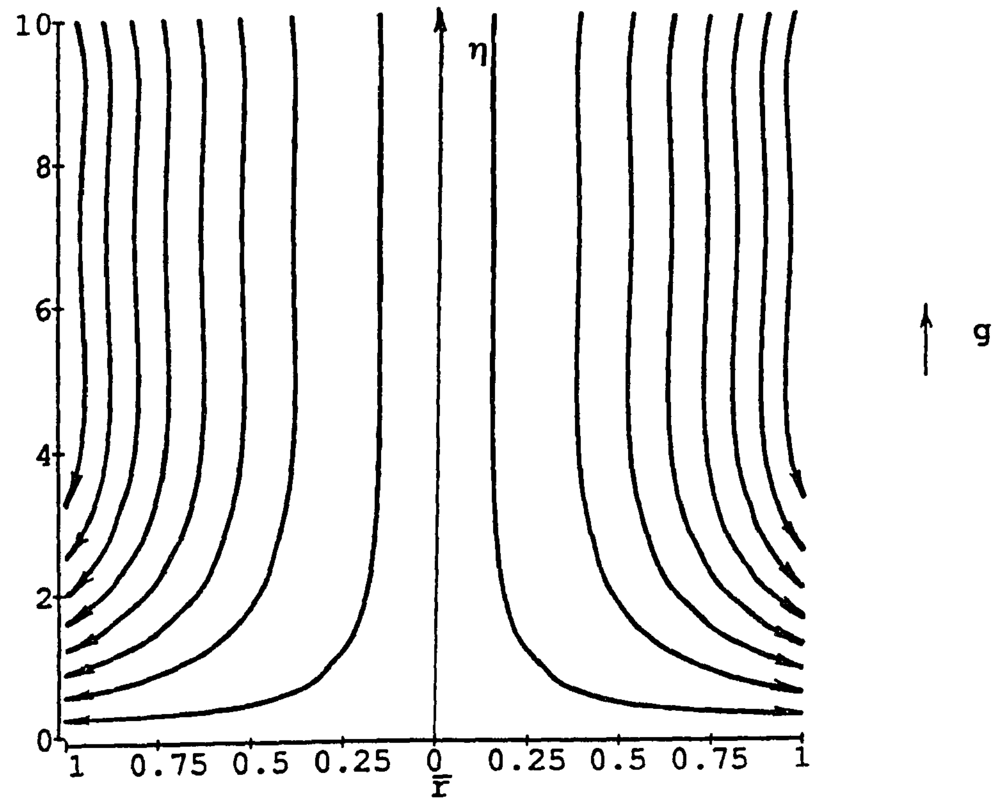

Fig.II-4.2.a Streamlines of Downward-Facing Heated Plate, One Assumed Temperature Function, and Prescribed Surface Temperature Case at Pr=0.72

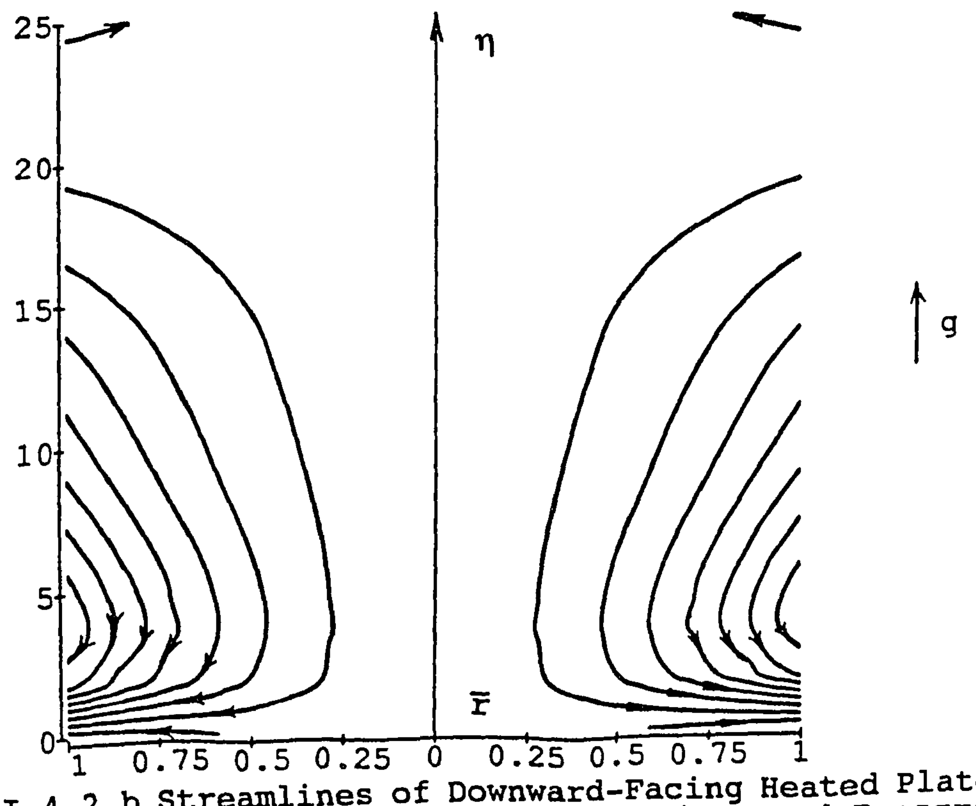

Fig.II-4.2.b Streamlines of Downward-Facing Heated Plate, One Assumed Temperature Function, and Prescribed Constant Surface Flux Case at Pr=0.72

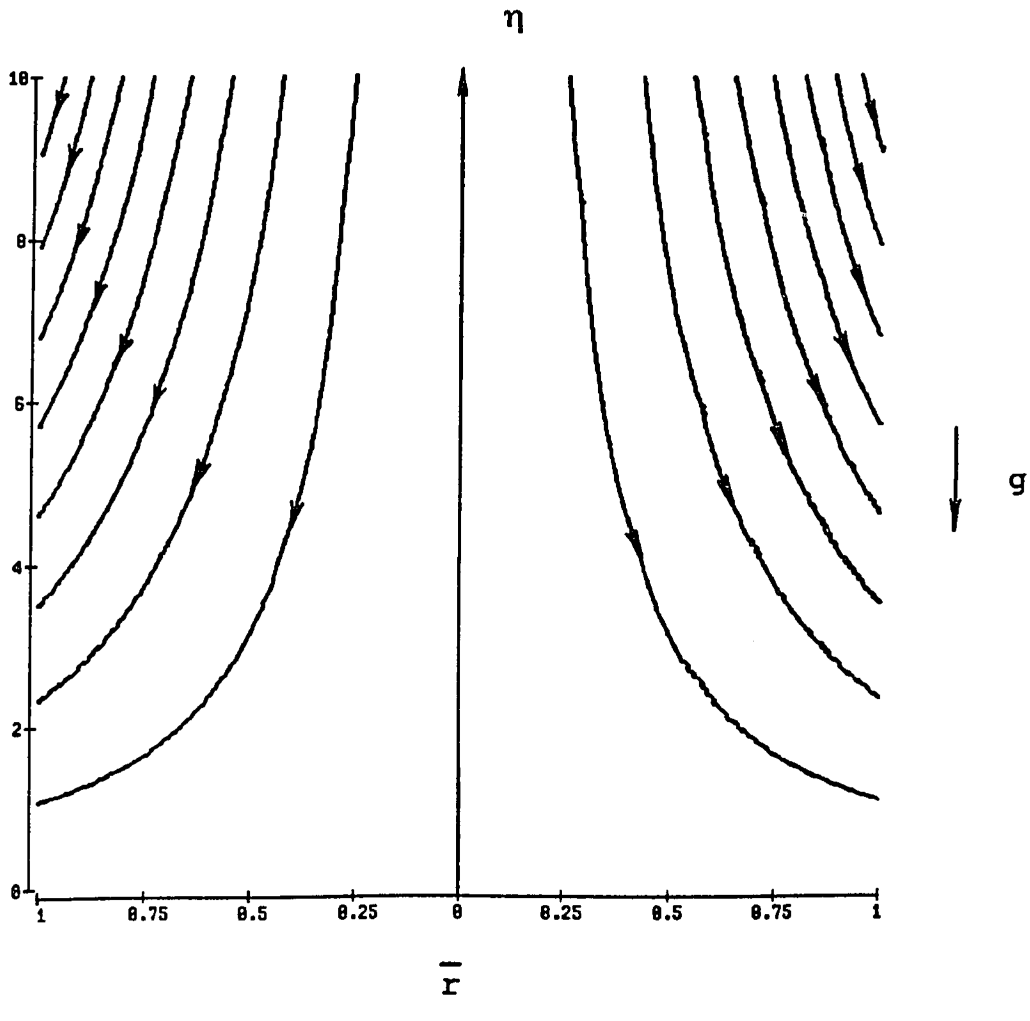

Fig.II-4.2.c Streamlines of Axisymmetric, Impinging, Stagnation flow

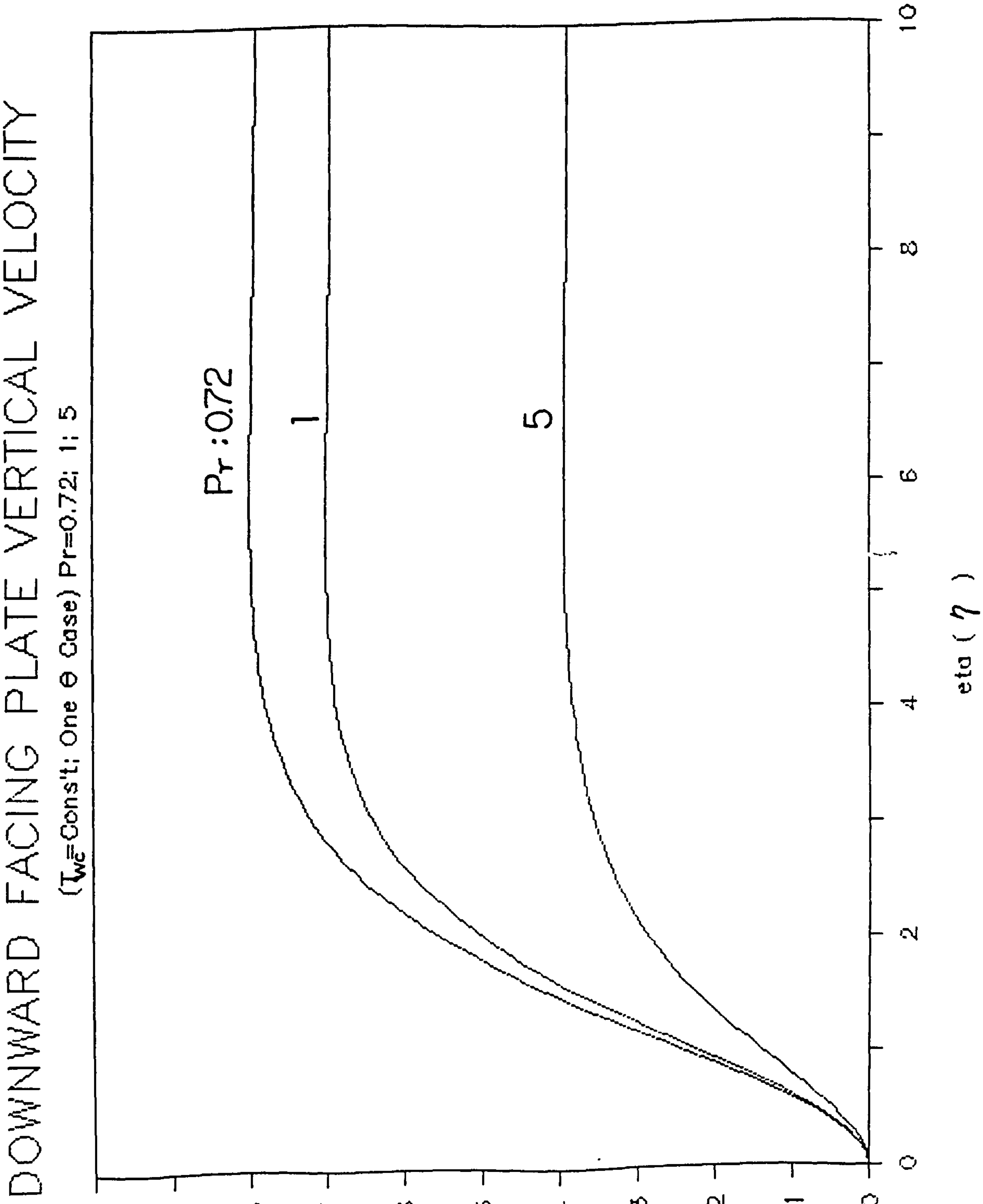

Fig.II-4.3 Vertical Velocity Function for Downward-Facing Heated Plate, One Assumed Temperature Function, Prescribed Surface Temperature Case at Pr=0.72, 1, 5

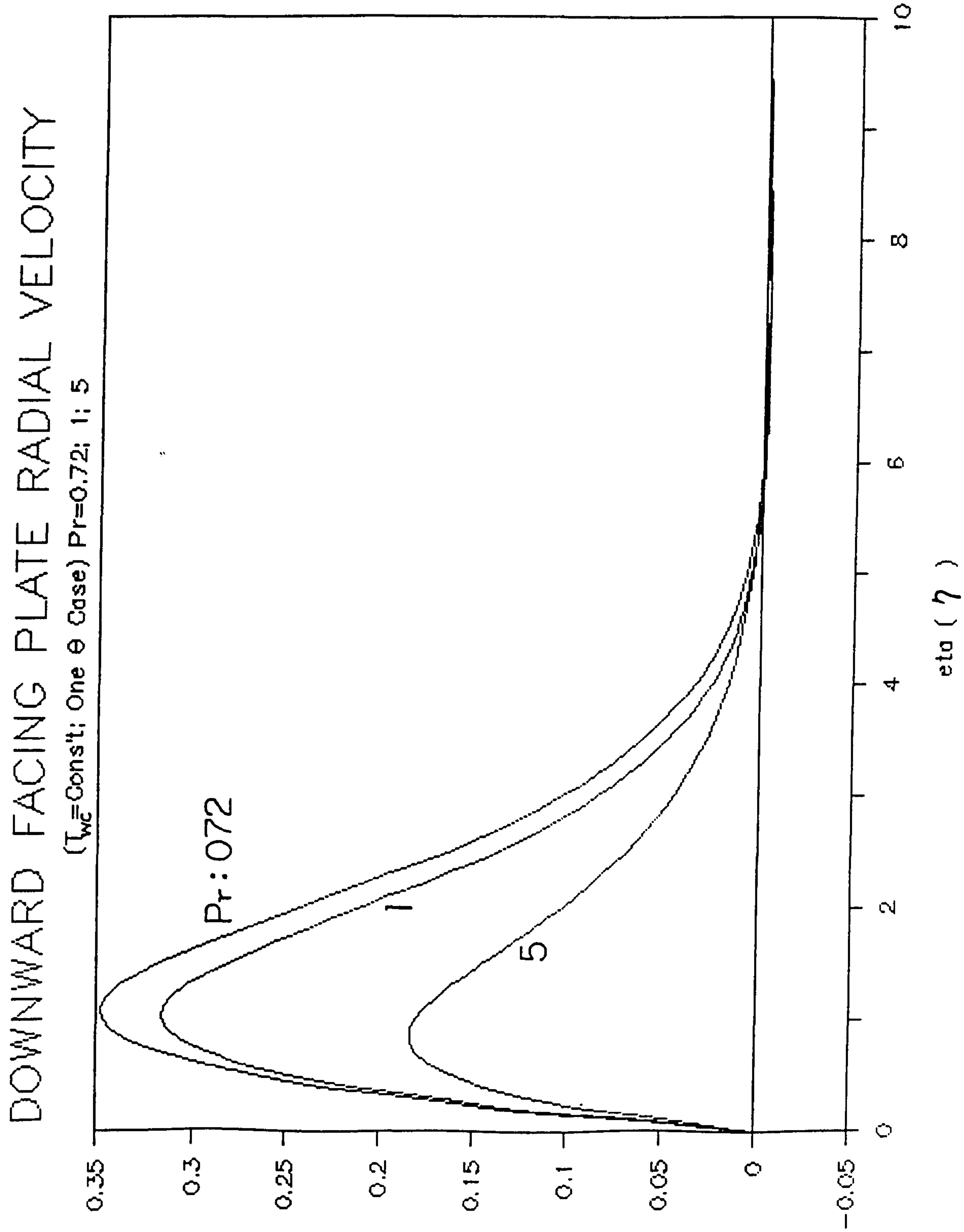

Fig.II-4.4 Radial Velocity Function for Downward-Facing Heated Plate, One Assumed Temperature Function, Prescribed Surface Temperature Case at Pr=0.72, 1, 5

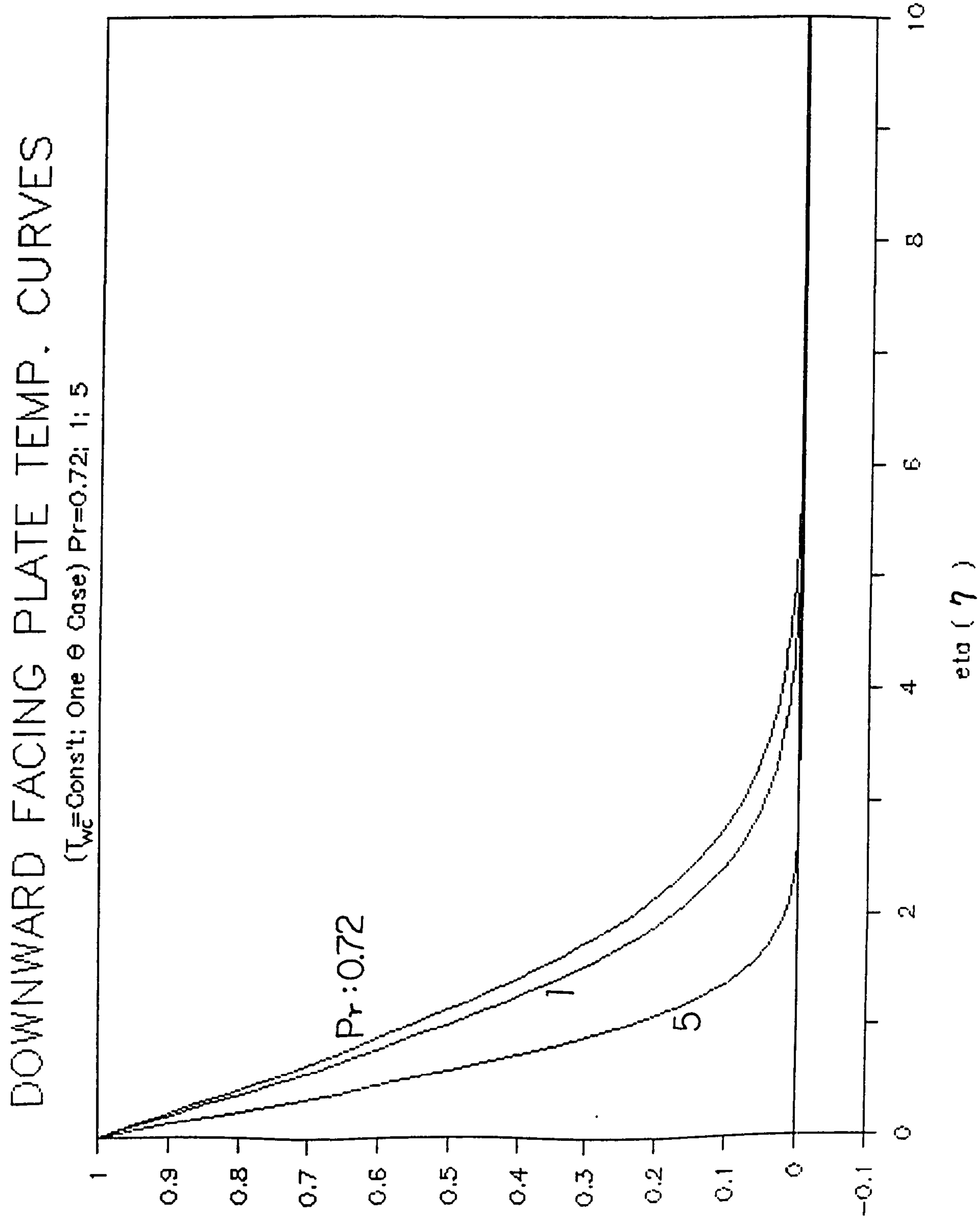

Fig.II-4.5 Temperature Function for Downward-Facing Heated Plate, One Assumed Temperature Function, Prescribed Surface Temperature Case at Pr=0.72, 1, 5

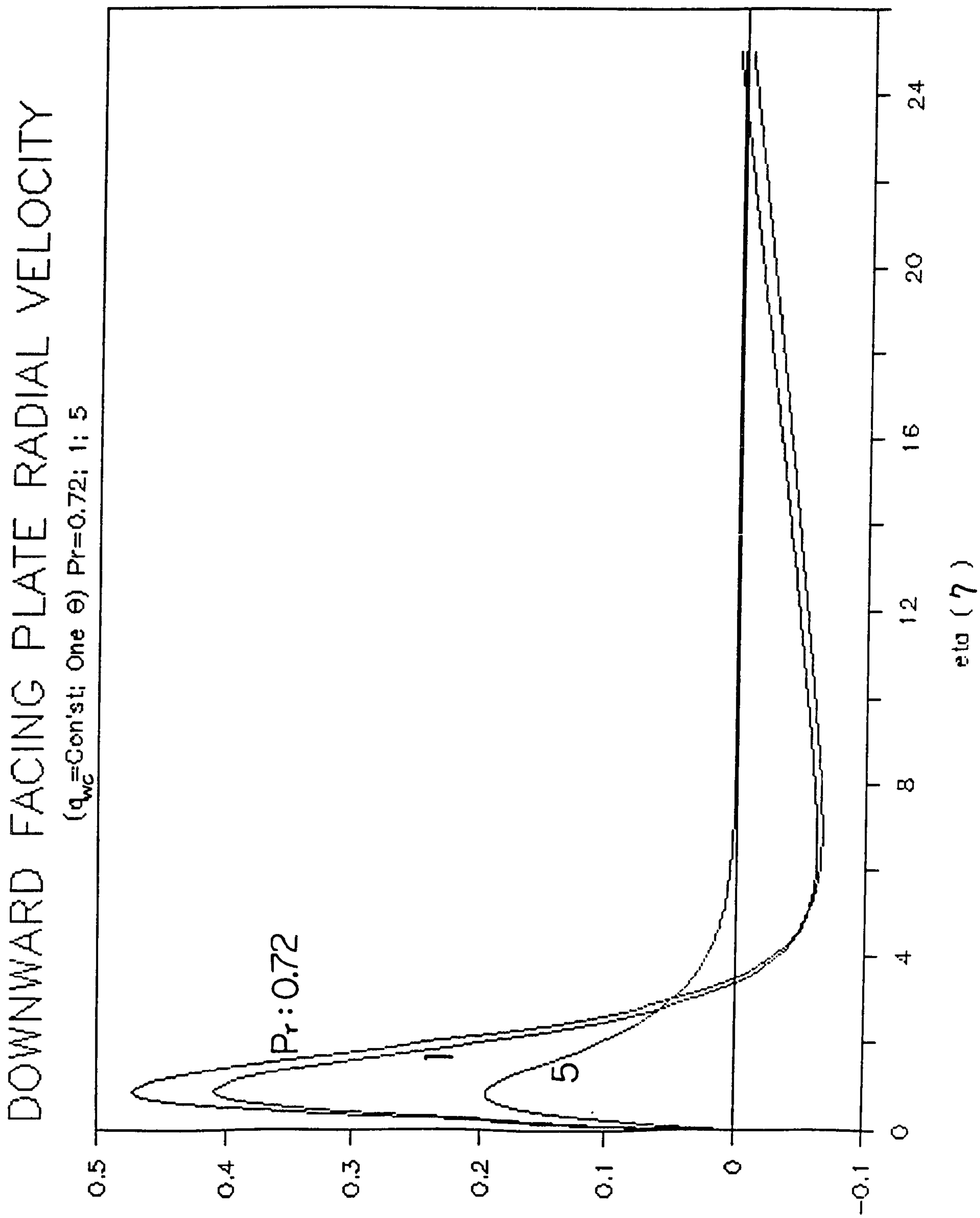

Fig.II-4.7 Radial Velocity Function for Downward-Facing Heated Plate, One Assumed Temperature Function, Prescribed Constant Surface Flux Case at Pr=0.72, 1, 5

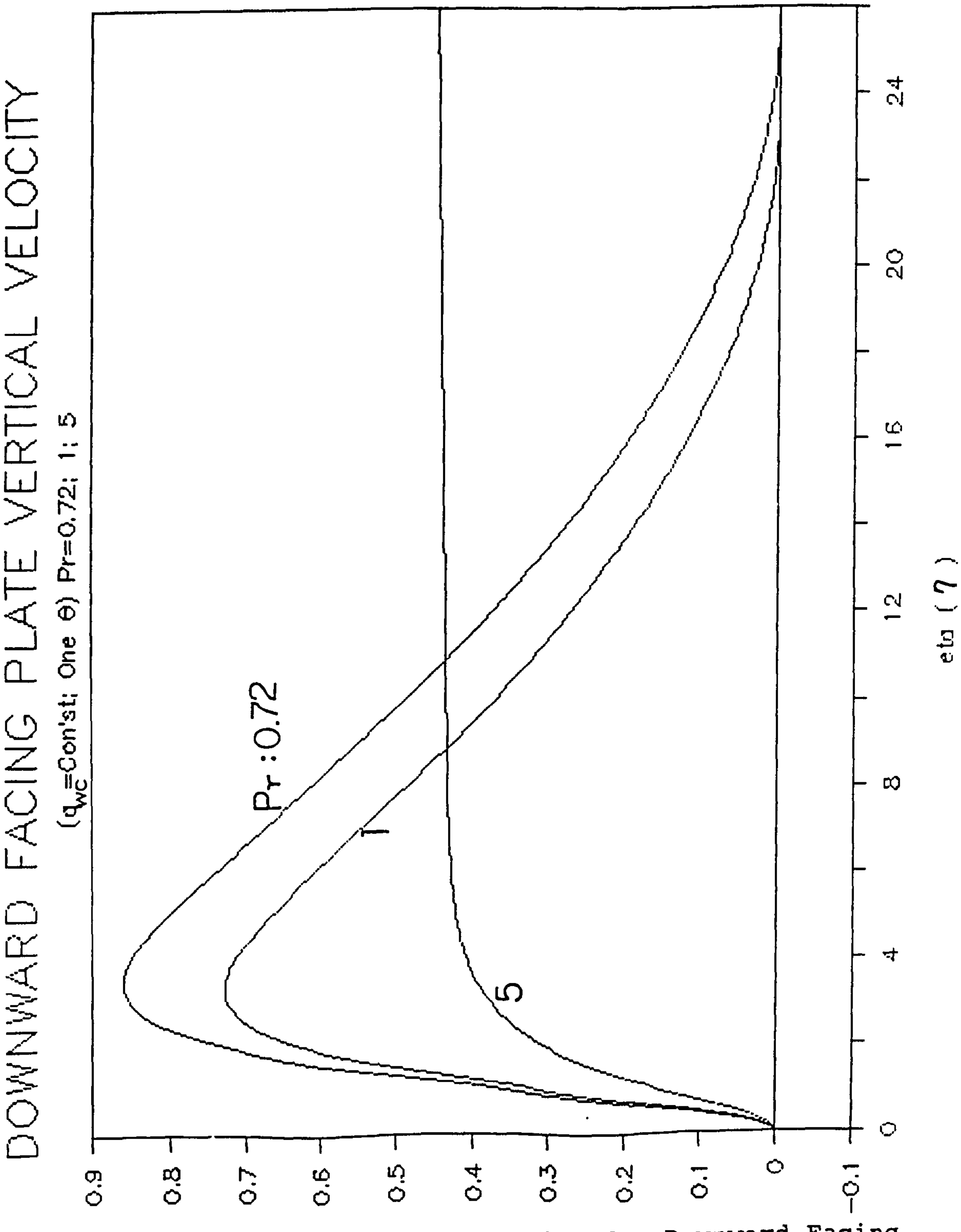

Fig.II-4.6 Vertical Velocity Function for Downward-Facing Heated Plate, One Assumed Temperature Function, Prescribed Constant Surface Flux Case at Pr=0.72, 1, 5

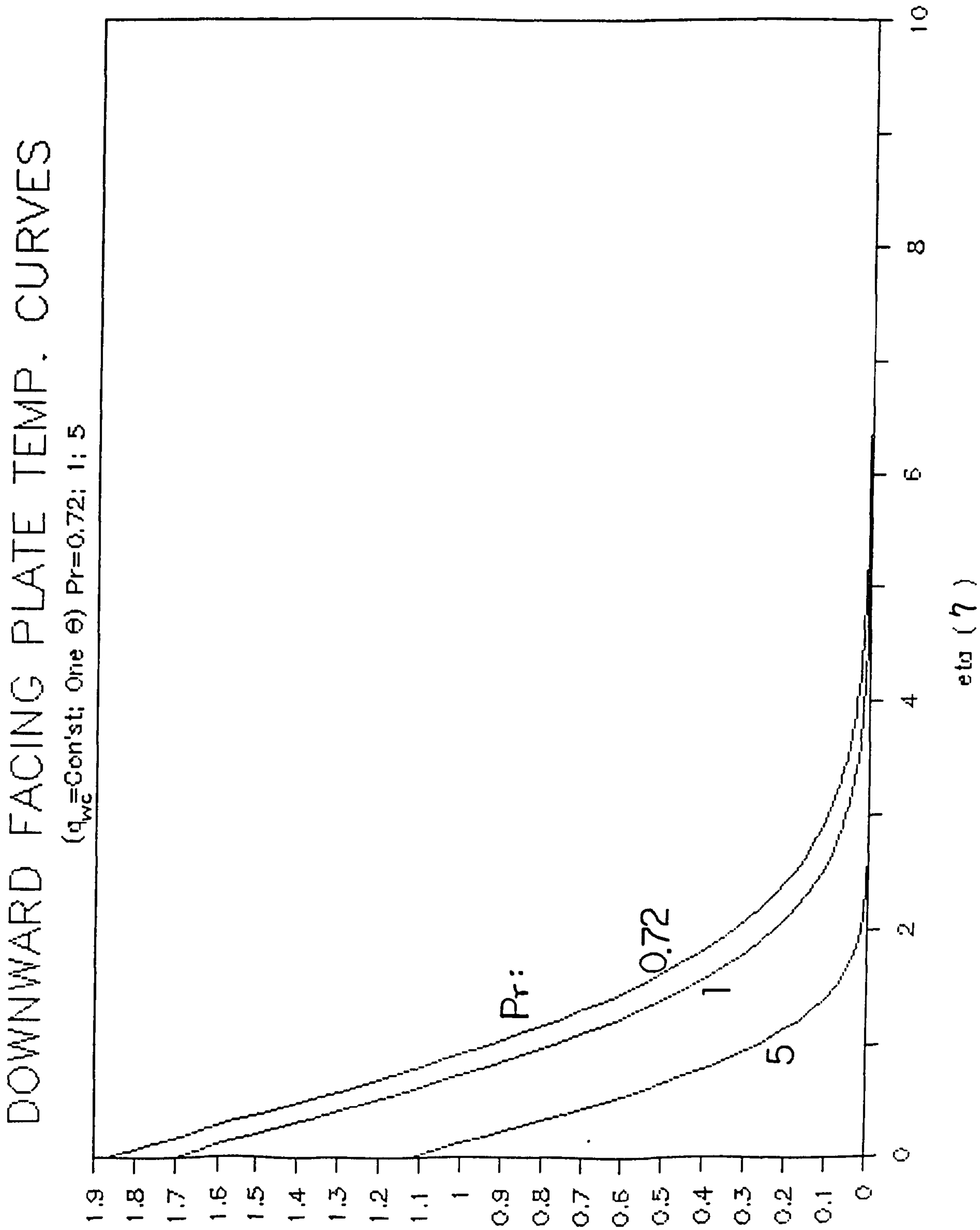

Fig.II-4.8 Temperature Function for Downward-Facing Heated Plate, One Assumed Temperature Function, Prescribed Constant Surface Flux Case at Pr=0.72, 1, 5

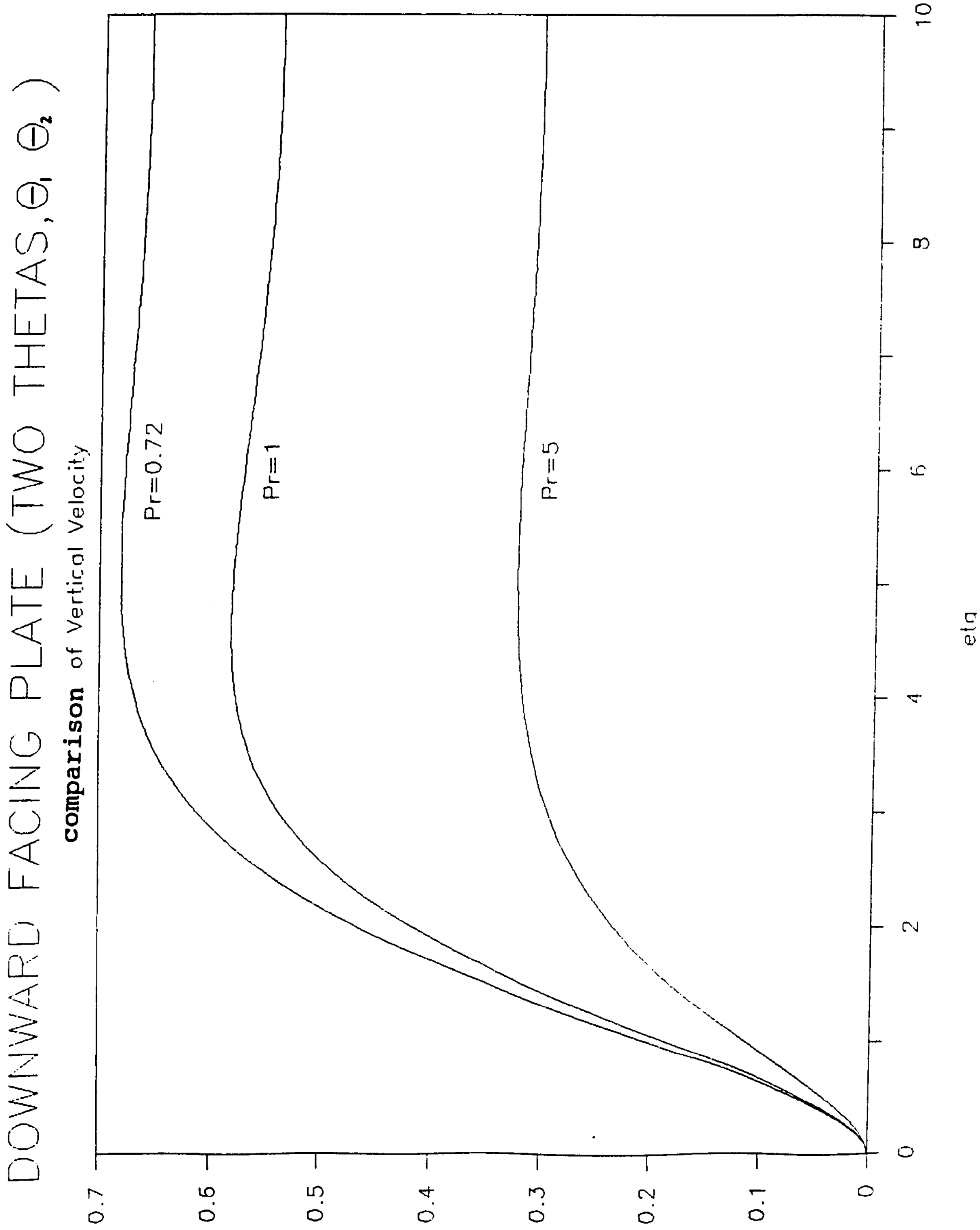

Fig.II-4.9 Vertical Velocity Function of Pr=0.72, 1, 5 for Downward-Facing Heated Plate, Two Assumed Temperature Functions, and Prescribed Surface Temperature Case at $\theta_2(0)=1$

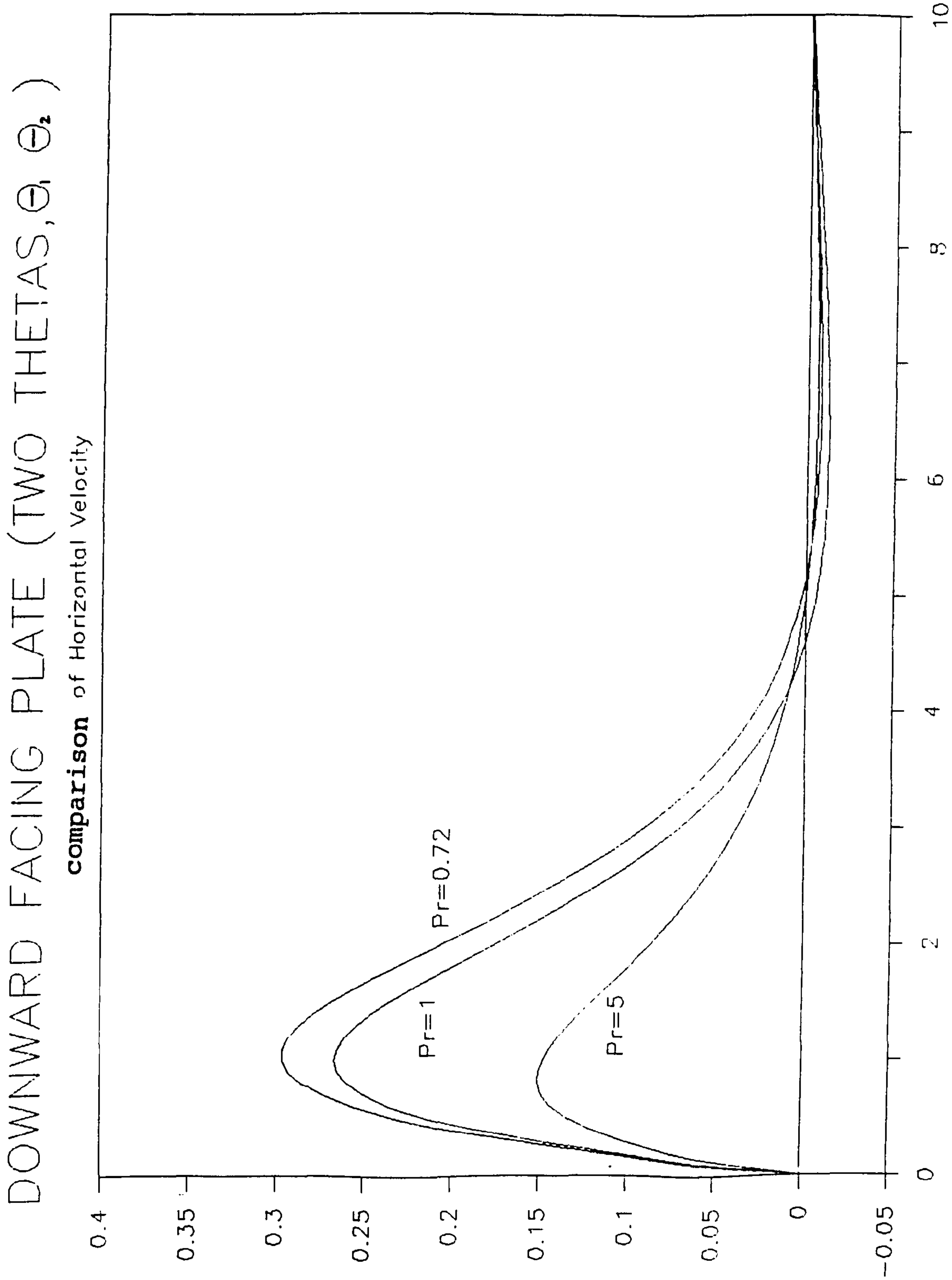

Fig.II-4.10 Radial Velocity Function of Pr=0.72, 1, 5 for Downward-Facing Heated Plate, Two Assumed Temperature Functions, and Prescribed Surface Temperature Case at $\theta_2(0)=1$

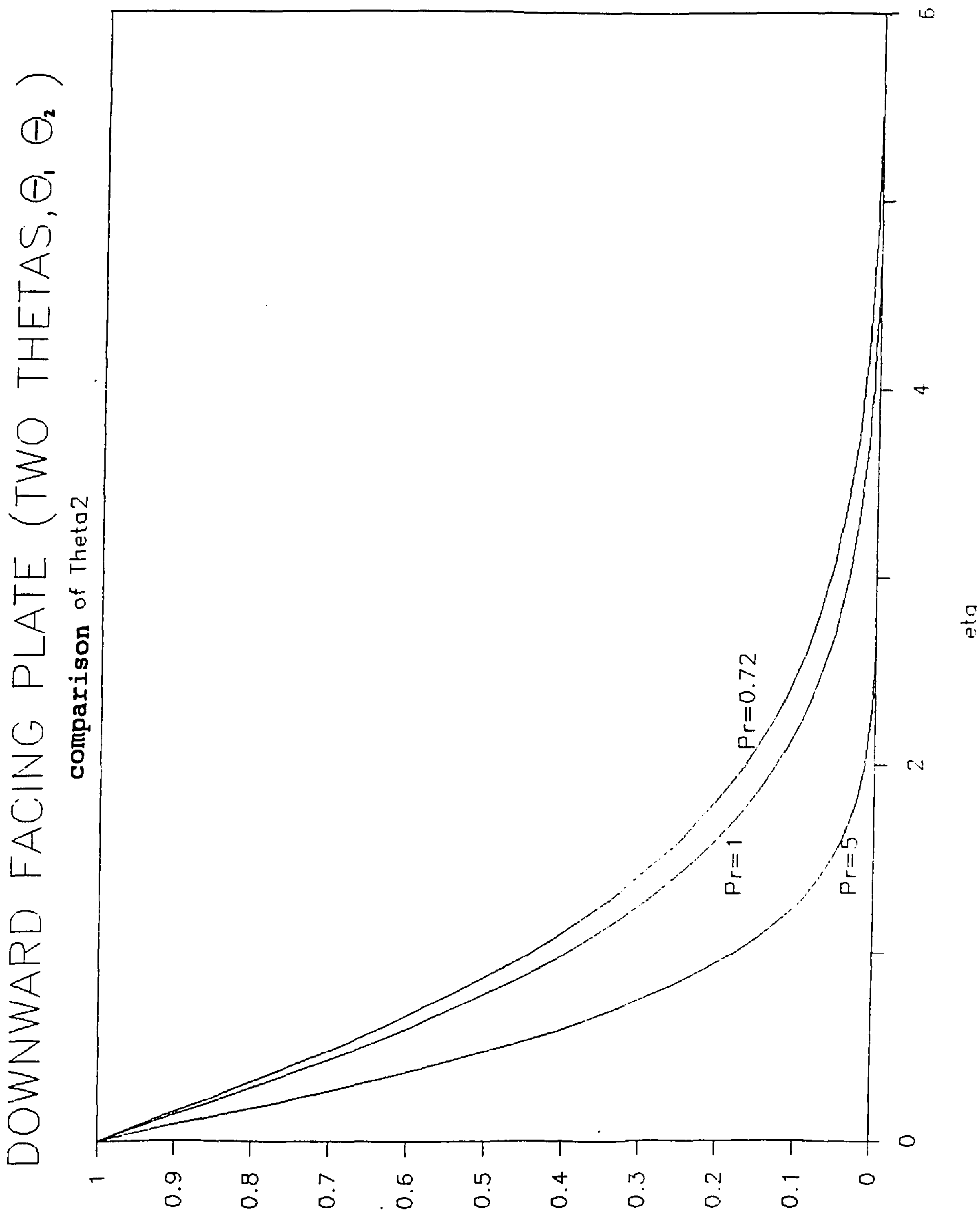

Fig.II-4.11 Solution of $\theta_2(\eta)$ of Pr=0.72, 1, 5 for Downward-Facing Heated Plate, Two Assumed Temperature Functions, and Prescribed Surface Temperature Case at $\theta_2(0)=1$

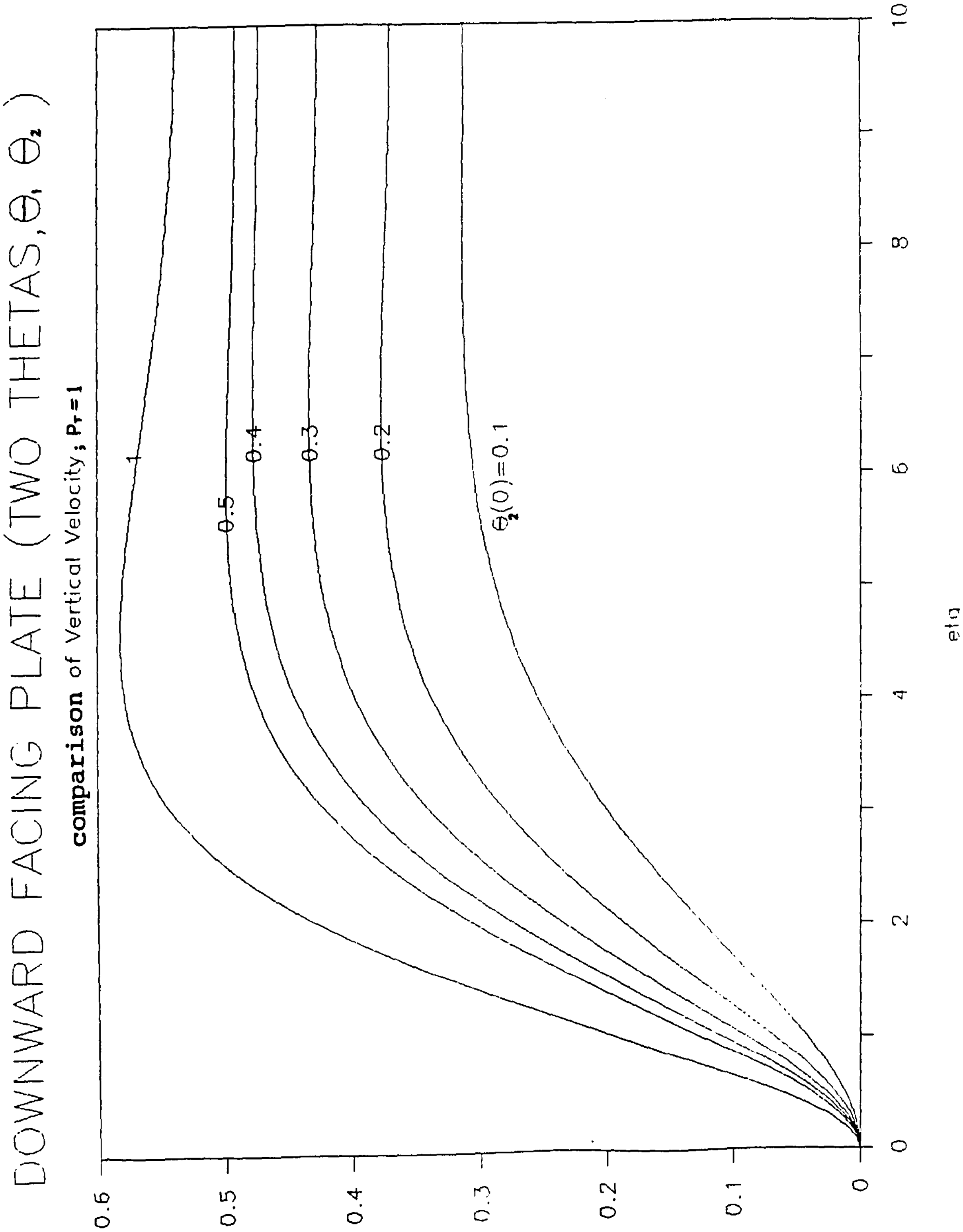

Fig.II-4.12 Vertical Velocity Function of Pr=1 for Downward-Facing Heated Plate, Two Assumed Temperature Functions, and Prescribed Surface Temperature Case at $\theta_2(0)=1$, 0.5, 0.4, 0.3, 0.2, 0.1

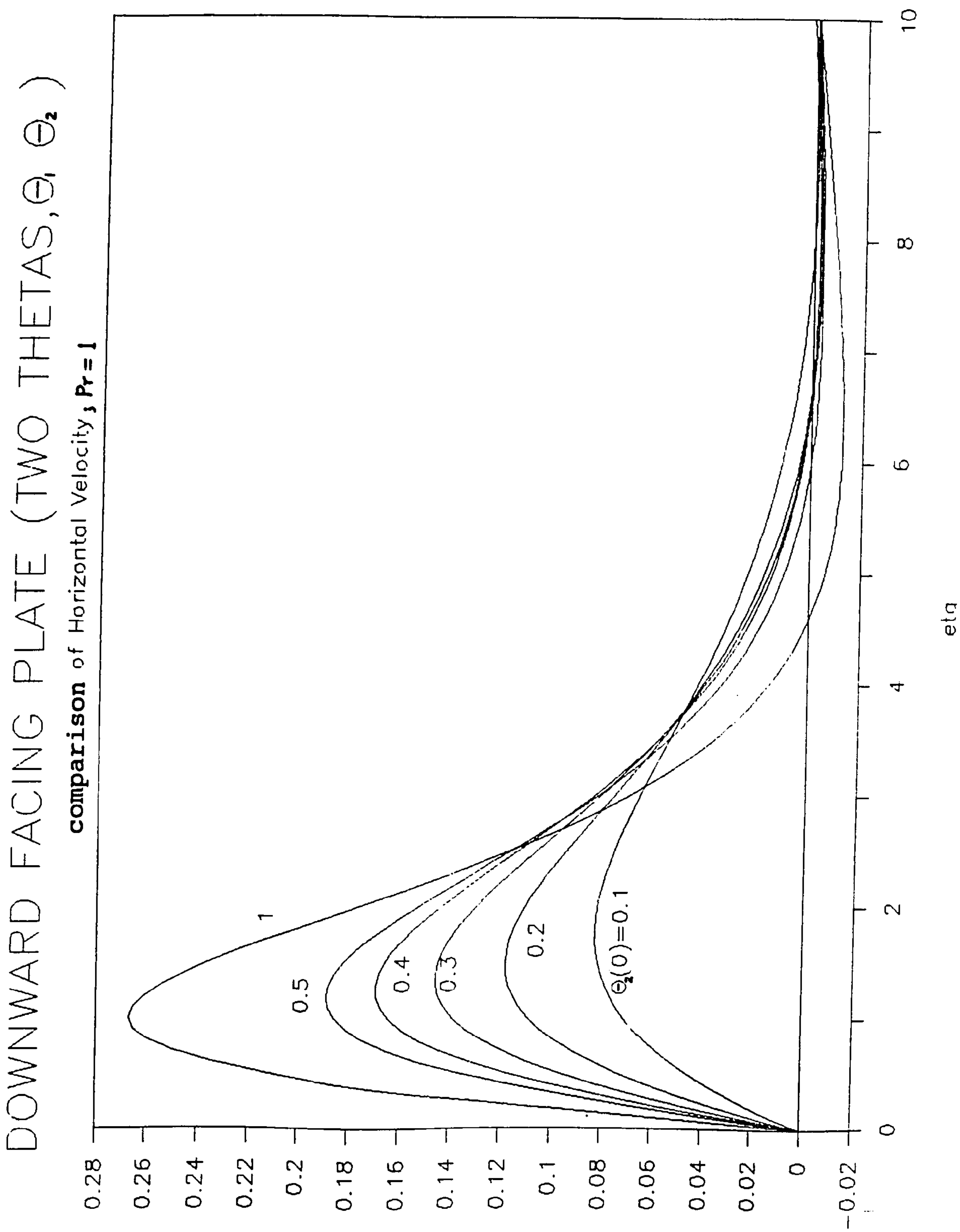

Fig.II-4.13 Radial Velocity Function of Pr=1 for Downward-Facing Heated Plate, Two Assumed Temperature Functions, and Prescribed Surface Temperature Case at $\theta_2(0)=1$, 0.5, 0.4, 0.3, 0.2, 0.1

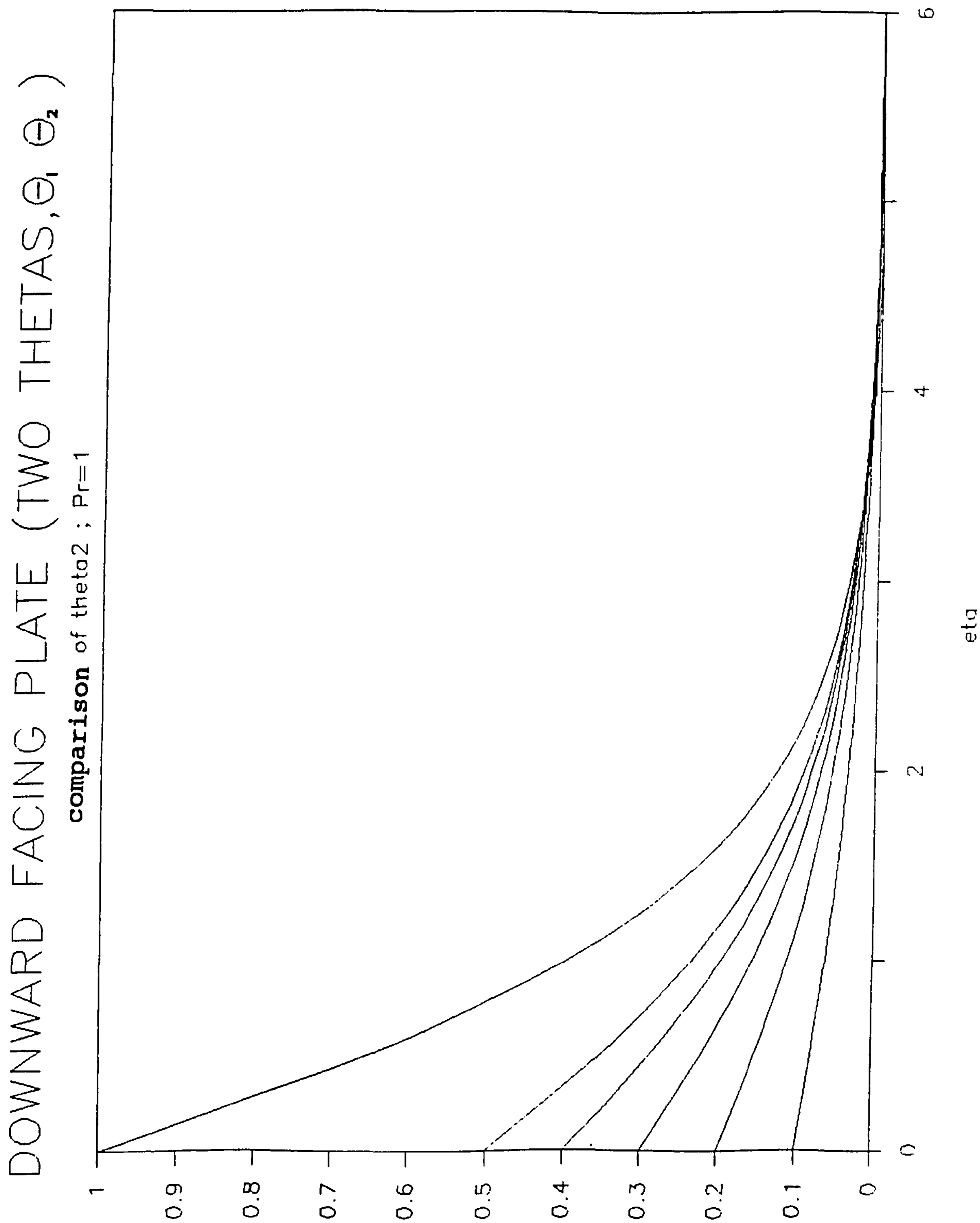

Fig.II-4.14 $\theta_2(\eta)$ of Pr=1 for Downward-Facing Heated Plate, Two Assumed Temperature Functions, and Prescribed Surface Temperature Case at $\theta_2(0)$=1, 0.5, 0.4, 0.3, 0.2, 0.1

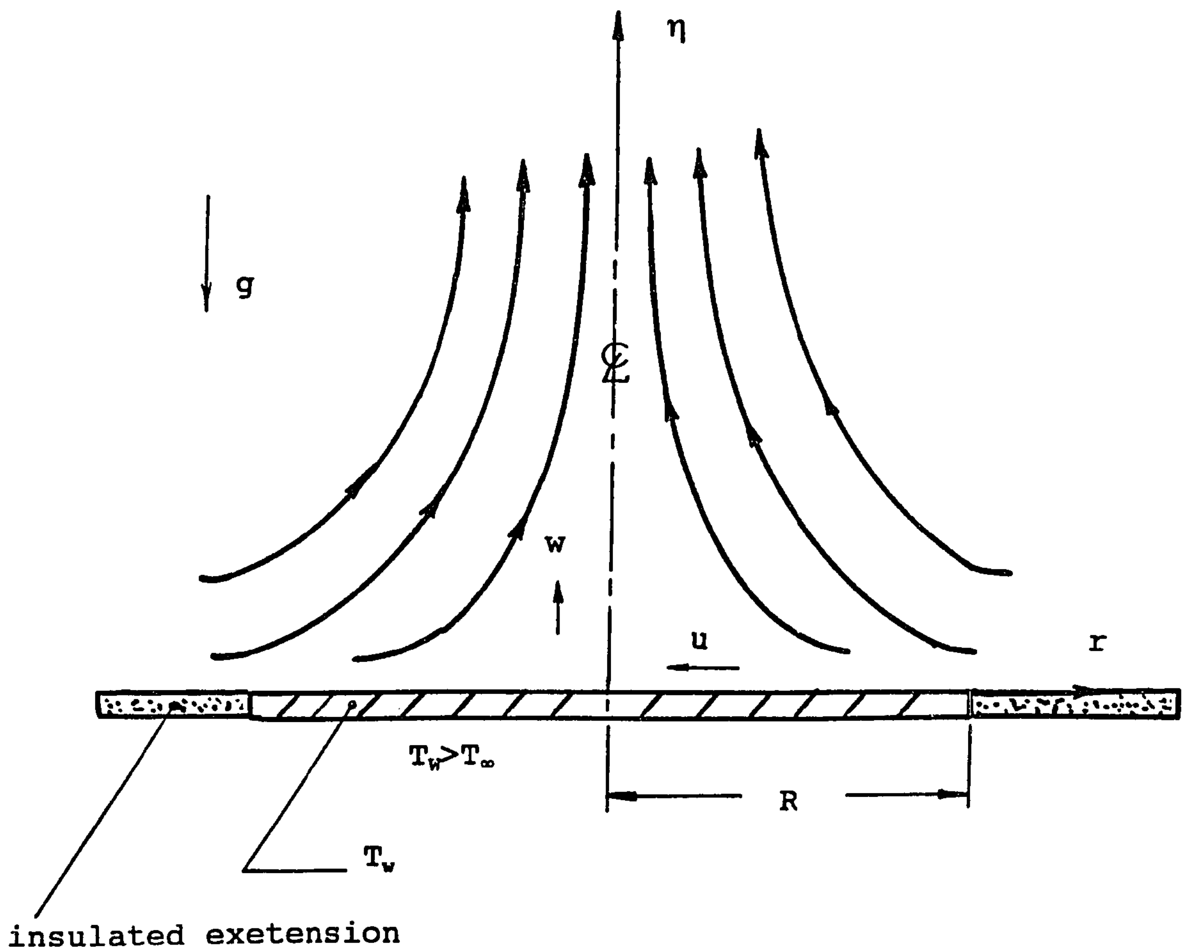

Fig.III-1.1 Flow Pattern and Coordinate System of Upward-Facing Heated Round Plate